

# **ANALYSIS OF PROVENANCE OF LATE CRETACEOUS – EOCENE TURBIDITE SEQUENCES IN NORTHERN VENEZUELA, TECTONIC IMPLICATIONS ON THE EVOLUTION OF THE CARIBBEAN**

by

MARIELA I. NOGUERA L.

(Under the Direction of James E. Wright)

## **ABSTRACT**

Provenance studies applying LA-ICP-MS U-Pb geochronology in detrital zircons and petrography were performed in Early Cretaceous passive margin and Paleogene turbidite sequences in northern Venezuela and Curacao, in hopes to understand the early Cenozoic history of the southern Caribbean and northern South America plates. The mature sediments of the passive margin deposits yielded ages between Late Proterozoic and Paleozoic and were primarily derived from the Guayana Shield. Grains with “Grenville ages” suggest an Andean source probably located in Colombia (Santa Marta and Santander Massifs). The detrital zircon data of the Maastrichtian-Miocene turbidite deposits record important magmatic events related to the Caribbean Large Igneous Province and its subduction below the South American margin. The petrographic and detrital zircon data indicate mixed continental and volcanic sources potentially located to the south (passive margin, Guayana Shield), north (Caribbean volcanic arc), and west (Colombian terranes and Perijá) of a foredeep basin.

**INDEX WORDS:** Turbidites, continental passive margin, Caribbean plate, Venezuela, provenance, geochronology, South America

**ANALYSIS OF PROVENANCE OF LATE CRETACEOUS – EOCENE TURBIDITE  
SEQUENCES IN NORTHERN VENEZUELA, TECTONIC IMPLICATIONS ON THE  
EVOLUTION OF THE CARIBBEAN**

by

MARIELA I. NOGUERA L.

Engineering Geologist, Universidad Central de Venezuela, Venezuela, 2002

A Thesis Submitted to the Graduate Faculty of The University of Georgia in Partial Fulfillment  
of the Requirements for the Degree

MASTER OF SCIENCE

ATHENS, GEORGIA

2009

© 2009

Mariela I. Noguera L.

All Rights Reserved

**ANALYSIS OF PROVENANCE OF LATE CRETACEOUS – EOCENE TURBIDITE  
SEQUENCES IN NORTHERN VENEZUELA, TECTONIC IMPLICATIONS ON THE  
EVOLUTION OF THE CARIBBEAN**

by

MARIELA I. NOGUERA L.

Major Professor: James E. Wright

Committee: Sandra Wyld  
Michael Roden

Electronic Version Approved:

Maureen Grasso  
Dean of the Graduate School  
The University of Georgia  
August 2009



## **DEDICATION**

To Luis and my parents for all the moral and economic support and for inspiring me in becoming  
a better professional

## **ACKNOWLEDGEMENTS**

I would like to express my most sincere thanks and to acknowledge all the people who either directly or indirectly, collaborated in the different stages of this work. Not all the names would fit in this space, the following are just a small fraction of them:

Dr. Jim Wright, my advisor and guide along all the way.

Dr. Franco Urbani, mi mentor and friend. From UCV, through UGA till the end.

My Committee board: Dr. Mike Roden and Dr. Sandra Wyld

Gustavo Malavé, Victor Cano, and Michael Schmitz from Funvisis and Patxi Viscarret for their help during the field work stage in Venezuela.

Meg Kinsella, Corin Stedman, Augie Parrinello, Emily First and Ted Lord for working through those long journeys at the Rock Preparation Room in UGA and in Arizona.

Victor Valencia and the people at the LaserChron Lab at the University of Arizona. Thanks for your assistance during those long days/nights analyzing zircons.

Marta Patiño, for her invaluable friendship and moral support

To all the students, professors and staff at the Geology Department, especially to Beatrice and Patty for their amazing work.

This work was supported by the National Science Foundation, through grants EAR-0087361 and EAR-0607533; the AAPG (Grants in Aid, 2008); and the University of Georgia, through the Miriam Watts – Wheeler Scholarship Fund 2008 (Geology Department) and the Tinker Foundation Travel Grant 2007 (Latin American and Caribbean Studies Institute).

## TABLE OF CONTENTS

	Page
ACKNOWLEDGEMENTS .....	v
CHAPTER	
1 INTRODUCTION .....	1
PURPOSE OF THE STUDY .....	1
UNITS AND AREA OF STUDY .....	3
METHODS .....	5
PREVIOUS STUDIES .....	6
EXPECTED RESULTS .....	10
2 EARLY CRETACEOUS PASSIVE MARGIN.....	11
INTRODUCTION.....	11
PASSIVE MARGIN SAMPLES.....	17
SANDSTONE PETROGRAPHY .....	24
DETRITAL ZIRCON AGES .....	34
PROVENANCE OF THE CRETACEOUS PASSIVE MARGIN.....	42
CONCLUSIONS .....	53
REFERENCES .....	54
3 PALEOCENE – EOCENE TURBIDITE UNITS.....	63
INTRODUCTION.....	63
TURBIDITE SAMPLES .....	65

SANDSTONE PETROGRAPHY .....	79
DETRITAL ZIRCON AGES .....	97
PROVENANCE OF THE MAASTRICHTIAN-MIOCENE TURBIDITES .....	108
CONCLUSIONS .....	117
REFERENCES .....	121
4 CONCLUSIONS.....	129
EARLY CRETACEOUS PASSIVE MARGIN UNITS .....	130
MAASTRICHTIAN – MIOCENE TURBIDITE DEPOSITS .....	131
REFERENCES .....	134
APPENDICES .....	150
A SAMPLES INVENTORY .....	151
B FIELD WORK PHOTOGRAPHS .....	154
C PETROGRAPHIC DATA .....	172
D DETRITAL ZIRCON DATA .....	175
E SAMPLE PREPARATION .....	188
F ANALYTICAL METHODS .....	196

# **CHAPTER 1**

## **INTRODUCTION**

### **PURPOSE OF THE STUDY**

Most accepted models for the evolution of the Caribbean (Pindell & Keenan, 2001; Pindell et al., 2006; Meschede & Frisch, 2002; James, 2006) suggest a Late Cretaceous – Paleocene configuration where a volcanic arc (Aves Ridge) on the eastern edge of the Caribbean plate moved eastwardly as a consequence of the oblique collision between the Caribbean and South American plates. During migration of this arc to its present location, turbidite sequences were deposited on the continental margin along the northern edge of the South American plate in Venezuela. As a consequence of this, turbidite sequences in Venezuela outcrop along the Cordilleran Belt from Western to Eastern Venezuela.

Earlier studies on turbidite deposits in Western and Central Venezuela by Yoris & Albertos (1989), and James (1997) suggest a strong contribution from a source of volcanic nature located to the north, with much less contribution from a source to the south (probably the Guayana craton or Early Cretaceous units deposited in passive margins). However, these estimations of provenance are supported only by petrography and field data (measurements of palaeocurrents in blocks that went through tectonic rotations of almost unknown magnitudes and directions). In addition, the tectonically active environment in which the turbidites were deposited may lead to problems of age determination by conventional biostratigraphic methods

(most turbidites are poor in fossil content, or may have a mixture of fossils that do not correspond to the same environment or age range, giving inconclusive results).

Recent studies of detrital zircons from turbidite units (Midden Curacao and Lagoen Formations) on Curacao island by Wright et al., (2008) showed ages between 65-75 Ma and a mixed provenance related to both a continental margin (South America) and volcanic arc (probably from exhumation of the Aves Ridge).

By studying detrital zircons from both turbidite (Chapter 3) and passive margin units (Chapter 2) along northern Venezuela, it is expected to find a relationship between the parental material of these rocks and either continental (southern source) or volcanic arc (northern source) rocks. These results will also provide new insights into the role of these sequences within the tectonic assemblage of the Caribbean and South American plates during the period from Late Cretaceous to Eocene.

The hypothesis to test with this work is the claim that the sediments composing the turbidite sequences had a primary source in the Early Cretaceous passive margin units and an extinct volcanic arc. From this statement arises the main objective, which is to determine the provenance of the sediments that formed the most important turbidite sequences along northern Venezuela, and their significance within the tectonic evolution of the Caribbean. Secondary objectives are listed below.

- To determine the age of detrital zircons in both turbidite and passive margin sequences.
- To determine age of post-cooling events (such as deposition) when possible.
- To identify the possible source(s) of the sediments that composes the turbidite units and to fit the results within the tectonic models for the evolution of the Caribbean plate.
- To determine the petrologic and tectonic affinity of the parental rock.

## UNITS AND AREA OF STUDY

The area of study is located in the southern part of the Caribbean, which structurally represents the boundary zone between the Caribbean and the South American plates. The research is focused on northern Venezuela (Figure 1.1), which includes part of the mainland and the Leeward Antilles islands from Aruba (west) to Margarita (east).

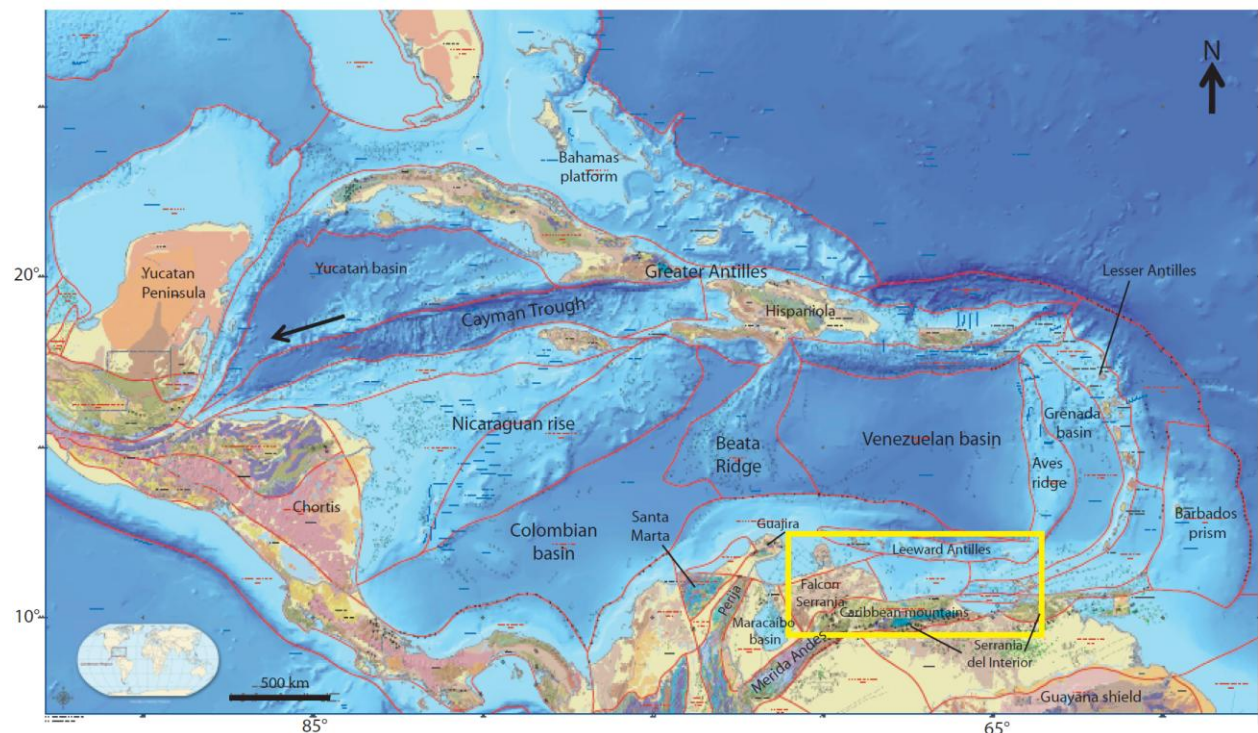


Figure 1.1. Location of the area of study (yellow box). Modified from French & Schenk (2004).

For this study, a total of 38 samples were collected (9 samples correspond to passive margin and 29 to turbidite units). An inventory of these samples is presented in Appendix A. Samples from Curacao were collected and provided by James Wright. The units under study are distributed from west to east in northern Venezuela (Figure 1.2) and are listed below (Table 1.1).

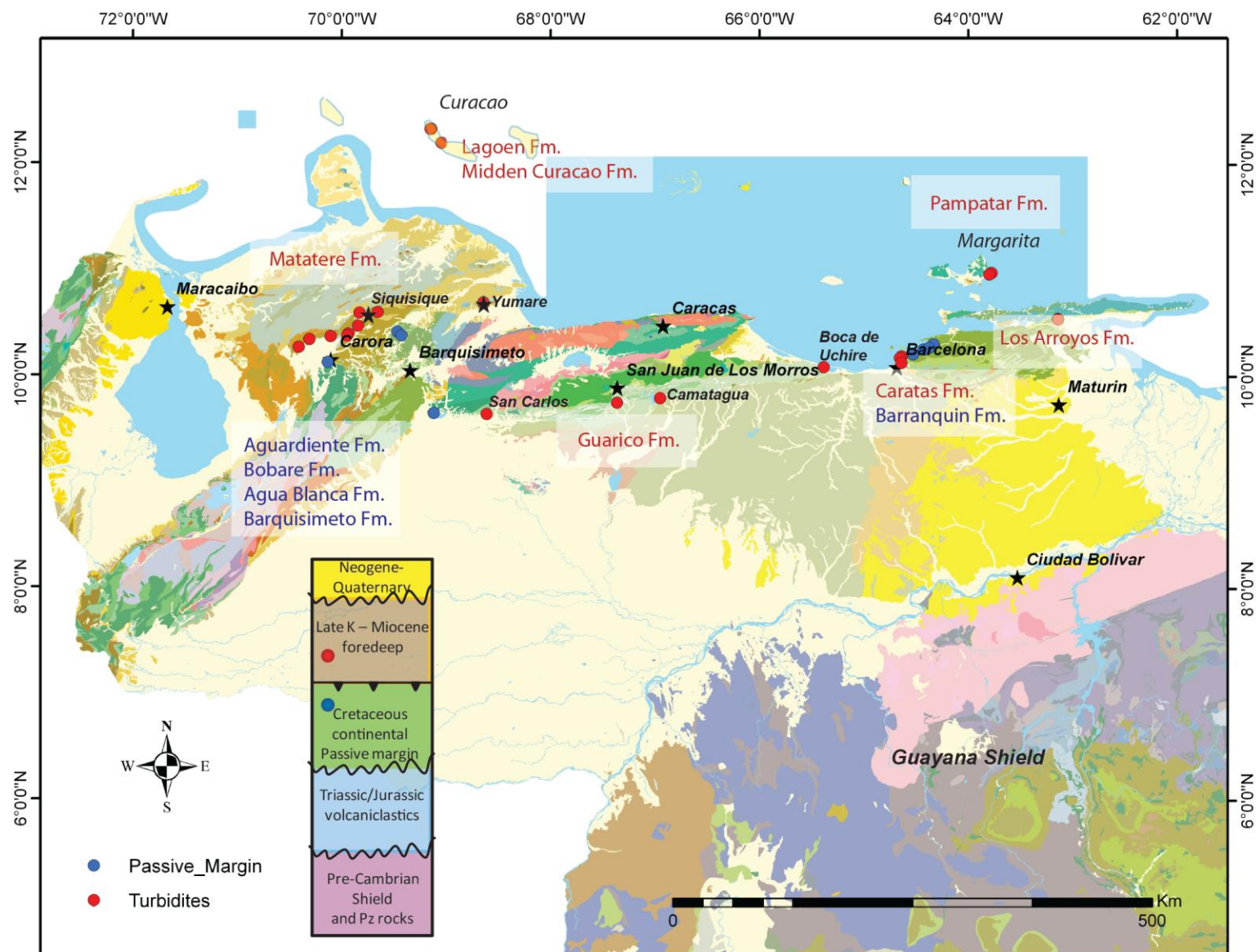


Figure 1.2. Location of the sampling sites and distribution of the units under study. Map modified after Hackley et al. (2005).



Table 1.1. Units under study and number of collected samples

<i>Passive Margin</i>	<i>Turbidites</i>
Aguardiente Formation (1*)	Lagoen Formation (2)
Bobare Formation (2)	Midden Curacao Formation (1)
Agua Blanca Formation (1)	Guarico Formation (4)
Barranquin Formation (4)	Matatere Formation (14)
Barquisimeto Formation (1)	Pampatar Formation (3)
	Caratas Formation (3)
	Los Arroyos Formation (2)

(\*) number of samples collected from each unit

## METHODS

U-Pb isotopic dating techniques were employed to determine ages of crystallization of detrital zircons. For the provenance study, and given the number of collected samples, the method of laser ablation –inductively coupled plasma mass spectrometry (LA-ICPMS) was applied. The equipment used is located at The University of Arizona (LA-ICPMS). The information presented in Appendix F explains the basics of this technique.

Conventional petrography and grain counting of framework grains was also performed on thin sections for each of the samples, in order to determine the mineralogical composition of the rocks and to obtain better control for identifying the parental material of the units.

A systematic collection of samples was executed on each of the units listed earlier. Both sampling and selection of the sites were based on the following criteria:

- Ease of access: Sites located in relatively accessible places were selected. Most of the samples collected were extracted from outcrops along rivers, streams and roads.
- Weathering degree: Ideal samples for this study were relatively unweathered. Also, rocks containing veins were avoided wherever possible.

- Quartz content: Zircon is usually associated with quartz, so samples containing quartz were targeted.
- Grain size: Coarse-grained clastic rocks (sandstones, conglomeratic sandstones and conglomerates) were preferred, since the hydraulic conditions related to their deposition increase the probability for accumulation of heavy minerals such as zircon. This also was the main reason why passive margin units of Early Cretaceous age were selected for this study rather than Upper Cretaceous units (Upper Cretaceous passive margin sequences in Venezuela are mainly carbonates; Gonzalez de Juana et. al, 1980; Yoris & Ostos, 1997).
- A minimum of five kilograms (about 11 pounds) and a maximum of ten kilograms (22 pounds) of rock per sample were collected when possible. Since zircons usually represent less than 1% of the mineral framework in a sedimentary rock, the probabilities of extracting significant amounts of these grains increase with the amount of rock collected.
- Samples were stored in sealed plastic and fabric bags, preventing any contamination by mixing with other samples, dirt or dust.

Information regarding zircon grain separation and sample preparation for the LA-ICP-MS analysis is presented in Appendix E.

## **PREVIOUS STUDIES**

There is a considerable amount of published studies on the Late Mesozoic-Cenozoic turbidite sequences in northern Venezuela and Trinidad. Early works are mere descriptions of the lithology, sedimentology and areal extent of these units, while later works (mentioned in the following) are more focused on their possible origins, and tectono-stratigraphic significance. However, to a much lesser extent, works related to provenance using thermochronology techniques in Venezuela and Colombia have also been published.

Moreno & Casas (1986) performed modal count methods on sandstones from the Eocene-age Pampatar and Punta Carnero Formations on Margarita Island (Figures 1.2 and 1.3). When plotted on the provenance discrimination diagrams of Dickinson et. al (1983), their results indicate affinities to recycled orogen and magmatic arc sources.

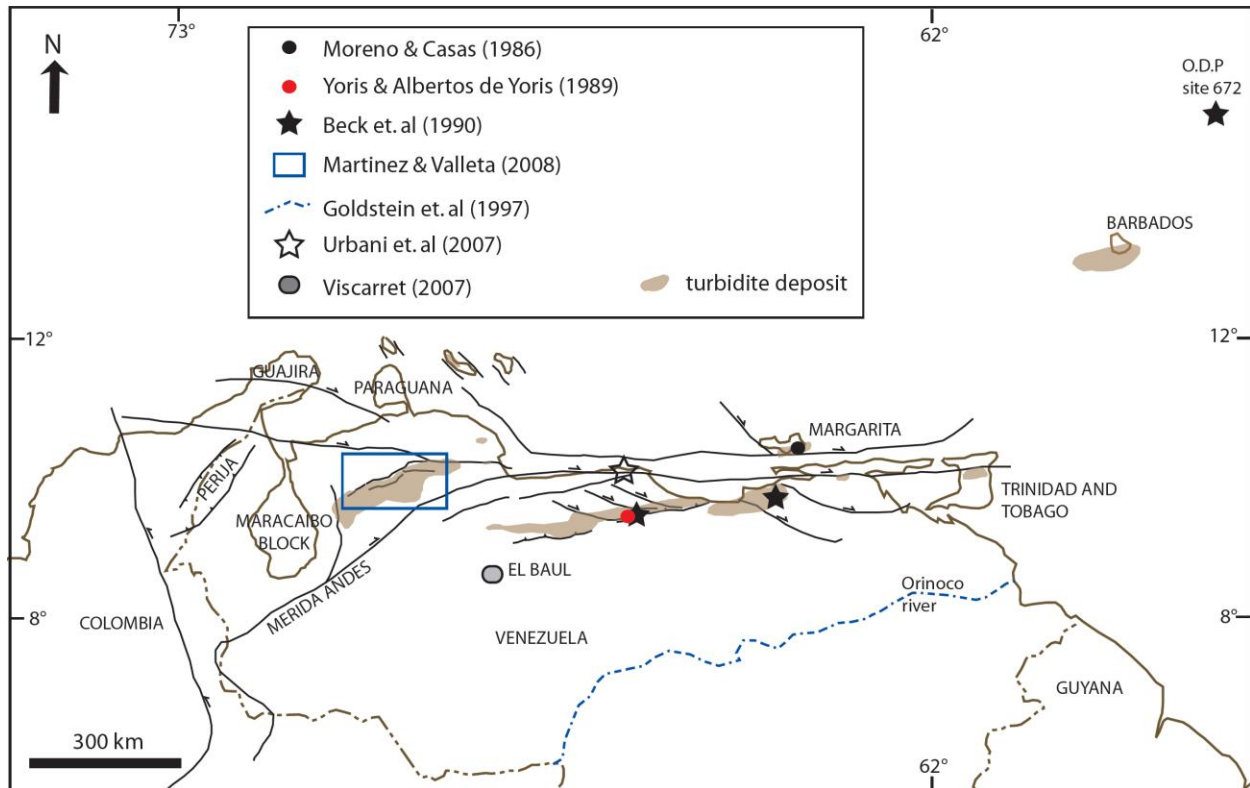


Figure 1.3. Map of northern Venezuela showing the areas previously targeted for studies on turbidite deposits and geochronology

Yoris & Albertos de Yoris (1989) used palaeocurrents to determine the provenance of the sediments of Guárico Formation in central Venezuela (Figure 1.3). They determined a primary source located to the north (probably from an extinct volcanic arc) but could not prove earlier theories about different sources located to the south and to the west (Bell, 1968; Kasper & Larue, 1986); however, they considered these as second-order sources. In this work, Guárico Formation

is assigned a “Dissected Magmatic Arc” affinity, with a deviation to “Transitional Continental” provenances.

Beck et. al (1990) studied a core section from the Atlantic abyssal plain at Ocean Drilling Program site 672 (Figure 1.3) and compared its Middle – Upper Eocene sediments to turbidite sequences in central and eastern Venezuela (Guárico and Caratas Formations). They suggested that deposition of these sequences is related with the eastward displacement of the Caribbean plate during the Eocene-Oligocene. Turbidite currents were formed on the southern part of an accretionary complex, on the South American slope, and moved eastward as the prism grew.

James (1997) summarized and made an inventory of turbidite units in Venezuela and Trinidad. He concluded that these units record an event that occurred from Late Cretaceous to Middle Eocene, which was related to the convergence between the Caribbean and South American plate. He suggested that sediments sources were to the north and the possibility of that these units are also found in the Interior Range in eastern Venezuela and in the substratum of the offshore area that includes the islands of Aruba to La Blanquilla.

The most recent work on provenance is that of Martinez & Valleta (2008), who used conventional petrographic analyses to compare the coarse grained facies of Matatere Formation to units located in adjacent areas of the Barquisimeto Trough. They suggested potential sources than include the Guajira Peninsula, Perijá Range, Merida Andes, El Baúl Massif and Paraguaná Peninsula (Figure 1.3).

Information on the geochronology of Venezuelan rocks is relatively poor. Most of the work done in the geochronology field is old. Most recent works apply detrital zircon techniques for objectives similar to those of this research, but since this is a “newly discovered tool” in this country, publications are scarce.

Probably the first study in Venezuela using U-Pb geochronology was that of Dasch (1982), who dated igneous and metamorphic rocks from the Sierra de Perijá and Isla de Toas, in northwestern Venezuela. These ages helped to constrain magmatic and metamorphic events during the Paleozoic and to reveal the influence of tectonic episodes in the region.

The provenance study of Goldstein et al. (1997) determined the relationship between the ages of detrital components in Quaternary sediments from the Orinoco River (Figure 1.3) and the growth and evolution of its basement precursor (Guayana Shield). SHRIMP U-Pb ages from detrital zircons and Sm-Nd isotopes were used, in an attempt to address many of the questions regarding the rate and mechanism of continental growth.

Sisson et al. (2005) presented results of geochronology of the allochthonous belts in northern Venezuela. The results come from different radiometric techniques (Rb-Sr,  $^{40}\text{Ar}/^{39}\text{Ar}$ , U-Pb, and apatite and zircon fission tracks). With the U-Pb technique they reported an age for the Guaremal Granite of 471 Ma. They also suggested the existence of an inherited component from the pre-Cambrian rocks of Roraima or Cuchivero provinces, located in the Guayana Shield.

The most recent work using SHRIMP U-Pb ages is from Urbani et al. (2007), who dated a meta-diorite body (Metadiorita de Todasana) from the metamorphic belt of Cordillera de la Costa (Figure 1.3). The new information (508 Ma, Mid Cambrian) constitute an improvement on previous ages determined by different authors with different methods.

New ages in the Venezuelan basement were also presented by Viscarret (2007), who determined SHRIMP U-Pb ages of granitic and volcanic rocks of the El Baúl region in western Venezuela (286 to 493 Ma; Figure 1.3). Again, the new ages showed differences with previous reports using other geochronologic methods.

## **EXPECTED RESULTS**

By analyzing some of the most representative Early Cretaceous passive margin units in northern Venezuela it is expected to obtain a characteristic detrital zircon signature to be compared with the foredeep deposits. If the Paleogene turbidite deposits were indeed formed by sediments derived from the Early Cretaceous continental rocks, then this “passive margin signature” is expected to be registered in the turbidite detrital fraction. Additional comparisons between the detrital components of the turbidite deposits of Venezuela and Curacao will determine if the Venezuelan deposits received either an additional or exclusive component from the Caribbean volcanic arc terranes.

## **CHAPTER 2**

### **EARLY CRETACEOUS PASSIVE MARGIN**

#### **INTRODUCTION**

A number of provenance studies have been performed on Late Cretaceous - Eocene turbidite deposits (Lopez, 1976; Zapata, 1976; Valdes D' Gregorio, 1980; Yoris & Albertos de Yoris, 1989; Albertos, 1989; Ghosh & Zambrano, 1996; Martinez & Valleta, 2008) in hope of understanding the Cenozoic basin evolution in northern Venezuela. Previous petrographic analyses and paleocurrent measurements in turbidite units (Matatere, Guárico, Garrapata, and Pampatar Formations) have pointed to a mixed continental margin (Guayana Shield) and volcanic arc provenance (Yoris & Albertos de Yoris, 1989). However, a complete study of the early Cenozoic processes that generated these deposits cannot be achieved without having a good understanding of the events that preceded them. Characterization of siliciclastic passive margin units in Venezuela (Aguardiente, Bobare, Agua Blanca and Barranquín Formations) by means of U-Pb detrital zircon ages and framework grains will contribute in identifying the original sources of sediment that built such sequences in the Early Cretaceous; subsequent comparison of the passive margin data with those from the Paleogene turbidites will help to constrain the contribution of this passive margin to the Tertiary basins and will add some new constraints to the current interpretations about the complex Cenozoic evolution of the Caribbean.

The Mesozoic tectonic evolution of northern South America was relatively simple. Separation of North America and South America, during the breakup of western Pangaea, was the dominant event at this time and provided the conditions for the generation of new oceanic crust (proto-Caribbean plate). Diachronously, an Atlantic-type continental passive margin developed in northern South America (Villamil & Pindell, 1998; Pindell et. al, 2005; Figure 2.1). By the end of the Cretaceous the Caribbean plate arrived at the north-western part of South America. Deformation associated with plate interactions between the Caribbean and the Americas affected the areas related to the present-time Yucatan Block, the Bahamas and the Greater Antilles (Figure 1.1, Chapter 1) since the end of the Mesozoic to present time (Villamil & Pindell, 1998). The most significant regional events that occurred during the Jurassic-Mesozoic evolution of northern South America are summarized below.

Spreading responsible for the separation of North America and South America probably began in Early Jurassic time. By Late Jurassic- Early Cretaceous, east-west rift propagation triggered the counterclockwise rotation and movement of the Yucatan Block, from its original location between Venezuela-Trinidad and Texas (Figure 2.1) to its present position relative to North America (Villamil & Pindell, 1998; Pindell & Kennan, 2001).

This continental rifting marked the initiation of a passive margin in northern South America, from the Guajira Peninsula to Trinidad (Figure 2.2; Villamil & Pindell, 1998). A series of rift basins formed to the west as a consequence of lithospheric extension in the Andean magmatic arc system: Machiques, Trujillo, Uribante, Cocuy and Arcabuco rifts (Figure 2.2). Numerous extensional faults associated with the main rifts occur in northwestern Venezuela (e.g.



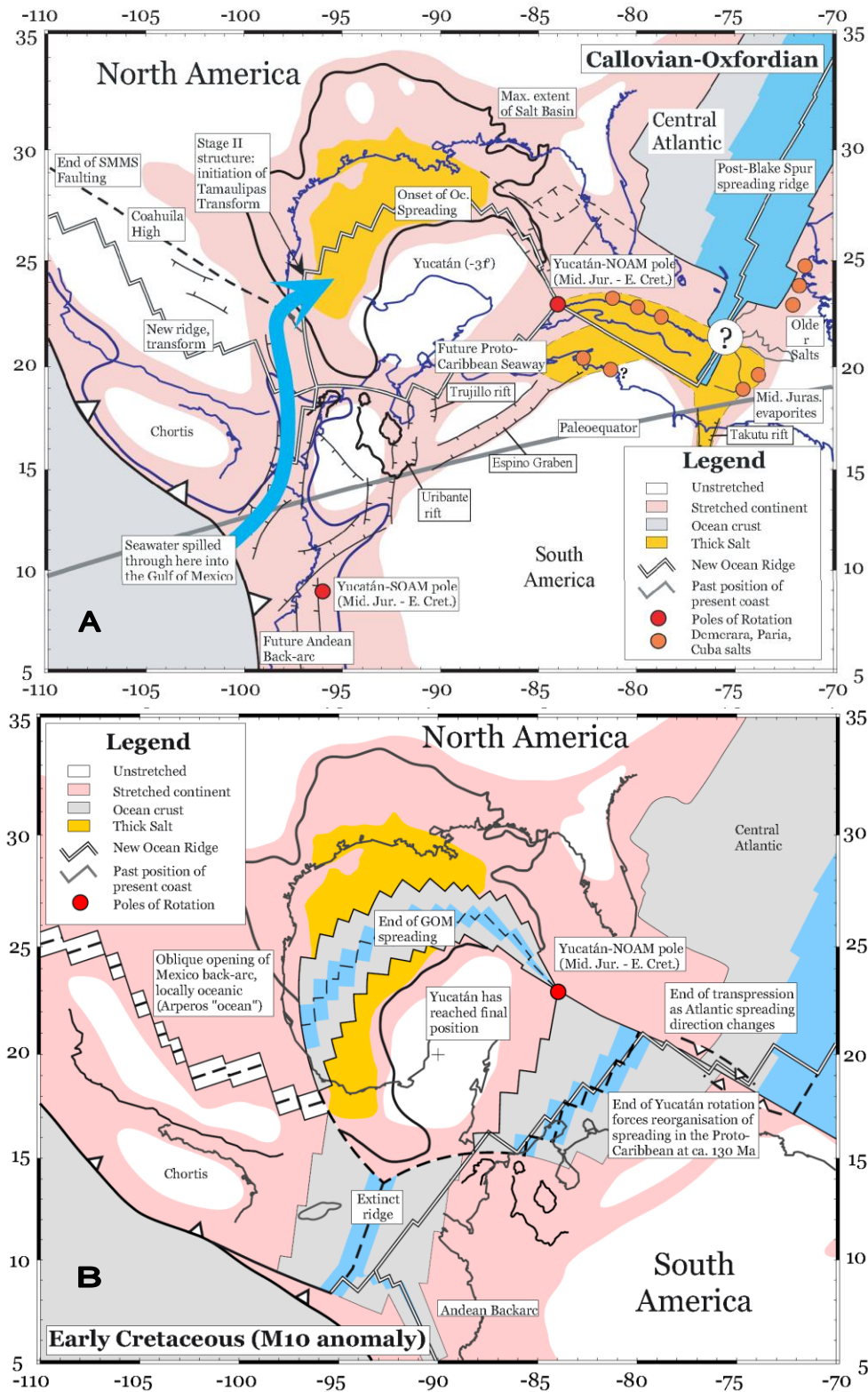


Figure 2.1. Plate reconstruction of the Caribbean area by (A) Late Jurassic time, (B) Early Cretaceous time (Pindell & Kennan, 2001).

Icotea half graben); other rifts, such as the Espino Graben (Figures 2.1a and 2.2), are found in western and eastern Venezuela (Villamil & Pindell, 1998).

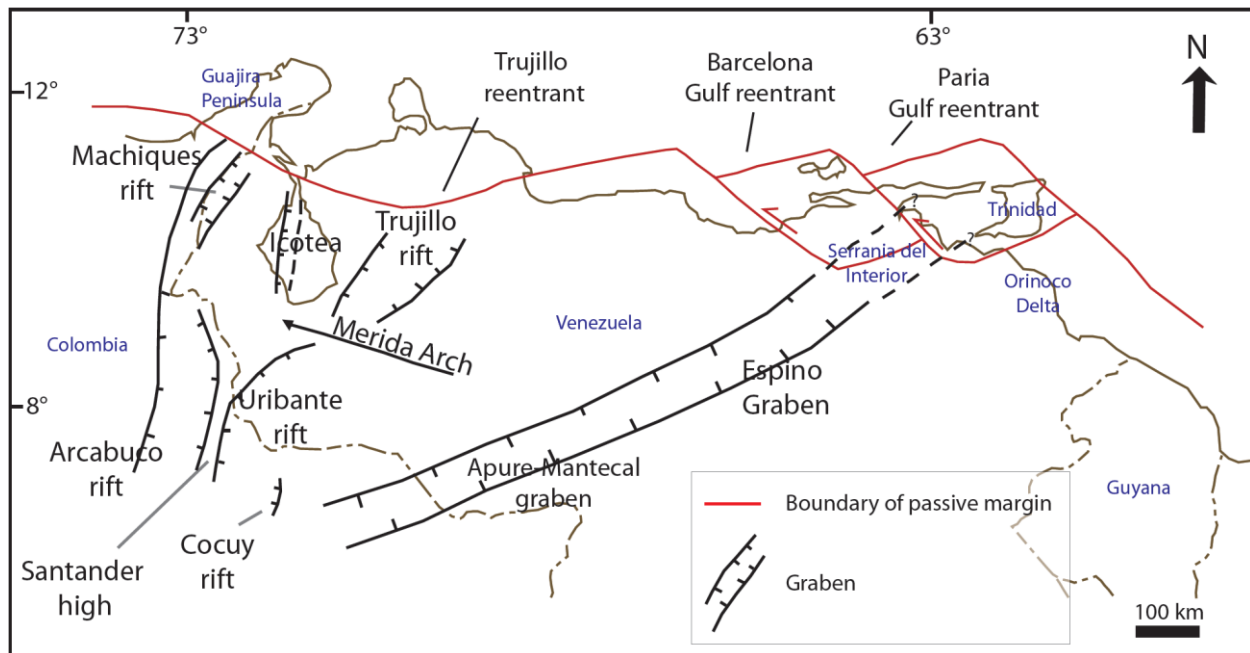


Figure 2.2. Distribution of Jurassic structures in Venezuela. Modified after Villamil & Pindell (1998) and Pindell & Kennan (2001).

This rifted margin had several re-entrants in South America: Trujillo Trough, Gulf of Barcelona and Gulf of Paria (Figure 2.2). The ENE orientation of these segments allows them to be considered as main rift zones associated with the NNW-SSE separation of the Yucatan Block from South America. NNW-oriented segments are associated with transfer zones that developed during the rifting (Villamil & Pindell, 1998).

The Apure-Mantecal and the Espino grabens (Figure 2.2) are probably the most important features that have controlled the sedimentation and basin evolution in Venezuela since the Jurassic. These structures run in a SW-NE trend and, although separated by the Paleozoic-age

plutonic rocks of the El Baúl High, they are considered in this paper as a single structure (Espino Graben) that extends from Eastern Venezuela to Colombia.

The Espino Graben, the Amazon Valley graben and the Takutu Rift in Guyana (Figure 2.1a) have been interpreted as failed rifts (aulacogens; Persad, 1990). This implies that the Espino Graben might extend toward the ENE beneath the Serranía del Interior, Gulf of Paria and/or Orinoco Delta, reaching into the Trinidad area (Figure 2.2; Persad, 1990; Villamil & Pindell, 1998; Pindell et al. 1998). Gravity and magnetic data tend to support this idea, but more research and data is still needed (Persad, 1990).

Rocks associated with the rifting phase are found in Venezuela at the base of the Jurassic grabens and are of continental and volcanoclastic nature. Magnetic, gravimetric and well data identified about 8,000 feet of Jurassic red beds (probably La Quinta and/or Ipire Formations) and volcanics of similar age (162 my) in the Espino graben (Persad, 1990; Rodríguez & Rodríguez, 2003). About 20,000 feet of Cambrian to Carboniferous sedimentary and meta-sedimentary rocks have also been reported in this graben (Persad, 1990).

The Cretaceous in northern South America is marked by a regional transgression which reached a maximum in Early Turonian time (Yoris & Ostos, 1997; Villamil & Pindell, 1998). By the end of the Neocomian, a proto-Caribbean sea was already formed, due to the advanced extension between Yucatan and South America (Figure 2.1b). Differential subsidence, caused by deactivation of the rift complexes, favored the development of shallow-water belts away from the Guayana Shield and rapid sedimentation in the adjacent troughs (Rio Negro, Aguardiente, Barranquín Formations, Figure 2.3).

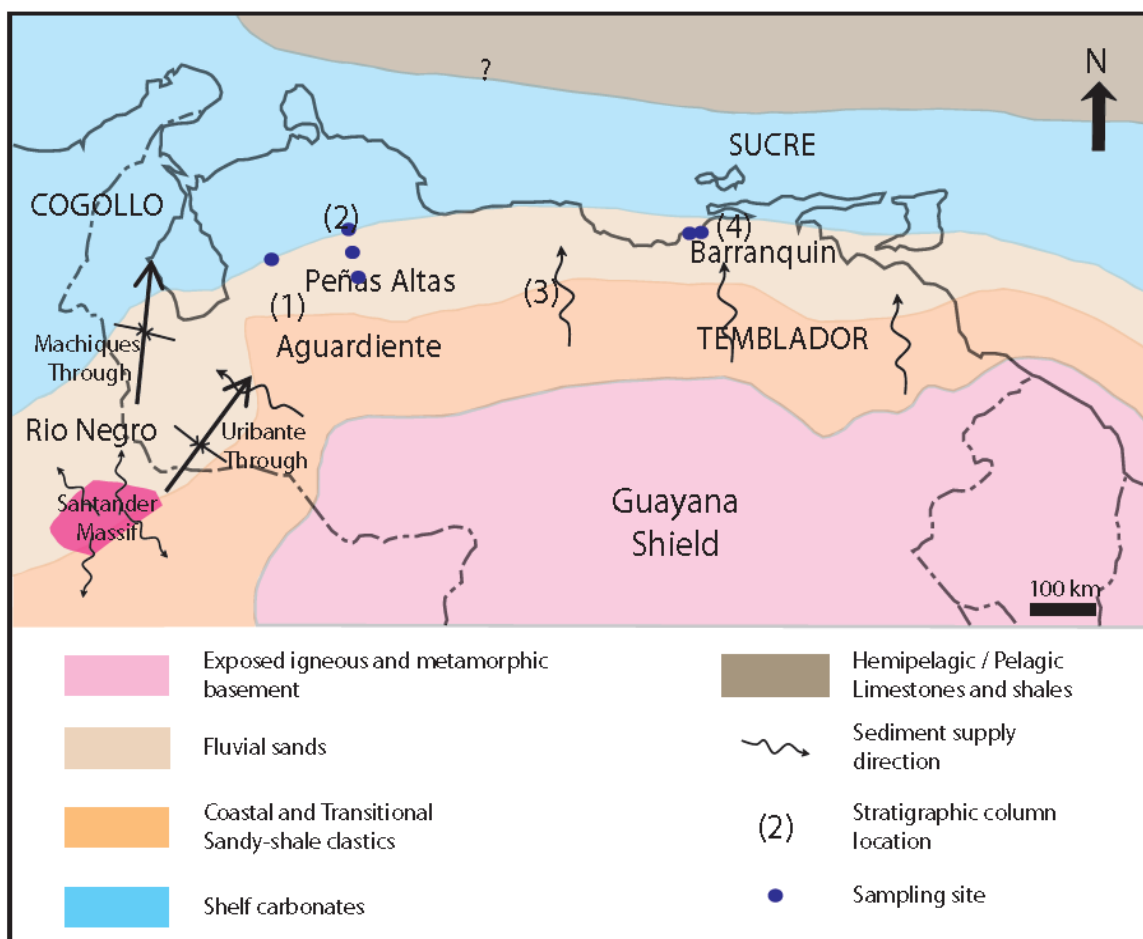


Figure 2.3. Paleogeographic map of Venezuela during the Early Cretaceous (modified from Yoris & Ostos, 1997).

Onlapping of deep water facies over shallow to continental facies occurred as transgression developed and is reflected in the Cretaceous stratigraphic record as a gradual change from continental clastics (Early Cretaceous Rio Negro and Barranquín Formations) to shale and carbonate facies (Late Cretaceous La Luna and Querecual Formations) (Figures 2.3 and 2.4). The Late Cretaceous in Venezuela ends with a regressive event associated with the arrival of the Caribbean Plate at northern South America (Yoris & Ostos, 1997).

The new petrographic and LA-ICP-MS U-Pb detrital zircon data of quartz-rich passive margin units (Barranquín, Aguardiente, Bobare, Agua Blanca Formations) are consistent with a

shield provenance. Additionally, U-Pb ages show an unexpected “Grenville age” not previously reported in Venezuela (but suspected from petrographic studies by Grande et al., 2007), that can possibly be related to an Andean source (Santa Marta and Santander Massifs in north-eastern Colombia; Cordani et al., 2005; Molina et al., 2006). Even more surprising is the finding of Grenville-age grains in deltaic sediments of the easternmost Barranquín Formation, considerably distant from the Andean sources. Interpretations of these data include an alternative paleogeographic model for the Early Cretaceous time, which considers a different conception of the main drainage system in Venezuela (proto-Orinoco River).

## **PASSIVE MARGIN SAMPLES**

A total of nine (9) samples of sandstones were collected from different Early Cretaceous units of the passive margin in western (Aguardiente, Bobare, Agua Blanca and Barquisimeto Formations) and eastern Venezuela (Barranquín Formation); (Figure 2.4). The Figure 2.5 shows the stratigraphic record from Jurassic to Late Cretaceous time in western and eastern Venezuela.

### **Barranquín Formation (Neocomian – Aptian)**

The Barranquín Formation is part of the Eastern Venezuela passive margin (Figures 2.3 and 2.4). It is composed of quartz sandstones, intercalated with shales and occasional layers of limestone at the intermediate level of the section. The sequence is divided into three members (from base to top):

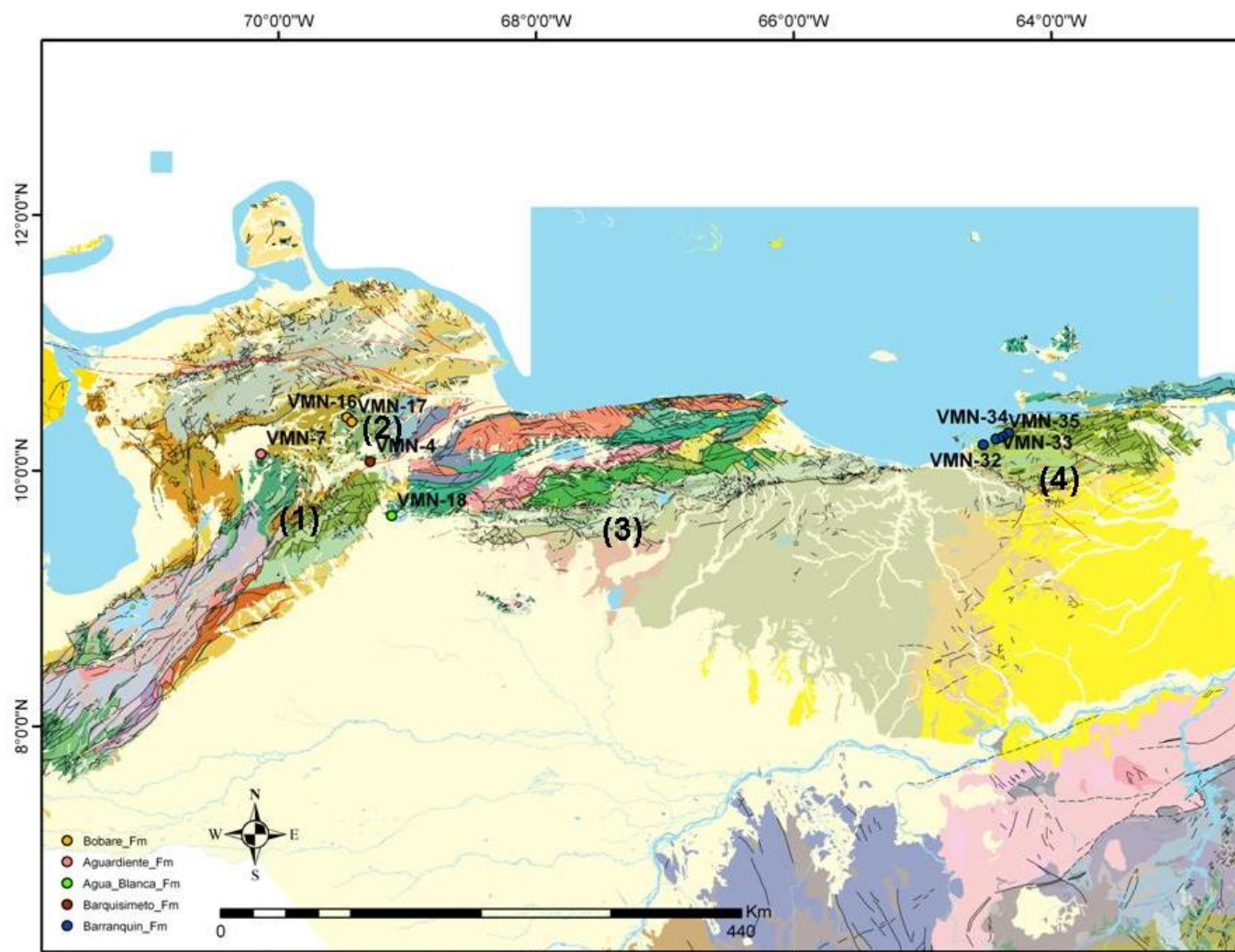


Figure 2.4. Distribution of samples collected from passive margin units in western and eastern Venezuela. Modified from Hackley et al. (2005). Numbers correspond to the location of stratigraphic columns from figure 2.5.



AGE		1	2	3	4	Tectonic Setting		
		Northern Andes	Lara	Northern Guarico	Eastern Venezuela			
Late Cretaceous	Maastrichtian	Mito Juan		Guarico	Vidoño	Passive Margin		
		Colon	BARQUISIMETO	G U A Y U T A	San Juan			
	Tres Esquinas	Mucaria, San Antonio, Rio Chavez, Querecual formations			San Antonio			
	Santonian			?	Exotic Blocks		Querecual	
	Coniacian							
	Turonian	Guayacan						
	Cenomanian	Capacho						
	Early Cretaceous	Albian		Capacho	BOBARE, Cojedes		?	Macaira limestone
AGUARDIENTE			El Cantil					
Aptian		Apon	BOBARE, AGUA BLANCA	Garcia				
		Rio Negro		Taguarumo				
Barremian			BOBARE	BARRANQUIN				
Neocomian			Mamey					
			Aroa					
Jurassic			La Quinta		Ipire			

Figure 2.5. Simplified correlation chart of the passive margin stage in northern Venezuela. Sampled units are in capitals. Numbers at headers indicate location according to the map in Figure 2.4. (Modified after Yoris & Ostos, 1997 and LEV, 2008).

- Venados Member (Pre-Valanginian): Shelf margin sequence of cross-bedded quartz sandstones intercalated with sandy shales with no fossils (Von der Osten 1954, in LEV 2008).
- Morro Blanco Member (Neocomian): Sequence of bioclastic limestones with silty and sandy intervals, less than 10 meters thick and deposited on an upward-deepening shelf (Erikson & Pindell, 1998b).

- Picuda Member and Taguarumo Formation (Barremian – Aptian): This interval records rapid accumulation of siliciclastics (Figure 2.6), with minor carbonate, in shelf and shoreface environments. Limestone content increases at the uppermost part of Taguarumo Formation, indicating the initiation of a transgression (Erikson & Pindell, 1998b).

The lower contact of Barranquín is not exposed and the underlying units are unknown, but hypotheses point to the existence of either a metamorphic basement or sedimentary sequences of Cambrian age (LEV, 2008). The upper contact is transitional with Taguarumo Formation and El Cantil Formation (Figure 2.5).



Figure 2.6. Barranquín Formation in the Mochima area. Site GPS-370, sample VMN-34.

The age of the Barranquín Formation is imprecise; biostratigraphic reports are often conflicting (Erikson & Pindell, 1998a; Villamil & Pindell, 1998; LEV 2008) and as a result, the unit has been assigned to different times within the Early Cretaceous (Figure 2.5). Erikson & Pindell (1998b) assign a deposition age of about 112 Ma for the beds of Barranquín Formation. Interpretations of the depositional environment of the Barranquín Formation in different locations of the Eastern Serranía (LEV, 2008; Erikson & Pindell, 1998a), suggest that the unit



was deposited in a transitional environment grading from deltaic to internal shelf. The Guayana Shield and Paleozoic to Jurassic sediments deposited along the northern margin of the shield have been interpreted as the sources of Barranquín Formation and younger units within the Sucre Group (Figure 2.5; Ostos et al. 2005).

### **Bobare Formation (Barremian?-Albian)**

The Bobare Formation (Figure 2.5) is mainly composed of shales and quartz-rich sandstones (Figure 2.7), in which grain size varies from very coarse to fine. Bellizia (1986, in LEV 2008) describes the Bobare Formation as composed of massive, sometime conglomeratic, quartz-rich meta-sandstones, phyllites and siltstones. Some limestone lenses and limestone olistoliths occur locally.



Figure 2.7. Outcrop of the Bobare Formation in Site GPS-348.

Bellizia & Rodriguez (1966, in LEV 2008) suggested a depositional environment of unstable shelf with sporadic transport, caused by turbidite currents, based on the scarce fauna and ripple marks. Macsotay (1972, in LEV 2008) considers the Bobare Formation to have accumulated in an epicontinental slope, under bathyal conditions combined with a dominant gravitational accumulation of terrigenous material.

The age of Bobare Formation has been the subject of discussion; it has been considered as of Early Cretaceous or Early Tertiary age, due to its confusing stratigraphic characteristics and relations with other units (Gonzalez de Juana et al., 1980). Barremian – Albian ages have been proposed from the few fauna reported by Macsotay et al. (1987, in LEV 2008). A hiatus has been interpreted to occur at the contact between the Bobare and Late Cretaceous Barquisimeto Formation; however, sometimes the relations reverse and the Barquisimeto Formation is found underlying the Bobare Formation with apparent concordance (LEV, 2008). Structural complications in the area may be responsible of these stratigraphic inconsistencies. Definition of the contact between Bobare and Mamey Formations (Figure 2.4) is not clear either and needs further study.

### **Agua Blanca Formation (Aptian?)**

The most representative lithology in the Agua Blanca Formation (Figure 2.5) is thickly bedded laminated limestones. Additionally, contorted phyllites, calcareous and feldspathic sandstones and conglomerates, the latter found at the base of the section, are usually found. It probably represents a shelf environment of shallow waters, with occasional contribution of terrigenous sediments (LEV, 2008). The advanced level of fragmentation and re-crystallization of the fossil content has complicated the determination of the age of the Agua Blanca Formation;

however, a probable Albian age was estimated by Renz & Short (1960, in LEV 2008). The unit lies unconformably over the Early Cretaceous(?) Araure Formation.

### **Aguardiente Formation (Albian)**

The Albian-age Aguardiente Formation (Figures 2.3, 2.5, 2.8) is composed of calcareous sandstones, intercalated with micaceous and carbonaceous shales and some limestones in the upper part. Some sandstones have such a high calcareous content that approximate sandy limestones (LEV, 2008). Its lower contact is with Apón Formation (Aptian – Albian, Figure 2.5), although near the Andes, the Aguardiente Formation overlies the conglomerates of the Río Negro Formation (Early Cretaceous). Also contacts with underlying La Quinta, Mucuchachí Formations and Iglesias Group are reported.



Figure 2.8. Outcrop of the Aguardiente Formation near Carora, Lara state. Site GPS-332, sample VMN-7.

### **Barquisimeto Formation (Cenomanian – Maastrichtian)**

The Barquisimeto Formation is generally composed of shales, siltstones, cherts, and limestones of dark colors (characteristic at the lower levels of the unit). Calcareous phyllites

associated with this unit indicate low degrees of metamorphism (LEV, 2008) and are found at site GPS-328 (Figure 2.9).

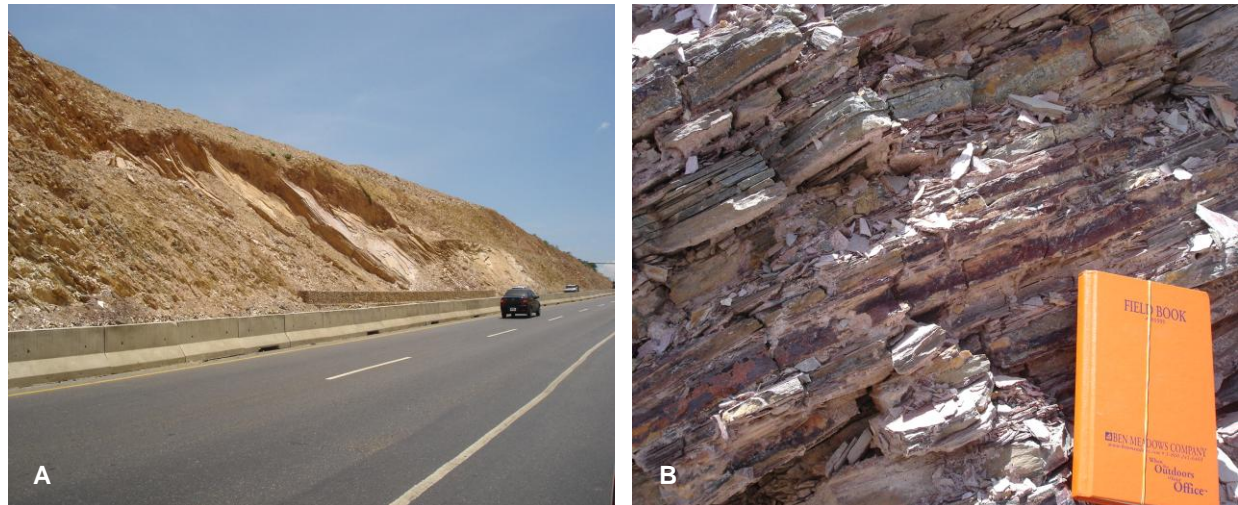


Figure 2.9. Barquisimeto Formation at site GPS-328 (sample VMN-4). (a) Outcrop view; (b) Phyllites.

This unit has been considered as part of an allochthonous block emplaced at the north of the Barquisimeto trough. Heterogeneities in the lithology exemplified by the presence of Cretaceous olistoliths and olistostromes (Gonzalez de Juana et al., 1980; LEV, 2008) support this idea. The unit has a transitional contact with the underlying sandy limestones of the Carorita Formation (of Lower Cretaceous age), although it can also be found through a hiatus overlying rocks from the Bobare Formation (Figure 2.5; LEV, 2008). Its upper contact is transitional with the Paleocene-Eocene Moran Formation or erosional with the Matatere Formation (Paleocene-Eocene).

## SANDSTONE PETROGRAPHY

Conventional petrographic analysis and counting of framework grains were performed for the siliciclastic samples of Aguardiente, Agua Blanca, Bobare, Barquisimeto, and Barranquín



Formations. The grain count data were consequently plotted in QtFLt (total quartz vs. Feldspar vs. total lithics), QmFLt (monocrystalline quartz vs. feldspar vs. total lithics) and QpLvLs (polycrystalline quartz vs. volcanic lithics vs. sedimentary lithics) provenance triangles. Detailed results from the petrography and modal grain count are presented in Appendix C.

### **Barranquín Formation**

Arenites and sublitharenites of the Barranquín Formation (samples VMN-32 through VMN-35) are both texturally and mineralogically mature (Figure 2.10). Sorting is excellent in these rocks, and the grains are usually very well rounded. The quartz content of these rocks is very high (Table 2.1), with the monocrystalline varieties representing about 98% of the quartz grains population versus 2% for the polycrystalline species (Figure 2.10). Feldspars are practically absent and, when their existence is suspected, they are altering to clay. Accessory minerals are also rare (up to ~2% of the grain framework) and are mainly represented by muscovite, biotite, zircon, leucoxene, tourmaline, rutile and sphene. A few fragments of quartzite and siltstone are also observed.

The sandstones of the Barranquín Formation are cement- and grain-supported. The cement is usually composed of silica and clay, filling pores and enveloping grains. The matrix is mostly represented by clay minerals (illite/smectite). Sutured contacts between grains, dissolution of matrix and grains, and deformed micas are evidence of pressure-solution effects during advance stages of diagenesis on these rocks.

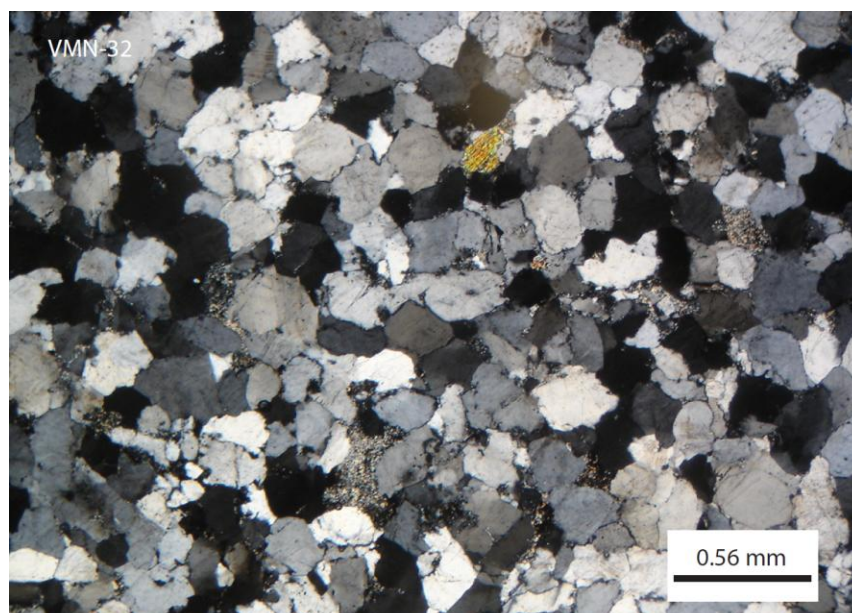


Figure 2.10. Quartz-arenite of Barranquín Formation. Sample VMN-32.

Table 2.1. General composition of samples of Barranquín Formation using modal analysis (values are in %).

		VMN-32	VMN-33	VMN-34	VMN-35
Framework grains	Quartz*	98.3	95.4	94.24	99.2
	Plagioclases	0	2.8	0	0
	K-Feldspar	0	0	1.43	0
	Micas	0.3	0	0.86	0.26
	Heavy minerals	0.56	0	1.43	0.26
	Sedimentary lithics	0.84	1.52	1.43	0.26
	Metamorphic lithics	0	0.25	0	0
	Volcanic lithics	0	0	0	0
	Alteration products	0	0	0.57	0
Whole rock	<b>Grains</b>	<b>90.5</b>	<b>90.16</b>	<b>88.54</b>	<b>91.04</b>
	<b>Cement</b>	<b>5.1</b>	<b>2.74</b>	<b>3.56</b>	<b>8.47</b>
	<b>Matrix</b>	<b>4.34</b>	<b>2.51</b>	<b>7.63</b>	<b>0</b>
	<b>Porosity</b>	<b>0</b>	<b>4.57</b>	<b>0.25</b>	<b>0.48</b>

(\*) Includes monocrystalline and polycrystalline species (chert, chalcedony and opal)

## Bobare Formation

Texturally and mineralogically mature samples (VMN-16 and VMN-17) collected from Bobare Formation were classified as quartz-arenites (Figure 2.11). They are rich in quartz (Table

2.2) and lack most of the relatively unstable elements in their framework (feldspars, lithic fragments, and other grains highly susceptible to weathering or alteration). Accessory minerals are usually zircon, tourmaline, sphene, leucoxene and pyrite. These sandstones are supported by cement, of either clay, hematite or quartz composition; the matrix is usually clay. The rocks of Bobare Formation have undergone processes related to the most advanced degrees of diagenesis. Pressure-solution is evidenced as dissolution of grains, sutured contacts between grains and deformation on ductile grains such as micas.

### **Agua Blanca Formation**

One sample of meta-sandstone (VMN-18) was collected from Agua Blanca Formation. This rock has a schistose texture (Figure 2.12) of quartz grains embedded in a fine grained matrix (secondary porphyroblastic texture). Quartz is the major component of these rocks (Table 2.3); monocrystalline species are about 88% of the grain population, while polycrystalline varieties are less than 3%. Feldspars are rare and, when present, are too altered to be differentiated into plagioclase or K-Feldspar.

Muscovite is the only identified mica in the sample of Agua Blanca Formation and, together with some heavy minerals such as zircon, leucoxene, sphene, rutile, tourmaline and hematite, represents about 10% of the rock framework. According to their nature and mineralogical composition, the rocks from Agua Blanca Formation are considered para-quartz-muscovite schists. Although these rocks have metamorphic texture, their mineralogical composition allows locating them within the quartzarenite field in the classification triangle for sandstones by Pettijohn et al. (1987).

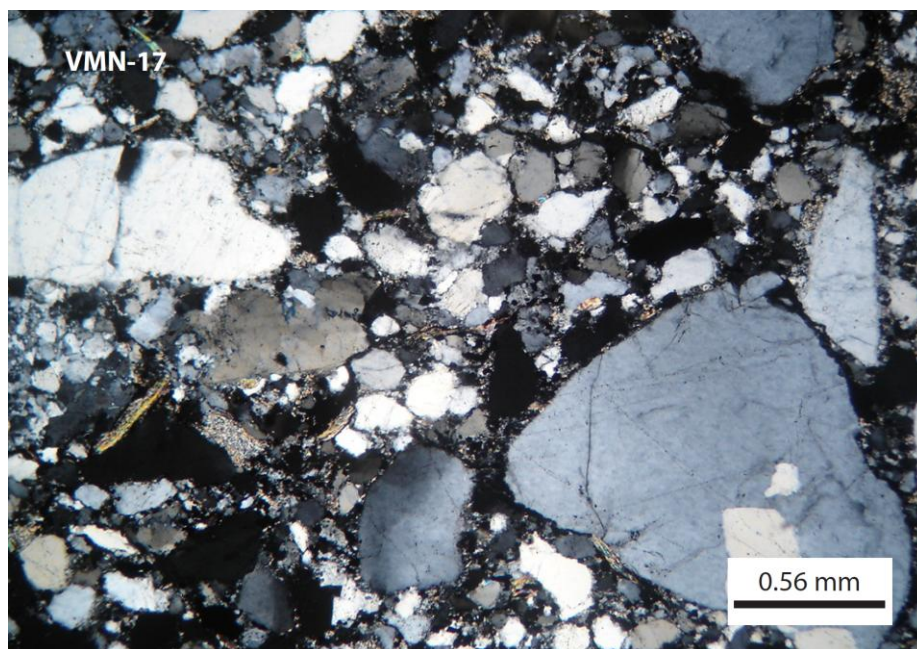


Figure 2.11. Quartz-arenite of Bobare Formation. Sample VMN-17.

Table 2.2. General composition of sandstones from Bobare Formation using grain count results (values are in %).

		VMN-16	VMN-17
Framework grains	Quartz*	94.6	94.5
	Plagioclases	0	0.64
	K-Feldspar	0.3	0
	Micas	2.85	2.9
	Heavy minerals	0.85	0.96
	Sedimentary lithics	0.3	0.96
	Metamorphic lithics	0	0
	Igneous lithics	0	0
	Alteration products	1	0
Whole rock	<b>Grains</b>	<b>78.3</b>	<b>59.5</b>
	<b>Cement</b>	<b>15.7</b>	<b>21.2</b>
	<b>Matrix</b>	<b>5.7</b>	<b>8.03</b>
	<b>Porosity</b>	<b>0.3</b>	<b>11.25</b>

(\*) Includes monocrystalline and polycrystalline species (chert, chalcedony and opal)



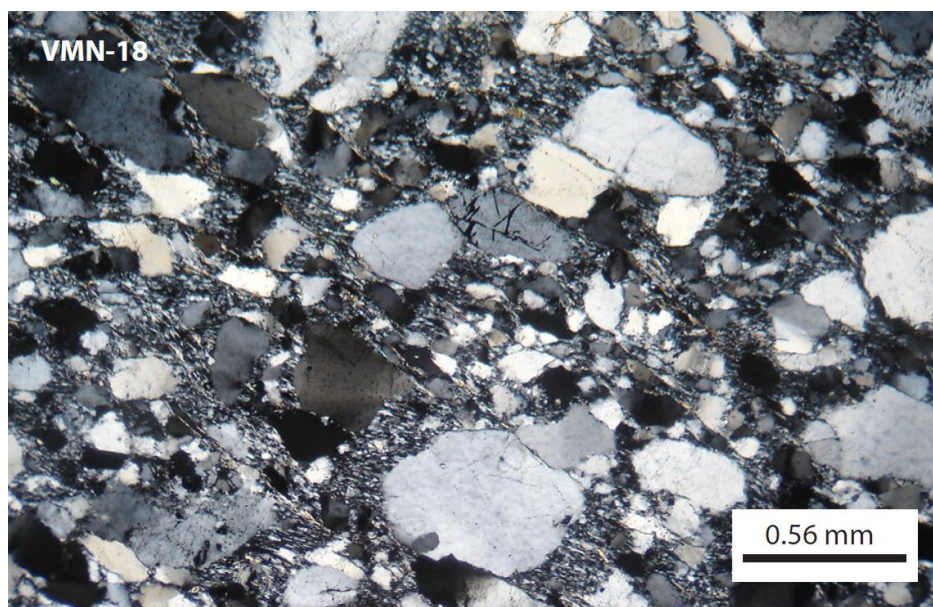


Figure 2.12. Meta-sandstone of Agua Blanca Formation. Sample VMN-18.

Table 2.3. General composition of meta-sandstones from Agua Blanca Formation using grain count results (values are in %).

		VMN-18
Framework grains	Quartz*	90
	Plagioclases	0
	K-Feldspar	0.3
	Micas	9
	Heavy minerals	0.6
	Sedimentary lithics	0
	Metamorphic lithics	0
	Igneous lithics	0
	Alteration products	0

(\*) Includes monocrystalline and polycrystalline species  
(chert, chalcedony and opal)

## Aguardiente Formation

One sample of sandstone (VMN-7, Figure 13) from the Aguardiente Formation was collected at the Carora area (Figure 2.8). This rock is quartz-rich (91.5% monocrystalline and 1.45% polycrystalline grains, Table 2.4), and its lack of feldspar and carbonates makes the rocks at this location different from other sandstones of the same unit in other areas close to the Merida

Andes, where both feldspathic and calcareous sandstones have been reported. Other components of the sandstones are accessory minerals including muscovite, zircon, hematite, pyrite, sphene and leucoxene, which together represent about 6% of the rock grain composition. This rock is a quartz-arenite according to Pettijohn et al. (1987).

Porosity in the sands of Aguardiente Formation is mostly of the secondary type, most probably as a result of dissolution of feldspars (given the square shape of the pores). Cement is the main support for the grains; it is often in the form of clays (illite/smectite, as rings or envelopes), quartz (as overgrowths) and Fe-oxides (as envelopes and filling pores). The matrix is practically absent but, when present, it is composed of clays (illite/smectite) and Fe-oxide. Diagenetic effects are indicated by the orientation of clays and polygonization of some quartz grains. Additionally, deformation of micas and overgrowth of quartz grains are indication of high levels of compaction and pressure-solution during an advanced diagenetic stage.

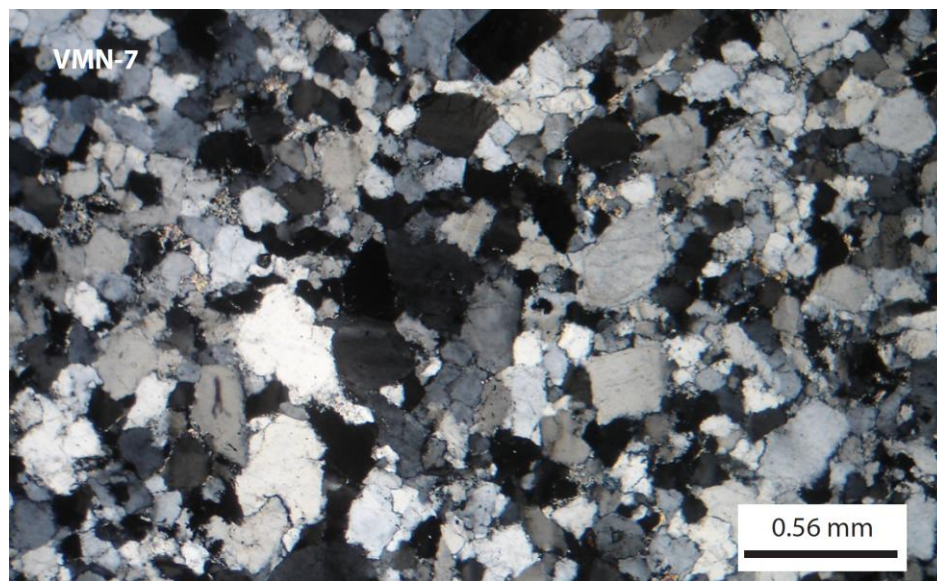


Figure 2.13. Quartz-arenite of the Aguardiente Formation. Sample VMN-7.

Table 2.4. General composition of sandstones from Aguardiente Formation using grain count results (numbers are in %).

		VMN-7
Framework grains	Quartz*	93
	Plagioclases	0
	K-Feldspar	0
	Micas	3.5
	Heavy minerals	2.6
	Sedimentary lithics	0
	Metamorphic lithics	0.29
	Igneous lithics	0
	Alteration products	0
Whole rock	<b>Grains</b>	<b>90</b>
	<b>Cement</b>	<b>6.82</b>
	<b>Matrix</b>	<b>0.26</b>
	<b>Porosity</b>	<b>2.88</b>

(\*) Includes monocrystalline and polycrystalline species (chert, chalcedony and opal)

## Barquisimeto Formation

At site GPS-328 (Figure 2.9), the Barquisimeto Formation is mostly represented by calcareous phyllites. Thin sections of sample VMN-4 show quartz crystals of sand size (up to 5%), deformed and embedded in a carbonate matrix (~94%, Figure 2.14). Crystals of pumpellyite as reported in LEV (2008) were not found. The protolith of this rock is interpreted as a sandy limestone that underwent low grade metamorphism. The mineral composition of this rock makes it unsuitable for detrital zircon analysis.

## Discussion

Sandy facies from the passive margin units under study are all compositionally and texturally mature. Their mineral content is basically quartz-rich and lack most, if not all, of the unstable mineral components. Feldspars are practically absent, probably due to tropical weathering rather than transport, given the proximity of the passive margin deposition centers from their potential source, the Guayana Shield.



Figure 2.14. Phyllite of Barquisimeto Formation. Notice advanced replacement of quartz (arrow) by calcite. Sample VMN-4.

Results from grain count, using the method of Dickinson (1985), relate all the units to a continental setting (Figure 2.15). Sandstones from the Barranquín Formation have a secondary orogenic influence that is reflected in a low content of sedimentary lithics (Table 2.1), and may be linked to a Hauterivian subsidence event preceded by a Late Jurassic uplift along the northeastern Venezuelan margin, due to a change in the movement between the North American and South American-African plates (Erikson & Pindell, 1998b).



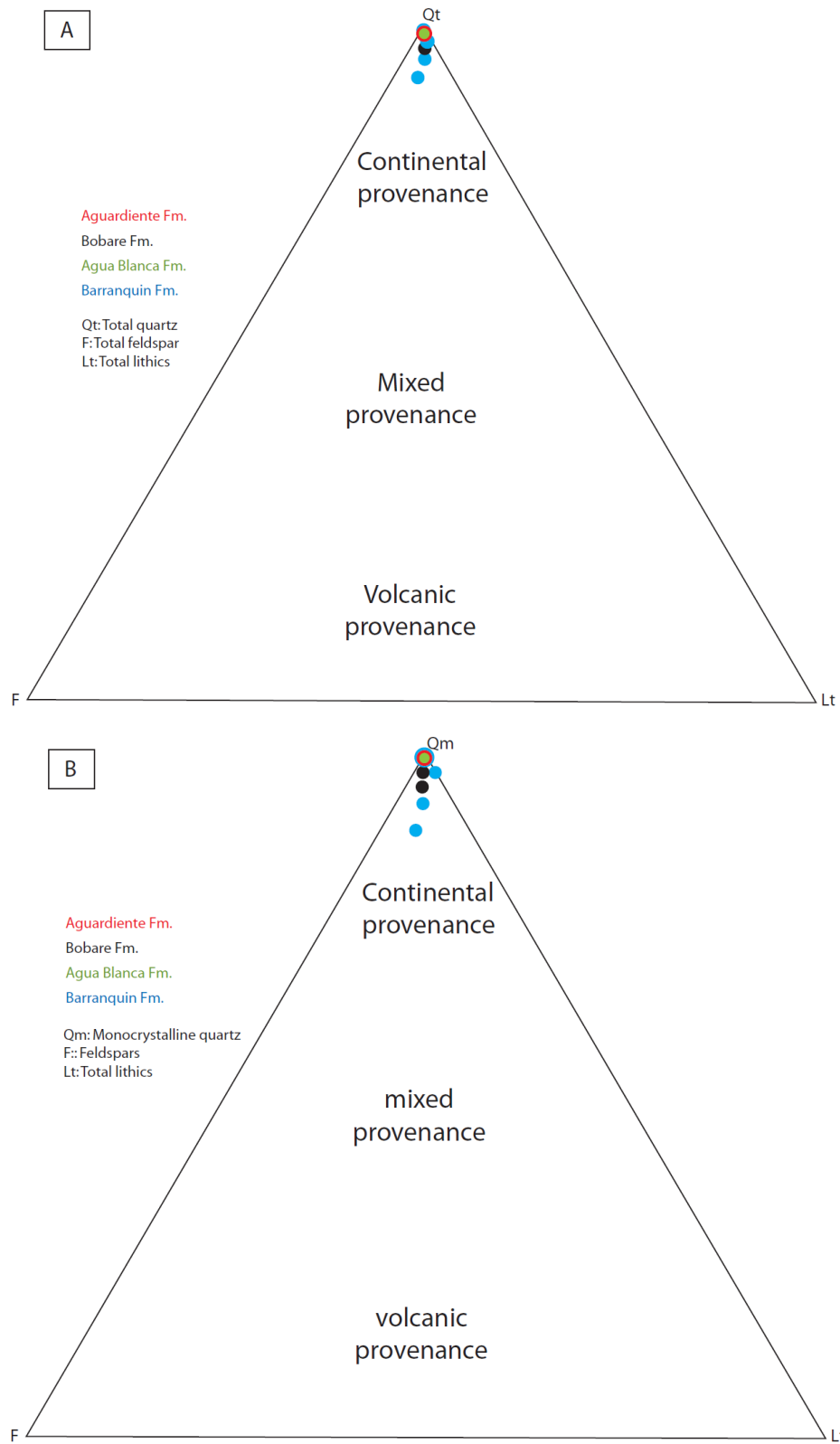


Figure 2.15. Provenance of passive margin samples (modified after Dickinson, 1985).

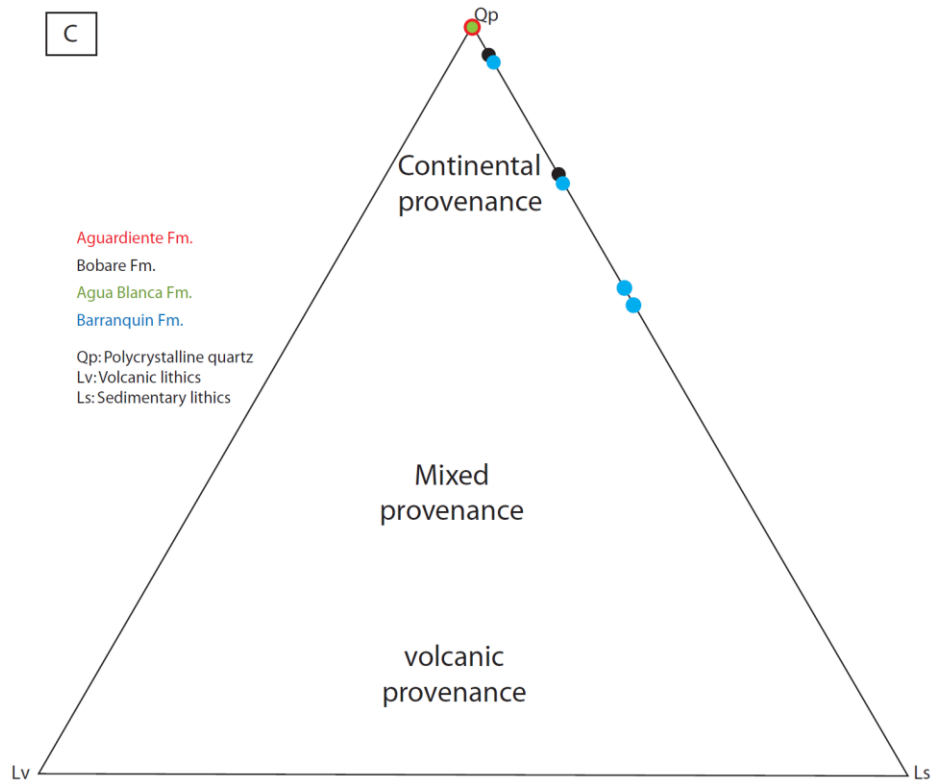


Figure 2.15 (cont.). Provenance of passive margin samples (modified after Dickinson, 1985).

## DETRITAL ZIRCON AGES

LA-ICP-MS U-Pb detrital zircon ages of each analyzed sample are presented in Appendix D. Histograms were generated to plot the distribution of these ages for each unit (Figures 2.16, 2.17, 2.18 and 2.19).

### Barranquín Formation

Detrital zircon ages for the rocks of Barranquín Formation range between  $427 \pm 4.1$  Ma (Silurian) and  $2731 \pm 26.7$  Ma (Late Archean). The histogram of Figure 2.16 shows the distribution of ages of two samples of the Barranquín Formation. These ages tend to group into 4

time slots: Archean (~2700 Ma), Early Proterozoic (major peaks at ~1815 and 1516 Ma), Middle Proterozoic (1019 – 1218 Ma) and Cambrian to Silurian (~500 Ma).

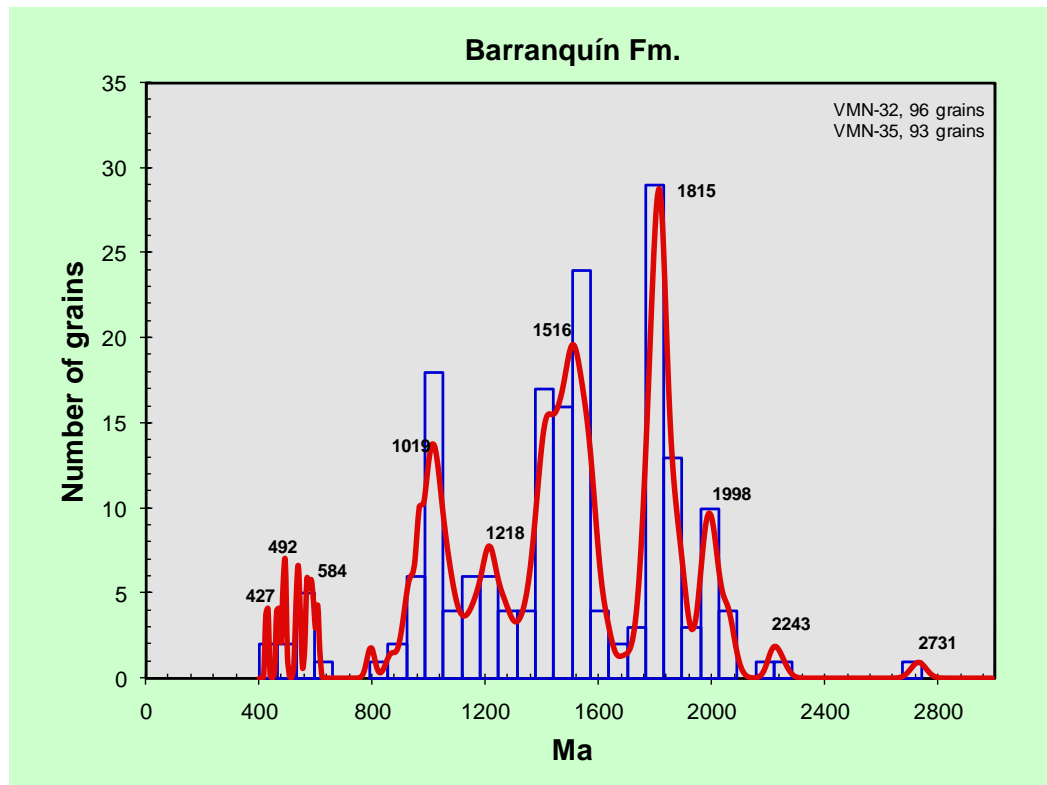


Figure 2.16. Age distribution of detrital zircons from Barranquín Formation.

### Bobare Formation

The oldest and youngest zircon grains of Bobare Formation are about  $2151 \pm 35.3$  Ma (Early Proterozoic) and  $451 \pm 4.4$  (Ordovician) Ma, respectively (Figure 2.17). The majority of zircon grains are of Proterozoic age (peaks occurring at 965 Ma, 1535 and 1812 Ma); the rest have Ordovician (453 Ma) or Neo-Proterozoic (~635 Ma) ages.

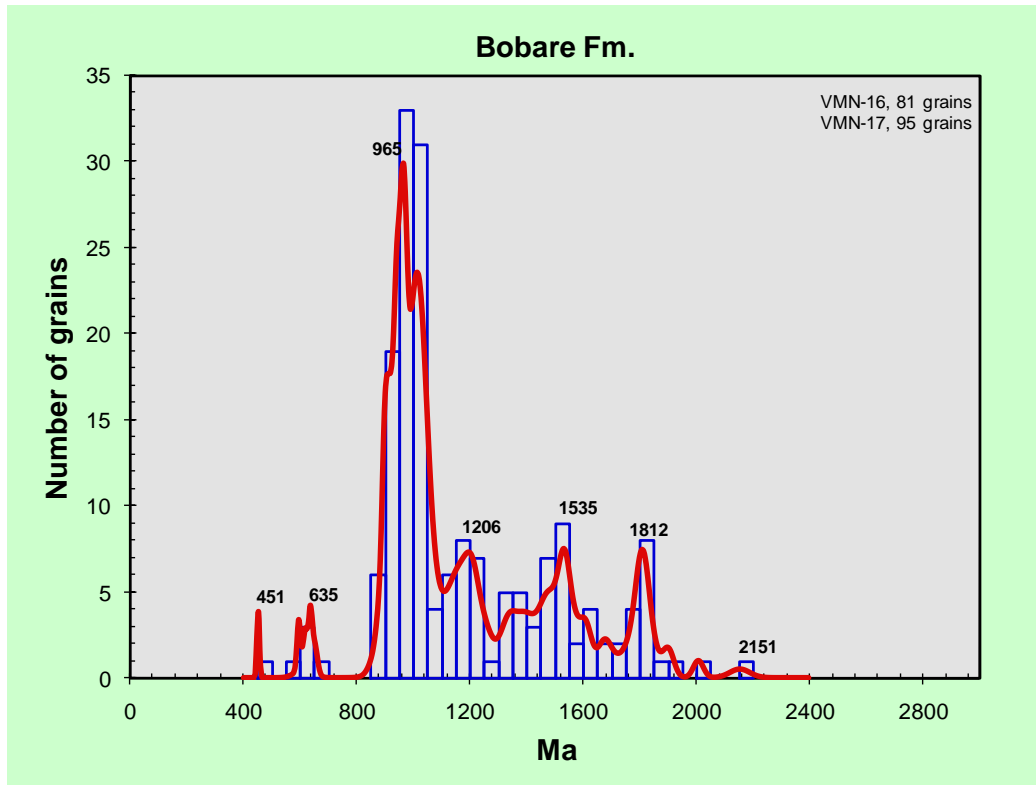


Figure 2.17. Age distribution of detrital zircons of Bobare Formation.

### Agua Blanca Formation

Detrital zircon grains of Agua Blanca Formation yield Early Proterozoic to Cambrian ages ( $2134 \pm 18.0$  Ma to  $491 \pm 6.7$  Ma). Major peaks are from Proterozoic grains (1435 Ma, 1812 Ma, and 1988 Ma, Figure 2.18).

### Aguardiente Formation

Ages from ninety four (94) detrital zircon grains from one sample of Aguardiente Formation were analyzed (Figure 2.19). These grains are as old as  $2719 \pm 24.6$  Ma (Late Archean) and as young as  $415 \pm 4.1$  Ma (Silurian). The largest peaks occur at Proterozoic (around 1814 Ma and 1439 Ma) and Silurian (422 Ma) times.



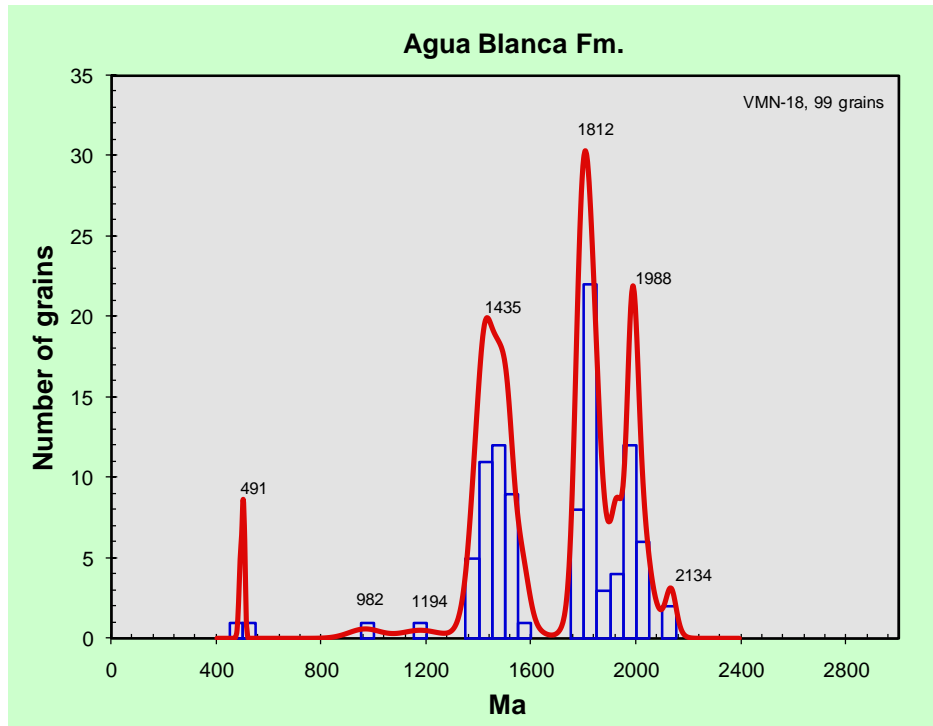


Figure 2.18. Age distribution of detrital zircons of the Agua Blanca Formation.

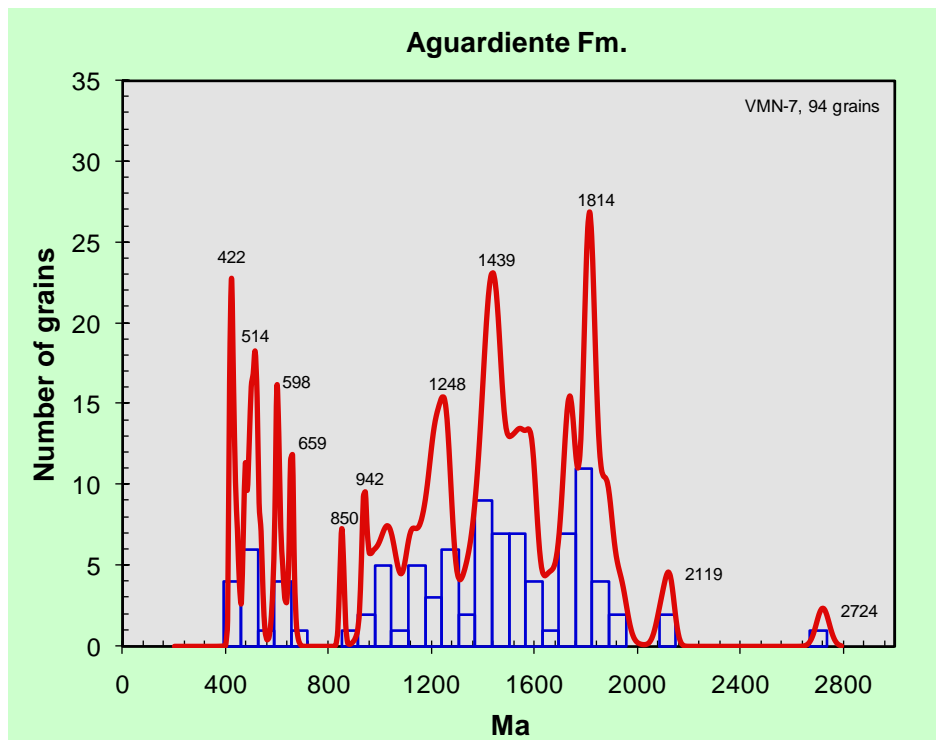


Figure 2.19. Age distribution of detrital zircons, Aguardiente Formation.

## Barquisimeto Formation

Due to the mineral composition of these rocks, no samples were analyzed for U-Pb detrital zircon geochronology in the Barquisimeto Formation.

## Discussion

In general, detrital zircon ages from the Barranquín, Bobare, Agua Blanca and Aguardiente Formations show similar distribution patterns. The data as a whole plot in three major age intervals (Figure 2.20): Early to Middle Proterozoic (~2200 – 1400 Ma), Late-Middle Proterozoic (1200-900 Ma) and Late Proterozoic to Silurian (669 – 422 Ma). A fourth, minor age interval is present at about 2700 Ma (Late Archean), and is only observed in the detrital fraction of the Bobare and Agua Blanca Formations (Figures 2.17 and 2.18).

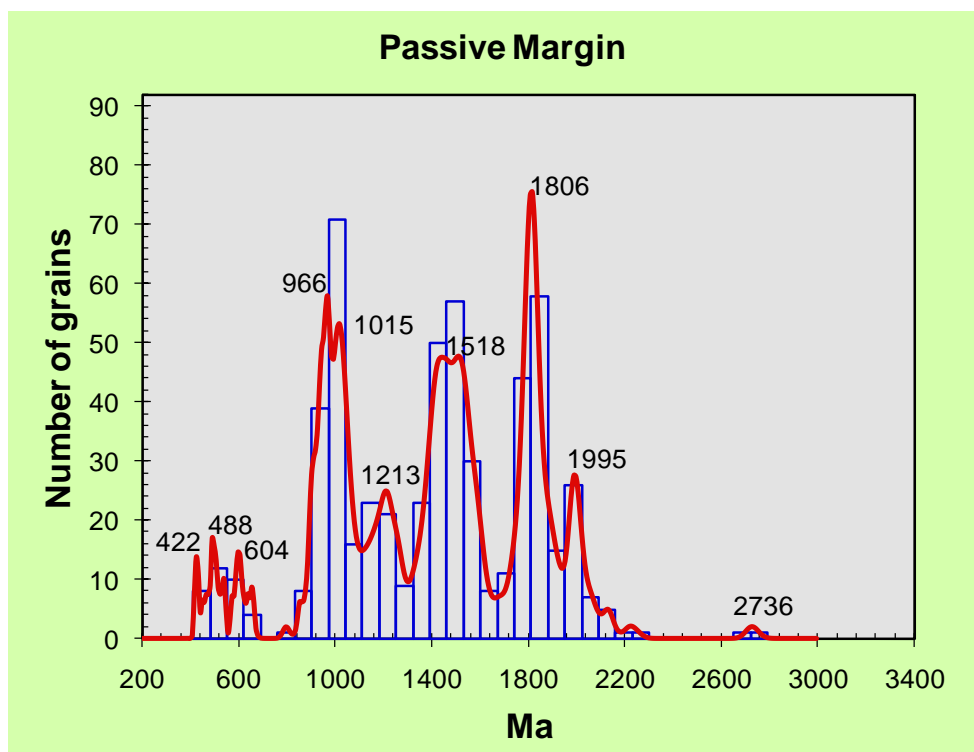


Figure 2.20. General age distribution of detrital zircon grains from the passive margin (Barranquín, Agua Blanca, Bobare and Aguardiente Formations combined).

Probably the most remarkable result from the passive margin data is the existence of detrital zircons with ages ranging between 1213 Ma and 966 Ma (Figure 2.20). Rocks of these ages have been reported in South America (Sunsás Belt), Central America (Oaxaquia Belt), and North America (Grenville Belt), (Rogers & Santosh, 2004), and are related to the origin of Rodinia during the Grenvillian Orogeny (1.33 – 0.98 Ga, Schneider Santos et al., 2003); (Figure 2.21). However, and not until very recently (Ruiz et al., 1999; Cordani et al., 2005; Molina et al., 2006), existence of rocks related to this event had not been confirmed in the areas of northern South America proximal to Colombia or Venezuela.

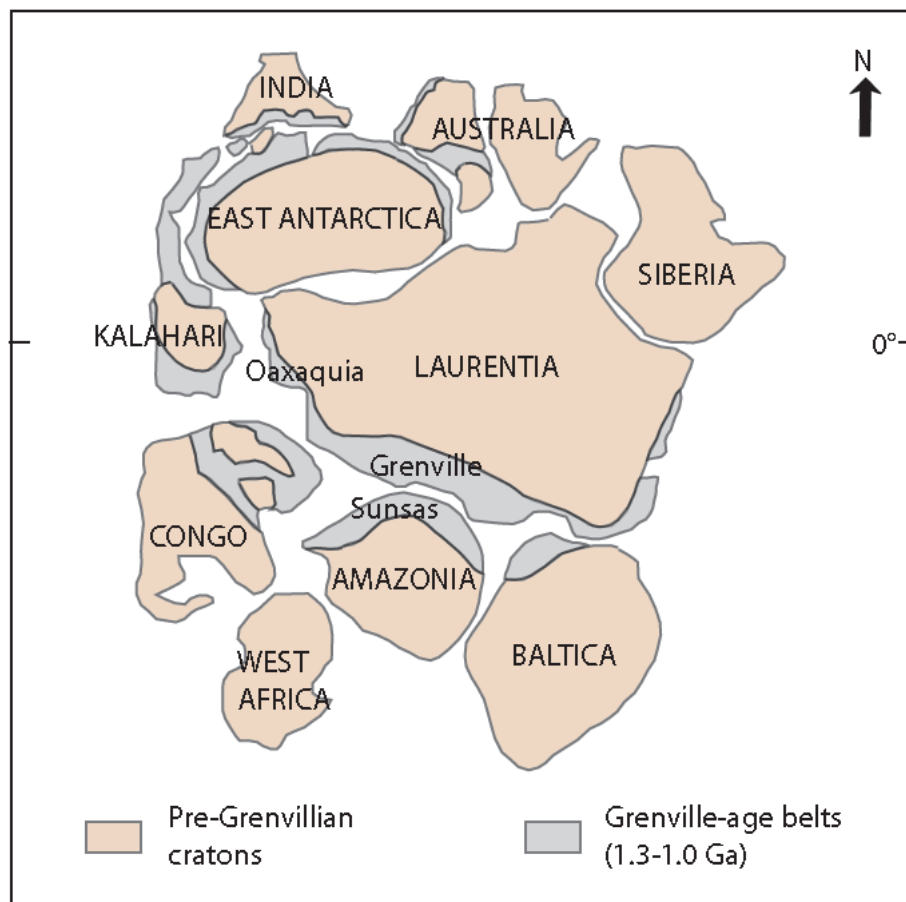


Figure 2.21. Distribution of Grenville-age belts during the formation of the super-continent Rodinia (1.3 – 1.0 Ga). Adapted after Kroner & Cordani (2003).

Kolmogorov-Smirnoff (K-S) statistical tests were performed to compare the cumulative distributions of zircon ages between the passive margin samples. Distances between the samples (D-values, Figure 2.22) represent the maximum difference between the Cumulative Distribution Functions (CDFs), and are related to the probability that the samples come from the same population (Guynn, 2006). For instance, small values of D from two distributions of detrital zircon ages will result in a high probability (P-value) that the samples under comparison were shed from the same or a similar source. The Figure 2.22 shows the pattern of the CDF for each sample, while Tables 2.5 and 2.6 show the P and D values for each separate comparison.

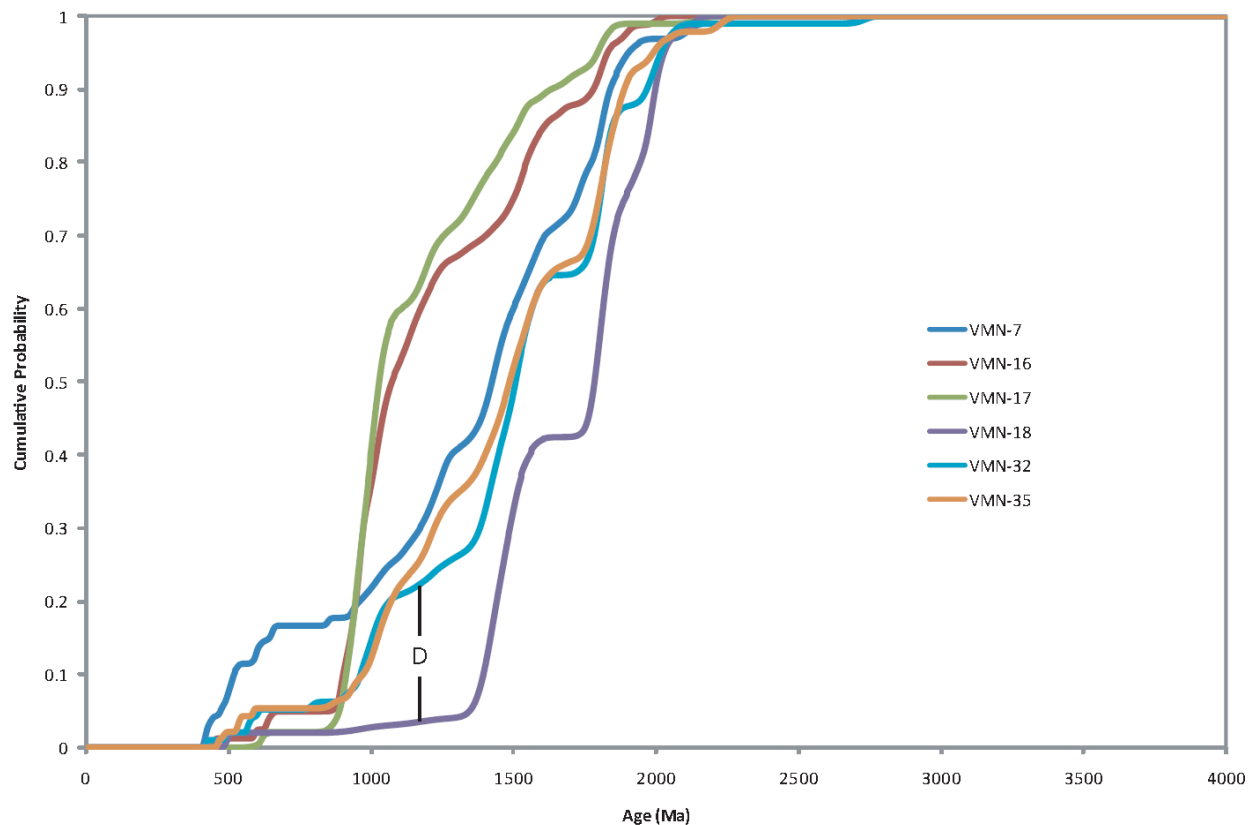


Figure 2.22. Cumulative Distribution Functions (CDFs) for the detrital zircon ages in samples from passive margin units: Aguardiente (VMN-7), Bobare (VMN-16 and 17), Agua Blanca (VMN-18) and Barranquín (VMN-32 and 35) Formations.

Table 2.5. Probability values for comparison of passive margin samples using the Kolmogorov-Smirnoff test.

K-S P-values using error in the CDF						
	VMN-7	VMN-16	VMN-17	VMN-18	VMN-32	VMN-35
VMN-7		0.001	0.000	0.000	<b>0.240</b>	<b>0.533</b>
VMN-16	0.001		<b>0.848</b>	0.000	0.000	0.000
VMN-17	0.000	<b>0.848</b>		0.000	0.000	0.000
VMN-18	0.000	0.000	0.000		0.014	0.000
VMN-32	<b>0.240</b>	0.000	0.000	0.014		<b>0.847</b>
VMN-35	<b>0.533</b>	0.000	0.000	0.000	<b>0.847</b>	

Table 2.6. D-values between compared Cumulative Distribution Functions.

D-values using error in the CDF						
	VMN-7	VMN-16	VMN-17	VMN-18	VMN-32	VMN-35
VMN-7		0.301	0.341	0.372	0.149	0.117
VMN-16	0.301		0.093	0.634	0.411	0.344
VMN-17	0.341	0.093		0.693	0.470	0.383
VMN-18	0.372	0.634	0.693		0.225	0.313
VMN-32	0.149	0.411	0.470	0.225		0.089
VMN-35	0.117	0.344	0.383	0.313	0.089	

According to this analysis, zircon age CDFs for samples from the same unit are expected to share almost identical patterns and to separate along very small distances of cumulative probability. As a consequence, P-values should be high (close to 1). Samples from Bobare (VMN-16 and VMN-17) and Barranquín (VMN-32 and VMN-35) Formations are obvious examples of this situation (Figure 2.22, Tables 2.5 and 2.6).

The cumulative distribution functions (CDFs) for samples of the Bobare Formation (maroon and green lines, Figure 2.22) are separated from other samples, probably indicating that zircons from Bobare Formation were shed from a different source than the other units.

Young grains (i.e. < 875 Ma) from Aguardiente Formation seem to have a separate source from the other units, as its CDF (navy blue line) has a very high D-distance from other functions

at the same age interval. However, older grains (>875 Ma) seem to share common characteristics with samples of Barranquín Formation.

The cumulative distribution line for zircons from Agua Blanca Formation (VMN-18, Figure 2.22) shows noticeably high D-separations from samples of other units, probably as an indication of a completely different origin

Differences between the CDFs seem to correlate with the petrographic results. Samples of Aguardiente and Barranquín Formations share more common textural and mineralogical characteristics than the meta-sandstones of Agua Blanca Formation and the quartz arenites of Bobare Formation. The sandstones of both Aguardiente and Barranquín Formations seem to be more mature than the rocks of the other units, probably offering an indication of different sources rather than a variation in sediment transportation processes.

## **PROVENANCE OF THE CRETACEOUS PASSIVE MARGIN**

Sandstones of Barranquín, Aguardiente, Bobare and Agua Blanca Formations are texturally and mineralogically mature and are consistent with a continental passive margin setting. Results from petrography and modal count support this information and add a secondary orogenic influence (Figure 2.15), reflected by the minor content of lithic fragments and polycrystalline quartz grains in some of the samples.

Additionally, LA-ICP-MS U-Pb detrital zircon data indicate ages that range from Silurian to Late Archean times for the detrital fraction of these units (Figure 2.20). Ages are grouped into three time-intervals: Early to Middle Proterozoic (2119 – 850 Ma), Late Proterozoic to Silurian (669 – 422 Ma) and Late Archean age (2.7 Ga), the latter being only observed in Aguardiente and Barranquín Formations. This distribution of ages probably indicates the existence of at least

three different sources for the sediments that accumulated along the passive margin. Such sources should have been originated in a continental setting, as previously discussed.

During Early Cretaceous times, siliciclastic sedimentation in transitional to shallow marine environments occurred in north Venezuela (Yoris & Ostos, 1997; Erikson & Pindell, 1998a), (Figure 2.3). Elevated areas were located in the south (Guayana Shield) and west (Santa Marta and Santander Massifs in Colombia) of Venezuela, and probably represent sources that fed the area north of the Guayana Shield during the passive margin stage. The following paragraphs will describe the potential rocks that may have contributed to the sediments forming the Early Cretaceous passive margin sequences under study.

### **Pre-Cambrian rocks**

Precambrian terranes are found in Venezuela (Guayana Shield, Apure Basin basement) and Colombia (Sierra Nevada of Santa Marta, Santander massif), (Figure 2.23; Yoris & Ostos, 1997). The Guayana Shield is the oldest and most extended terrane; it outcrops in the countries of Guyana, Suriname, Brazil and Colombia. In Venezuela, it has been divided in four provinces (Imataca, Pastora, Cuchivero, and Roraima; Figure 2.23), each one is associated with a regional-scale magmatic/deformational event. Published ages of these provinces are listed in Table 2.7.

The oldest detrital zircons (1500 Ma and older) of the passive margin units (Figure 2.20) correlate very well with rocks from the Guayana Shield. Grains that are approximately 2700 Ma old can be related to the crystalline rocks from the Imataca Complex, while age peaks of 1995 Ma and 1806 Ma are diagnostic of the Cuchivero and Roraima provinces respectively. On the other hand, zircons with ages near 1500 Ma are interpreted to be diagnostic of the Parguazan province (Goldstein et al., 1997).

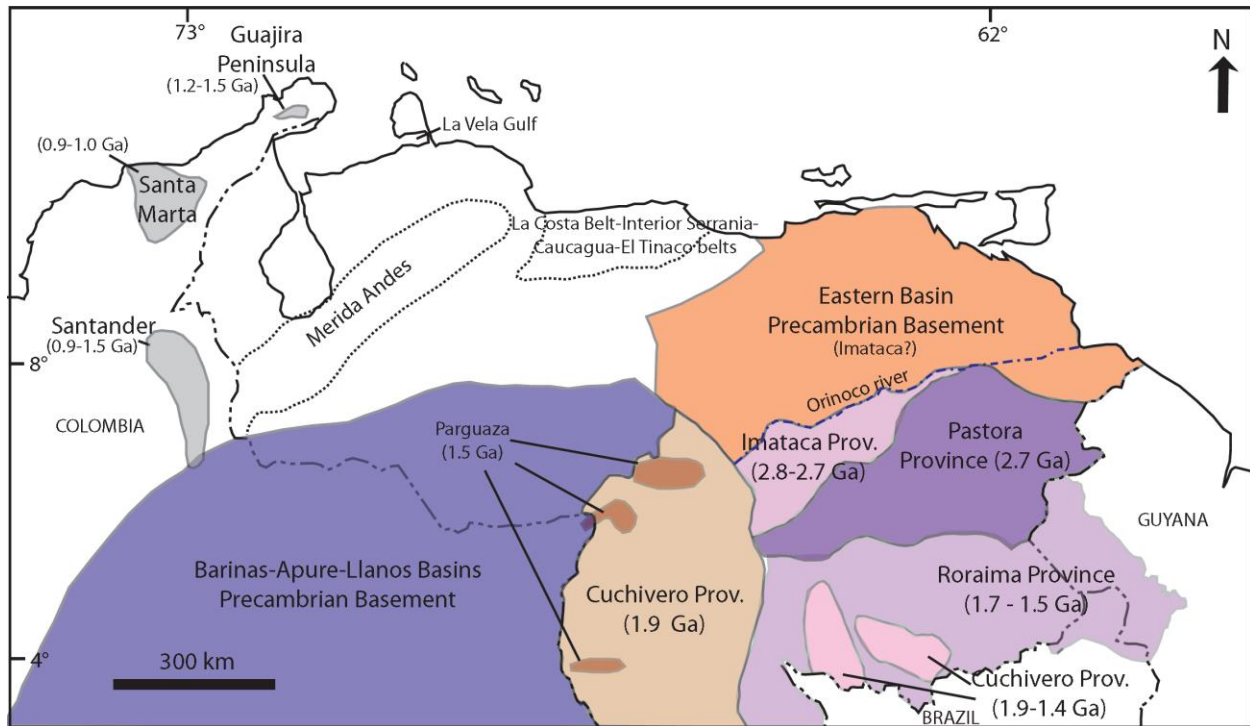


Figure 2.23. Precambrian terranes in Venezuela and Colombia. Allochthonous terranes are in grey. Ages are based on published U-Pb zircon ages (adapted after Yoris & Ostos, 1997).

Zircon U-Pb ages of 1.2 – 0.9 Ga are reported in metamorphic belts in Colombia (Sierra Nevada de Santa Marta and Santander massifs, and Guajira Peninsula; Ruiz et al. 1999, Cordani et al. 2005, Molina et al., 2006; Table 2.8), and from river sediments in southern Venezuela (Orinoco river and tributaries; Goldstein et al., 1997; Cordani et al., 2005; Bizzi, 2005).

Ages and metamorphic evolution of these rocks are comparable to Proterozoic belts in Mexico (Oaxaquia, Ruiz et al., 1999; Keppie & Ortega-Gutierrez 1999) and Central Andes (Sunsás, Cordani et al. 2005, Molina et al. 2006, Chew et al. 2007). Consequently, the Proterozoic domains encountered in Colombia can be considered as fragments of a larger collisional belt (probably Sunsás), related to the juxtaposition of the Western Amazonian Craton with Laurentia in Meso-Proterozoic times (Figure 2.21; Kroner & Cordani, 2003; Molina et al., 2006).



Table 2.7. Reported ages of the Precambrian provinces of the Guayana Shield.

Province	Unit	Age (Ma) / Method		Reference	Orogenetic Event
Parguaza Batholith	Parguaza Granite	1550 - 1450	U-Pb	Goldstein et al., (1997)	
		1490	Rb-Sr	Gonzalez de Juana et al. (1980)	
		1545 ± 20	U-Pb	LEV (2009)	
		1590	(zircon)		
Roraima - Uatuma Group - Rio Negro - Juruena Belt	Roraima, Rio Negro - Juruena	2000 - 1500	U-Pb	Goldstein et al., (1997)	Transamazonian
		1600 - 1520	U-Pb (zircon)	Schneider Santos et al., (2003)	
	Roraima Group (Venezuela, Brasil, Guyana, Surinam)	1593 ± 66	Rb-Sr	Gonzalez de Juana et al. (1980)	
		1599 ± 18	?		
		1603 - 1699	?	Schneider Santos et al., (2003)	
		1782 ± 3	U-Pb (zircon)	LEV (2009)	
Cuchivero	?	1900 -1400	?	Yoris & Ostos (1997); Ostos et al. (2005)	Transamazonian
	Caicara Fm.	1850 1975	Rb-Sr	Gonzalez de Juana et al., (1980)	
		1990 - 1950	U-Pb (zircon)	Schneider Santos et al., (2003)	
	Burro Burro Group (Guyana)	1815-1980	?	Gonzalez de Juana et al., (1980)	
	Cuchivero Group	2100-1900			
Pastora	"Young plutons"	1300 1419 1510	K/Ar	Gonzalez de Juana et al., (1980)	Orinocan / Nickerian
		Supamo Complex	2100		Rb-Sr
	2817 ± 57 2660 ± 30		Rb-Sr U-Pb	LEV (2009)	
	?	2700 - 2000	Rb-Sr, U-Pb	Gonzalez de Juana et al., (1980)	
		2700 - 2000	?		
	Imataca	Imataca Complex	2250 - 2080	?	Yoris & Ostos (1997); Ostos et al. (2005)
2700 - 2800			U-Pb	Goldstein et al., (1997)	
2100 2700			?	Gonzalez de Juana et al., (1980)	
2153 2900			Rb-Sr	LEV (2009)	
3500-3600			Rb-Sr, U-Pb	Gonzalez de Juana et al., (1980)	

Table 2.8. Proterozoic units of the collision belts of Eastern Colombia.

Belt	Unit	Age (Ma)	Reference
Sierra Nevada of Santa Marta	Dibulla Gneiss	1081 ± 14 991 ± 12 930 ( <sup>207</sup> Pb/ <sup>206</sup> U) (Ar-Ar)	Cordani et al. (2005)
	Sevilla Complex	1380 - 1120 614 ± 13 732 ± 16 ( <sup>206</sup> Pb/ <sup>238</sup> U)	Molina et al. (2006)
Santander Massif	Bucaramanga Gneiss	1550 - 900 (U-Pb SHRIMP)	Cordani et al. (2005)
Guajira Peninsula	Jojoncito Gneiss	1529 ± 43 1342 ± 25 1236 ± 16 ( <sup>207</sup> Pb/ <sup>206</sup> Pb)	Cordani et al. (2005)

No outcropping rocks of 1.2 – 0.9 Ga in age have been reported in Venezuela. Nevertheless, geochronological evidence from modern fluvial sediments in Guayana (Goldstein et al. 1997, Cordani et al. 2005, Bizzi 2005) and petrographic studies of rocks from the basement of La Vela Gulf (Figure 2.23; Grande et al. 2007) point to the existence of a “Grenvillian” basement in, or near, Western Venezuela. Gneisses 1200 Ma old have also been reported in the Guajira Peninsula (Irving 1971, in Priem et al., 1986). Other evidence of a Grenvillian collision are seen in metamorphic rocks from the Guayana Shield, which record a deformation event (Nickerian/Orinocan orogenesis) that affected older rocks (Chew et al. 2007; Mendoza, 2005). In summary, the probable existence of rocks of this age in the basement of northwestern Venezuela is not precluded; however, more study is needed.

The “Grenville” signature observed in the passive margin detrital zircons (Figure 2.20) supports the idea of the existence of a 980-1200 Ma exposed basement in the nearest areas to the deposition centers during Early Cretaceous times. The most likely source is located in the Eastern Cordillera of Colombia (Santander and Santa Marta massifs), as previously proposed by Cordani et al. (2005). Grenville-age distributions of zircons from Colombia and the Orinoco River are remarkably similar to those from the passive margin units in Venezuela (Figure 2.24),

and suggest that 0.9 – 1.2 Ma crystalline rocks from Eastern Colombia were responsible for a fraction of the sediments shed to the Venezuelan passive margin basins during Early Cretaceous time.

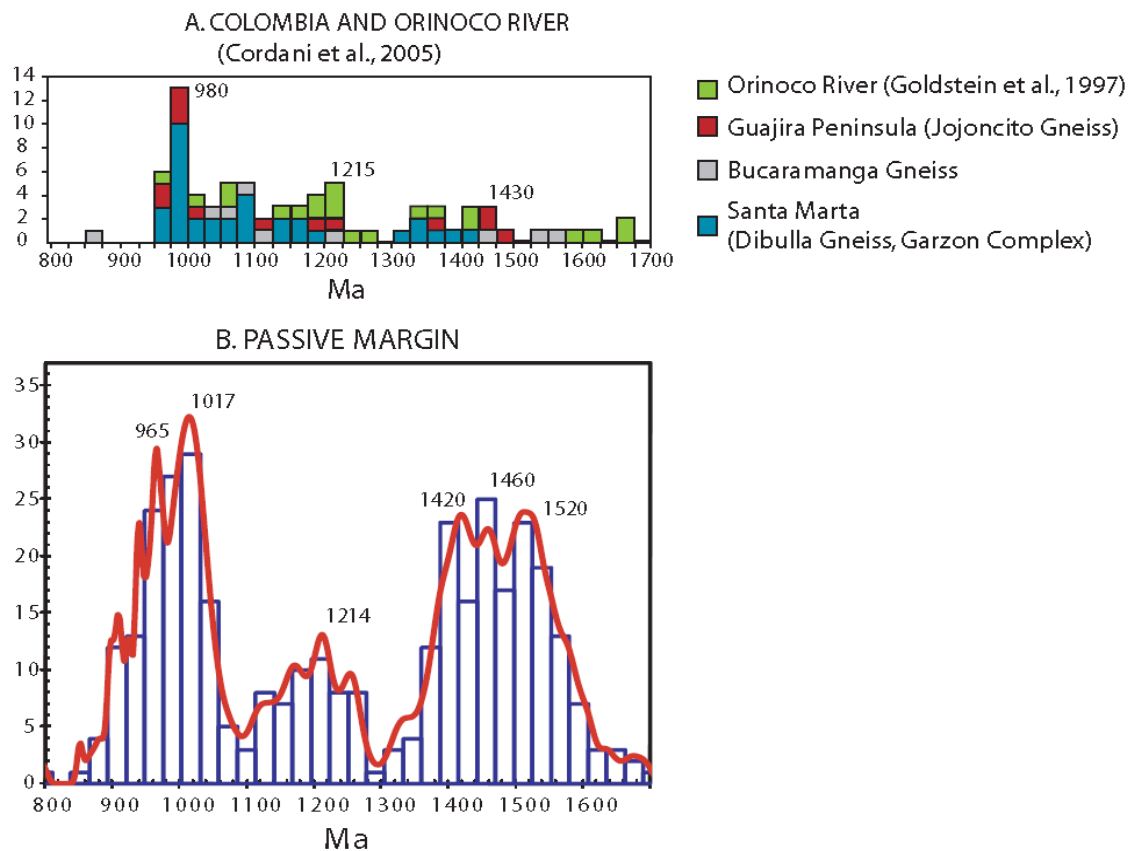


Figure 2.24. Distributions of U-Pb detrital zircon ages for the time interval between 800 Ma and 1700 Ma. A) Colombia and Orinoco River (Goldstein et al., 1997; Cordani et al., 2005). B) Passive margin units.

U-Pb detrital zircons ages ranging 633 - 605 Ma identified from the passive margin samples may correspond to intrusive rocks from the Iglesias Complex or the Bella Vista Association in the northern Merida Andes, which had reported U-Pb zircon ages of 595 Ma and 585 – 660 Ma respectively (Gonzalez de Juana et al., 1980). Other rocks in Venezuela with

similar ages are located in allochthonous belts (La Costa Range, Interior Serranía, Caucagua- El Tinaco; Figure 2.23) accreted to the Guayana Shield (Sisson et al., 2005).

## Paleozoic rocks

Paleozoic autochthonous terranes are found only in the subsurface in the Barinas-Apure and Eastern Basins (Figure 2.25; Early Cambrian Hato Viejo and Devonian Carrizal Formations). These rocks are syn-rift red beds typical of Gondwana and Laurentia (Pimentel de Bellizzia, 1992 in Ostos et al. 2005).

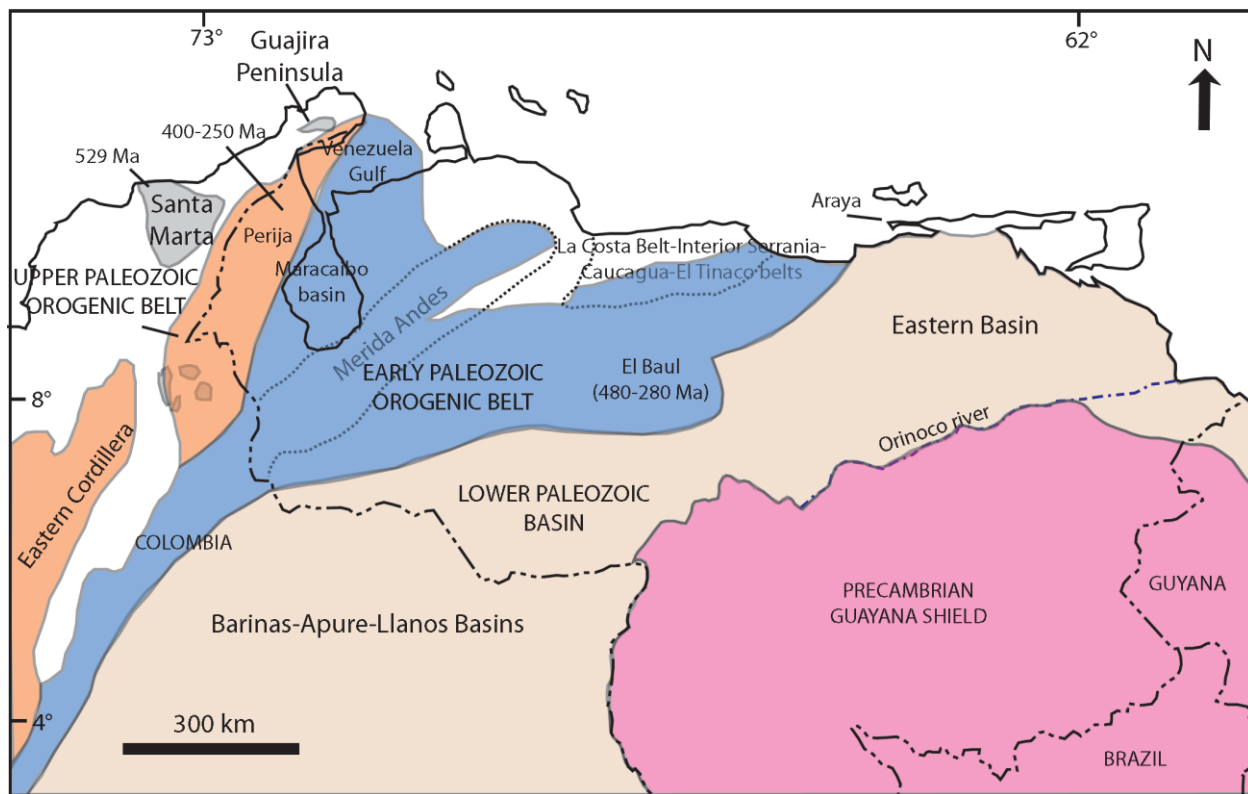


Figure 2.25. Paleozoic provinces in Venezuela and Colombia. Ages correspond to published U-Pb zircon data (modified after Yoris & Ostos, 1997).

Allochthonous Paleozoic terranes accreted to the northern portion of South America are of Early Paleozoic, Late Paleozoic and Mesozoic ages (Yoris & Ostos, 1997). Early Paleozoic rocks include Ordovician metamorphosed granitic and shelf-slope sedimentary rocks in the basement of the Maracaibo Basin and in the Andes, and Devonian rocks in the Perijá Mountains. Late Paleozoic terranes are represented by granitic rocks of the El Baúl massif (Permian), the subsurface of Eastern, Barinas-Apure and Maracaibo Basins (Carboniferous age), and sequences outcropping in the Perijá and Andes mountains (Carboniferous and Permian age). In the Caribbean Mountain System (from Guajira to Araya Peninsulas, including the basement of the Gulf of Venezuela and La Costa Cordillera, Figure 2.25) rocks of Devonian to Permian age are also found.

Published geochronologic data of the Paleozoic rocks in Venezuela and Colombia is summarized in the Table 2.9. Age information about the autochthonous basement in the Llanos and Barinas-Apure basins (Figure 2.25) is currently reduced to a number of reports based on old data released from the oil companies (i.e. Feo-Codecido et al., 1984). However, the dating methods applied on these studies (K-Ar, Rb-Sr) usually register the last thermal event, adding uncertainty to the determination of the initial crystallization age of the mineral grains.

The detrital zircon data from the passive margin units indicate sources with ages between Cambrian-Ordovician (488 Ma) and Silurian-Devonian (415-422 Ma) times. The Cambrian granitic units of the El Baúl Massif (El Baúl Granitic Suite) and probably plutonic bodies in the Merida Andes such as the Cerro Azul Granite are the potential sources.

Table 2.9. Ages of Paleozoic rocks in Venezuela and Colombia

Belt	Unit	Age (Ma) / Method		Reference
Paraguana Peninsula	El Amparo metagranodiorite	262-265	U-Pb (Sphene)	Grande (2005)
Perija and Guajira Peninsula Region	Toas Island granite	252 ± 50	U-Pb SHRIMP	Molina et al. (2006)
	Lajas Granite	310-385	U-Pb (zircon)	Dasch (1982)
	Siapana Granodiorite	456 ± 9.7		
El Baul Region	Segoviera Rhyolite	283.3 ± 2.5	U-Pb SHRIMP	Viscarret et al. (2007)
	Corcovado Rhyolite	286.4 ± 2.8		
	El Baul Granitic Suite	289 ± 2.9		
		294.1 ± 3.1		
		493.8 ± 5.2		
Sierra Nevada of Santa Marta	Sevilla Complex	529 ± 16	U-Pb SHRIMP	Molina et al. (2006)
Merida Arch and Caparo Block	Cerro Azul granite	400 ± 7	K-Ar	LEV (2009)
	Soledad granite	299 ± 5	?	
		475 ± 65		
	Bella Vista Association	460 ± 15	K-Ar	

In summary, the mature sediments of the Lower Cretaceous passive margin units have a detrital zircon signature that indicates a clear Guayana Shield provenance (2.7 – 1.5 Ga). Additionally, abundant grains show unexpected “Grenville ages” ranging 980-1200 Ma that may indicate Andean sources (Santa Marta and Santander Massifs). Younger grains are Early and Middle Paleozoic in age and correlate with the plutons of El Baúl Massif and Andean rocks, respectively. No Triassic or Jurassic grains were identified in the passive margin samples.

Similarities in the detrital zircon data (Figure 2.22) for grains older than 875 Ma in the Aguardiente and Barranquín Formations could indicate influence from a common source(s). Their relatively close proximity to the Guayana Shield compared to other units explains the rich content of Archean and Late Proterozoic grains. Additionally, “Grenville” age grains suggest that a connection between Aguardiente and Barranquín sedimentary basins should have existed between Neocomian and Albian times. The Espino Graben may have provided such a connection, given its extension and strategic location at the northern edge of the Guayana Shield.

This graben could have acted as a conduct for transportation of 1.2 – 0.9 Ga old sediments from the positive areas of the Colombian Andes to the northeastern Venezuelan basin.

### **Venezuelan Early Cretaceous tectonic scenario and Paleogeography**

Figure 2.26 shows the proposed paleogeographic configuration of the Venezuelan passive margin in Early Cretaceous time.

The northwestern Venezuelan passive margin was initially affected by tectonics probably related to the collision of the Nazca Plate with Western Colombia. By Aptian time, the Merida Arch formed due to the existence of a transfer zone between the Trujillo and Uribante troughs (Figure 2.2, Pindell et al., 1998), controlling the accumulation of sediments of the Aguardiente Formation and Agua Blanca and Bobare Formations in its southern and northern flanks, respectively.

Diachronously, the Eastern Venezuela margin acted as a typical Atlantic passive margin (Ostos et al. 2005). From Berriasian to Albian times, a relatively stable siliciclastic shelf system existed and was fed by a fluvio-deltaic system (Barranquín Formation) that prograded from south-west of today's Interior Range (Erikson & Pindell, 1998a).

For both Western and Eastern Venezuela, the Early Cretaceous sedimentary record is a transgressive sequence that is generally composed of shallow-water siliciclastics mixed with carbonate buildups and localized reefs which gradually onlapped onto the Jurassic red beds and the Guayana Shield (Villamil & Pindell, 1998). By the end of Early Aptian, a sudden transgression occurred and abruptly interrupted the siliciclastic supply into the basins, deepening the water column and promoting the accumulation of shales.

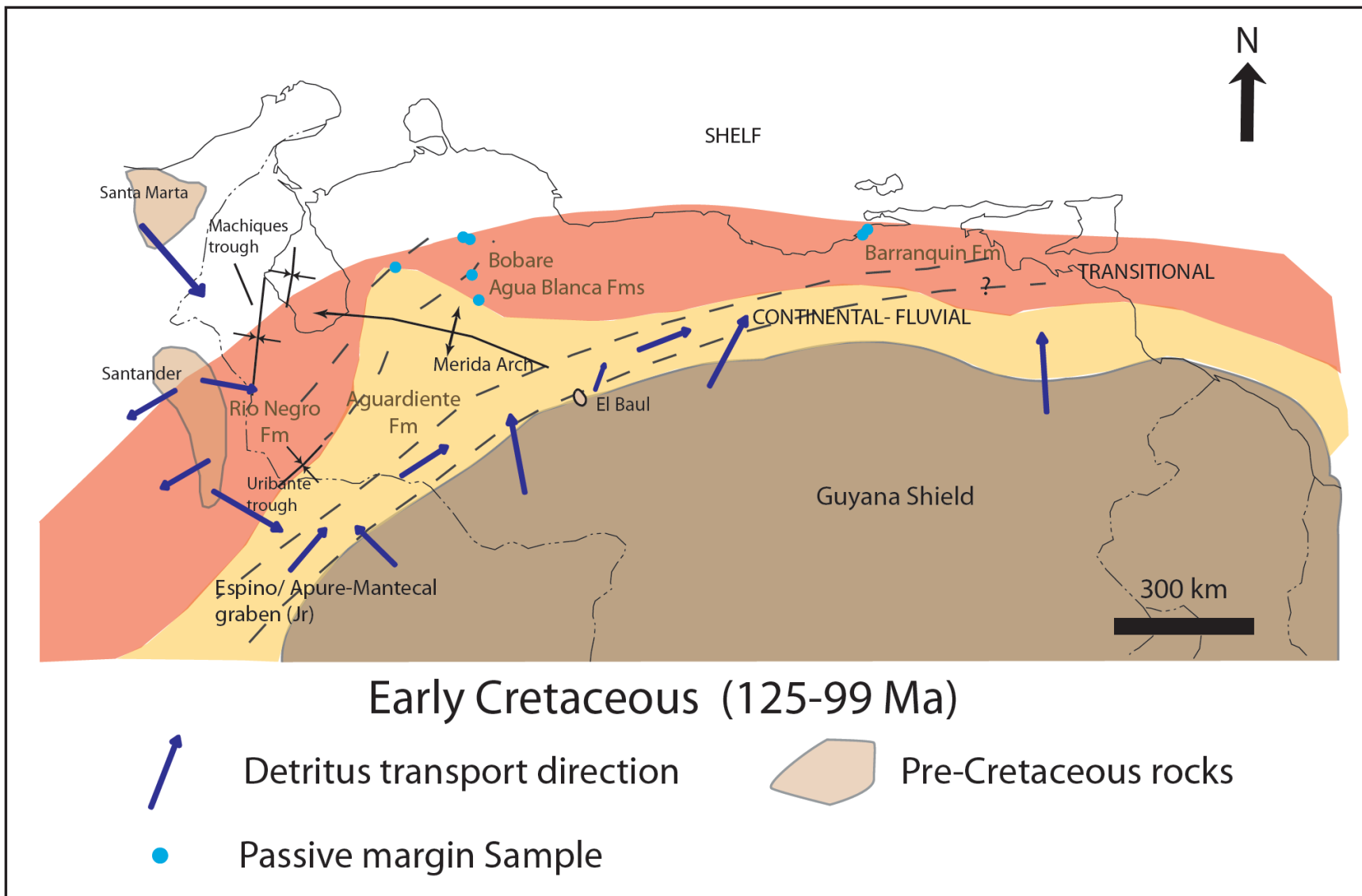


Figure 2.26. Proposed palaeogeographic configuration of the passive margin in Venezuela.



The siliciclastic influx to the deposition centers was provided by drainage from the exposed Guayana Shield, El Baúl Massif, the Colombian Andes (Santa Marta and Santander) and probably the Merida Arch. Deposition was primarily controlled by the Jurassic Espino Graben (Yoris & Ostos, 1997; Ostos et al., 2005), which because of regional extension and its proximity to the exposed areas could have provided an optimum pathway for fluvial sediment transportation in a SW-NE direction. The deltaic deposits of Barranquín Formation may represent the outlet of this “Proto-Orinoco” river.

## CONCLUSIONS

LA-ICP-MS U-Pb detrital zircon geochronology was applied to four siliciclastic units representing the Early Cretaceous passive margin in Northern Venezuela (Barranquín, Aguardiente, Bobare and Agua Blanca Formations). In general, ages of these units range between Late Archean and Early Devonian. No Triassic or Jurassic grains were identified. Maximum and minimum ages of the detrital components determined in this study are listed below (Table 2.10).

Table 2.10. Age ranges of the detrital fraction of the northern Venezuela Early Cretaceous units

Unit	Oldest grain (Ma)	Youngest grain (Ma)
Barranquin Fm	2731.8 ± 26.7	427 ± 4.1
Aguardiente Fm.	2719 ± 24.6	415 ± 4.1
Bobare Fm.	2151 ± 35.3	451.4 ± 4.4
Agua Blanca Fm.	2134 ± 18	491 ± 6.7

The detrital zircon data show signatures that indicate the presence of at least three different sources:

- Precambrian (2.7 – 1.5 Ga) source: Grains of these age correlate very closely to rocks from the Guayana Shield: Imataca (2736 Ma), Cuchivero (1995 Ma) and Roraima (1806 Ma) provinces. Detrital zircons with ages of about 1518 Ma seem to be diagnostic of the Parguazan Granite of the same shield.
- “Grenville” (1.3 – 1.0 Ga) source: Not reported from outcrops nor in the basement of Venezuela, but identified in fluvial grains in the Orinoco basin (Goldstein et al., 1997). Meta-igneous rocks from the Eastern Cordillera of Colombia (Santa Marta and Santander Massifs) are the potential source of the 960 and 1200 Ma detrital component.
- Paleozoic (415 – 490 Ma) source: Peaks of 488 Ma and 422 Ma could be related to Cambrian-Ordovician rocks of the El Baúl Massif (El Baúl Granitic Suite) and probably to Silurian-Devonian plutonic bodies in the Mérida Andes (Cerro Azul Granite).

Deposition during Early Cretaceous times was controlled by extensional structures, which received siliciclastics drained from the exposed Guayana Shield, El Baúl Massif, the Colombian Andes (Santa Marta and Santander) and probably the Merida Arch. Location of these sources indicate general sediment transport directions as S-N (Guayana Shield) and W-E/SW-E. A proposed proto-Orinoco River could have flown along the structural depressions of a SW-NE oriented structure (Espino Graben) and delivered prograded siliciclastic sediments from Colombia to north-eastern Venezuela. The deltaic deposits of Barranquín Formation may represent the outlet of this “Proto-Orinoco” river.

## REFERENCES

Albertos, María A. 1989. Estudio Geológico de las Secciones Altagracia de Orituco – Agua Blanca y Gamelotal – San Francisco de Caira (estados Guárico y Miranda): Análisis

- Petrográfico y estadístico de la Formación Guárico (Geologic Study of the sections Altigracia de Orituco and Gamelotal – San Francisco de Caira, Guárico and Miranda states: Petrographic and statistical analysis of the Guárico Formation). Universidad Central de Venezuela, Thesis.
- Bellizia, A., 1986. Sistema montañoso del Caribe: Una Cordillera alóctona en la parte norte de América del Sur (Caribbean Mountain system: an allochthonous cordillera in northern South America). *VI Congreso Geológico Venezolano*, 10: 6657-6836.
- Bellizia G., Alirio and Domingo Rodríguez G. 1966. Excursión a la Región de Duaca – Barquisimeto – Bobare (Field trip to Duaca – Barquisimeto - Bobare region). In: LEV, 2008, <http://www.pdvsa.com/lexico/excursio/exc-66.htm>
- Bizzi A. L. 2005. The Venezuelan Guayana Shield Basement dating Project. Progress Report. *Geos*, Universidad Central de Venezuela, 38:112-194, in CD.
- Chew, David M.; Urs Schaltegger; Jan Kosler; Martin J. Whitehouse; Marcus Gutjahr, Richard A. Spikings and Aleksandar Miskovic. 2007. U-Pb Geochronologic evidence for the evolution of the Gondwanan margin of the north-central Andes, *GSA Bulletin*, 119(5): 697-711.
- Cordani U.G, A. Cardona, D.M. Jimenez, D. Liu, and A.P Nutman. 2005. Geochronology of Proterozoic Basement Inliers in the Colombian Andes: Tectonic History of remnants of a fragmented Grenville Belt. In: Vaughan A.P.M., Leat P.T. and R.J. Pankhurst (eds.), *Terrane Processes at the margins of Gondwana*, Geological Society of London, Special Publications, 246:329-346.

- Dickinson, William R. 1985. Interpreting provenance relations from detrital modes of sandstones. In: G. G. Zuffa (ed.), *Provenance of Arenites*, p.333-361.
- Erickson J. P. and J. Pindell. 1998a. Cretaceous through Eocene sedimentation and Paleogeography of a Passive Margin in northeastern Venezuela. In: Paleogeographic Evolution and Non-Glacial Eustasy, Northern South America, SEPM Special Publication No 58, p. 218-259.
- Erickson J. P. and J. Pindell. 1998b. Sequence stratigraphy and relative sea-level history of the Cretaceous to Eocene passive margin of North-East Venezuela and the possible tectonic and eustatic causes of stratigraphic development. In: Paleogeographic Evolution and Non-Glacial Eustasy, Northern South America, SEPM Special Publication No 58, p. 261-281.
- Feo-Codecido Gustavo, Foster D. Smith Jr., Nelson Aboud and Estela Di Giacomo. 1984. Basement and Paleozoic rocks of the Venezuelan Llanos Basin. Geological Society of America, Memoir 162, p.175-187.
- Ghosh, S.K. and E. Zambrano. 1996. The Eocene turbidites of the Trujillo Formation, Venezuelan Andes, *AAPG Bulletin*, 80(8):1294.
- Goldstein S. L., N. T. Arndt and R. F. Stallard. 1997. The history of a continent from U-Pb ages of zircons from Orinoco basin river sediments. *Chemical Geology*, 139:271-286.
- González de Juana C., J.M. Iturralde de Arozena, X. and Piccard Cadillay. 1980. *Geología de Venezuela y de sus Cuencas Petrolíferas*, Caracas, Foninves, 1031 p.

- Grande, Sebastian. 2005. Rocas ígneas de la Península de Paraguaná (Igneous Rocks of the Paraguaná Peninsula, Venezuela. I Jornadas de Geología de Rocas Ígneas y Metamórficas, Programa General y Libro de Resúmenes. P. 28-30.
- Grande Sebastian, Franco Urbani and David Mendi. 2007. Presencia de un basamento Grenvilliano de alto grado en Venezuela noroccidental (Presence of a High-grade Basement in Northwest Venezuela of possible Grenville Affinity). *Geos* 39:90.
- Guynn, Jerome. 2006. Comparison of Detrital Zircon Age Distributions using the K-S Test. Arizona LaserChron Center. <http://www.geo.arizona.edu/alc/Analysis%20Tools.htm>
- Hackley P. C., F. Urbani, A.W. Karslen and C. Garrity. 2005. Geologic Shaded Relief Map of Venezuela. U.S. Geological Survey Open File Report 2005-1038. <http://pubs.usgs.gov/of/2005/1038/>.
- Keppie J. Duncan and F. Ortega-Gutierrez. 1999. Middle American Precambrian basement: A missing piece of the reconstructed 1-Ga orogen. *In*: Ramos Victor and J. Duncan Keppie (eds.), Laurentia-Gondwana connections before Pangea. Geological Society of America, Special Paper 336:199-210.
- Kroner, Alfred and Umberto Cordani. 2003. African, southern Indian and South American cratons were not part of the Rodinia supercontinent: evidence from field relationships and geochronology. *Tectonophysics*, 375: 325-352.
- Léxico Estratigráfico Venezolano (LEV). <http://www.pdvsa.com/lexico/>. (November 2008).

- Lopez, Rafael. 1976. Estudio de la Formación Matatere en el área de Carora, estado Lara (Study of the Matatere Formation in the area of Carora, Lara state). Universidad Central de Venezuela, Thesis.
- Macsotay O., 1972. Observaciones acerca de la edad y paleoecología de algunas formaciones de la región de Barquisimeto, Estado Lara, Venezuela (Observations about age and paleoecology in some formations of the Barquisimeto region, Lara state). *Memorias IV Congreso Geológico Venezolano.*, Ministerio de Minas e Hidrocarburos, Caracas, 3: 1673-1701.
- Macsotay O.; J. F., Stephan, and E. Alvarez, 1987. Grupo Lara: Sedimentitas oceánicas y peninsulares en el Cretáceo alóctono de Venezuela occidental (Lara Group: Oceanic and peninsula sedimentites in the Cretaceous allochthonous of western Venezuela). *Bol. Geol.*, (28): 3-78.
- Martínez Gladys and Graziana Valleta. 2008. Petrografía de las facies gruesas de la Formación Matatere y otras unidades del Centro-Occidente de Venezuela (Petrography of the coarse grained facies of Matatere Formation and other units from Central-Western Venezuela), Universidad Central de Venezuela, Thesis, 280 p.
- Mendoza V. 2005. Geología de Venezuela. *Geos* 38, CD.
- Molina Agustin Cardona, Unberto G. Cordani and William D. MacDonald. 2006. Tectonic correlations of Pre-Mesozoic crust from the Northern termination of the Colombian Andes, Caribbean region. *Journal of South American Earth Sciences* 21:337-354.

- Ostos M., F. Yoris, and H. A. Lallemand. 2005. Overview of the Southeast Caribbean – South American Plate Boundary Zone. *In: Lallemand H. and V. Sisson, Caribbean-South American Plate Interactions, Venezuela. The Geological Society of America, Special paper 394, p. 53-89.*
- Persad, K.M. 1990. The Espino Graben – An Aulacogen?, *Transactions of the Geological Conference of the Geological Society of Trinidad & Tobago*, 2:25.
- Pettijohn F.J., P.E. Potter and R. Siever. 1987. *Sand and Sandstone*, 2<sup>nd</sup> edition, Berlin, Springer-Verlag. 553 p.
- Pindell J. L., R. Higgs, and J. F. Dewey. 1998. Cenozoic palinspatic reconstruction, paleogeographic evolution and hydrocarbon setting of the northern margin of South America. *In: Paleogeographic Evolution and Non-Glacial Eustasy, Northern South America, SEPM Special Publication No 58, p.45-85.*
- Pindell James and Lorcan Keenan. 2001. Kinematic Evolution of Mexico and the Caribbean. *GCSSEPM Foundation 21st Annual Research Conference, Petroleum Systems of Deep Water Basins*, p. 193-220.
- Pindell, James; Lorcan, Keenan; Walter V., Maresch; Klaus-Peter, Stanek, Grenville, Draper and Roger, Higgs. 2005. Plate-Kinematics and crustal dynamics of circum-Caribbean arc-continent interactions: Tectonic controls on basin development in Proto-Caribbean margins. *In: Lallemand H. and V. Sisson, Caribbean-South American Plate Interactions, Venezuela. The Geological Society of America, Special paper 394, p. 7-52.*

- Priem, H.N.A; D.J. Beets and E.A.Th. Verdurmen. 1986. Precambrian rocks in an Early Tertiary conglomerate on Bonaire, Netherlands Antilles (southern Caribbean borderland): evidence for a 300 km eastward displacement relative to the South American mainland?, *Geologie en Mijnbouw* 65:35-40.
- Renz, O. y K. C. Short, 1960. Estratigrafía de la región comprendida entre el Pao y Acarigua, estados Cojedes y Portuguesa (Stratigraphy of the region between El Pao and Acarigua, Cojedes and Portuguesa states). *III Congreso Geológico Venezolano*, Caracas, 1: 277-315.
- Rodriguez Inirida and Josmat Rodriguez. 2003. Gravity and Magnetic Modelling across the Guárico Sub-basin, Espino Graben, Venezuela. *Andean Geodynamics: Extended Abstracts*. Institut de Reserche pour le développement IRD – Université Paul Sabatier. p. 533-536.
- Rogers, J. W. and M. Santosh. 2004. *Continents and Supercontinents*. Oxford University Press, 289 p.
- Ruiz Joaquin, Richard M. Tosdal, Pedro A. Restrepo and Gustavo Murillo-Muneton. 1999. Pb Isotope evidence for Colombia-southern Mexico connections in the Proterozoic. *In*: Ramos Victor and J. Duncan Keppie (eds.), *Laurentia-Gondwana connections before Pangea*. Geological Society of America, Special Paper, 336:183-197.
- Schneider Santos J.O., P.E. Potter, N.J. Reis, L.A. Hartmaun, I.R. Fletcher and N.J. McNaughton. 2003. Age, source, and regional stratigraphy of the Roraima Supergroup and Roraima-like outliers in Northern South America based on U-Pb geochronology. *GSA Bulletin*, 115(3):331-348.



- Sisson V., M. Ostos, A. E. Blythe, L. W. Snee, P. Copeland, J. Wright, R. Donelick and L. R. Guth. 2005. Overview of radiometric ages in three allochthonous belts of northern Venezuela: Old ones, new ones, and their impact on regional geology. *In*: Lallemant H. and V. Sisson, Caribbean-South American Plate Interactions, Venezuela. The Geological Society of America, Special paper 394, p: 91-117.
- Valdes D'Gregorio, Carmen. 1980. Geología de superficie, Sedimentología, Estratigrafía y Tectónica de un Área entre Carora – Barquisimeto, estado Lara (Las Peñitas – Pozo Guapo). (Surface Geology, Sedimentology, Stratigraphy and Tectonic of an area between Carora – Barquisimeto, Lara state; Las Peñitas – Pozo Guapo). Universidad Central de Venezuela, Thesis.
- Van Andel, Tjeerd. 1958. Origin and Classification of Cretaceous, Paleocene and Eocene sandstones of Western Venezuela. *Bulletin of the American Association of Petroleum Geologists*, 42(4):734-763.
- Villamil Tomas and James Pindell. 1998. Mesozoic Paleogeographic Evolution of Northern South America: Foundations for sequence stratigraphic studies in passive margin strata deposited during non-glacial times. *In*: Paleogeographic Evolution and Non-Glacial Eustasy, Northern South America, SEPM Special Publication No 58, p. 283-318.
- Viscarret Patxi, James Wright and Franco Urbani (2007). Dataciones U/Pb SHRIMP en circon de rocas del Macizo El Baúl, estado Cojedes, Venezuela (U-Pb SHRIMP zircon geochronology of El Baúl massif, Cojedes state, Venezuela). *Geos*, 39:94-95.
- Von der Osten, E., 1954. Geología de la región de la bahía de Santa Fé, estado Sucre (Geology of the region of Santa Fe bay, Sucre state). Venezuela, *Boletín de Geología* 3(8): 123-211.

- Yoris F. and Albertos de Yoris M. A. 1989: Medidas de Paleocorrientes en la secuencia de la Formación Guárico y sus equivalentes en las secciones: Altagracia de Orituco, Guatopo y Gamelotal – San Francisco de Macaira, estados Guárico y Miranda (Paleocurrents in Guárico Formation and equivalents, Altagracia de Orituco-Guatopo and Gamelotal-San Francisco de Macaira sections, Guárico and Miranda States). Caracas, *Geos*, 29:152-159.
- Yoris F. and M. Ostos. 1997. Petroleum Geology of Venezuela, *in*: Singer J. M. (ed.) 1997. *Well Evaluation Conference*. Caracas, Schlumberger, p. 1-44.
- Zapata, Eglee. 1976. Estudio de la Formación Guárico en el área de la Laguna de Unare, estado Anzoátegui (Study of the Guárico Formation in the area of Laguna de Unare, Anzoátegui state). Universidad Central de Venezuela, Thesis.

## **CHAPTER 3**

### **LATE CRETACEOUS – MIOCENE TURBIDITES**

#### **INTRODUCTION**

Maastrichtian-Miocene turbidite deposits occur in northern Venezuela (Matatere Formation, Martínez & Valleta, 2008; Guárico Formation, Zapata, 1976, Albertos, 1989; Pampatar Formation, Muñoz 1973; Los Arroyos Formation, Alvarez et al., 1985; Caratas Formation, Galea, 1986), Curacao (Lagoen and Midden Curacao Formations; Beets, 1972), Trinidad (Chaudière and Point-a-Pierre Formations) and Barbados (Scotland Formation, Pudsey & Reading, 1982); (Figure 3.1). The quartz-rich and lithic sandstones, polymict conglomerates, and shales of these units currently overlie Cretaceous sediments and record the first interactions between the Caribbean and the South American plates since Late Cretaceous time (Kasper & Larue, 1986; James, 1997; Meschede & Frisch, 2002; Pindell et al., 1998). Provenance studies in turbidite sections in Venezuela (based on petrographic and paleocurrent data) indicate at least two different sources of sediments: a northern volcanic arc source and a southern continental margin source (Matatere Formation, Kasper & Larue, 1986; Martinez & Valleta, 2008; Guárico Formation, Albertos, 1989; Yoris & Albertos, 1989; Pampatar Formation, Moreno & Casas, 1986). Sources located to the west (Colombian Andes) have also been suggested (Van Andel, 1958; Kasper & Larue, 1986).

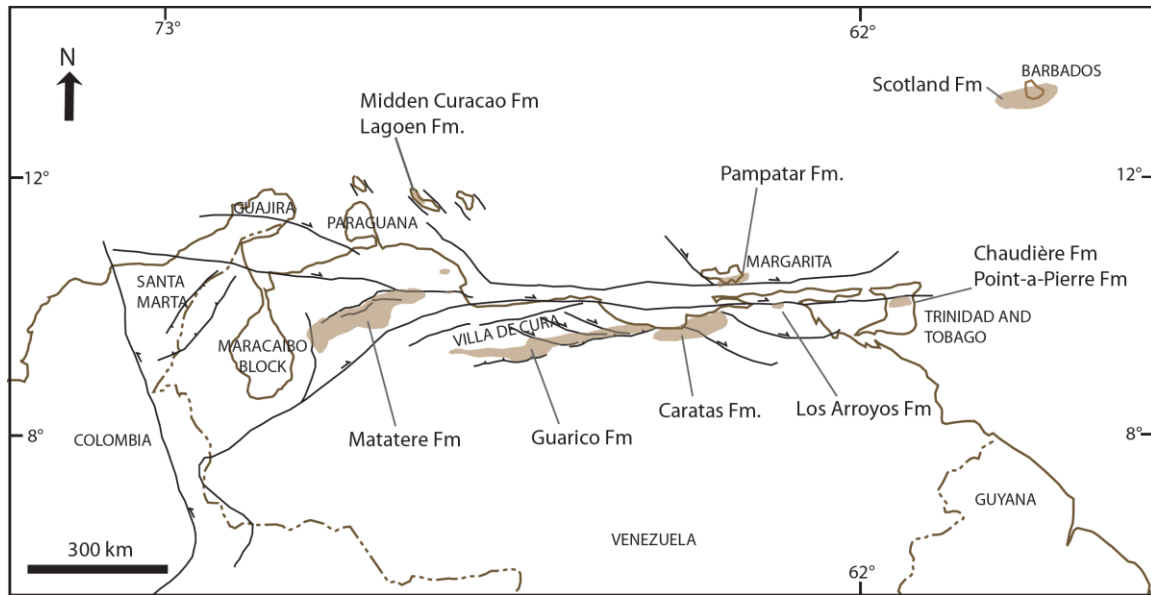


Figure 3.1. Distribution of Maastrichtian – Middle Miocene-age turbidite deposits in northern Venezuela and the Caribbean.

The combination of petrographic and LA-ICP-MS U/Pb detrital zircon geochronologic studies on turbidite sequences in northern Venezuela and Curacao help to constrain the potential sources for these deposits and the timeframe of their deposition. The new petrographic and detrital zircon data for the sandstones and conglomerates of Matatere, Guárico, Pampatar, Midden Curacao, and Lagoen Formations, including the sandstones of Caratas and Los Arroyos Formations, is consistent with previous provenance interpretations, indicating a mixed provenance. The older detrital fraction resembles a passive margin detrital zircon signature (Chapter 2), including “Grenville” ages only seen in Colombia; whereas younger grains (Maastrichtian - Eocene) reflect a volcanic component and indicate a strong Caribbean-arc influence. Important magmatic events are also recorded in the detrital zircon data, and can be related to the evolution of the Caribbean region at:

- ca. 90 Ma: generation of the Leeward Antilles arc on the basement of the Caribbean Large Igneous Province (CLIP).
- ca. 64 Ma: Cessation of arc magmatism caused by the collision of the arc with western Colombia and Ecuador.
- ca. 55 - 50 Ma: Renewed magmatic activity following collision of the arc with Colombia.

## **TURBIDITE SAMPLES**

Twenty nine (29) samples of sandstones and conglomerates of turbidite units from western (Matatere Formation), central (Guárico Formation) and eastern Venezuela (Pampatar, Caratas and Los Arroyos Formations) were collected (Figure 3.2). Additionally, three samples of the Midden Curacao and Lagoen Formations from the island of Curacao were used for this study. Units representing the Late Cretaceous to middle Eocene time in northern Venezuela are summarized in Figure 3.3.

### **Lagoen and Midden Curacao Formations (Upper Cretaceous – Middle Eocene)**

The Maastrichtian-age Lagoen Formation is a fine-grained turbidite sequence, composed of an alternation of siltstones, fine-grained sandstones, silica-rich mudstones and marls (Beets, 1972). It represents the upper-middle section of the complex Knip Group, which overlies the Santonian Curacao Lava Formation (Figure 3.4). Vitric tuffs at the base (Newtown tuff zone) and a massive bed of green volcanoclastic sandstone (Koea Joeda Member) located at the middle of the Lagoen Formation are identified. The unit is interpreted to be deposited by submarine sliding in a deep-water environment.

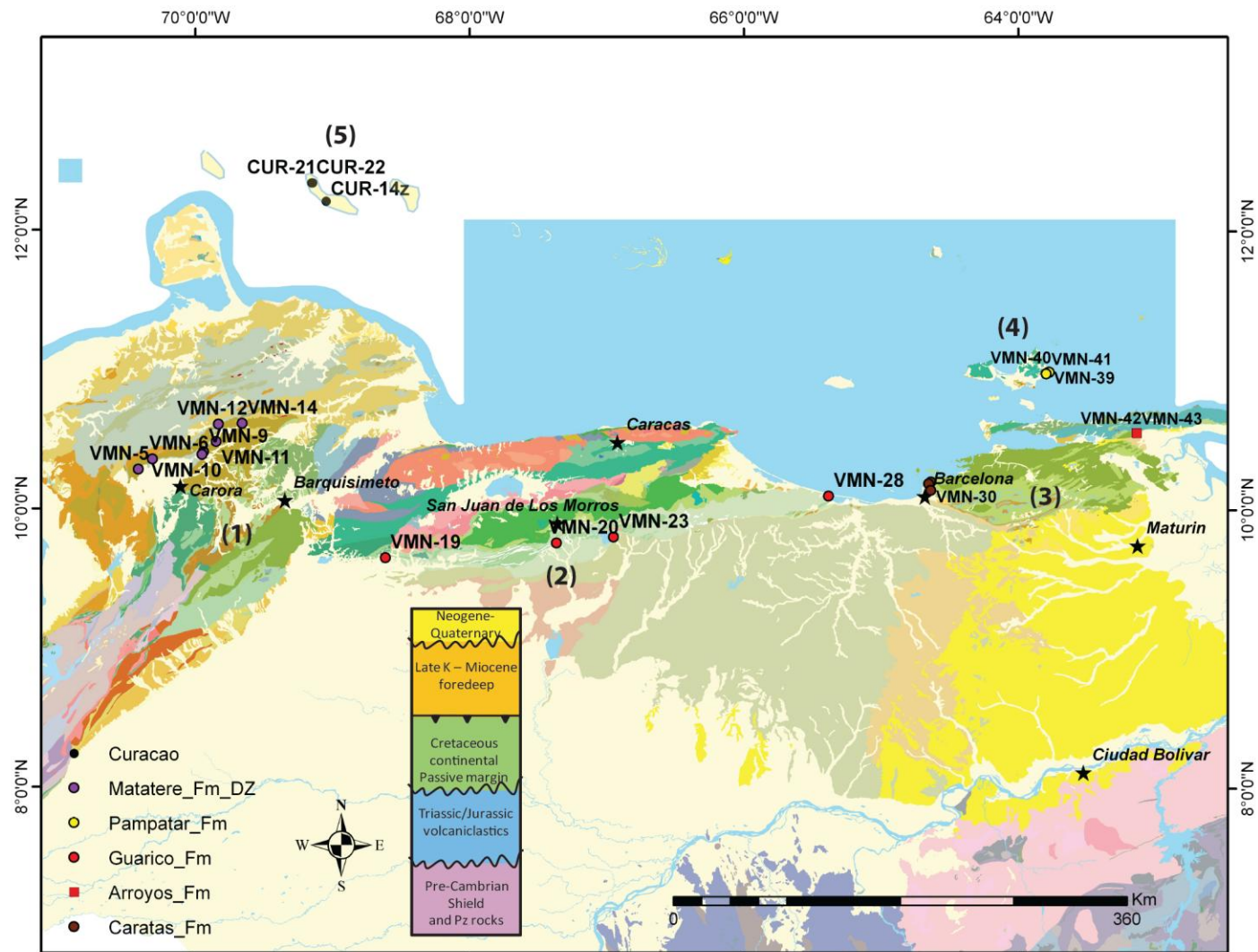


Figure 3.2. Distribution of samples collected from turbidite units in northern Venezuela. Modified from Hackley et. al (2005). Numbers in map correspond to the location of stratigraphic columns from figure 3.3.

AGE			1	2	3	4	5	Tectonic Setting
			Lara	Northern Guarico	Eastern Venezuela	Margarita	Curacao	
Neogene	Miocene	Late				Cubagua	?	Foredeep
		Middle	Capadare	Chaguaramas	LOS ARROYOS / Capiricual / Uchirito	?	?	
		Early	Agua Clara		Carapita			
Paleogene	Oligocene		Castillo / Churuguara	Naricual	Naricual	?	?	Foredeep
				Quebradon	?			
				?	Areo		?	
				?	Los Jabillos			
	Eocene	Late	Santa Rita / Jarillal / Pauji / Misoa	Roblecito / La Pascua	La Pascua	?		Foredeep (West Vzla) Passive margin (East Vzla), (*)
				Peñas Blancas			Seroe di Cueva / Mainsji	
		Middle	?	?	Tinajitas			
			MATATERE	?	CARATAS	Punta Carnero	?	
	Paleocene	Early						
			MATATERE, Humocaro	GUARICO	Vidoño	PAMPATAR		
	Late K	Maastrichtian						Passive margin
			Colon	?	San Juan		LAGOEN/MIDDEN CURACAO	

(\*) Excludes Curacao

Figure 3.3. Generalized stratigraphic chart of the Late Cretaceous – Miocene in northern Venezuela. Units under study are in capital and bold letters.

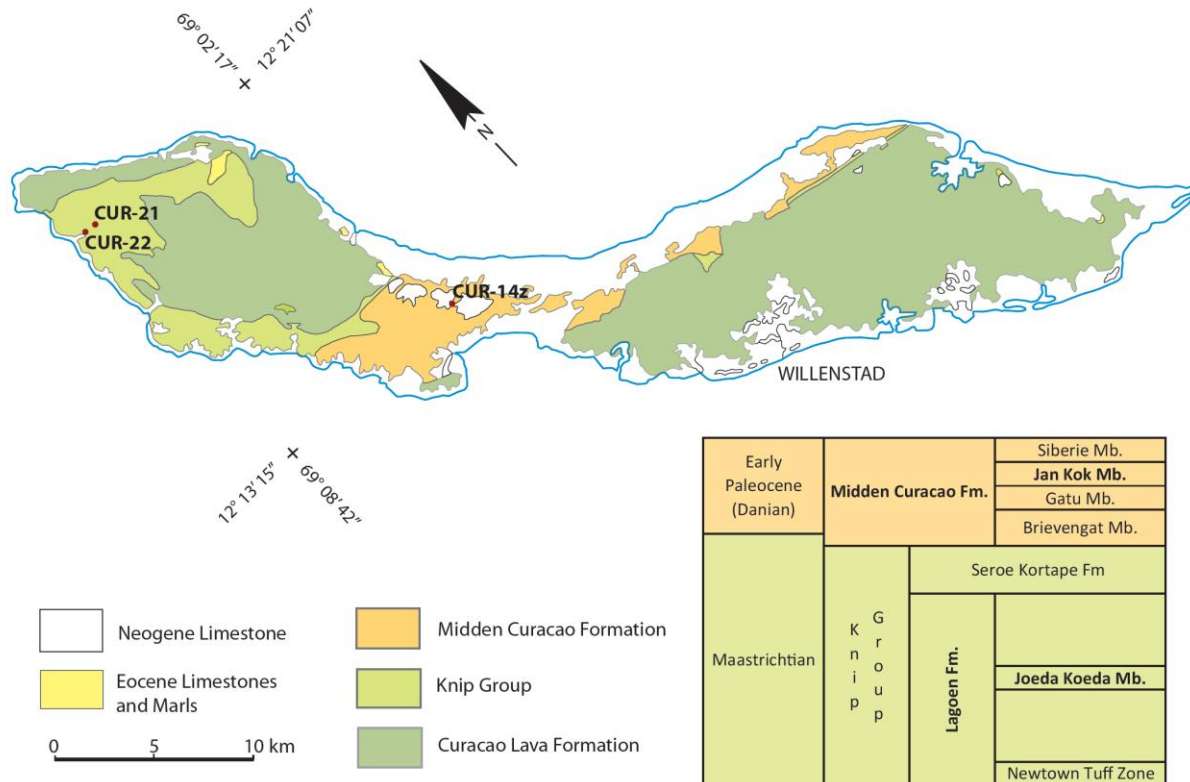


Figure 3.4. Geologic map and stratigraphic table of the Late Cretaceous and Paleocene rocks of the Curacao Island. Units under study are in bold letters. Modified after Beets (1972).

The Early Paleocene Midden Curacao Formation consists of conglomerates, fine-grained sandstones and shales or mudstones (Beets, 1972). It overlies the Knip Group and it is subdivided into four members (Figure 3.4):

- Brievengat Member: Shales with thin intercalations of fine-grained turbidites.
- Gatu Member: Slump deposits of conglomerates and sandstones.
- Jan Kok Member: a sandy turbidite sequence, consisting of alternating sandstones, siltstones and shales.
- Siberië Member: Slump deposits of conglomerates and conglomeratic sandstones and turbidite sandstones with subordinate shales.



### **Guárico Formation (Maastrichtian – Eocene)**

Outcrops of the Guárico Formation (Figures 3.2, 3.5) are located in north-central Venezuela (Figure 3.6) and are composed of a monotonous sequence of sandstones, siltstones and shales that overlie continental passive margin rocks. The sandstones are quartz-rich and also of the greywacke type and their composition varies according to the geographic location (Gonzalez de Juana et al., 1980). Olistoliths and other evidence of gravitational collapse have also been reported (LEV, 2008). Other units have been included within the Guárico Formation (Los Cajones, Caramacate, Garrapata members; LEV, 2008). However, they are now considered to be allochthonous material not related to the Guárico Formation (Pindell et al., 2005; Figure 3.7).



Figure 3.5. Outcrop of Guárico Formation near San Juan de los Morros. Site GPS-352, sample VMN-20.

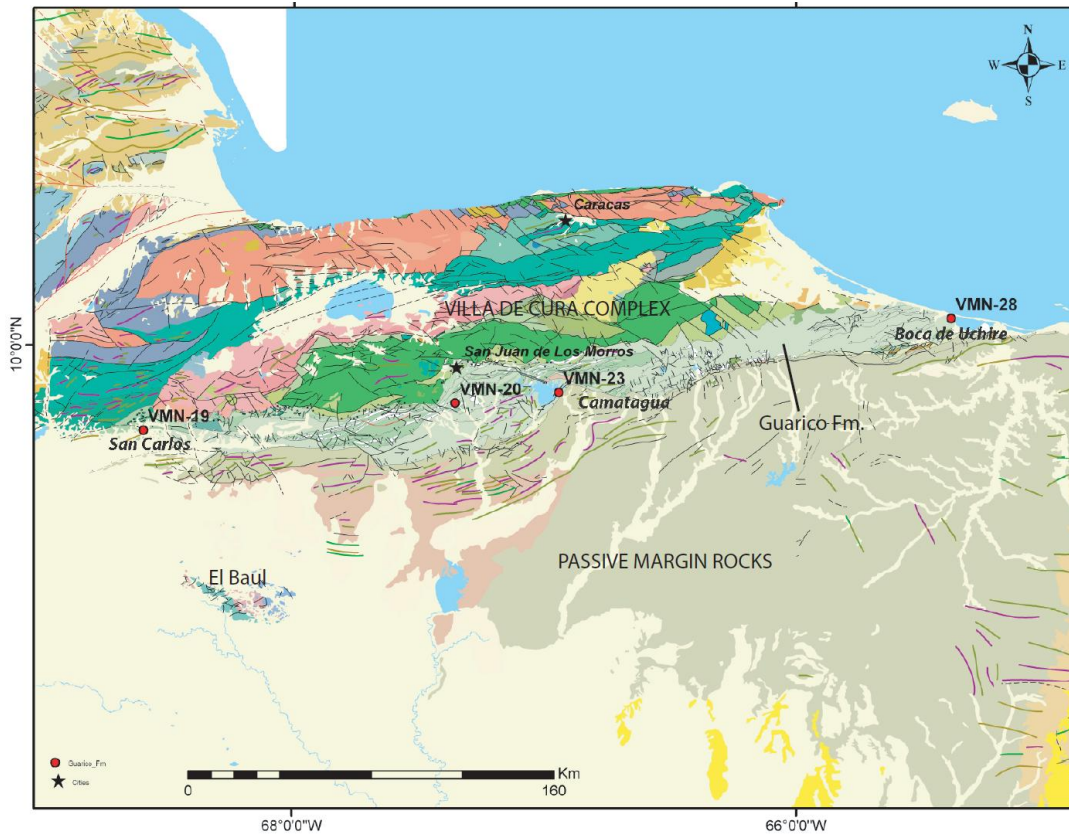


Figure 3.6. Distribution of samples of the Guárico Formation. Modified from Hackley et. al (2005).

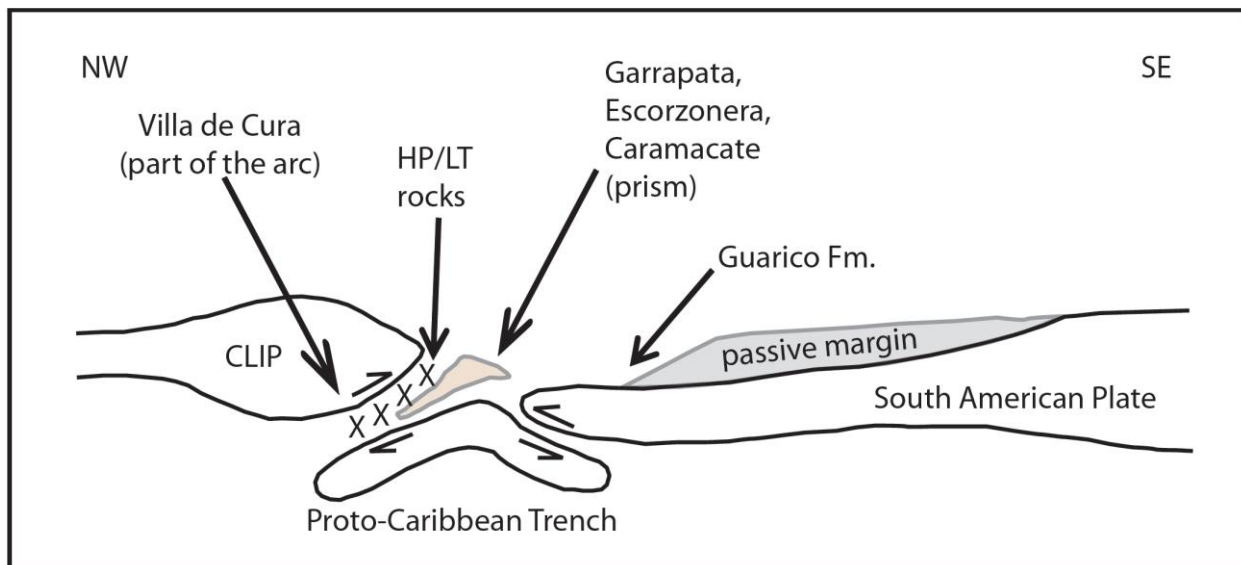


Figure 3.7. Schematic cross section describing the emplacement of the allochthonous Villa de Cura Complex on the continental north-Venezuelan margin at ca. 55 Ma (modified after Pindell et al., 2005).



## Matatere Formation (Paleocene – Eocene)

The Matatere Formation is located in northwestern Venezuela, outcropping along a SW-NW-oriented thrust belt north of Barquisimeto city (Figure 3.8). It consists of an alternating sequence of sandstones that vary from lithic to arkosic, conglomeratic sandstones, and shales (Figure 3.9); polymict conglomerates are also present (LEV, 2008). Some blocks identified within this unit, as the result of collapse in a submarine environment during orogenic episodes, are characteristic of passive margin strata of the Barquisimeto Formation (Chapter 2).

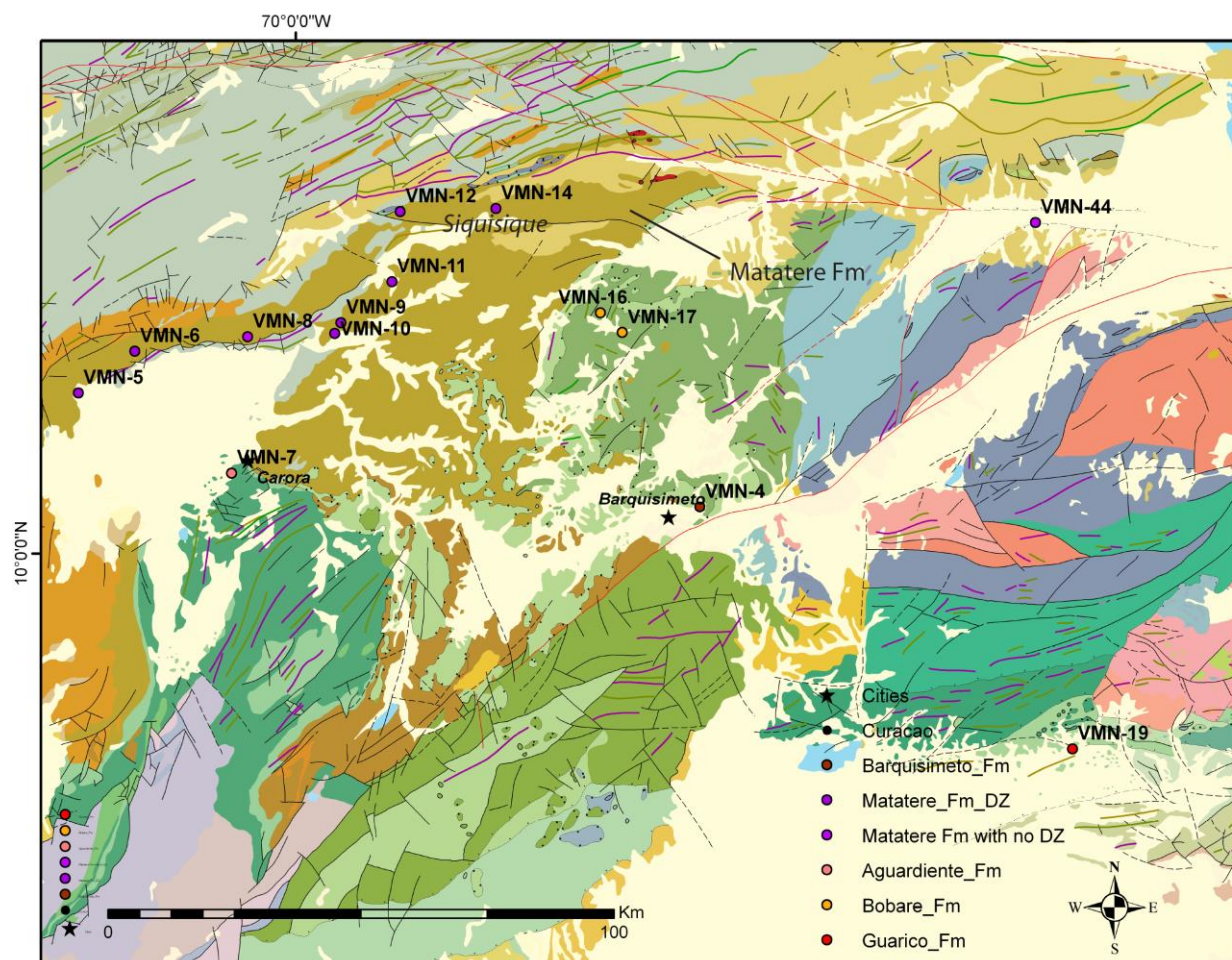


Figure 3.8. Distribution of samples of the Matatere Formation. Modified from Hackley et al., (2005).



Figure 3.9. Outcrop of the Matatere Formation at El Palito stream. Site GPS-333, sample VMN-8b.

The lower contact of Matatere Formation has been reported as unknown (LEV, 2008; Gonzalez de Juana et al., 1980). In some areas, and due to the complex structural conditions, the Paleocene-Eocene Matatere Formation lies in thrust-fault contact over Oligocene-Miocene rocks of the Castillo Formation (Martinez & Valleta 2008; Figure 3.11a). The immature clastic sediments of Matatere Formation were deposited in an accretionary prism that was subsequently emplaced onto the Venezuelan margin (Pindell et al., 2005) as the Caribbean plate moved southeastwardly. Therefore, the lower contact of Matatere Formation is inferred as a thrust fault contact overriding Cretaceous continental sequences. The top of Matatere is usually found as an angular unconformity below younger units (Figure 3.11b-c).



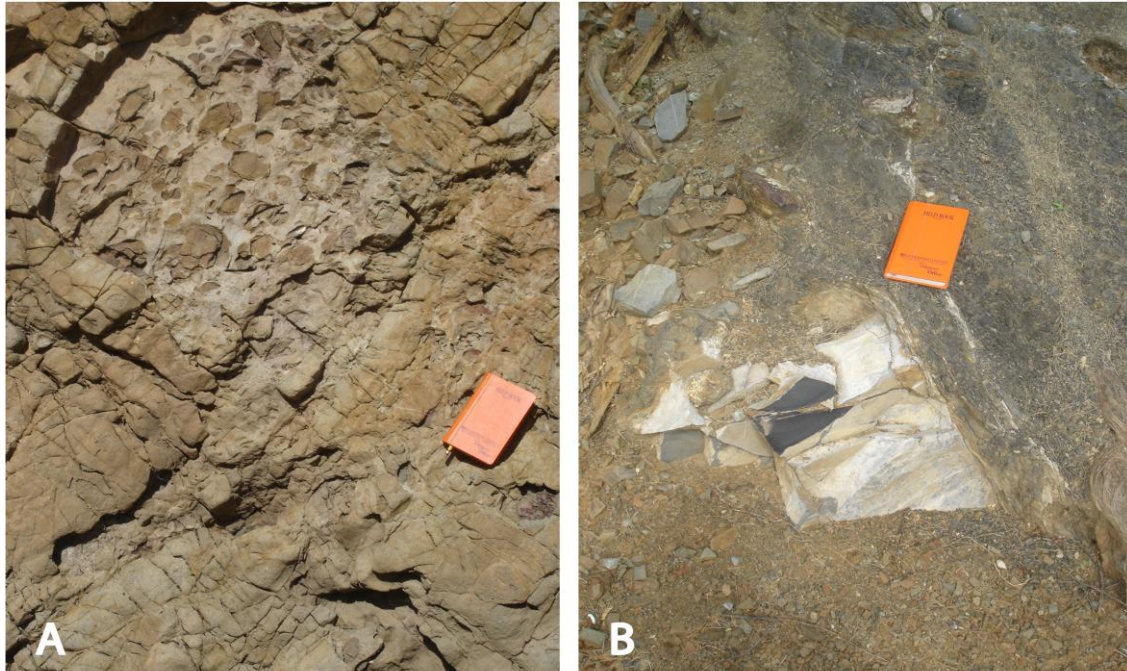


Figure 3.10. Olistoliths embedded in sections of Matatere Formation. (A) Conglomerate, La Peñita stream, Site GPS-329. (B) Limestone fragment, Los Carrillos stream, Site GPS-339.

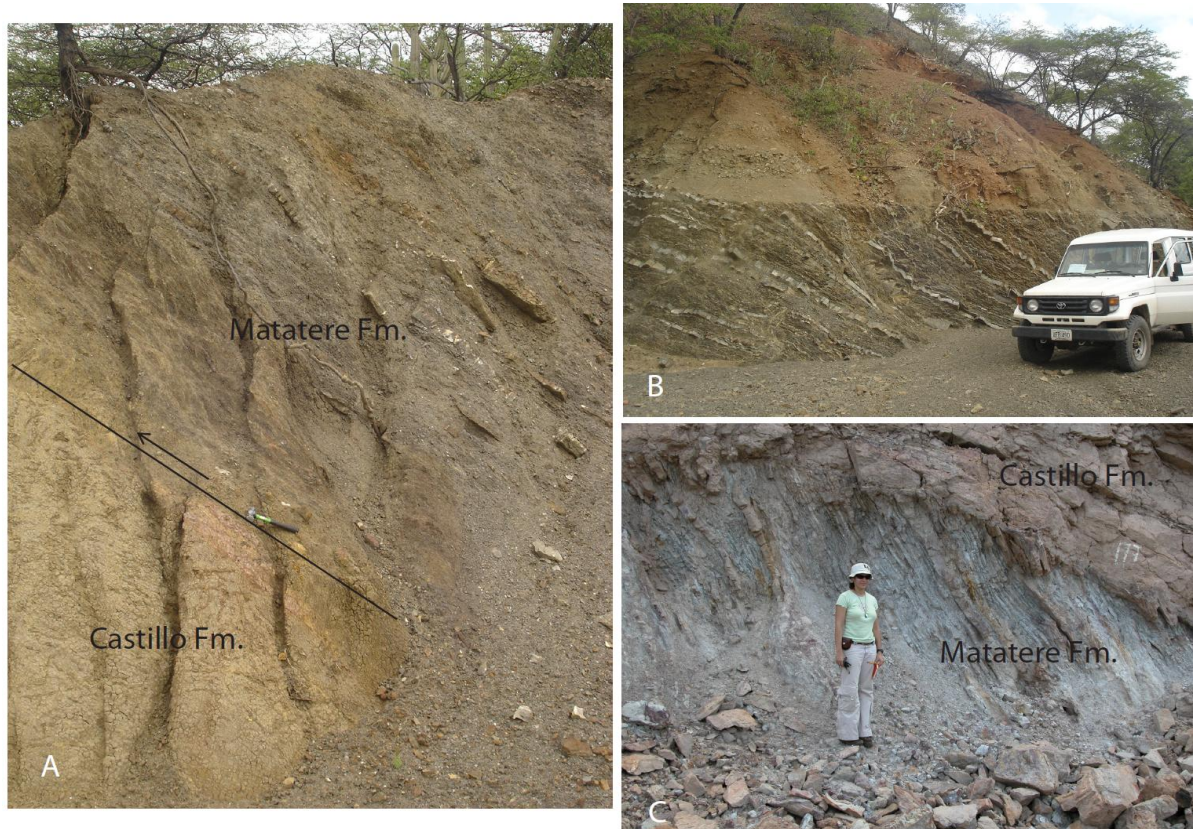


Figure 3.11. Matatere Formation. (A) Fault contact with Oligocene-Early Miocene Castillo Formation, site GPS-335; (B) Erosional contact with Quaternary sediments, site GPS-339; (C) Angular unconformity with Castillo Formation, site GPS-342.

### Pampatar Formation (Eocene)

The Pampatar Formation of Margarita Island (Figures 3.2, 3.12) is composed of a succession of conglomerates, graywackes and shales, with allochthonous blocks of carbonates of Cretaceous age (Gonzalez de Juana et al., 1980; LEV, 2008). The polymict conglomerates are located at the bottom of the unit (Figure 3.13); and underlie a turbidite sequence of graywackes intercalated with shales (Muñoz, 1973). The Pampatar Formation has a non-conformable contact with the underlying Los Robles Formation, of Cenomanian age (LEV, 2008; Figure 3.12); its top is either eroded or covered by Recent sediments. The Pampatar Formation laterally changes to the carbonate turbidite sequences of the Eocene Punta Carnero Group (LEV, 2008).

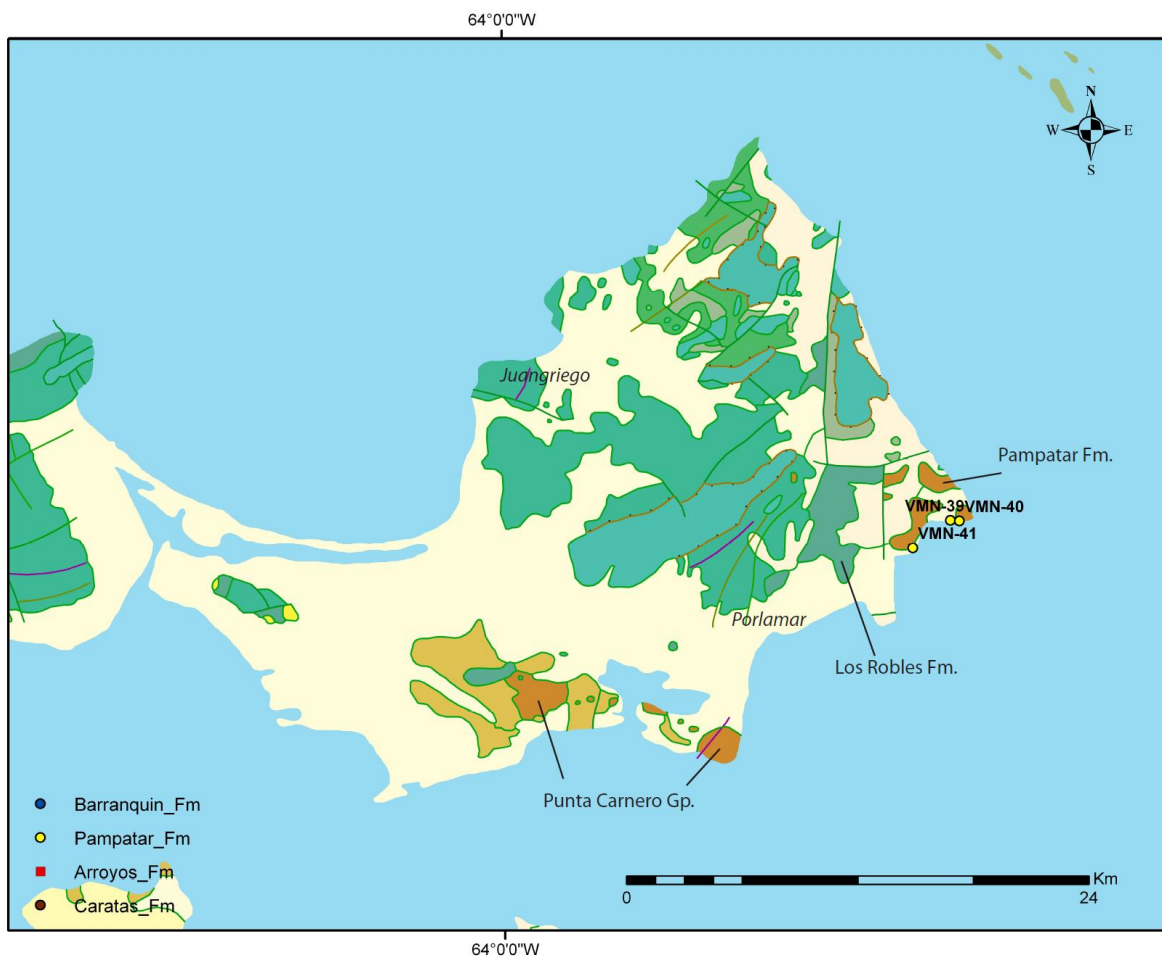


Figure 3.12. Distribution of samples of Pampatar Formation on Margarita Island. Modified from Hackley et al., (2005).





Figure 3.13. Conglomeratic section of Pampatar Formation. Site GPS-380, sample VMN-40.

### **Caratas Formation (Early – Middle Eocene)**

The Caratas Formation (Figures 3.2, 3.14, 3.15) is composed of a sequence of shales and fine-grained quartz-rich sandstones, topped by a thick carbonate sequence (Tinajitas Member, LEV, 2008). The sandstones are also frequently glauconitic and carbonate-rich. The Caratas Formation lies conformably over the shales of Late Cretaceous Vidoño Formation (Figure 3.2); its upper contact with the shales of Oligocene-age Jabillos Formation (Figure 3.2, 3.15) is erosional and marks a regional hiatus, indicated by the absence of Late Eocene fauna. The Punta Carnero Group of Margarita Island is the chronologic equivalent to the Caratas Formation (Figures 3.3, 3.12; Gonzalez de Juana et al., 1980; Macsotay et al., 1986; LEV, 2008).

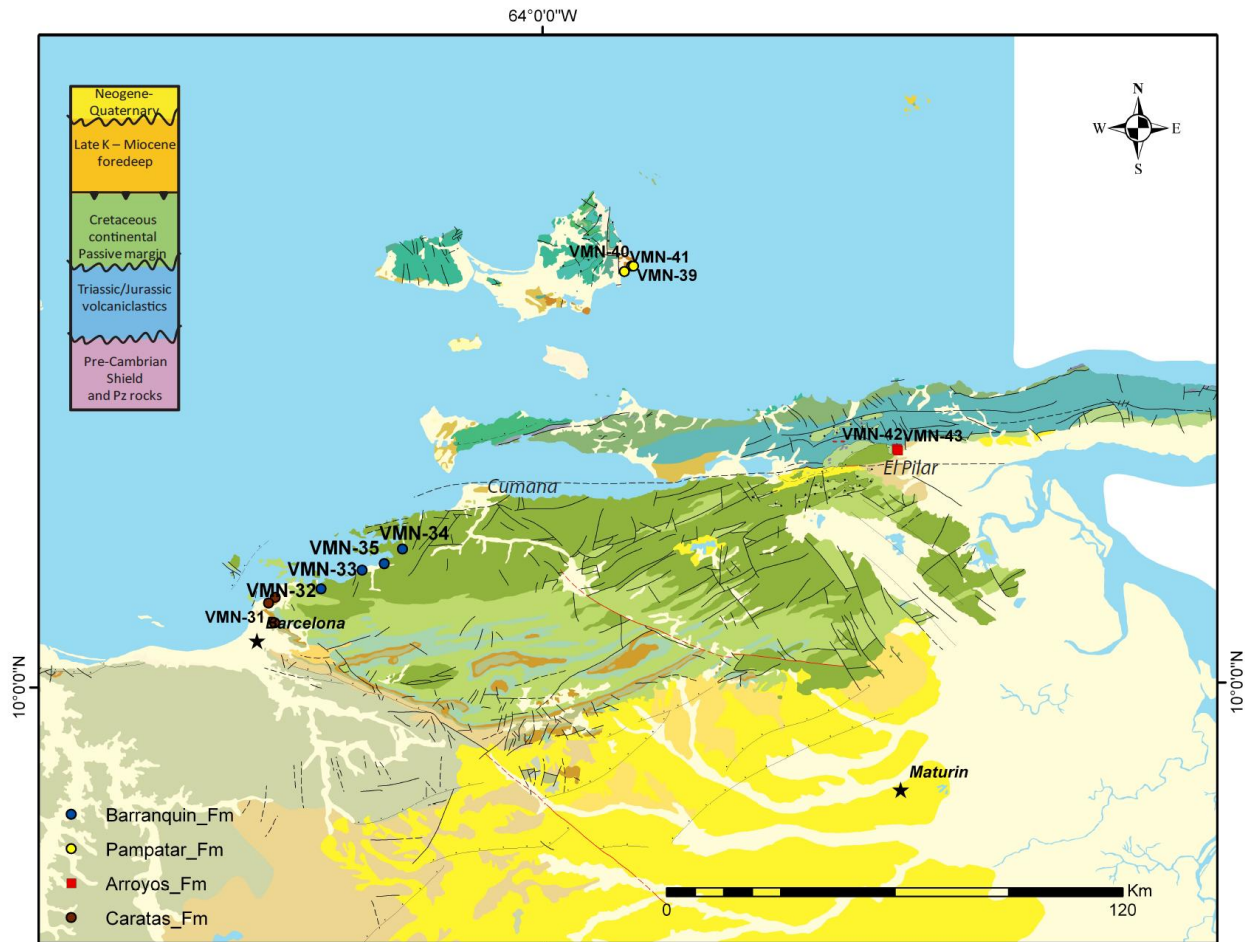


Figure 3.14. Distribution of samples of Caratas and Los Arroyos Formations in Eastern Venezuela. Modified from Hackley et al., (2005).

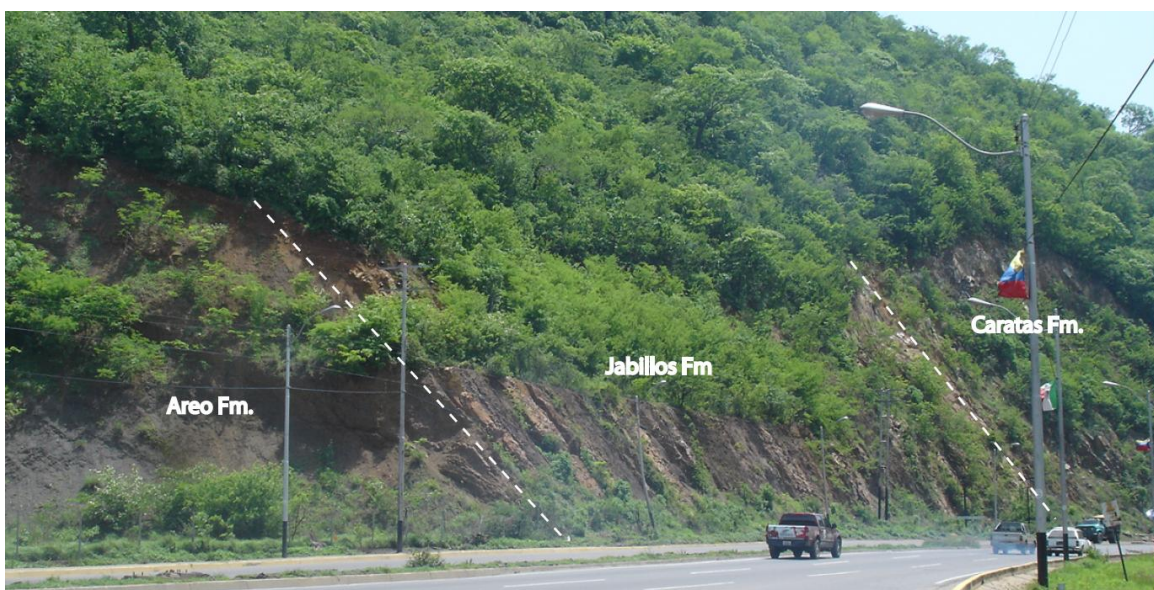


Figure 3.15. The Caratas Formation at site GPS-384



Galea (1986) indicated the depositional environment of the Caratas Formation as turbidite flows on a continental slope, as suggested by the foraminifera. The Tinajitas limestones form a biostrome deposited on the exposed platform edge. Benthic fauna associated with a deep marine environment was also reported by Aguasuelos Ingenieria (1991). Additionally, Pindell et al. (2005) interpreted a trough (referred to as the Vidoño trough) approximately oriented SW-NE, separated from the ocean by a flexural bulge. This trough was fed mostly by shield-derived sands of Caratas Formation and to a lesser degree by sediments derived from the exposed passive margin rocks at the bulge (Figure 3.16).

### **Los Arroyos Formation (Middle Miocene)**

The Los Arroyos Formation (Figures 3.2, 3.14, 3.17) is a terrigenous-carbonate turbidite deposit which includes conglomerates, shales, siltstones, lithic arenites and limestones (Alvarez et al., 1985). From base to top, three facies are identified: lower facies, composed of conglomerates with metamorphic pebbles, an intermediate facies dominated by shales, and an upper facies, represented by a typical turbidite sequence. Structures suggesting gravitational collapse are observed in the upper section of Los Arroyos. The unit is poor in autochthonous fauna; however, Middle Miocene ages were reported from the scarce foraminifera content. Distal platform environments were also interpreted from planktonic foraminifera and gastropods (Alvarez et al., 1985). In the El Pilar area (Figure 3.14), the Los Arroyos Formation is in non-conformable contact over phyllites of undetermined age. Its upper contact is erosional and covered with Pleistocene-age gravels (LEV, 2008; Alvarez et al., 1985).

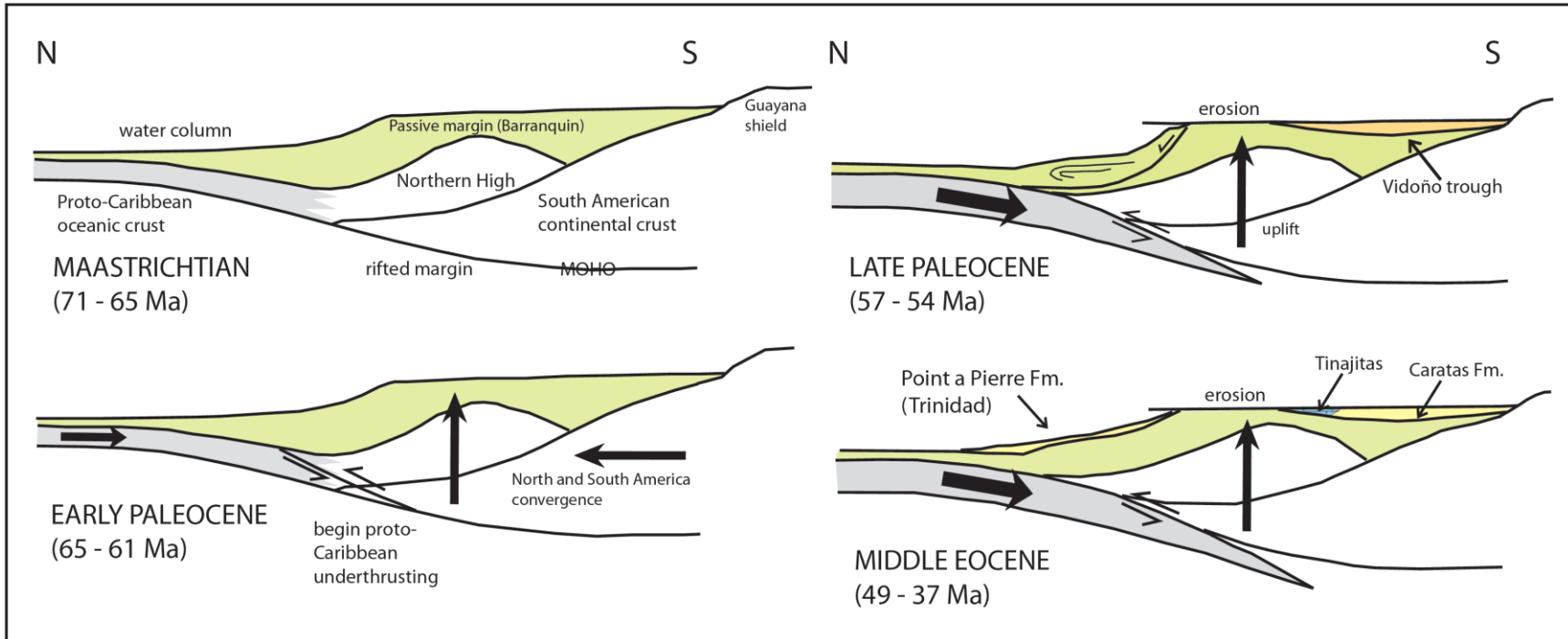


Figure 3.16. Subduction model between the Caribbean and the South American plates in Eastern Venezuela (modified after Pindell et al., 2005)



Figure 3.19. The Los Arroyos Formation in El Pilar area, site GPS-382

## **SANDSTONE PETROGRAPHY**

Mineral composition description and modal counting analyses were performed in samples of the turbidite units. Detailed results of these analyses are presented in Appendix C. Grain count results were also plotted in QtFLt, QpLvLs and QmFLt triangles (Dickinson, 1985) for provenance studies.

### **Lagoen and Midden Curacao Formations**

Lithic graywackes of the Curacao Island have a wide variety of detrital components (Figure 3.18; Table 3.1). Quartz represents 51% and less of the framework grains, with monocrystalline varieties more dominant over the polycrystalline ones. Chert and chalcedony are also found. Alteration in most of the plagioclase grains is advanced but, when possible, albite, oligoclase, andesine and andesine-labradorite compositions were determined through the Michel-Levi method (Kerr, 1959). Accessory minerals are represented by muscovite, leucoxene,

magnetite, pyrite, and hornblende and, less commonly, pyroxenes, apatite and glauconite. Hornblende grains in these samples are subhedral and minimally altered.

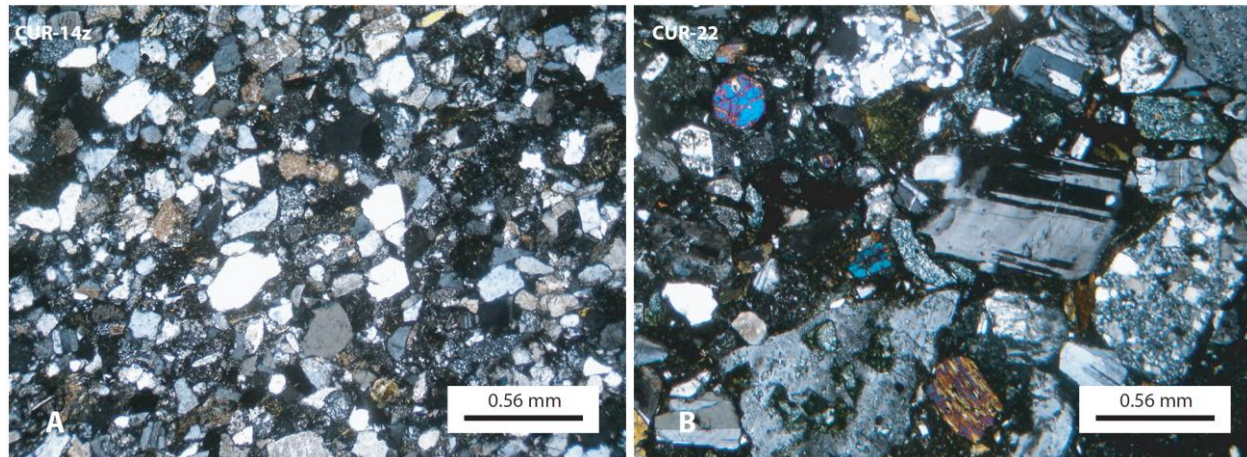


Figure 3.18. Graywackes of the Midden Curacao Formation (A) and Lagoen Formation (B), Curacao Island.

Table 3.1. General composition of sandstones from the island of Curacao (Lagoen Formation in purple and Midden Curacao Formation in blue) using modal analysis (values are in %).

		CUR-14z	CUR-21	CUR-22
Framework grains	Quartz*	51.8	15.1	6.4
	Plagioclases	20.44	35.22	32.41
	K-Feldspar	1.4	0.28	0
	Micas	6.44	3.12	6.11
	Heavy minerals	0	3.12	3.66
	Sedimentary lithics	0.84	0.28	2.75
	Metamorphic lithics	1.68	3.12	7.64
	Volcanic lithics	7.84	24.14	25.07
	Alteration products	6.16	3.12	2.44
	Hornblende	0.28	7.95	7.33
	Fossils	0.28	0.56	0
	Accessories	1.1	4	5.3
	Unknowns	1.68	0	0.91
Whole rock	<b>Grains</b>	<b>65</b>	<b>73</b>	<b>75</b>
	<b>Cement</b>	<b>20</b>	<b>5</b>	<b>0</b>
	<b>Matrix</b>	<b>15</b>	<b>20</b>	<b>25</b>
	<b>Porosity</b>	<b>&lt;1</b>	<b>2</b>	<b>0</b>

(\*) Includes monocrystalline and polycrystalline species (chert, chalcedony and opal)

Lithic fragments in sandstones of Midden Curacao Formation and Lagoen Formation (Figures 3.18) are composed of metamorphic (biotite-phyllite, phyllite, quartz-mica-schist and quartzite), sedimentary (quartz-rich sandstones, graywackes, chert, shales and limestones) and a compositionally wide spectra of volcanic rocks, which includes rhyolites, andesites, basalts and undifferentiated mafic and ultramafic volcanoclastic rocks. Undifferentiated volcanic fragments were usually heavily altered to chlorite and serpentine, which indicates an original mafic or ultramafic composition.

### **Guárico Formation**

Compositions of the sandstones of the Guárico Formation are presented in Table 3.2. The quartz content in these rocks is relatively higher than in the samples from Curacao Island. Quartz grains are generally anhedral, subangular and either fractured or strained. Monocrystalline crystals are more abundant than the polycrystalline varieties (Figure 3.19). Chert is present in small, rounded grains. Plagioclases in these rocks are highly altered to clay and mostly dissolved by advanced diagenesis (pressure-solution); when identification through extinction angles was possible, they were of intermediate composition (andesine-labradorite). Micas are represented by muscovite, biotite and detrital chlorite. Other accessories include sphene, zircon, magnetite, pyrite, hornblende, rutile, detrital calcite and rarely glauconite.

Rock fragments in the Guárico Formation sandstones are of sedimentary (shale, siltstone), metamorphic (quartz-biotite-phyllite, quartz-mica-schist and quartzite) and volcanic (andesite and undifferentiated volcanoclastic) nature. Volcanic lithics are aphanitic and, of probable intermediate to felsic composition; they are mostly altered to chlorite.



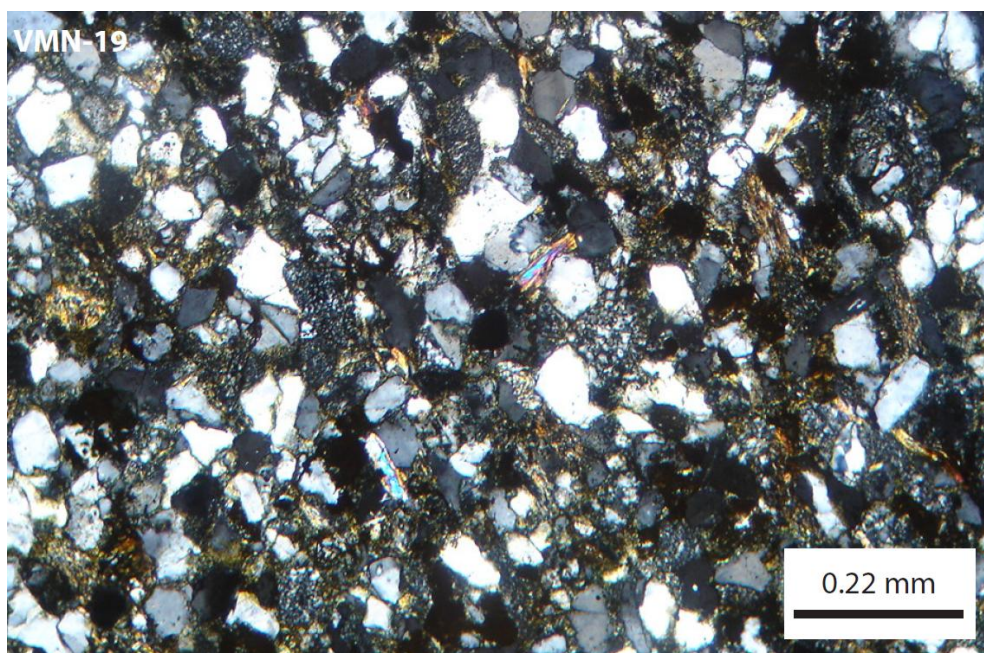


Figure 3.19. Graywacke of Guárico Formation. Sample VMN-19.

Table 3.2. General composition of sandstones of Guárico Formation using modal analysis (values are in %).

		VMN-19	VMN-20	VMN-23	VMN-28
Framework grains	Quartz*	75.5	63.2	89.8	73.1
	Plagioclases	3.98	4.84	1.42	9.83
	K-Feldspar	0	0	0	0
	Micas	1.06	6.77	0.94	2.81
	Heavy minerals	0	0.48	0.23	0.23
	Sedimentary lithics	2.39	5.08	3.31	11.47
	Metamorphic lithics	1.06	3.87	2.36	1.4
	Volcanic lithics	10.37	12.1	0.71	0.7
	Alteration products	5.31	3.14	0.23	0.46
	Hornblende	0.26	0.24	0.47	0
	Fossils	0	0	0	0
	Unknowns	0	0	0	0
Whole rock	<b>Grains</b>	<b>50</b>	<b>54</b>	<b>79</b>	<b>70</b>
	<b>Cement</b>	<b>25</b>	<b>20</b>	<b>8</b>	<b>10</b>
	<b>Matrix</b>	<b>20</b>	<b>25</b>	<b>5</b>	<b>15</b>
	<b>Porosity</b>	<b>5</b>	<b>1</b>	<b>8</b>	<b>5</b>

(\*) Includes monocrystalline and polycrystalline species (chert, chalcedony and opal)

The composition of the sandstones of the Guárico Formation seems to be different depending on location. Samples located to the west (VMN-19 and VMN-20) have a higher

content of volcanic lithics than the easternmost samples (VMN-23 and VMN-28), (Figure 3.6). The proportion of alteration products (mostly clays) is also diminishing towards the east, and is probably related to the lack of susceptible materials like volcanic lithics and iron-magnesium-rich minerals in the eastern areas. The content of sedimentary lithics also seems to increase towards the east.

### **Matatere Formation**

General composition of the sandstones of the Matatere Formation is presented in Table 3.3. Lithic arenites and lithic graywackes of this unit are of medium to coarse grain-size (Figure 3.20). The bigger grains are usually monocrystalline quartz, well rounded and usually strained. Polycrystalline quartz is rare in most of the samples and, when found, grains are very well rounded. Potassic feldspars are absent in all of the samples excepting one located in the area of Yumare (VMN-44, Figure 3.8), from which a few grains of orthoclase were identified. Cryptocrystalline quartz occurs as either chalcedony or chert. Subhedral plagioclase crystals with different levels of alteration are present only in the graywackes (Table 3.3); identification using the angle of extinction was not feasible, but labradorite and andesine compositions were determined in a few grains. Accessory minerals include muscovite, biotite, and detrital hornblende, all altering to clay; the heavy mineral fraction is represented by zircon, pyrite, tourmaline, rutile and sphene.

Conglomerates are widely distributed along Matatere Formation, and have been identified at the north of Carora (Los Carrillos stream, site GPS-336 and Siquisique, GPS-343); (Figure 3.8). Pebbles from the conglomerates are also of a vast variety and are basically represented by chert, plutonic (quartz-monzo-diorites), volcanic, metamorphic (phyllites, quartz-mica-schists and quartzites) and sedimentary (limestones) rocks (Figure 3.21).

Table 3.3. General composition of arenites (in pink) and graywackes (white) of Matatere Formation using modal analysis (values are in %).

		VMN-5a	VMN-5b	VMN-6a	VMN-8a	VMN-10	VMN-6b	VMN-8b	VMN-9	VMN-11	VMN-12	VMN-14	VMN-44
Framework grains	Quartz*	93.0	91.5	95.0	95.5	50.7	87.1	89.6	52.1	58.9	49.2	50.8	52.4
	Plagioclases	0	0	0	0	19.06	0.63	0	6.06	11.71	14.89	13.17	12.27
	K-Feldspar	0	0	0	0	0	0	0	0	0	0	0	3.29
	Micas	0.25	1.08	0	0	6.54	0.94	0.28	0.9	2.45	4.04	11.55	11.97
	Heavy minerals	2.31	2.6	1.86	0	0.18	3.47	0.28	0.3	0.81	0.25	0.53	0.59
	Sedimentary lithics	0.77	0.65	0	2.83	1.12	0.63	4.03	1.51	1.08	0	0.26	0
	Metamorphic lithics	2.06	1.08	0.93	0.23	5.42	0.63	0	3.03	3.81	1.76	1.61	1.79
	Volcanic lithics	0.25	0	0.31	0	11.4	0.31	0.28	13.93	10.89	25.75	16.12	15.86
	Alteration products	1.28	3.04	1.86	1.17	5.04	5.36	0.28	19.69	6.53	3.78	6.91	1.49
	Hornblende	0	0	0	0	0.37	0.94	0	0	0	0.25	0	0.29
	Fossils	0	0	0	0	0.18	0	4.89	2.42	3.81	0	0	0
	Unknowns	0	0	0	0	0	0	0.28	0	0	0	0	0
Whole rock	<b>Grains</b>	<b>85</b>	<b>80</b>	<b>80</b>	<b>80</b>	<b>60</b>	<b>60</b>	<b>45</b>	<b>62</b>	<b>60</b>	<b>70</b>	<b>65</b>	<b>73</b>
	<b>Cement</b>	<b>10</b>	<b>10</b>	<b>10</b>	<b>7</b>	<b>29</b>	<b>15</b>	<b>35</b>	<b>20</b>	<b>10</b>	<b>15</b>	<b>20</b>	<b>10</b>
	<b>Matrix</b>	<b>5</b>	<b>10</b>	<b>5</b>	<b>13</b>	<b>10</b>	<b>25</b>	<b>20</b>	<b>15</b>	<b>30</b>	<b>15</b>	<b>15</b>	<b>15</b>
	<b>Porosity</b>	<b>&lt;1</b>	<b>0</b>	<b>5</b>	<b>0</b>	<b>1</b>	<b>0</b>	<b>0</b>	<b>3</b>	<b>0</b>	<b>0</b>	<b>0</b>	<b>2</b>

(\*) Includes monocrystalline and polycrystalline species (chert, chalcedony and opal)



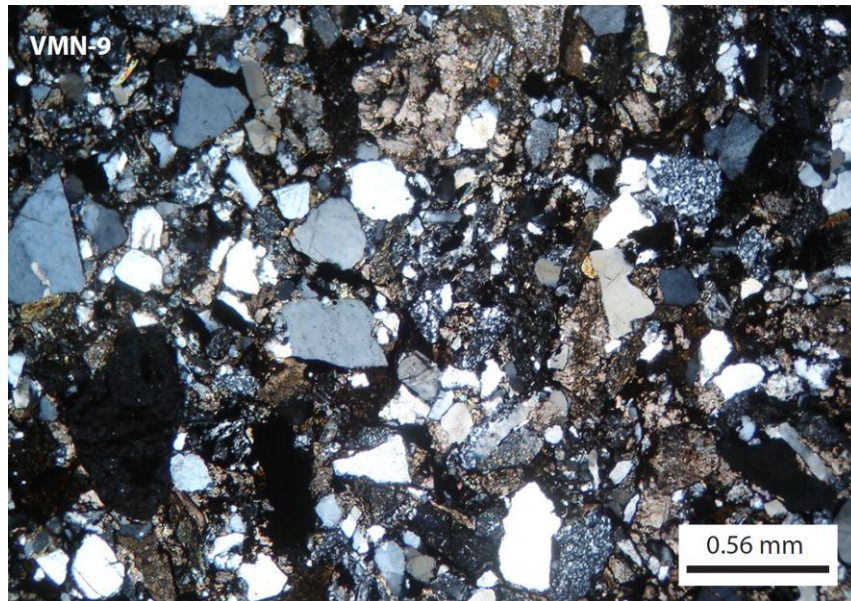


Figure 3.20. Lithic graywacke of Matatere Formation. Sample VMN-09.

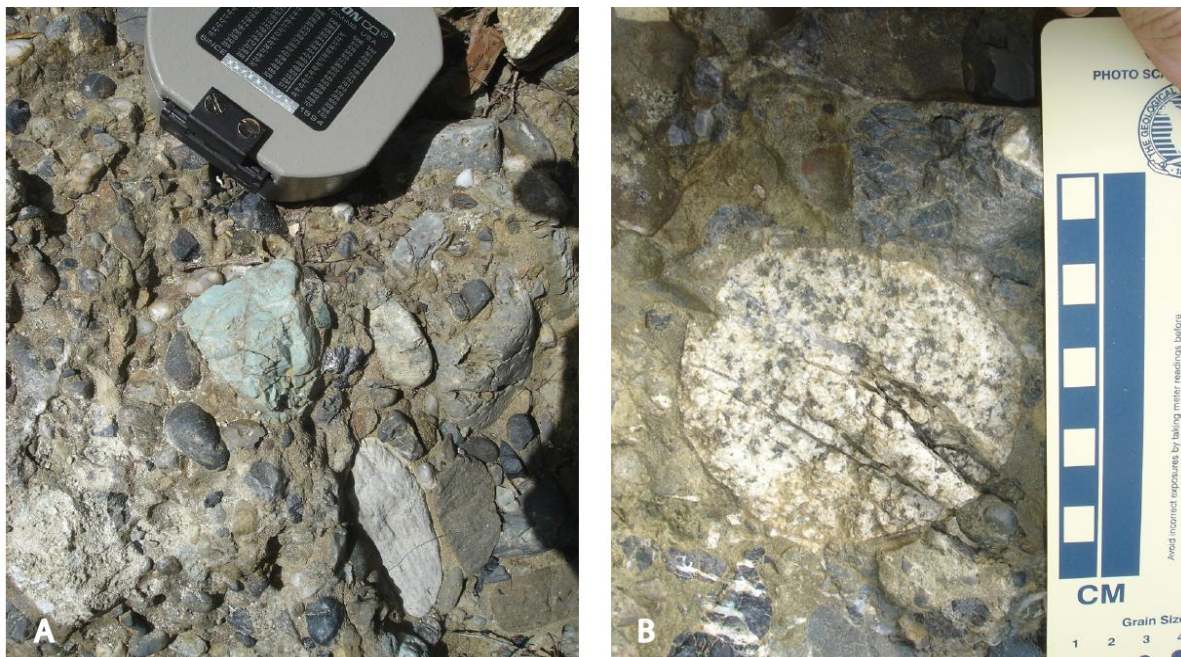


Figure 3.21. Pebbles in conglomerates of the Matatere Formation in the Siquisique area, site GPS-343. A) Volcanic fragments (in green and black colors); sample VMN-13. B) Monzodiorite (Sample VMN-15).

Volcanic fragments are present in most rocks; they are aphanitic and porphyritic, mostly altered to chlorite, and of a wide variety from intermediate to mafic composition (dacites, rhyolites, andesites and undifferentiated rocks). Metamorphic lithics (phyllites, quartz-mica-

schists and occasional quartzites) are also found. Sedimentary lithics are not so abundant, but fragments of shale, limestone and siltstone were observed. Reworked fossils were identified in samples located near Siquisique (Figure 3.8) and include fragments of foraminifera, brachiopods, echinoderms and algae.

The siliciclastic rocks of the Matatere Formation are very similar in texture and mineralogical composition to the lithic sandstones described on the island of Curacao. However, the detrital volcanic components of the Midden Curacao Formation have undergone much less weathering and alteration than the Matatere Formation. The sample of Lagoen Formation (CUR-14z; Figure 3.18a) also resembles the textural and mineralogical characteristics of the sandstones of Matatere Formation, at more similar alteration levels. This suggests the existence of a common source that fed the deposition centers of Midden Curacao and Matatere Formations, Curacao being more proximal to that source.

A general variation in composition, from southwest to northeast, is observed in the samples of the Matatere Formation (Figure 3.8, Table 3.3). In the southernmost areas lithic arenites coexist with lithic graywackes. To the north arenites are not found, and the proportions of volcanic lithics increase towards Siquisique, which is consistent with the information reported by Gonzalez de Juana et al. (1980) and Van Andel (1958). The content of chlorite also seems to increase towards the north, reflecting a higher content of unstable materials (intermediate volcanic rocks and/or ferromagnesian minerals) in the sediments of Matatere Formation. The increase of the volcanic content in the sandstones and conglomerates of Matatere Formation towards Siquisique may be a consequence of proximity to the Leeward Antilles volcanic arc at times of deposition.



## Pampatar Formation

Conglomeratic sandstones (samples VMN-39 and VMN-40) and carbonate sandstones (sample VMN-41) of the Pampatar Formation are moderately to poorly sorted and have angular to subangular grains (Figure 3.22). Their general composition is explained in Table 3.4. Volcanic quartz is abundant in these rocks and is usually less altered than the plutonic and metamorphic varieties. Feldspar grains are generally euhedral to subhedral. Alteration to sericite is very advanced in plagioclases, sometimes masking the mineral for a positive identification; however, a few grains could be identified as andesine, labradorite and, less altered, albite. Sheet silicates include detrital chlorite, muscovite and altered biotite. Other accessories are zircon, tourmaline, epidote, detrital calcite, chloritized hornblende and pyroxene, and pyrite.

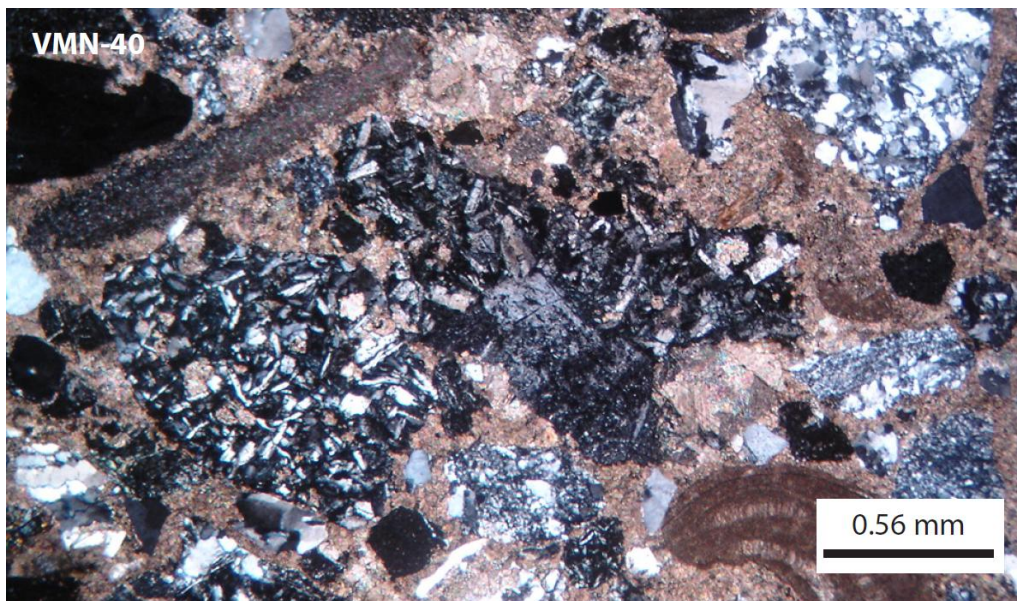


Figure 3.22. Lithic graywacke with carbonate matrix, Pampatar Formation. Sample VMN-40.

Fossils were often identified in the Pampatar samples. Fragments of foraminifera, mollusks, echinoderms and corals were found completely replaced by calcite (either spar or micrite) and chlorite (sample VMN-40). Additionally, sponge spicules, red and green algae, fragments of fusulinids, pelecypods, archaeocyathids and bryozoans occur in sample VMN-41.

Table 3.4. General composition of samples of Pampatar Formation using modal analysis (values are in %).

		VMN-39	VMN-40			VMN-41
Framework grains	Quartz*	40.5	22.5	Framework grains	Quartz*	19.7
	Plagioclases	18.07	7.12		Plagioclases	4.52
	K-Feldspar	2.28	1.09		K-Feldspar	0.79
	Micas	7.09	2.46		Micas	1.06
	Heavy minerals	0.45	0.27		Heavy minerals	0
	Sedimentary lithics	2.74	1.09		Sedimentary lithics	0.79
	Metamorphic lithics	2.28	1.91		Metamorphic lithics	1.58
	Volcanic lithics	21.51	43.01		Volcanic lithics	24.73
	Alteration products	3.2	6.3		Alteration products	17.28
	Hornblende	0.68	0		Hornblende	0
	Fossils	0	13.15		Fossils	29.52
	Unknowns	0.68	0.27		Unknowns	0
Whole rock	<b>Grains</b>	<b>69</b>	<b>40</b>	Whole rock	<b>Extraclasts</b>	<b>38</b>
	<b>Cement</b>	<b>15</b>	<b>30</b>		<b>Allochemicals</b>	<b>15</b>
	<b>Matrix</b>	<b>15</b>	<b>30</b>		<b>Orthochemicals</b>	<b>47</b>
	<b>Porosity</b>	<b>1</b>	<b>&lt;1</b>		<b>Porosity</b>	<b>&lt;1</b>

(\*) Includes monocrystalline and polycrystalline species (chert, chalcedony and opal)

The rocks of Pampatar Formation have a rich variety of lithic fragments. Shales, chert and fragments of micritic limestones are part of the sedimentary fraction. Metamorphic fragments of quartzite, meta-chert, quartz-mica-schist, phyllite and epidote-rich rocks are also found. The volcanic lithic fraction is large and it is generally represented by fragments of andesites, rhyolites, dacites, volcanoclastics and a high amount of aphanitic fragments that could not be differentiated due to alteration. Chlorite and serpentine are the most common alteration products in the volcanic unknowns, suggesting an originally mafic composition. Plutonic fragments were not identified in the collected samples; however Muñoz (1973) and Moreno & Casas (1986, in Rekowski & Rivas 2005) report hornblende-tonalite and granodiorite in conglomerates of the Pampatar Formation. Porphyritic andesite, pyroxene meta-andesite, porphyritic dacite, porphyritic meta-dacite, meta-tuff and meta-sandstone are also reported by the above mentioned authors.

## Caratas Formation

Three samples of the Caratas Formation were collected in northeastern Venezuela, in the surroundings of Barcelona City (Figure 3.14). Petrographic results show differences in the composition of these rocks (Table 3.5, Figure 3.23). Monocrystalline quartz is the most abundant mineral. Feldspars are present in variable concentrations as microcline and plagioclases. Glauconite grains are common in the sands of the Caratas Formation. Accessory minerals in these rocks are usually rutile, zircon, tourmaline, muscovite, and biotite. Fossils are frequent in the carbonate sands of the Caratas Formation, most commonly as planktonic foraminifera (sample VMN-29, Figure 3.23a).

Table 3.5. General composition of samples of the Caratas Formation (values are in %).

		VMN-29			VMN-30	VMN-31
Framework grains	Quartz*	19	Framework grains	Quartz*	55	45
	Plagioclases	0		Plagioclases	4	1
	K-Feldspar	0		K-Feldspar	6	2
	Micas	<1		Micas	1	1
	Heavy minerals	0		Heavy minerals	2	2
	Sedimentary lithics	1		Sedimentary lithics	4	0
	Metamorphic lithics	0		Metamorphic lithics	0	1
	Volcanic lithics	0		Volcanic lithics	1	0
	Alteration products	0		Alteration products	5	9
	Hornblende	0		Hornblende	0	0
	Glauconite	5		Fossils	0	1
	Accessories	<1		Glauconite	2	7
Whole rock	Extraclasts	25	Whole rock	Grains	80	69
	Allochemicals	30		Cement	10	25
	Orthochemicals	45		Matrix	10	5
	Porosity	<1		Porosity	<1	1
Name of the rock		Packstone	Name of the rock		lithic arenite	lithic Graywacke

The lithic fraction in the sandstones of the Caratas Formation is not as rich as in samples of other turbidite units (e.g. Guárico, Matatere, Midden Curacao Formations); however, fragments of chert and biotite-phyllite are observed. Advanced substitution by calcite, dolomite, and clay masked some lithic fragments, making their identification difficult.

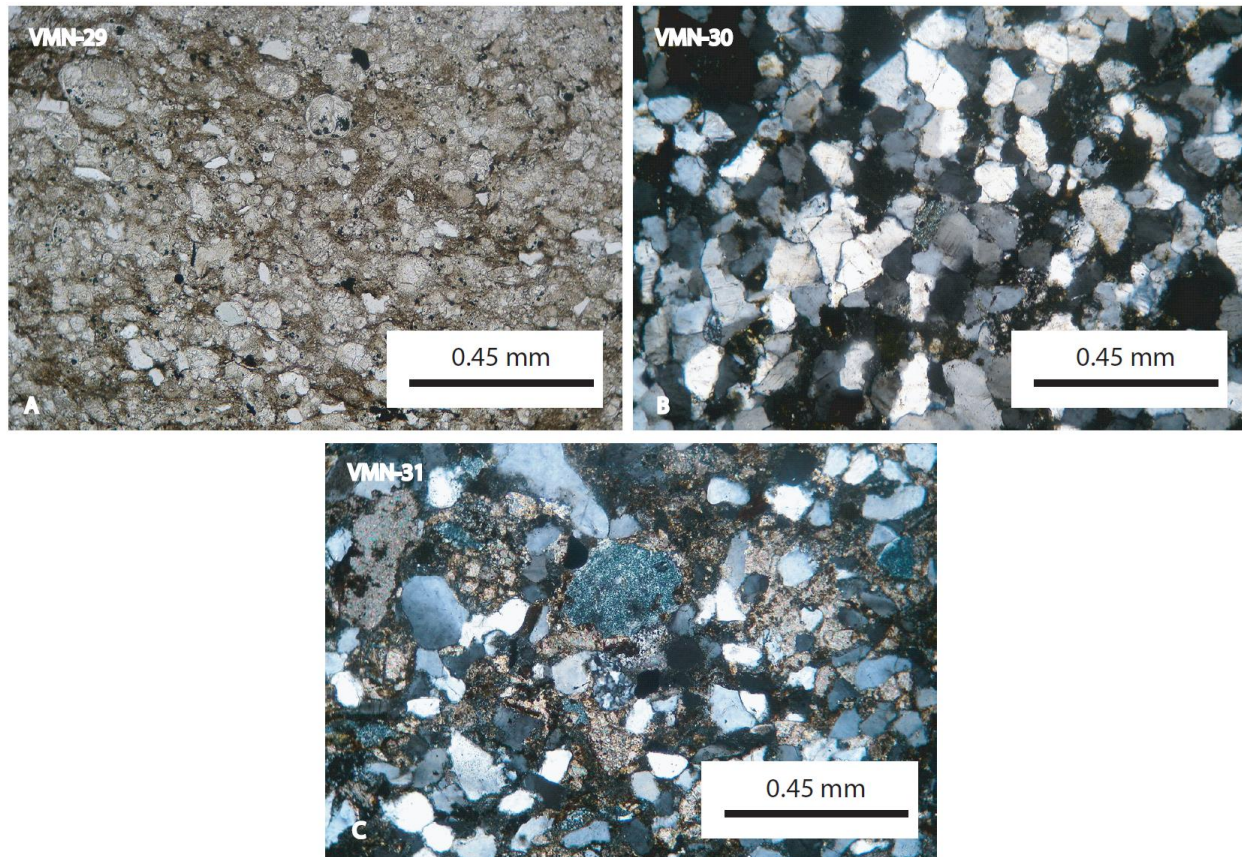


Figure 3.23. Facies of the Caratas Formation. (A) Packstone; (B) Lithic arenite; (C) Lithic graywacke.

### Los Arroyos Formation

Sandstones in Los Arroyos Formation (Figure 3.24) are medium-grained to conglomeratic. Quartz usually represents the coarse fraction of the grains; monocrystalline quartz is dominant over the polycrystalline varieties in these rocks (Table 3.6). Feldspars are generally absent in the samples of the Los Arroyos Formation. Accessory minerals include biotite, muscovite, zircon, tourmaline, apatite, sphene, detrital calcite and detrital glauconite.

Metamorphic and sedimentary rock fragments are abundant in the turbidite sands of the Los Arroyos Formation. Biotite-phyllite, quartz-muscovite-schist, and quartzite are present, along with fragments of chert, limestone, and sandstones. Volcanic fragments were also identified; they are usually aphanitic and with abundant vesicles filled with quartz. This volcanic



variety was identified in all the turbidite units under study, with the exception of Caratas Formation. Most of the lithic grains are usually rounded to well rounded, contrasting with the sub-angular mineral grains. Micas within the metamorphic lithics show alteration to clay minerals, probably as a result of tropical weathering.

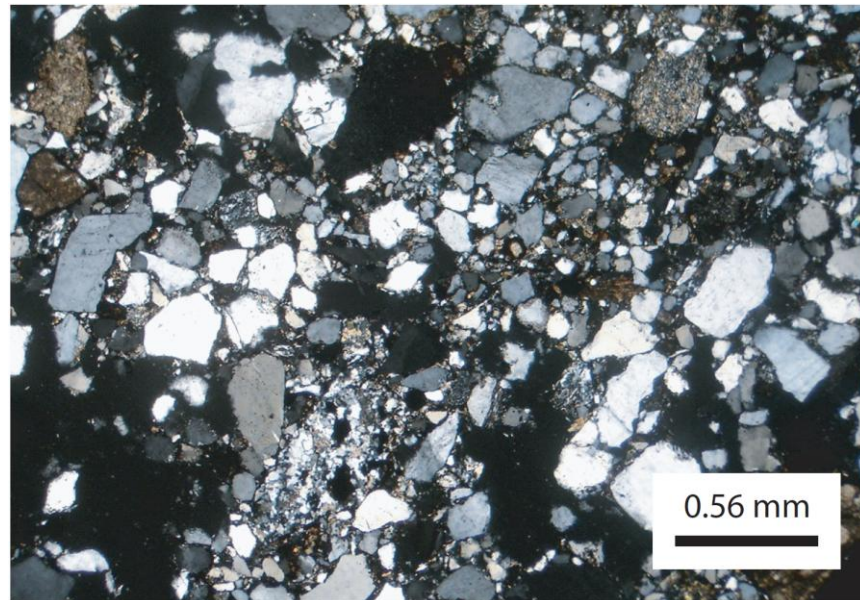


Figure 3.26. Lithic graywacke of the Los Arroyos Formation. Sample VMN-42.

Table 3.6. General composition of samples of the Los Arroyos Formation (values are in %).

		VMN-42	VMN-43
Framework grains	Quartz*	39	44
	Plagioclases	0	0
	K-Feldspar	0	0
	Micas	1	1
	Heavy minerals	5	3
	Sedimentary lithics	3	6
	Metamorphic lithics	5	6
	Volcanic lithics	7	4
	Alteration products	0	0
	Hornblende	0	0
	Fossils	0	1
	Glauconite	<1	0
Whole rock	<b>Grains</b>	<b>60</b>	<b>65</b>
	<b>Cement</b>	<b>15</b>	<b>10</b>
	<b>Matrix</b>	<b>15</b>	<b>20</b>
	<b>Porosity</b>	<b>10</b>	<b>5</b>

## Discussion

In general, sandstones from Matatere, Guárico, Pampatar, Lagoen, Midden Curacao, Caratas and Los Arroyos Formations are generally quartz-lithic (graywackes) or quartz-rich (arenites), and contain a wide variety of lithics, including chert, limestones, shales, phyllites, quartz-mica-schists, plutonic fragments of acidic composition and volcanic fragments in a spectra that ranges from felsic to mafic and ultramafic compositions. The volcanic content in the lithic graywackes dominates over the metamorphic and sedimentary rock fragments (except in Caratas and Los Arroyos Formations). Feldspars constitute a minority fraction in these rocks; potassium feldspars are rare, while plagioclase of intermediate (andesine-labradorite) composition were often identified.

The heterogeneous composition of the samples suggests a mixed provenance (volcanic and continental sources) that is consistent with previous reports on these turbidite deposits (Matatere Formation, Kasper & Larue, 1986; Martinez & Valleta, 2008; Guárico Formation, Albertos, 1989; Yoris & Albertos, 1989; Pampatar Formation, Moreno & Casas, 1986). When plotted in Quartz-Feldspar-Lithics (QFL) provenance diagrams, the modal count data separate the rocks into two major groups, represented by the quartz-rich (arenites of Matatere and Guárico Formations) and lithic facies (graywackes of Matatere, Guárico and Pampatar Formations, and Curacao island); (Figure 3.25a,b). Similar results were obtained when comparing the volcanic lithic fraction (Lv) versus the continental-related components (polycrystalline quartz, Qp, and sedimentary lithics, Ls); (Figure 3.25c).



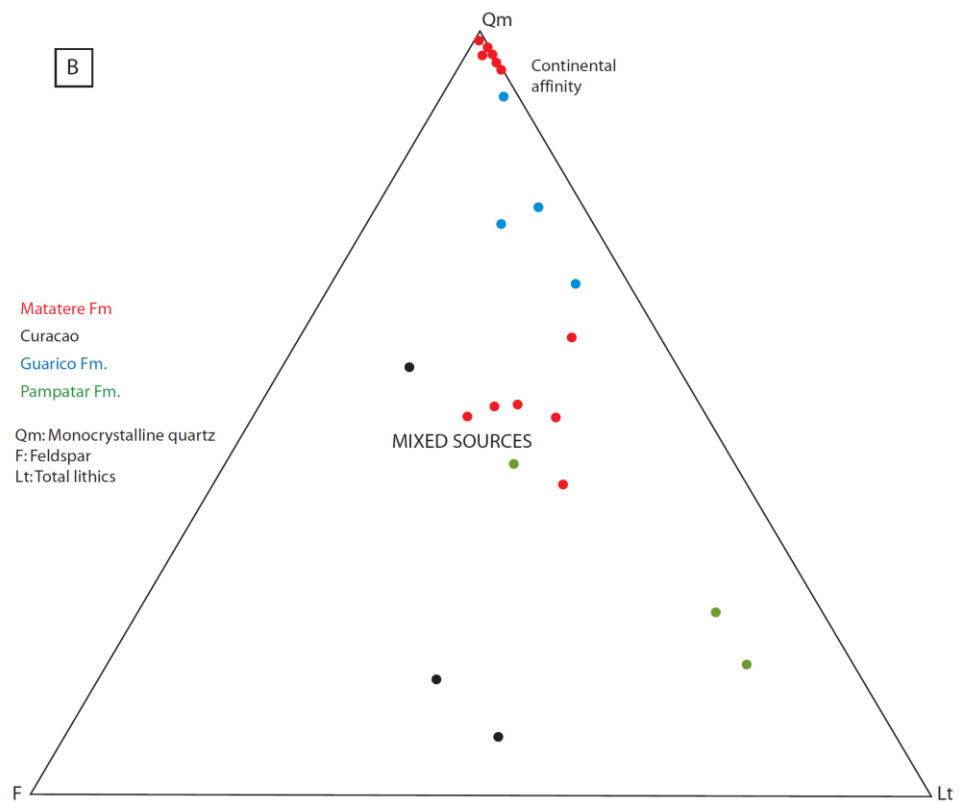
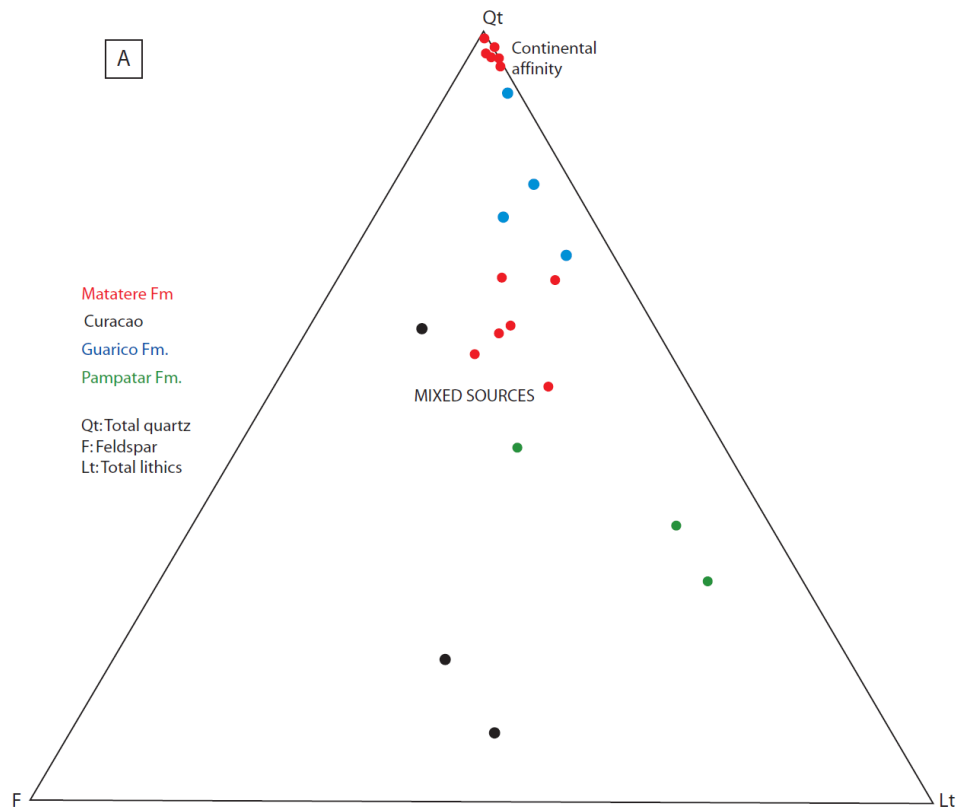


Figure 3.25. Provenance of the turbidite samples (modified after Dickinson, 1985).

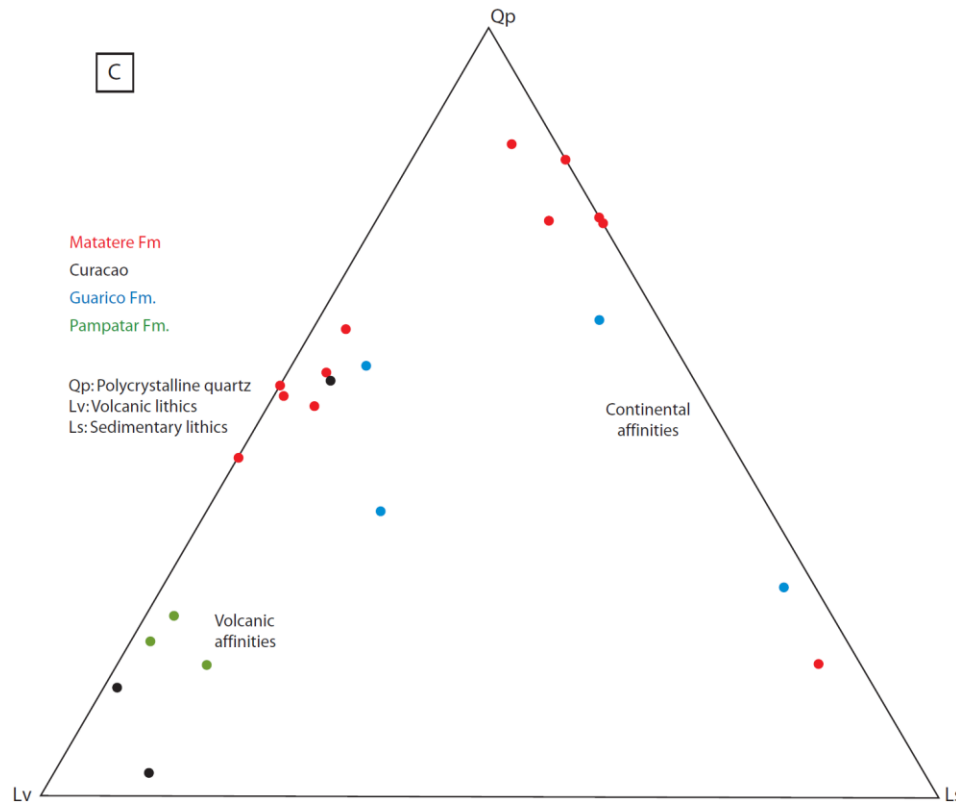


Figure 3.25. (cont.) Provenance of the turbidite samples (modified after Dickinson, 1985).

Variations in composition related to geographic location indicate a major influence of a volcanic source in the northwest of Venezuela (lithic-graywackes of Matatere Formation, Guárico Formation and Curacao Island) compared to the south, where continental facies are more abundant (arenites of Matatere and Guárico Formations, and sands of Caratas and Los Arroyos Formations). Proximity to a volcanic source (Leeward Antilles volcanic arc) located to the northwest of Venezuela must have controlled the deposition of the different facies of these turbidite sequences in Maastrichtian – Miocene time.

Principal Component Analyses (PCA) tested the distribution of the Early Cretaceous passive margin and Late Cretaceous – Middle Eocene turbidite samples (excluding Caratas and Los Arroyos Formations), using their framework components as variables (Figure 3.26). Results of this test are consistent with the petrographic data and with the results obtained from the

provenance triangles (mixed sources). Samples of the passive margin units, together with the quartz-rich fraction of Matatere Formation and Guárico Formation show a strong influence from the total quartz (Qt) and monocrystalline quartz (Qm) variables (continental influence). Graywackes of Matatere, Guárico, Pampatar and Curacao Formations correlate well with the volcanic lithics (Lv), which indicates a strong volcanic influence.

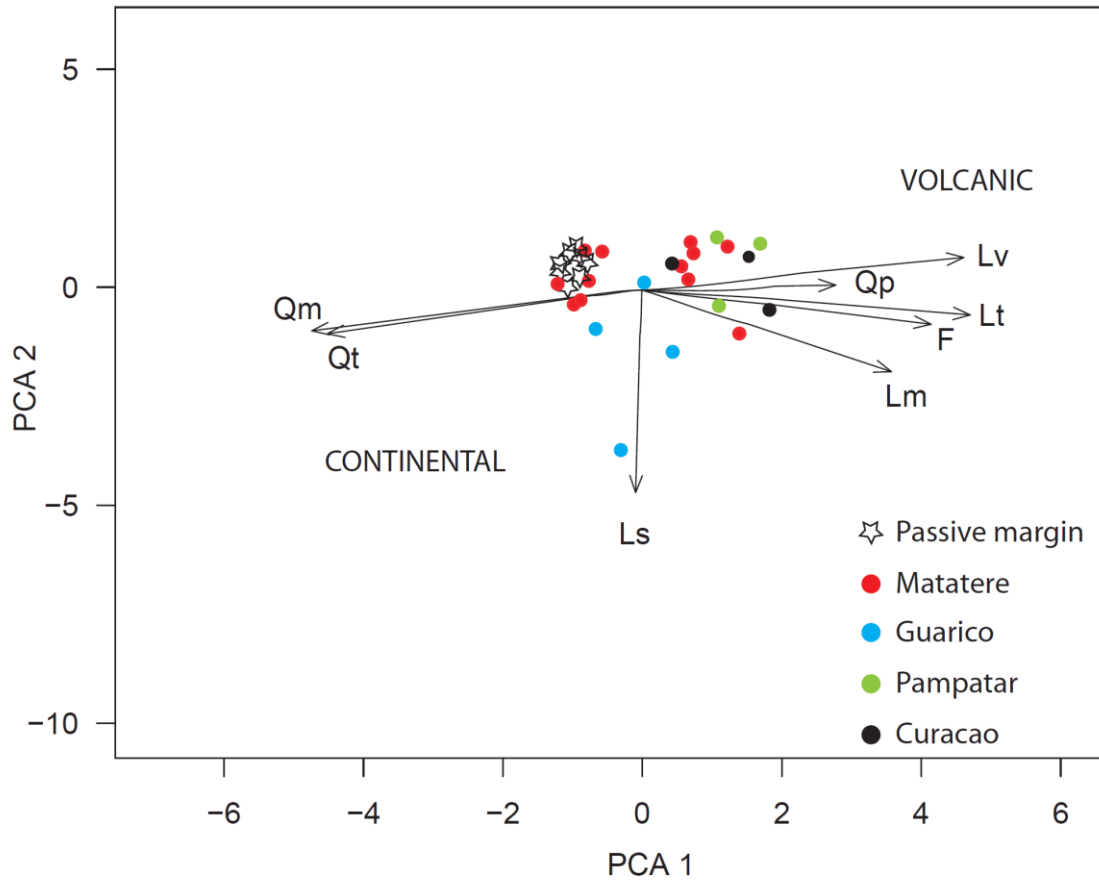


Figure 3.26. Principal Component Analysis correlation biplot comparing Early Cretaceous passive margin and Late Cretaceous-Eocene turbidite samples.

In conclusion, the components of the Maastrichtian – Miocene turbidite sequences were the result of a combined derivation from continental and volcanic-arc rocks. Deposition of these sequences was controlled by the development of a foredeep basin on the convex side of a volcanic arc (the Leeward Antilles volcanic arc, Figure 3.27). This foredeep basin received variable proportions of continental and volcanic sediments depending on the proximity of the

exposed terranes of the passive margin, Guayana Shield (south) and the Leeward Antilles (northwest). Continuous subsidence of this basin and accretion along the subduction front provided the tectonic instability responsible for the inclusion of allochthonous blocks (olistoliths) in these deposits.

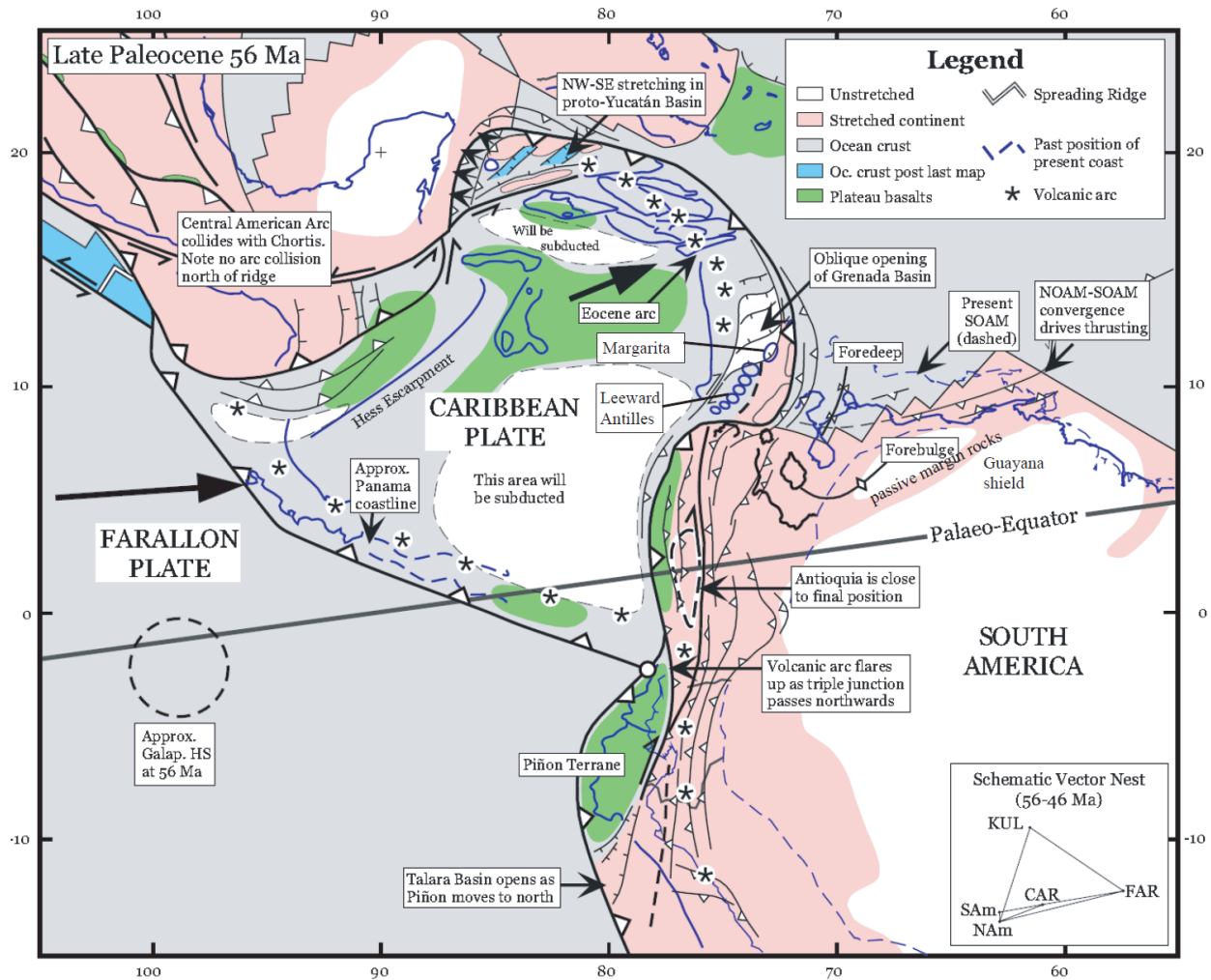


Figure 3.27. Tectonic reconstruction of the Caribbean region by Late Paleocene time (Pindell & Kennan, 2001)

## **DETRITAL ZIRCON AGES**

### **Lagoen and Midden Curacao Formations**

LA-ICP-MS detrital zircon ages from samples of the Midden Curacao and Lagoen Formations range between  $2684.9 \pm 16.8$  Ma (Late Archean) and  $66.4 \pm 3.8$  Ma (end of Maastrichtian); (Figure 3.28). Age distributions peaking at 2700 Ma (Late Archean), 1200 and 980 Ma (Middle Proterozoic) and 634 Ma (Late Proterozoic) are consistent with a passive margin signature, including the “Grenville” (Chapter 2). Detrital zircons of Early Triassic (247 Ma) and Campanian (74 Ma) ages are also identified in the younger fraction of the Curacao turbidites. Ages ranging 100 and 200 Ma are nonexistent (Figure 3.29) in these rocks.

### **Guárico Formation**

The detrital zircon ages of Guárico Formation vary between Late Archean ( $2962.1 \pm 26.1$  Ma) and Paleocene ( $63.1 \pm 4.6$  Ma); (Figure 3.29). Grains older than 400 Ma show a signature that is very similar to that of the passive margin units, also including the “Grenville” age (Figure 2.20, Chapter 2). New peaks are identified at 235 Ma (Middle Triassic), 160 Ma (Late-Middle Jurassic), and 66 Ma (Maastrichtian-Paleocene). Variations in the pattern of the cumulative distribution function (CDF; Guynn, 2006) in samples of the Guárico Formation may indicate differences in provenance (Figure 3.30). According to this scenario, the detrital fraction of samples VMN-20 and VMN-23 (located in the areas of San Juan de los Morros and Camatagua, Figure 3.6) was probably shed from a source different (or less similar) than the rocks from which samples VMN-19 (San Carlos) and VMN-20 (Boca de Uchire) were derived. Relative location of these samples (of heterogeneous composition, Table 3.2), combined with possible lateral facies variations, point to changes in the source(s) that fed the Guárico basin in Late Cretaceous-Paleocene time.

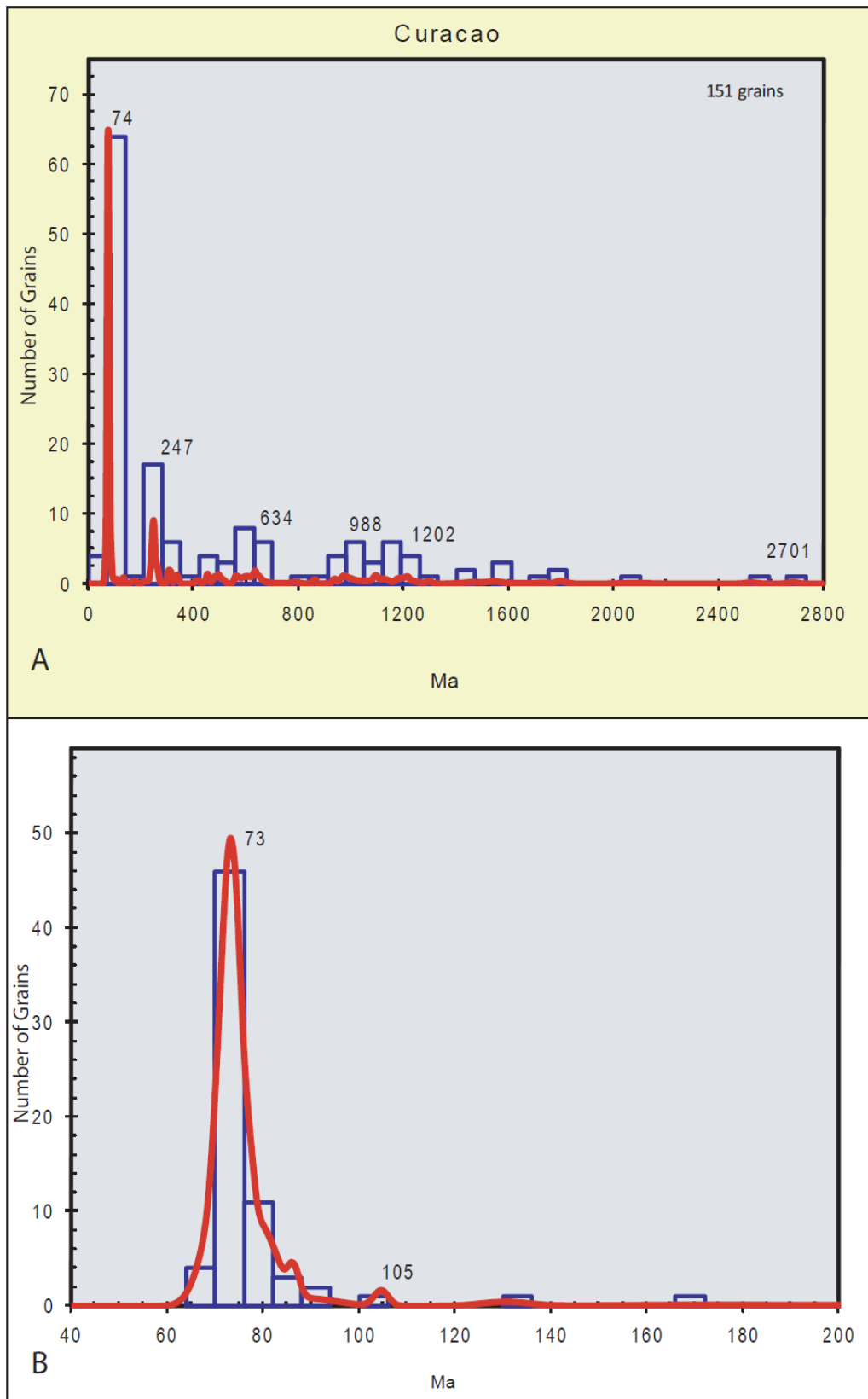


Figure 3.28. Age distribution of samples of the Midden Curacao and Lagoen Formations in Curacao island. A) 3000 – 0 Ma age interval. B) 200 – 20 Ma age interval.

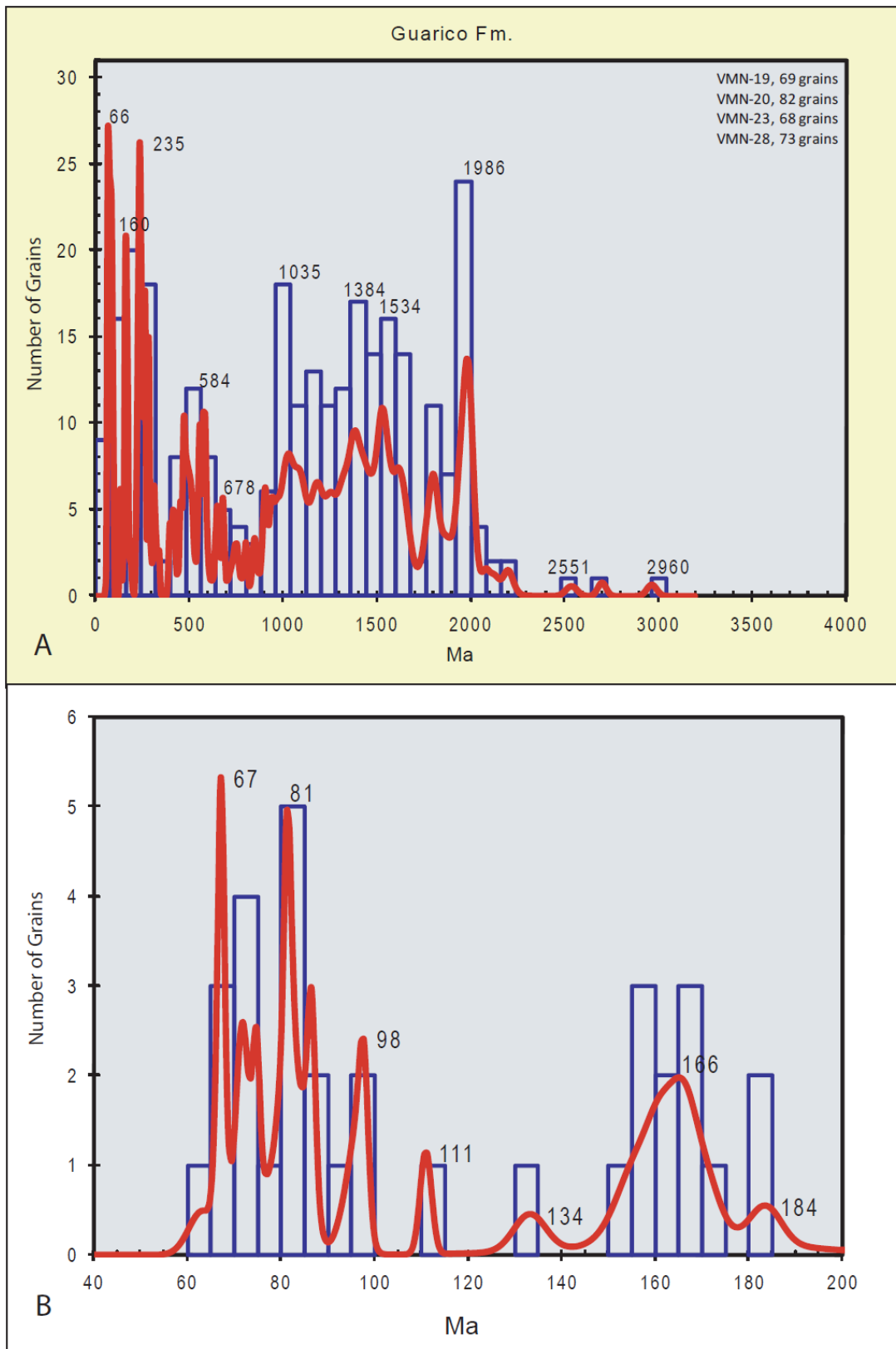


Figure 3.29. Age distribution of samples of the Guárico Formation. A) 3000 – 0 Ma age interval. B) 200 – 20 Ma age interval.

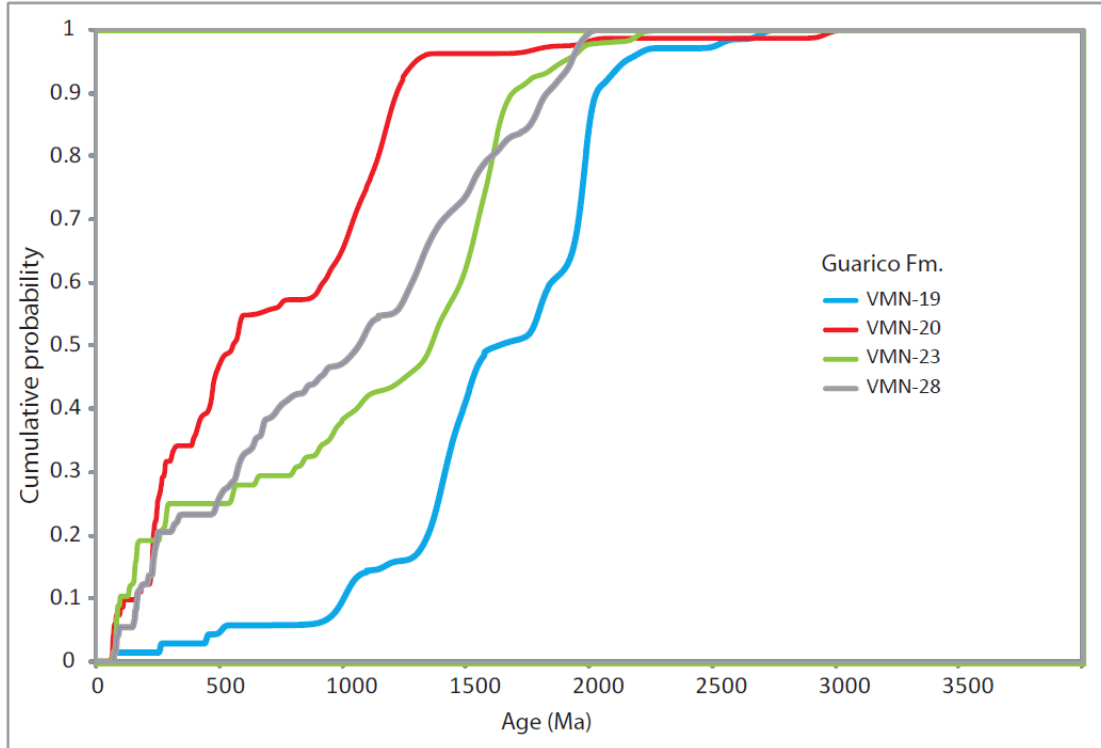


Figure 3.30. Cumulative Distribution Functions (CDFs) for the detrital zircon ages in samples of Guárico Formation.

### Matatere Formation

Detrital zircon ages from nine (9) samples of Matatere Formation range between  $2841 \pm 16.3$  Ma (Late Archean) and  $39.4 \pm 1.5$  Ma (Eocene); (Figure 3.31). As in samples of Guárico Formation, the age distribution patterns of Matatere Formation resemble that from the passive margin (main peaks at 2800, 1835, 1540, and 600 Ma, and the “Grenvillian” at 1000 and 1200 Ma). Additionally, peaks at 240 Ma (Early Triassic), 70 Ma (Campanian-Maastrichtian) and 53 Ma (Eocene) are seen in the detrital fraction of Matatere Formation (Figure 3.31b). No grains between 100 and 120 Ma are identified in the detrital zircons of this unit.



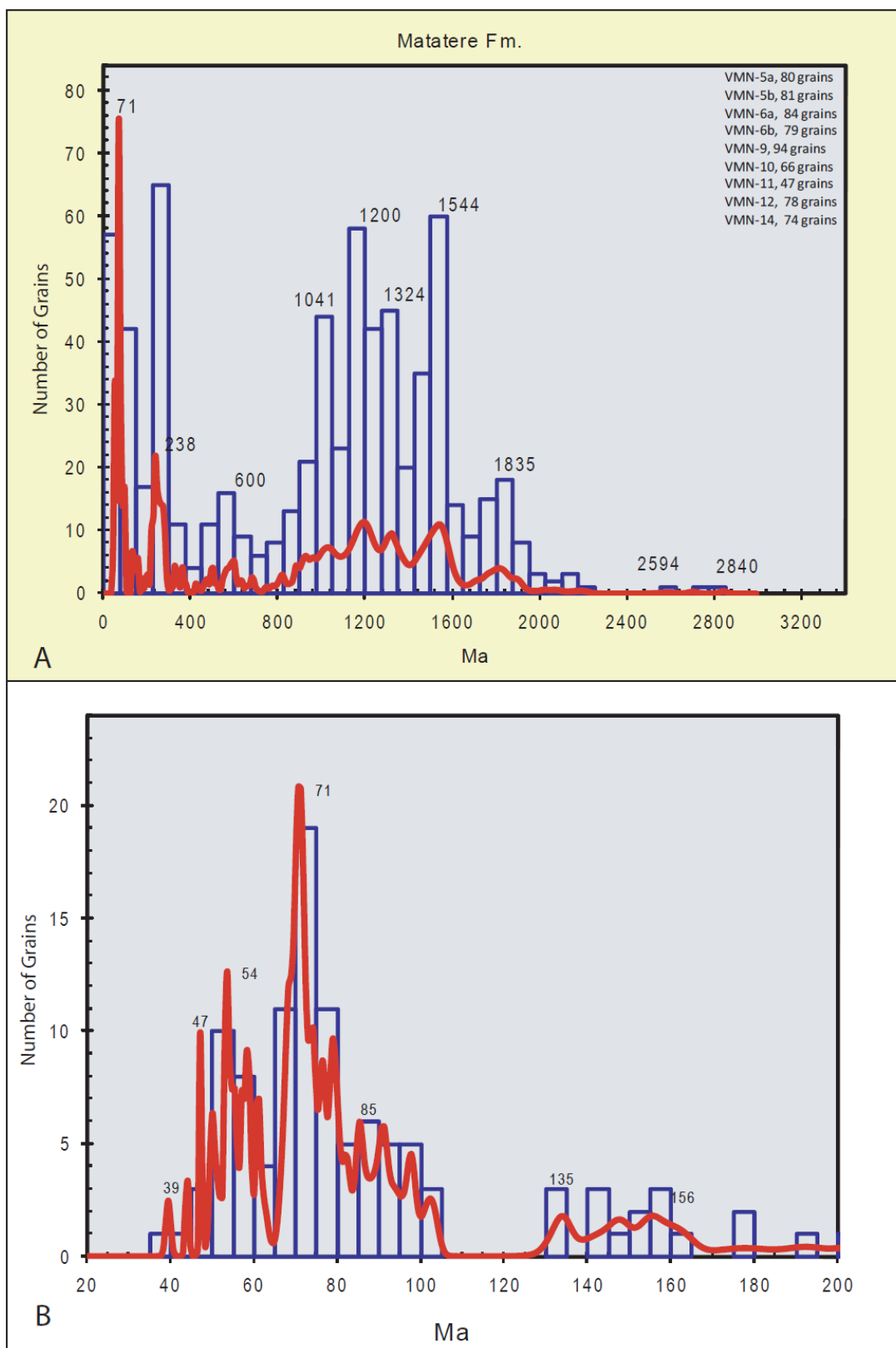


Figure 3.31. Detrital zircons age distributions of samples of the Matatere Formation. A) 3000 – 0 Ma age interval. B) 200 – 20 Ma age interval.

Cumulative distribution functions (CDFs) of the detrital zircon data of Matatere Formation (Figure 3.32) show variations between samples. About 50% of the detrital zircon population in samples of Siquisique (VMN-12 and VMN-14, Figure 3.8) is younger than 250 Ma (Permian-Triassic), compared to proportions of 10 – 25% in the rest of the samples. Additionally, 25% to 30% of the zircon population is younger than 100 Ma in the samples from Siquisique. The high volcanic content (both volcanic lithics and plagioclases) of these two samples is consistent with the data of the CDFs.

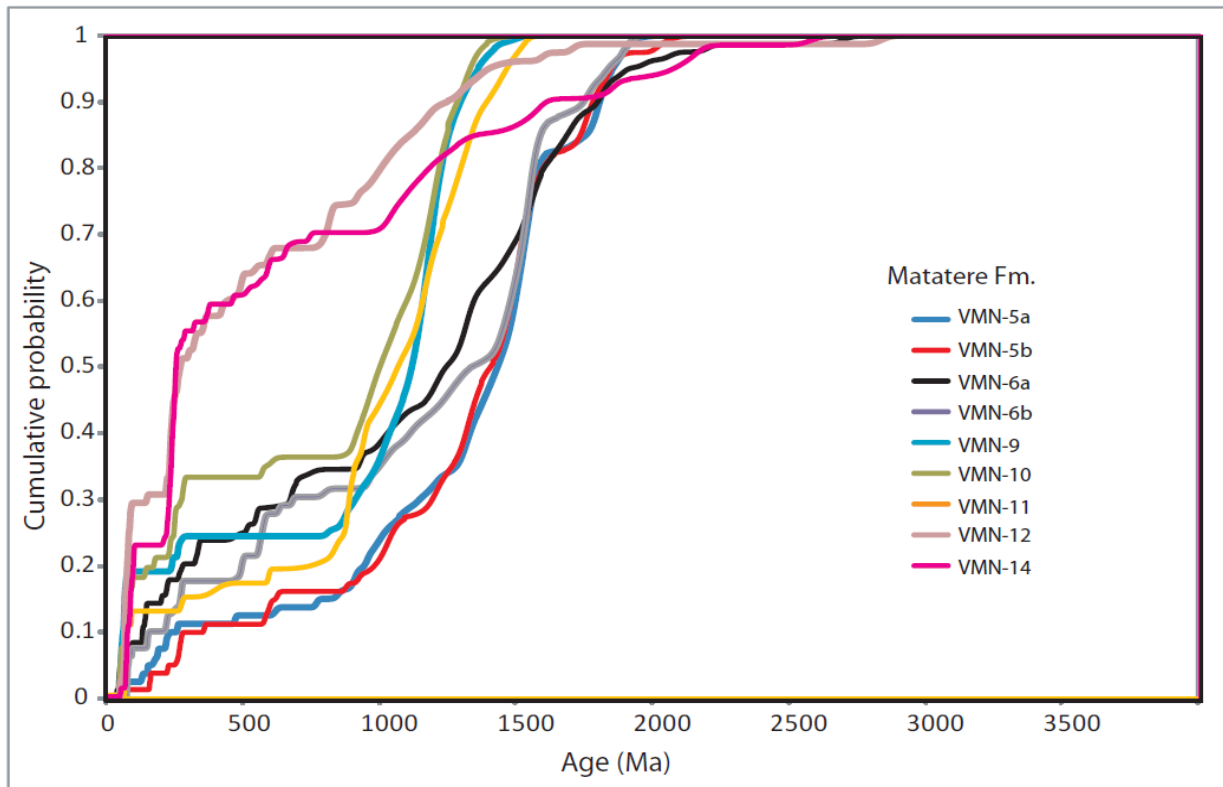


Figure 3.32. Cumulative Distribution Functions (CDFs) for the detrital zircon ages in samples of Matatere Formation.

### Pampatar Formation

The oldest detrital zircon grain from three samples of Pampatar Formation is of Late Archean age ( $2626.8 \pm 16.6$  Ma), while the youngest grain is of Eocene age ( $49.1 \pm 0.9$  Ma).

Older grains indicate ages of Early Proterozoic (2084 Ma), Middle Proterozoic (1220 Ma and 1054 Ma), Early Cambrian (535 Ma) and Middle Triassic (239 Ma). Younger grains group at 74 Ma (Campanian) and 49 Ma (Eocene). Grains of ages between 120 and 200 Ma are absent from the sandstones of Pampatar Formation (Figure 3.33).

### **Caratas and Los Arroyos Formations**

The detrital zircon data of Caratas and Los Arroyos Formations, in Eastern Venezuela, are distinctive from the other turbidite units. No grains of Cretaceous or younger age were found in the detrital fraction of these units. In Caratas Formation, ages range between  $2916 \pm 24.5$  Ma and  $1425 \pm 23.7$  Ma; whereas detrital zircon grains of the Los Arroyos Formation are constrained between  $2292.8 \pm 34.2$  Ma and  $499.1 \pm 9.4$  Ma (Figure 3.36).

For both Caratas and Los Arroyos Formations a strong continental derivation is indicated, although some variations occur. For instance, grains of Paleozoic (peaks at 500 Ma and 635 Ma) and Grenville ages (peaks at 1035 Ma and 1241) are present in the detrital fraction of Los Arroyos Formation (Figure 3.34), suggesting combined sources from Guayana Shield, El Baúl and the Colombian Andes, as previously seen in Early Cretaceous passive margin units of northern Venezuela, including the Barranquín Formation. The Caratas Formation, on the other hand, shows a detrital signature that is limited only to crystalline rocks of the Guayana Shield (Figure 2.23, Chapter 2).

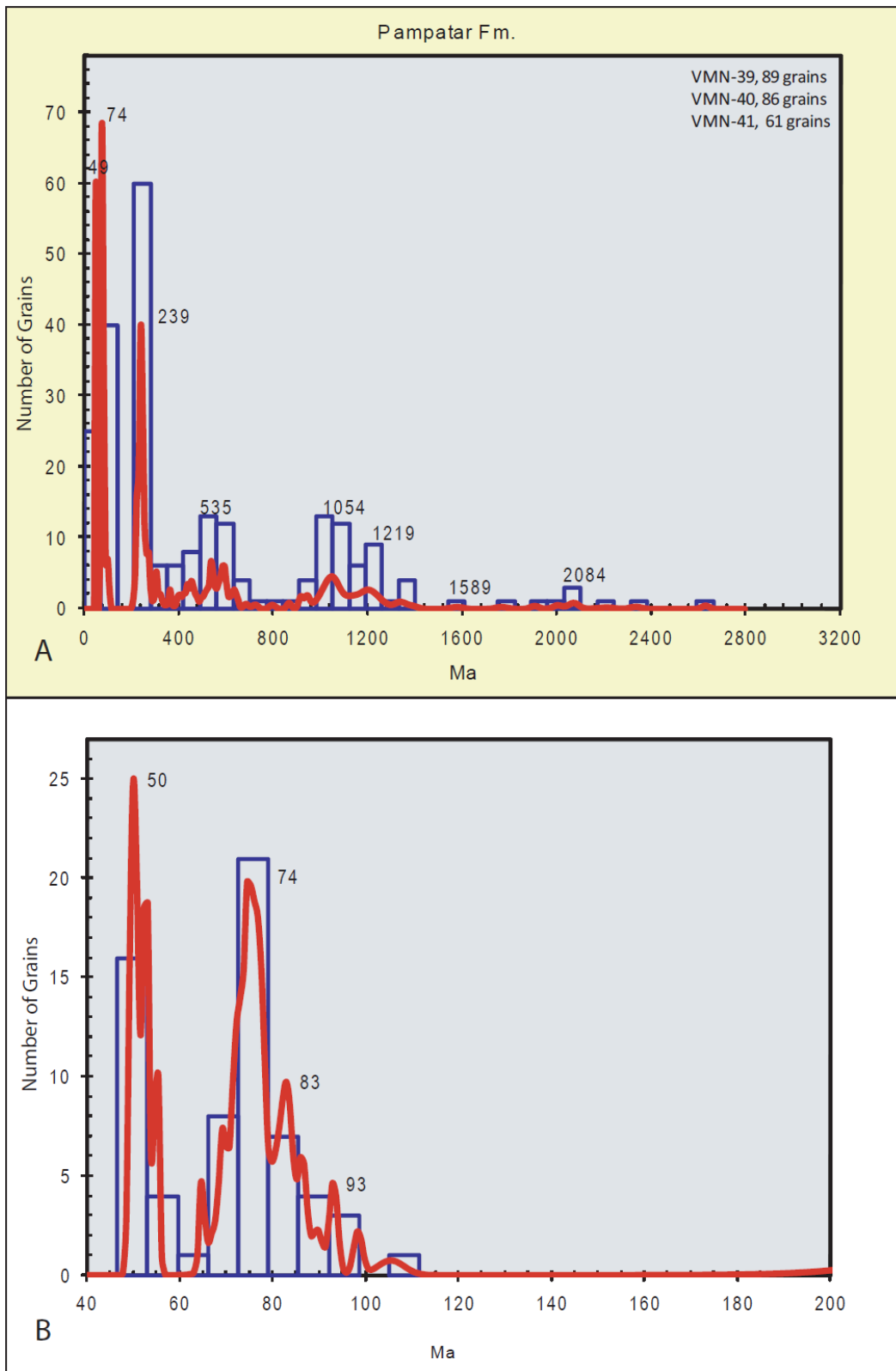


Figure 3.33. Age distribution of samples of the Pampatar Formation. A) 3000 – 0 Ma age interval. B) 200 – 20 Ma age interval.

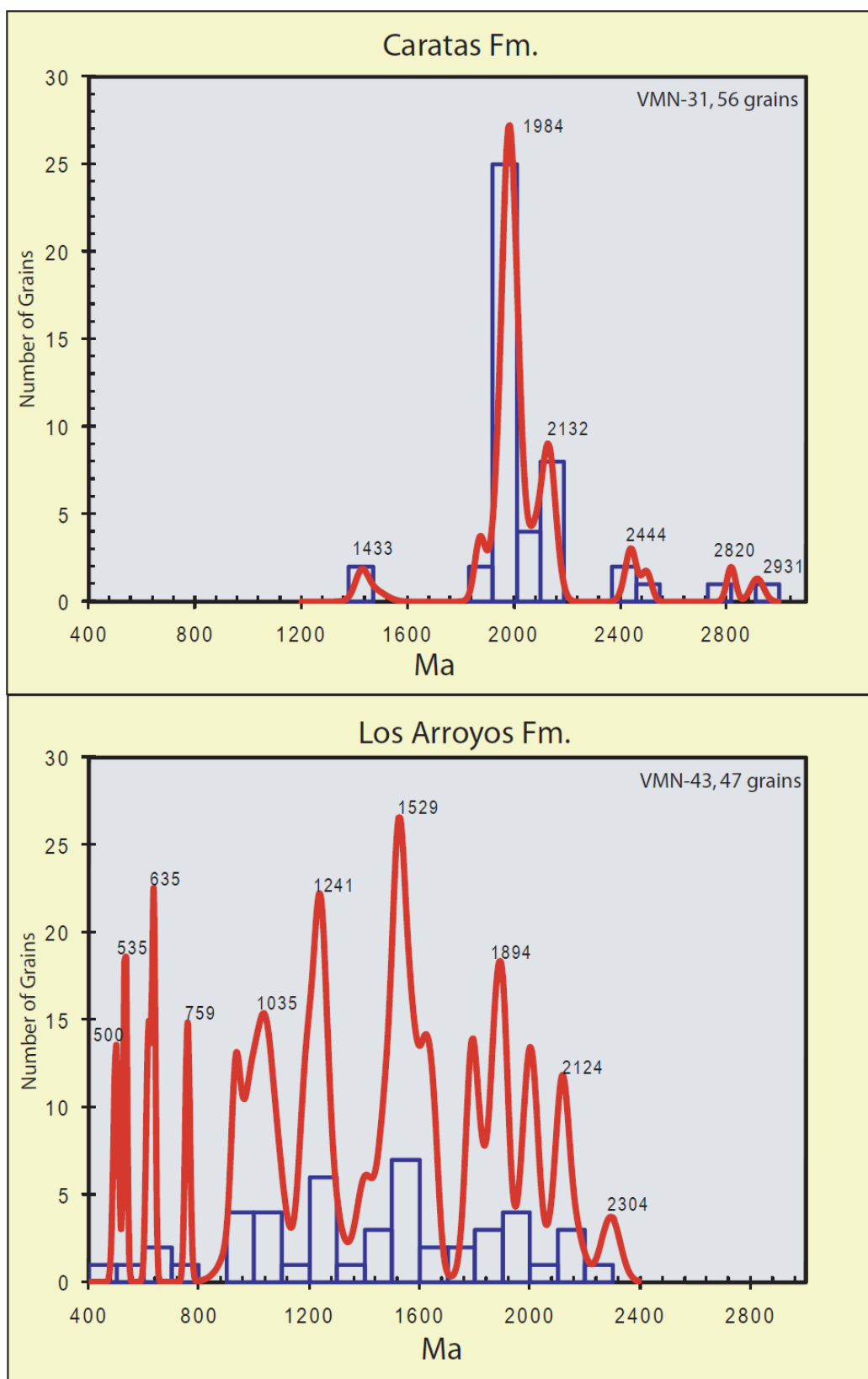


Figure 3.34. Age-distribution of detrital zircon grains of Caratas and Los Arroyos Formations, Eastern Venezuela.

## Discussion

In general, detrital zircon ages of the turbidite units range between 2800 Ma and 40 Ma (Figure 3.35). Ages older than 420 Ma have a distribution pattern resembling that from the continental passive margin units, suggesting that reworking of the Early Cretaceous units (Aguardiente, Agua Blanca, Bobare and Barranquín Formations) contributed to the building of the Maastrichtian – Miocene units. “Grenville” ages between 980 and 1200 Ma are identified in the Maastrichtian – Middle Eocene units (except Caratas Formation), and are associated with the detrital fraction of the passive margin. Ages of 240 Ma (Middle Triassic) are not identified in the Early Cretaceous units, suggesting exposition of a Triassic basement in times no earlier than Late Cretaceous. Detrital zircon ages between 200 Ma and 100 Ma are practically nonexistent, only in Guárico Formation ages of about 160 Ma are registered (Figure 3.29), and may indicate absence of magmatism or thermal events in the proximities of northern Venezuela at least during Early Cretaceous time (140-99 Ma). Finally, grains of Late Cretaceous age (100 Ma) and younger are indicative of magmatism associated with the subduction of the Caribbean Large Igneous Province and the Leeward Antilles volcanic arc.

Interpretations of dual provenance in the turbidites units are supported by the detrital and petrographic data. Cumulative distribution functions (Figure 3.36) are another example of the good correlation between the composition and age of these sediments. Units located in Margarita (Pampatar Formation) and Curacao islands (Lagoen and Midden Curacao Formations) have a strong volcanic influence (Leeward Antilles arc), with up to 40% of detrital grains of Late Cretaceous age. Matatere and Guárico Formations represent a mixture of volcanic and continental sources, with average values of 15% of Leeward Antilles-related zircons. The

Precambrian-age zircons of Caratas and Los Arroyos Formations separate these units from the rest, indicating a clearly dominant continental (passive margin) affinity.

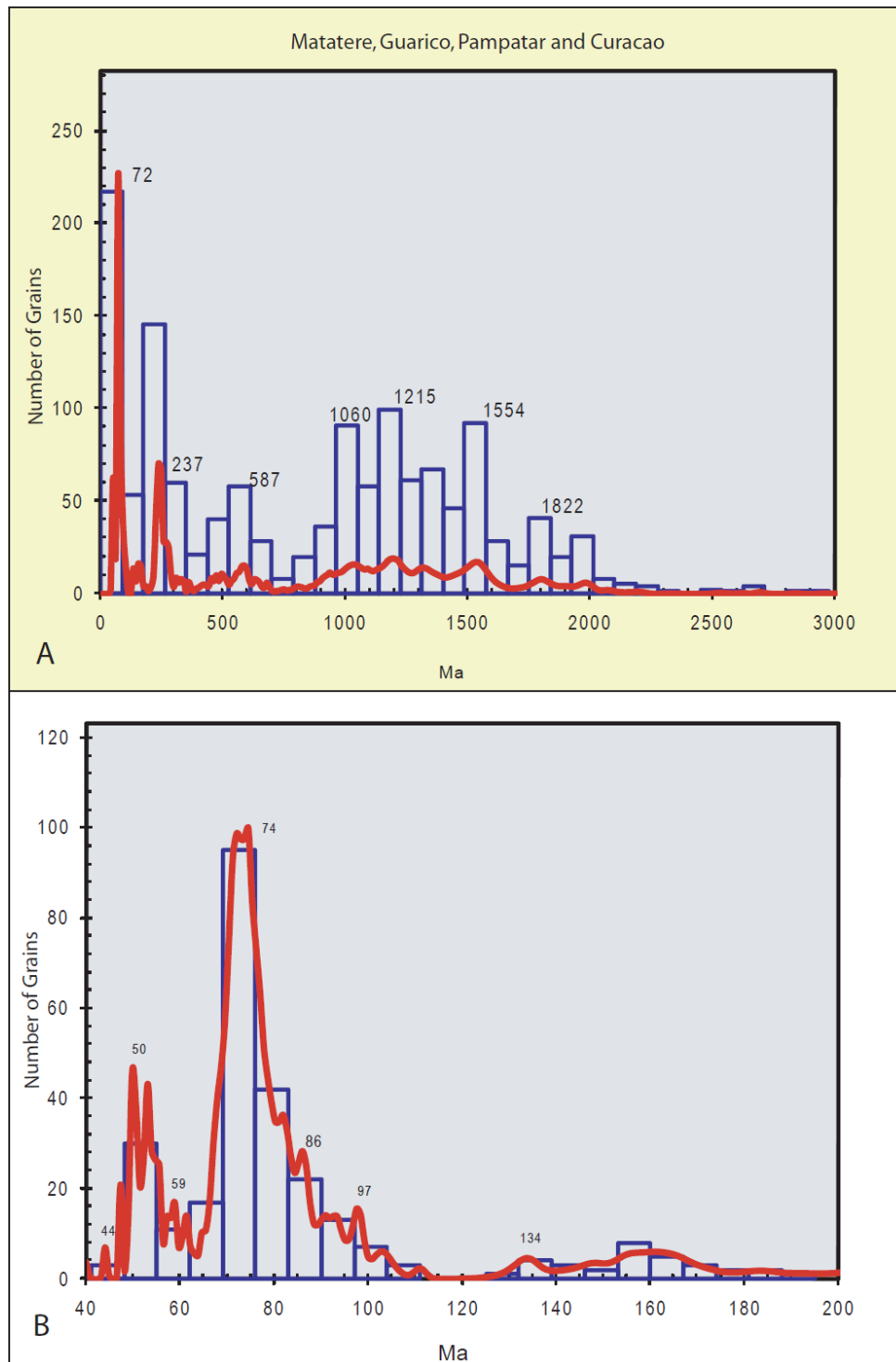


Figure 3.35. General age distribution of the Paleocene turbidites in northern Venezuela (Matatere, Guárico and Pampatar Formations) and Curacao (Lagoon and Midden Curacao Formations). A) 3000 – 0 Ma age interval. B) 200 – 20 Ma age interval.

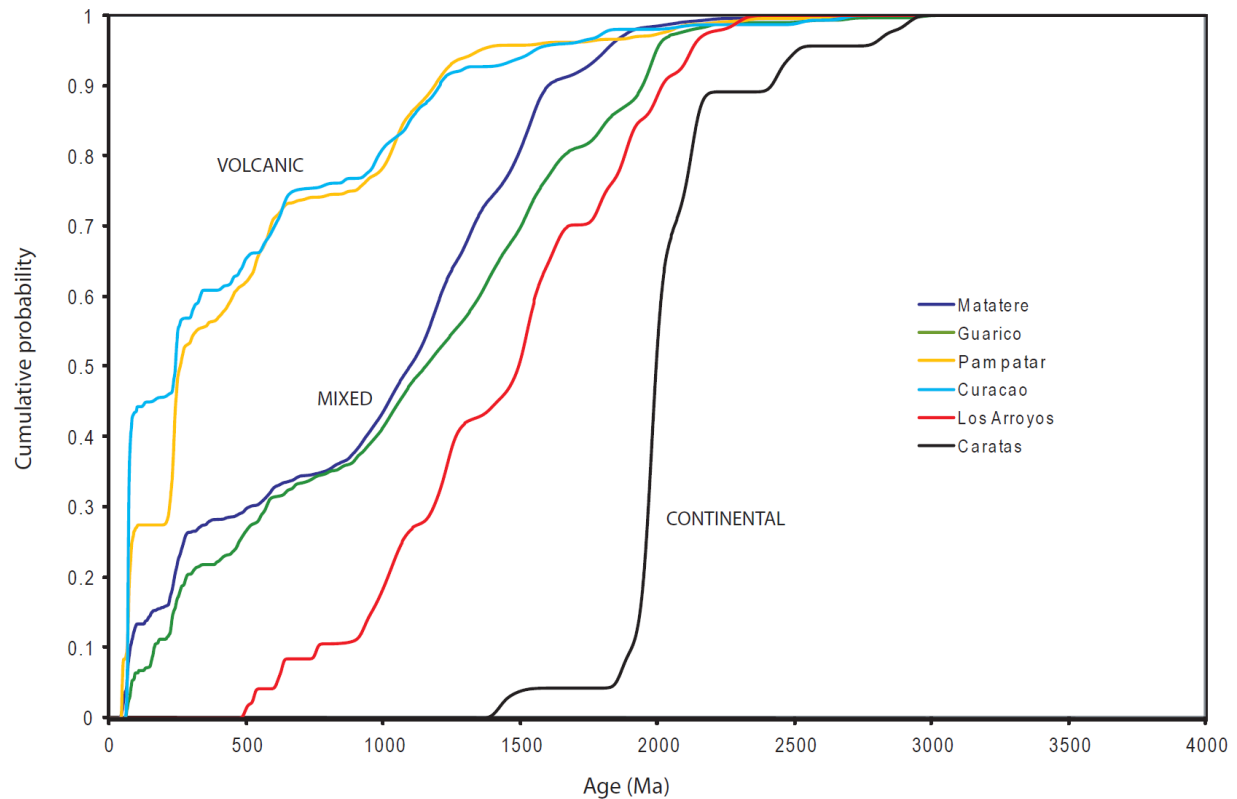


Figure 3.36. Cumulative Distribution Functions (CDFs) for the detrital zircon ages in samples of the turbidite units.

Additionally, good correlations are seen between the concentrations of detrital zircons younger than Late Cretaceous age (estimated age for initiation of subduction of the Caribbean plate and subsequent activation of the Leeward Antilles volcanic arc) and the proportions of volcanic grains in the sandstones (Figure 3.37). Northeastward variation in lithic contents is also consistent with the geochronologic data for the units located in the mainland (Matatere, Guárico, Caratas and Los Arroyos Formations).

### PROVENANCE OF THE MAASTRICHTIAN – MIOCENE TURBIDITES

From Late Cretaceous time, a series of tectonic and magmatic events (related to the evolution of the Caribbean plate) have controlled the paleogeography and sedimentation patterns in northern Venezuela. The potential source rocks that may have influenced the accumulation of the turbidite deposits between Maastrichtian and Miocene time are described below.



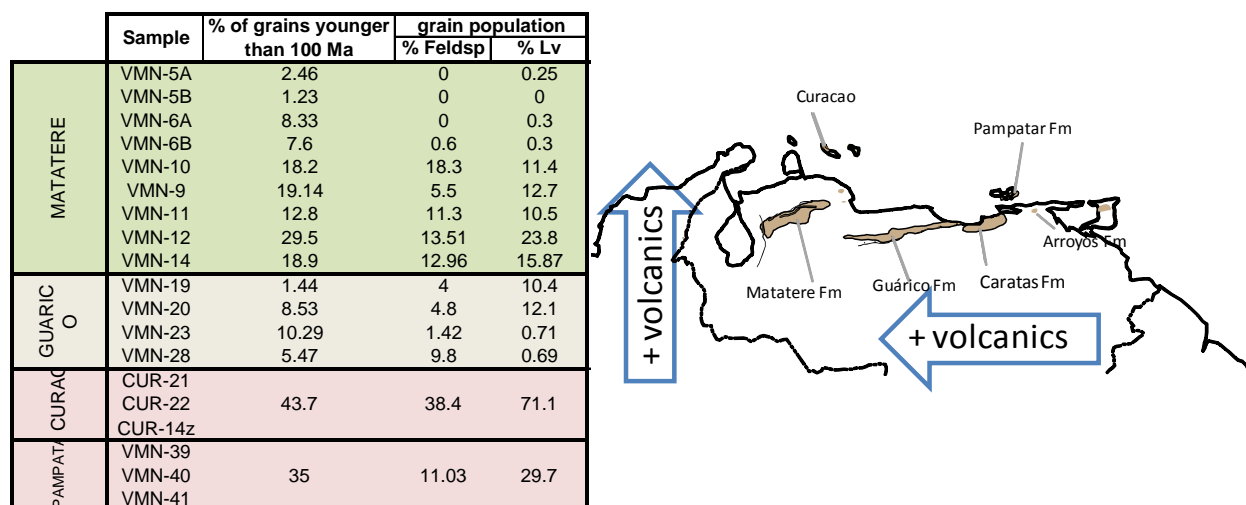


Figure 3.37. Northwestward variation of the content of volcanic components in the turbidites, indicating probable location of a volcanic source (Leeward Antilles volcanic arc)

### Precambrian – Paleozoic rocks

Detrital zircon age distributions ranging 2700 and 400 Ma in the turbidite deposits correspond with the detrital zircon signature of the Early Cretaceous passive margin units (Figure 3.34a). However, it is possible that some of the same provinces that provided sediments for the continental passive margin units (Guayana Shield and the Colombian Andes, discussed in Chapter 2) were still exposed in the Tertiary, adding secondary Proterozoic to Paleozoic detritus to the foredeep basins.

### Triassic – Jurassic rocks

U-Pb age peaks around 240 Ma observed in the detrital fraction of the turbidites (but absent in the Early Cretaceous passive margin signature) suggest exposure of a Middle Triassic basement at some point between the Late Cretaceous and the Paleocene. Permian-Triassic ages have been found in granitoids from Paraguaná Peninsula (265 Ma U/Pb, El Amparo granite; Feo Codecido et al., 1984), the Eastern Colombian Andes, Perijá and Guajira (220 Ma U/Pb, Macuira Formation; Cardona et al., 2006) and in Toas Island ( $252 \pm 50$  Ma; Dasch, 1982); (Figure 3.38).

Additionally, Kasper and Larue (1986) interpret topographic highs for the Guajira and Paraguaná peninsulas by the time of the deposition of the turbidite sequences.

Ages of 160 Ma (Upper Jurassic, Figure 3.35b) yielded by a few detrital zircon grains seem to correlate to 163 Ma (U-Pb, zircons) volcanic fragments reported in La Quinta Formation in Perijá (hornblende andesite; Dasch, 1982) and to  $162 \pm 4$  Ma (U-Pb, zircons) plutons in the Guajira Peninsula (Siapana granodiorite; Cardona et al., 2006); (Figure 3.38).

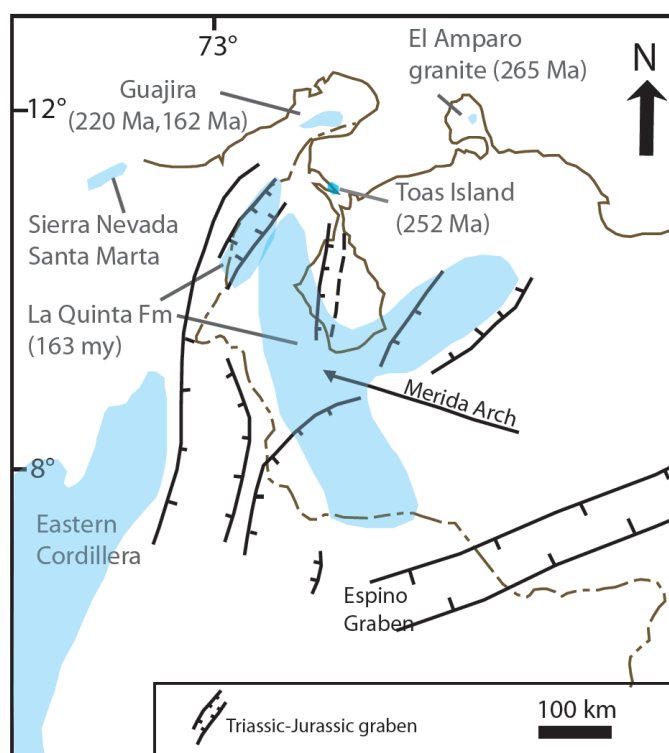


Figure 3.38. Triassic-Jurassic rocks in western Venezuela and Colombia. Ages based in U-Pb zircon ages.

### Cretaceous rocks

Reworking of Early Cretaceous passive margin rocks could have contributed to the sediments of the turbidite units, as seen in the similar distribution pattern exhibited by Precambrian – Paleozoic grains. The existence of olistoliths from other passive margin rocks

(e.g. Barquisimeto and La Luna Formations) in Matatere and Guárico Formations supports the idea of the Cretaceous passive margin as one of the main sources of sediments for the Late Cretaceous – Miocene turbidites.

Ages between 100 Ma and 65 Ma (peaks at 98 Ma, 86 Ma and 71, 74 Ma) record the first interactions between the Caribbean plate and the western margin of northern South America. Oceanic plateau rocks and intrusions of younger arc-type rocks in the basement of the Leeward Antilles (Caribbean Large Igneous Province, CLIP) have yielded ages indicated for the generation of the Caribbean plateau (90-93 Ma, Curacao and Aruba), and its immediate subduction under the South American plate (89-90 Ma, oldest intrusion; Table 3.7). Ages near 90 Ma may represent initiation of subduction along the southern margin of the CLIP and generation of the Leeward Antilles (Wright, personal communication, 2009). Ages of 71-74 Ma correlate to an extinct volcanic arc currently accreted in western Colombia (Western Cordillera) and Ecuador (Pallatanga Terrane), (Kerr et al, 2003; Vallejo et al., 2006; Figure 3.39). Cessation of magmatism at 65 Ma (from absence of zircons of this age, Figure 3.35b), indicates completion of the accretion of these arc-related terranes (Mamberti et al., 2003; Vallejo et al., 2006).

### **Paleocene – Eocene rocks**

Detrital zircon ages peaking at 59 Ma and 50 Ma (Paleocene, Figure 3.35b), are seen in samples of Matatere and Pampatar Formations (Figures 3.31b and 3.33b), and probably mark the arrival of the Leeward Antilles volcanic arc to western Venezuela (55 Ma, Levander et al., 2008). Rocks formed during the emplacement of the leading edge of the Caribbean plate are found in the Colombian Sierra Nevada de Santa Marta (65-50 Ma unroofed granitoids; Cardona et al., 2008).

Table 3.7. Radiometric ages of the Caribbean plateau and younger intrusions in the Netherlands and Leeward Antilles.

	Location	Age (Ma)	Method	Reference
Younger intrusions	Aruba (Aruba Batholith)	$89 \pm 1$	U-Pb (SHRIMP)	Wright et al (2008)
		91 – 67	K-Ar	Ostos et al. (2005)
	Curacao	$86.2 \pm 1.1$	U-Pb (SHRIMP)	Wright (2009, personal communication)
	Los Roques	66, 65	K-Ar	Santamaria & Schubert (1974)
	La Blanquilla	64-62		
		59	U-Pb (SHRIMP)	Wright et al (2008)
	Los Hermanos	71 – 67	K-Ar	Santamaria & Schubert (1974)
	Margarita	115-70	K-Ar, U-Pb	Ostos et al. (2005)
	Los Frailes	66	K-Ar	Santamaria & Schubert (1974)
	Los Testigos	47-44		
Caribbean plateau	Aruba (Aruba Lava Formation)	Turonian (~93 - 88)	Ammonites	Beets, 1977 and Beets et al., 1977 (in Ostos et al., 2005)
	Curacao (Curacao Lava Formation)	$89.5 \pm 1$	Ar-Ar	Sinton et al. (1998)
		$88 \pm 1.2$		
	Bonaire (lappilli tuffs and dacitic blocks)	$98.5 \pm 0.6$	U-Pb (SHRIMP)	Wright (2009, personal communication)
		$94.6 \pm 1.4$		
	Los Roques	130 - 127	K-Ar	Santamaria & Schubert (1974)
	Los Monjes	116, 114		

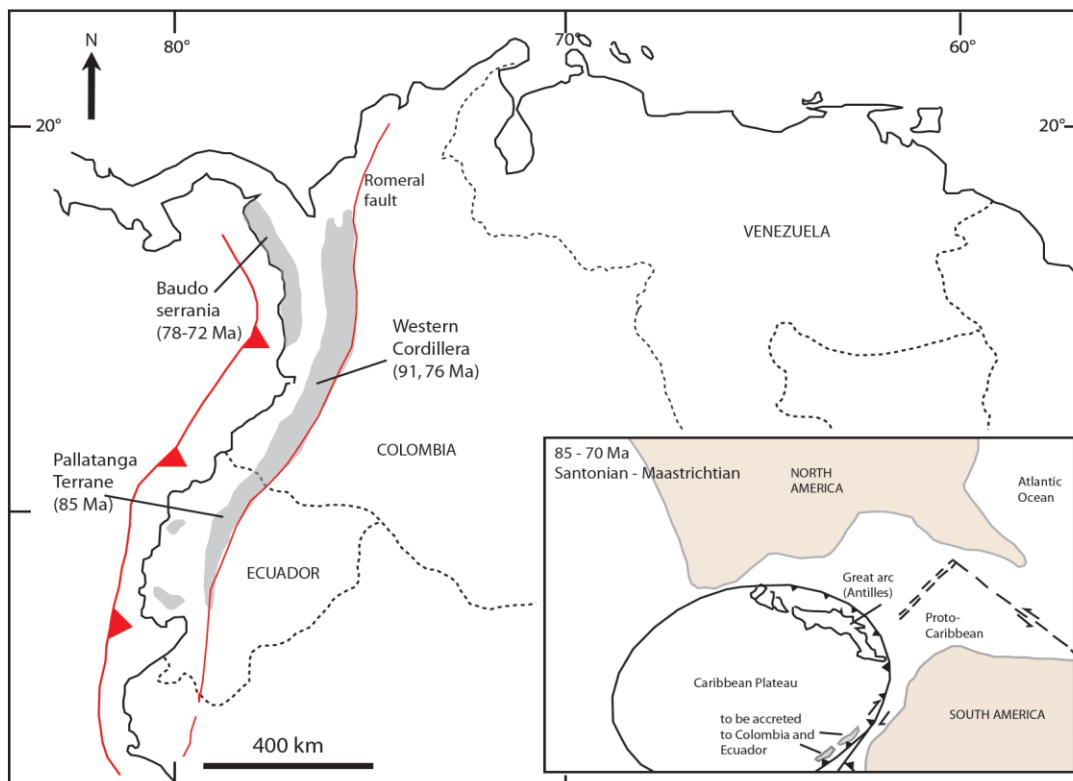


Figure 3.39. Accreted terranes in western Colombia and Ecuador. U/Pb SHRIMP ages from Kerr et al. (2003) and Vallejo et al. (2006). Modified after Kerr et al. (2003).

Ages between 50 and 40 Ma are only seen in grains of the Matatere and Pampatar Formations. By middle Eocene time, thrusts associated with the emplacement of the Lara nappes occurred (Pindell & Kennan, 2001; Pindell et al, 2005), probably involving some previous metamorphism of the accretionary complex (Pindell & Barrett, 1990). However, there is not enough information known about magmatism or thermal events occurring in the area during Eocene time to allow correlation with the current detrital zircon data. Therefore, more studies are necessary.

In summary, volcanic and continental sediments of the turbidite units were shed from at least three general locations:

- North - northwest: represented by the volcanic components from the Leeward Antilles arc.
- South: Continental passive margin rocks and Guayana Shield
- West and southwest: the Colombian Cordilleras (Western, Central and Eastern), Perijá and probably Guajira Peninsula

These results are consistent with previous interpretations (Van Andel, 1958; Kasper & Larue, 1986; Pindell et al., 1998; Ostos et al., 2005; Martinez & Valleta, 2008) and add new variables to the geologic frame of northern South America at the beginning of the Cenozoic.

### **Western Venezuela Paleocene tectonic scenario and paleogeography**

The map of Figure 3.40 shows the proposed paleogeographic reconstruction of the Paleocene in northern Venezuela, using the current data and interpretations from previous authors.

Convergence between the southern Caribbean plate and northern South America began in the Campanian (83-71 Ma) as the southern part of the Caribbean volcanic arc (age of about 90

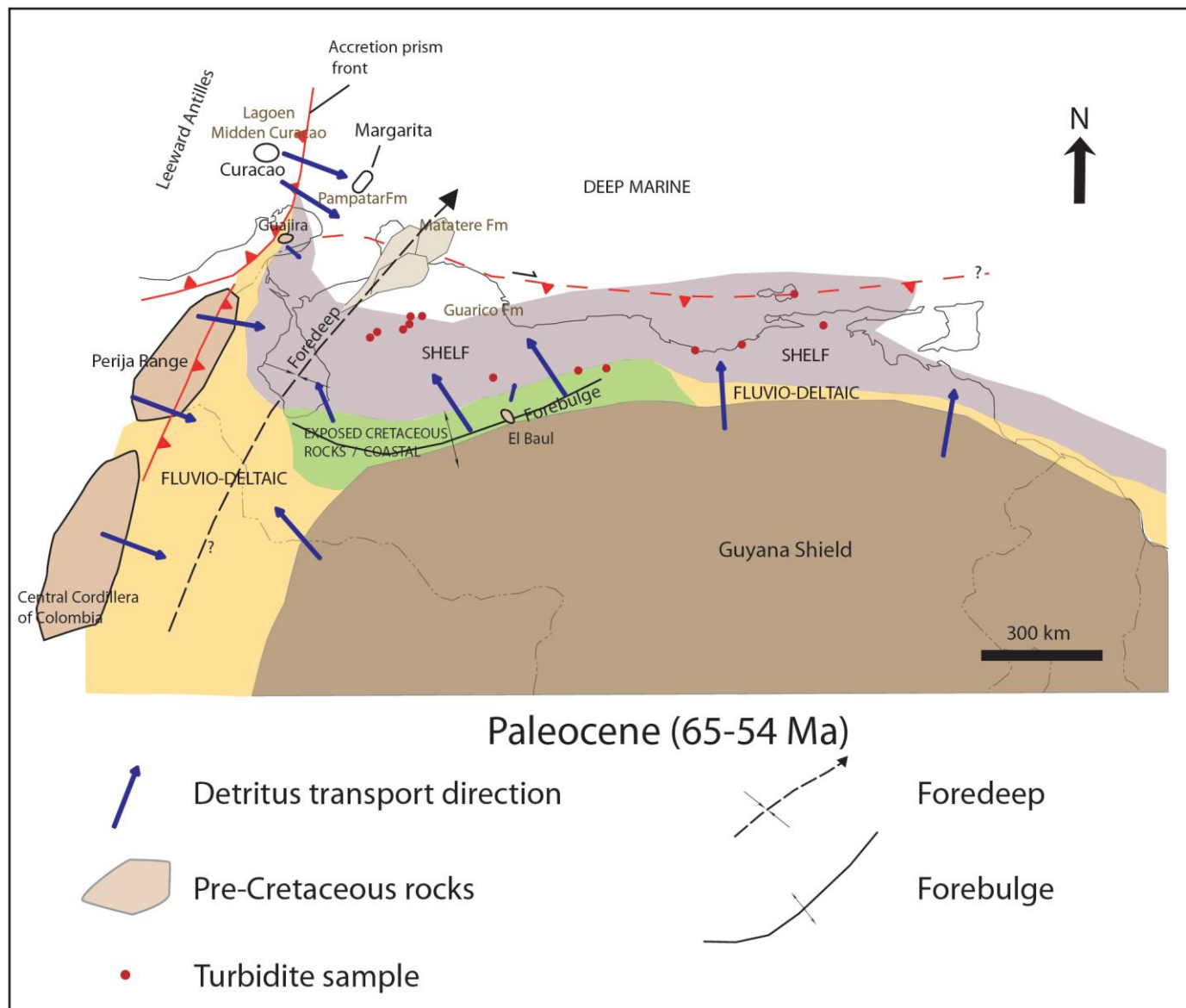


Figure 3.40. Proposed paleogeographic model for the Paleocene (65-54 Ma) in northern Venezuela.

Ma) collided with western Ecuador and Colombia. By Maastrichtian-Paleocene time (ca. 65 Ma), portions of this arc were accreted onto Ecuador and Colombia (Western Cordillera and Pallatanga terranes, Figure 3.39). Effects of this collision were manifested in western Venezuela as the arrival of a southeast migrating peripheral bulge followed by a foredeep across the Maracaibo basin (Pindell et al., 1998; Figure 3.27). Arrival of this deformation front was already reflected in the stratigraphic record since Maastrichtian time by the first pulses of a regression that exposed the northern areas of the Guayana Shield. Uplift associated with the bulge probably exposed Early and Late Cretaceous rocks originally deposited in a continental passive margin setting. These rocks provided the recently opened foredeep basins with mature, quartz-rich sediments and blocks of different sizes (olistoliths and olistostromes). Diachronously, sediments from the accretionary prism and sub-aerial areas of the Caribbean arc (Bonaire Basin and Leeward Antilles, Pindell et al., 1998; Aruba and Bonaire, Beardsley et al, 2008; Aruba, Curacao and Los Roques, Wright et al., 2008) were also incorporated into the foredeep from the north (volcanic fragments, plagioclases and hornblende).

A fluvial complex running in a SSW-NNE direction along the foredeep axis probably existed in the Paleocene. Such a system would have drained the positive areas of Perijá and the Central Cordillera of Colombia and probably Guajira Peninsula, providing Middle Triassic and Jurassic sediments to the foredeep. This Paleogene drainage system had been previously referred as proto-Maracaibo river (Escalona, 2004), paleo-Orinoco river (Kasper & Larue, 1986; Hoorn et al., 1995; Diaz de Gamero, 1996) and paleo-Magdalena river (Stephan, 1985 in Diaz de Gamero, 1986). This fluvial system may have actually been a tributary of the Magdalena River, given the existence of detrital zircon grains with ages consistent to the accreted terranes in the Western Cordillera of Colombia and Ecuador. The outlet of this river was presumably a delta complex



which included turbidite fan sediments of the Matatere Formation (a mix of “orogenic” and volcanic components); (Pindell et al., 1998).

The lithic graywackes and conglomerates of the Matatere Formation were deposited at the distal lobes of the outlet of this fluvial system, close to the volcanic arc and its associated accretionary prism (Figure 3.40); whereas arenites of this unit were deposited at the southern (“continental”) part of the foredeep (located at the present time near Carora, Figure 3.8), which received sediments from exposed areas of the passive margin, Colombian Andes and, to a lesser degree, the Guayana Shield. With the advance of the Caribbean plate toward the east, the turbidite fan was thrust into its present position.

Although the arrival of the migrating peripheral bulge to the Guárico basin did not occur until Middle Eocene time (Pindell et al., 1998), quartz-rich sediments of Guárico Formation were being already deposited in the distal parts of the foredeep (but more proximal to the exposed passive margin) since Maastrichtian time (Figure 3.40). These sediments were consequently thrust in their present location along the Interior Serranía as allochthonous terranes (Villa de Cura Complex and associated accretionary prism) and were accreted onto the passive margin, (Pindell et al., 2005; Ostos et al., 2005; Figure 3.7).

The Pampatar, Midden Curacao and Lagoen Formations deposited in the accretionary prism between the foredeep and the volcanic arc. Curacao was located closer to the volcanic arc, while Margarita was probably located in the distal area of the accretionary prism. Sediments of these units were primarily provided by the Leeward Antilles (volcanic components) and in a much lesser amount from the positive areas in Guajira and Perijá (metamorphic lithics).

Eastern Venezuela remained a continental passive margin until the gradual arrival of the peripheral bulge by Late Eocene time and the Caribbean foredeep by Oligocene time (Pindell et

al., 1998). The Eocene Caratas Formation marks the end of the continental passive margin stage in Eastern Venezuela. It was deposited in a dominantly continental environment, at the margins of the Guayana Shield and in the outer areas of the peripheral forebulge. Additionally, magmatism in the southern part of the Lesser Antilles (and probably in the Aves Ridge) may have ceased at some point between Eocene and Oligocene times, since no detrital zircon with ages younger than 40 Ma were found. Finally, deposition of the Los Arroyos Formation in Miocene time was probably contemporaneous to dextral oblique thrusting associated with uplifting of the Interior Serranía, given the abundance of metamorphic and sedimentary lithic fragments in its rocks.

## CONCLUSIONS

LA-ICP-MS U-Pb detrital zircon ages of Late Cretaceous-Miocene turbidite units in northern Venezuela (Matatere, Guárico, Pampatar, Caratas, and Los Arroyos Formations) and Curacao (Lagoen and Midden Curacao Formations) yielded ages that vary between 2800 Ma (Late Archean) and 40 Ma (Middle Eocene; Figure 3.35, Table 3.8).

Table 3.8. Age intervals of the detrital fraction of the northern Venezuela Late Cretaceous-Tertiary turbidite units

Unit	Oldest grain (Ma)	Youngest grain (Ma)
Matatere Fm.	2841.1 ± 13.3	39.4 ± 1.5
Guarico Fm.	2962.1 ± 26.1	63.1 ± 4.6
Pampatar Fm.	2626.8 ± 16.6	49.1 ± 0.9
Caratas Fm.	2916 ± 24.5	1425 ± 23.7
Los Arroyos Fm.	2292.8 ± 34.2	499.1 ± 9.4
Curacao	2684.9 ± 16.8	66.4 ± 3.8

The mineral composition of the arenites and graywackes, although variable from west to east, is consistent with the detrital zircon data and show volcanic lithics, plagioclases and in some cases detrital hornblende, which suggest the proximity of a volcanic source. The

petrographic data in general reflect mixed provenances of continental passive margin and volcanic island arc (Figure 3.25).

The sediments that compose these turbidite deposits were shed from three main areas:

- A southern, cratonic source represented by the Guayana Shield and exposed areas of the Early Cretaceous passive margin.
- A northern source located at the Caribbean volcanic arc and associated accretionary prism which fed the foredeep basin with Early Cretaceous – Eocene volcanic sediments.
- A western source found in the uplifted areas of the Western, Central and Eastern Cordillera of Colombia, Perijá and probably Guajira Peninsula, which provided Precambrian (Grenvillian-age), Paleozoic and Jurassic-Triassic meta-igneous components to the sediments.

Origin of the turbidite units is linked to right-lateral oblique collision between the southern Caribbean and the northern South American plates. By Maastrichtian-Paleocene time, arrival of the southern margin of the Caribbean plate to western Venezuela was marked by the emplacement of a southeast-migratory peripheral bulge and formation of a SSW-NNE-oriented foredeep. A fluvial system (probably a paleo-Magdalena river) drained in a south to north direction along this foredeep, eroding areas of the forebulge, Guayana Shield, Western, Central and Eastern Cordillera of Colombia, and Perijá, and transported continental and orogenic sediments into the distal parts of a delta complex in which mixing occurred with components from the Caribbean volcanic arc. This delta was located on an unstable platform, providing with the conditions for turbidity currents and gravitational slides (Matatere and Guárico Formations and associated olistoliths and olistostromes). Sediments of Pampatar formation probably

accumulated in distal areas of the accretionary prism, whereas turbidites of Curacao were deposited near the volcanic arc.

Starting in the Middle Eocene, continuous eastward advance of the Caribbean plate thrust the Paleogene sequences into their current positions, along with diachronous emplacement of allochthonous terranes in northern Venezuela.

The detrital zircon data also recorded important magmatic and deformation events linked to the evolution of the Caribbean and its interactions with the South American plate:

- ca. 90 Ma: initiation of subduction magmatism, responsible for the generation of the Leeward Antilles arc on the basement of the Caribbean Large Igneous Province (CLIP); (Figure 3.41).
- ca. 65 Ma: Cessation of arc magmatism caused by the collision of the arc with western Colombia and Ecuador (Figure 3.42).
- ca. 55 - 50 Ma: Renewed magmatic activation following collision of the arc with Colombia (Figure 3.43).

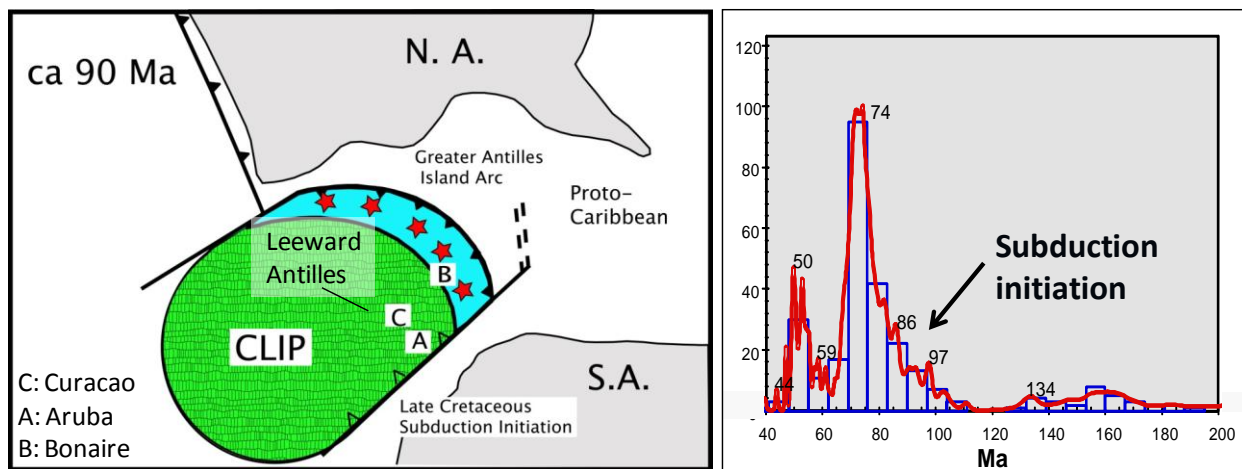


Figure 3.41. Initiation of subduction of the southern edge of the CLIP at ca. 90 Ma, responsible of the generation of the Leeward Antilles volcanic arc (model proposed by Wright, 2009). The histogram on the right shows an increment on the number of zircons at about 100 – 90 Ma, indicating initiation of magmatism.

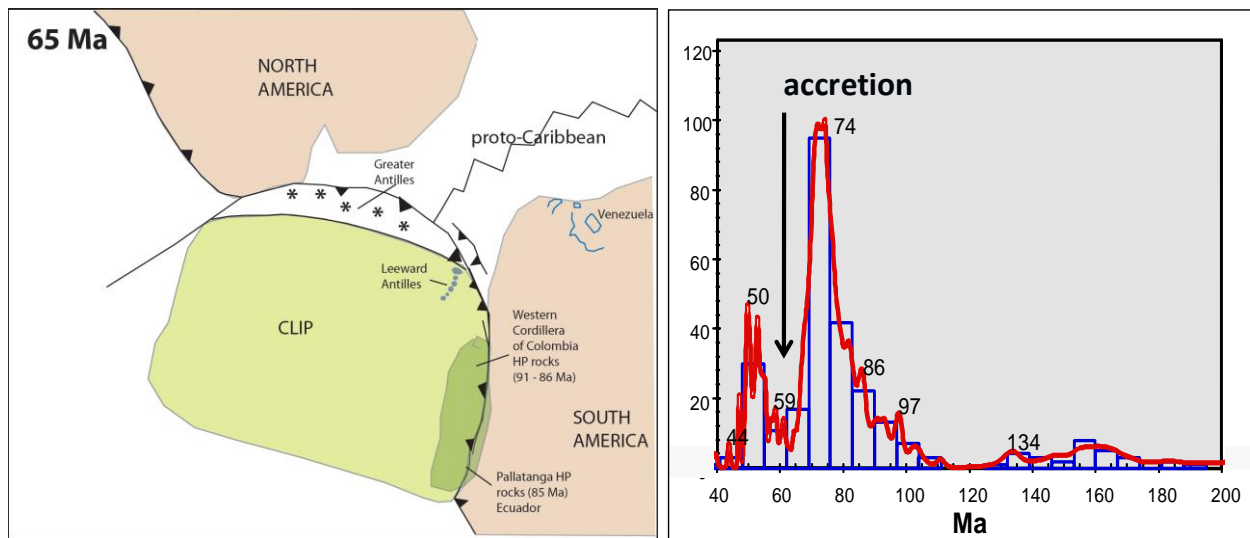


Figure 3.42. Diminished number of detrital zircons at about 65-60 Ma (diagram on right) may indicate cessation of magmatism as a consequence of accretion of the southern part of the volcanic arc to the western continental margin of Colombia and Ecuador (proposed model on left)

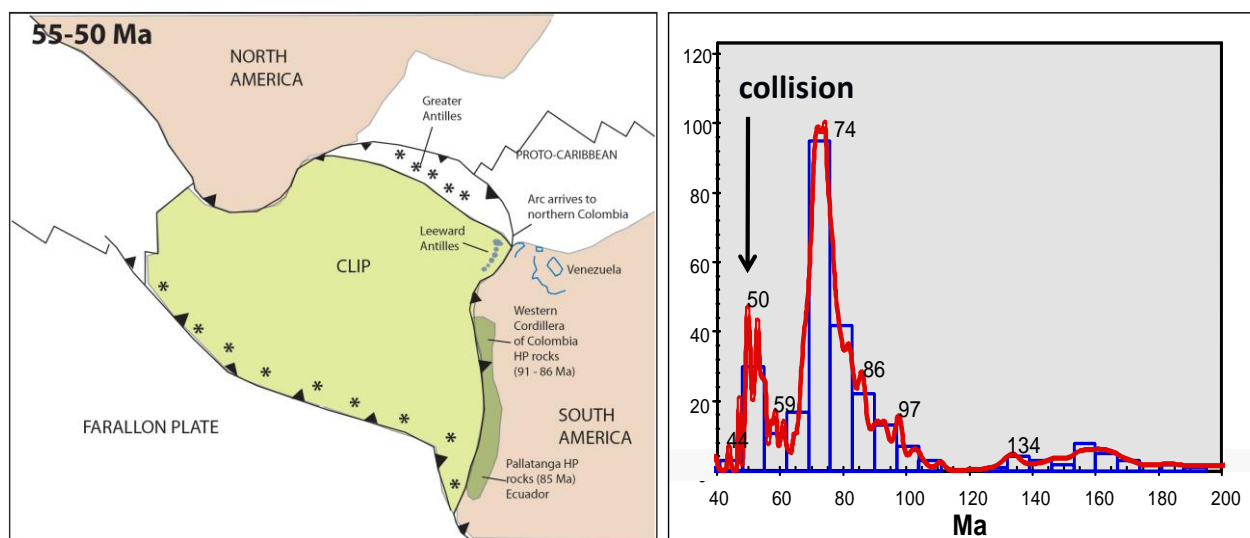


Figure 3.43. Arrival of the Leeward Antilles volcanic arc to northern Colombia at ca. 55-50 Ma (proposed model on left) may have triggered new magmatism, reflected in an increase of detrital zircon grains (diagram on right)

## REFERENCES

- Aguasuelos Ingeniería. 1991. Geología de la Serranía del Interior (Geology of the Serranía del Interior). Internal Corpoven Report. 237 p.
- Albertos, María. 1989. Estudio Geológico de las Secciones: Altagracia de Orituco – Agua Blanca y Gamelotal – San Francisco de Caira (estados Guárico y Miranda). Análisis Petrográfico y estadístico de la Formación Guárico (Geologic Study of the sections Altagracia de Orituco and Gamelotal – San Francisco de Caira, Guárico and Miranda states. Petrographic and statistical analysis of the Guárico Formation). Universidad Central de Venezuela, Thesis.
- Alvarez, Eduardo; Oliver Macsotay; Duggar Rivas and Victor Vivas. 1985. Formación Los Arroyos: Turbiditas de edad Mioceno Medio en la Región de El Pilar, edo. Sucre (Los Arroyos Formation: Turbidites of Middle Miocene age in the El Pilar Region, Sucre state). VI Congreso Geológico Venezolano, p. 1-32.
- Beardsley, Amanda G; Virginia G, Sisson and H. G, Lallemand. 2008. Exhumation history of the Leeward Antilles coeval with regional deformation and island arc accretion. 2008 Annual GSA Joint Annual Meeting, Abstracts with Programs, p. 171.
- Beets, D. J. 1972. Lithology and Stratigraphy of the Cretaceous and Danian Succession of Curacao, Uitgaven “Natuurwetenschappelijke Studiekring voor Suriname en de Nederlandse Antillen, Utrecht, No. 70, 153 pag.
- Cardona Molina Agustin, Umberto G. Cordani and William D. MacDonald. 2006. Tectonic correlations of Pre-Mesozoic crust from the Northern termination of the Colombian Andes, Caribbean region. *Journal of South American Earth Sciences* 21:337-354.
- Cardona, A.; V., Valencia; P., Reiners; J., Duque; C., Montes; S., Nicolescu; G., Ojeda and J., Ruiz. 2008. Cenozoic exhumation of the Sierra Nevada de Santa Marta, Colombia;

- implications on the interactions between the Caribbean and South American plate. 2008 GSA Joint Annual Meeting, Abstracts with Programs, pag 104.
- Dasch L. E. 1982. U-Pb Geochronology of the Sierra de Perijá, Venezuela. Case Western Reserve University, M.S. Thesis. 164 p.
- Diaz de Gamero, Maria L. 1995. The changing course of the Orinoco River during the Neogene: a review, *Palaeogeography, Palaeoclimatology, Palaeoecology*, 123:385-402.
- Dickinson William R. 1985. Interpreting provenance relations from detrital modes of sandstones. In: G. G. Zuffa (ed.), *Provenance of Arenites*, p.333-361.
- Erickson J. P. and J. Pindell. 1998. Sequence stratigraphy and relative sea-level history of the Cretaceous to Eocene passive margin of North-East Venezuela and the possible tectonic and eustatic causes of stratigraphic development. In: *Paleogeographic Evolution and Non-Glacial Eustasy, Northern South America*, SEPM Special Publication No 58, p. 261-281.
- Escalona, A. 2004. Tectonic reconstruction of sedimentary basins associated with the proto-Maracaibo and proto-Orinoco rivers: New constrains from BOLIVAR and GULFREX seismic data, *Eos Transactions AGU*, 85(47), Fall Meeting Suppl., Abstract T33B-1374.
- Feo-Codecido Gustavo, Foster D. Smith Jr., Nelson Aboud and Estela Di Giacomo. 1984. Basement and Paleozoic rocks of the Venezuelan Llanos Basin. In: Bonini, William E., Robert Hargraves and Reginald Shagam, *The Caribbean-South American Plate Boundary and Regional Tectonics*, Geological Society of America, Memoir 162, p.175-187.
- French, Christofer D. and Christopher J., Schenk. 2004. Map Showing Geology, Oil and gas Fields, and Geologic Provinces of the Caribbean Region. USGS Open-File Report 97-470-K.



- Galea F. 1986. Bioestratigrafia y ambiente sedimentario del Grupo Santa Anita del Cretáceo Superior – Eoceno, Venezuela nor-oriental (Biostratigraphy and sedimentary environment of the Upper Cretaceous – Eocene Santa Anita Group, Northeastern Venezuela). *Memoria VI Congreso Geológico Venezolano*, 1:703-721.
- Guynn, Jerome. 2006. Comparison of Detrital Zircon Age Distributions using the K-S Test. Arizona LaserChron Center. <http://www.geo.arizona.edu/alc/Analysis%20Tools.htm>
- Hackley Paul C., Franco Urbani and Alexander W. Karlsen. 2005. Geologic Shaded Relief Map of Venezuela. U.S. Geological Survey Open File Report 2005-1038. <http://pubs.usgs.gov/of/2005/1038/>.
- Hoorn, Carina; Javier Guerrero; Gustavo A. Sarmiento and Maria A. Lorente. 1995. Andean tectonics as a cause for changing drainage patterns in Miocene northern South America, *Geology*, 23(3):237-240.
- James K. H. 1997. Distribution and Tectonic significance of Cretaceous–Eocene Flysch–Wildflysch deposits of Venezuela and Trinidad. *Memoirs from VIII Congreso Geológico Venezolano*, Margarita Island, Venezuela, p. 415-421.
- James K. H. 2006. Arguments for and against the Pacific origin of the Caribbean plate: discussion, finding for an inter-American origin. *Geologica Acta* 4(1-2): 279-302.
- James K. H. 2007. The Caribbean Ocean Plateau – an overview, and a different understanding. <http://www.mantleplumes.org/WebDocuments/CaribbeanPlateau.pdf>.
- Kasper D. C. and D. K. Larue. 1986. Paleogeographic and tectonic implications of quartzose sandstones of Barbados, *Tectonics*, 5(6):837-854.
- Kerr, Paul F. 1959. *Optical Mineralogy*, Third edition, McGraw-Hill Book Company, 441 p.

- Kerr, A., R. V. White, P. M. E. Thompson, J. Tarney, and A. D. Saunders. 2003. No oceanic plateau – No Caribbean plate? The seminal role of an oceanic plateau in Caribbean plate evolution, *in*: Bartolini C., R.T. Buffler, and J. Blickwede (eds.), *The Circum-Gulf of Mexico and the Caribbean: Hydrocarbon habitats, basin formation, and plate tectonics*, AAPG Memoir 79, p. 126-168.
- Levander A. and the BOLIVAR working Group. 2005. BOLIVAR: Continental Growth and Deformation along South American – Caribbean Plate Boundary. *17<sup>th</sup> Caribbean Geological Conference, San Juan Puerto Rico*, pag. 46-47.
- Léxico Estratigráfico Venezolano (LEV). <http://www.pdvsa.com/lexico/>. (November 2008).
- Macsotay, Oliver; Victor Vivas; Nelly Pimentel de Bellizia and Alirio Bellizzia G. 1986. Excursion: Estratigrafía y Tectónica del Cretáceo – Paleógeno de las islas al norte de Puerto La Cruz – Santa Fe y regiones adyacentes (Field Trip: Stratigraphy and Tectonics of the Cretaceous – Paleogene of the islands north of Puerto La Cruz – Santa Fe and adjacent regions). *Memoria VI Congreso Geológico Venezolano*, 10:7125-7174.
- Magnani, M.B; C.A., Zelt; A., Levander and the BOLIVAR Working Group. 2005. BOLIVAR: A snapshot of the Caribbean – South american plate boundary at 67.5 W. *17th Caribbean Geological Conference 2005, San Juan, Puerto Rico*.
- Mamberti, Marc; Henriette, Lapierre; Delphine, Bosch; Etienne, Jaillard; Raynald, Ethien; Jean, Hernandez, and Mireille Polve. 2003. Accreted fragments of the Late Cretaceous Caribbean-Colombian Plateau in Ecuador. *Lithos*, 66:173-199.
- Martínez Gladys and Graziana Valleta. 2008. Petrografía de las facies gruesas de la Formación Matatere y otras unidades del Centro-Occidente de Venezuela (Petrography of the coarse

- grained facies of Matatere Formation and other units from Central-Western Venezuela), Universidad Central de Venezuela, Thesis, 280 p.
- Maze, W.B., 1984. Jurassic La Quinta formation in the Sierra de Perijá, northwestern Venezuela: geology and tectonic environment of red beds and volcanic rocks. *In*: Bonini, William E., Robert Hargraves and Reginald Shagam, The Caribbean-South American Plate Boundary and Regional Tectonics, Geological Society of America, Memoir 162, p. 263-282.
- Meschede Martin and Wolfgang Frisch. 2002. The Evolution of the Caribbean Plate and its Relation to Global Plate Motion Vectors: Geometric Constrains for an Inter-American Origin. *In*: Jackson, Trevor A. 2002. Caribbean Geology into the Third Millennium, *Transactions of the 15<sup>th</sup> Caribbean Geological Conference*, p.1-14.
- Moreno Joselys and Johnny Casas. 1986. Estudio Petrográfico y estadístico de la secuencia flysch Eocena de la Isla de Margarita (Petrographic and statistic study of the Eocene flysch sequence from Margarita Island), Universidad Central de Venezuela, Thesis.
- Muñoz J., Nicolas Gerardo. 1973. Geología Sedimentaria del Flysch Eoceno de la Isla de Margarita, Venezuela (Sedimentary Geology of the Eocene Flysch of Margarita Island, Venezuela). *Geos*, 20:5-64.
- Ostos M., F. Yoris, and H. A. Lallemand. 2005. Overview of the Southeast Caribbean – South American Plate Boundary Zone. *In*: Lallemand H. and V. Sisson, Caribbean-South American Plate Interactions, Venezuela. The Geological Society of America, Special paper 394, p. 53-89.

- Peirson III, A. L.; A. Salvador and R.M. Stainforth, 1966. The Guárico Formation of north-central Venezuela. (La Formación Guárico, Venezuela nor-central). Boletín Informativo, *Asociación Venezolana de Geología, Minas y Petróleo*, 9(7): 183-224.
- Pindell, James L. and Stephen F. Barrett. 1990. Geological evolution of the Caribbean region; A plate-tectonic perspective. In: Dengo, G. and Case, J. E. (eds.), The Caribbean region, Geological Society of America, The Geology of North America, H:405-431.
- Pindell J. L., R. Higgs and J. F. Dewey. 1998. Cenozoic palinspatic reconstruction, paleogeographic evolution and hydrocarbon setting of the northern margin of South America. In: Paleogeographic Evolution and Non-Glacial Eustasy, Northern South America, SEPM Special Publication No 58, p.45-85.
- Pindell James and Lorcan Keenan. 2001. Kinematic Evolution of Mexico and the Caribbean. *GCSSEPM Foundation 21st Annual Research Conference, Petroleum Systems of Deep Water Basins*, p. 193-220.
- Pindell, James; Lorcan, Keenan; Walter V., Maresch; Klaus-Peter, Stanek, Grenville, Draper and Roger, Higgs. 2005. Plate-Kinematics and crustal dynamics of circum-Caribbean arc-continent interactions: Tectonic controls on basin development in Proto-Caribbean margins. In: Lallemant H. and V. Sisson, Caribbean-South American Plate Interactions, Venezuela. The Geological Society of America, Special paper 394, p. 7-52.
- Pindell James, L. Kennan, K.-P. Stanek, W. V. Maresch and G. Draper. 2006. Foundations of Gulf of Mexico and Caribbean Evolution: Eight Controversies Resolved. *Geologica Acta*, 4(1-2):303-341.

- Pudsey, C. J. and H. G. Reading. 1982. Sedimentology and Structure of the Scotland Group, Barbados. *In*: Legget, J. K. (ed.): Trench Forearc Geology, Geological Society of London, Special Publication, 10:291-308.
- Rekowski F., and L. Rivas. 2005. Integración Geológica de la Isla de Margarita, estado Nueva Esparta (Geologic integration of Margarita Island, Nueva Esparta state). Universidad Central de Venezuela, Thesis.
- Santamaria, Francisco and Carlos Schubert. 1974. Geochemistry and Geochronology of the Southern Caribbean – Northern Venezuela plate boundary. *Geological Society of America Bulletin*, 7:1085-1098.
- Schubert, C.; R. S. Sifontes; V. E. Padrón; J. R. Vélez , J. R. and P. A. Loaiza, 1979. Formación La Quinta (Jurásico), andes merideños: geología de la sección tipo (Jurassic La Quinta Formation, Merida andes: Geology of the type section). *Acta Científica Venezolana*, 30: 42-55.
- Sinton, C.W.; R.A. Duncan, M. Storey, J. Lewis and J.J. Estrada. 1998. An Oceanic Flood Basalt Province within the Caribbean Plate. *Earth and Planetary Science Letters*, 155:221-235.
- Urbani, Franco. 2006. Geología de la region de Siquisique, estado Lara (Geologi of the Siquisique region, Lara state). *Geos* 39, 85 p.
- Vallejo Cristian, Richard A. Spikings, Leonard Luzieux, Wilfried Winkler, David Chew and Laurence Page. 2006. The early interaction between the Caribbean Plateau and the NW South American Plate. *Terra Nova*, 18:264-269.
- Van Andel, Tjeerd. 1958. Origin and Classification of Cretaceous, Paleocene and Eocene sandstones of Western Venezuela. *Bulletin of the American Association of Petroleum Geologists*, 42(4):734-763.

- Villamil Tomas and James Pindell. 1998. Mesozoic Paleogeographic Evolution of Northern South America: Foundations for sequence stratigraphic studies in passive margin strata deposited during non-glacial times. In: Paleogeographic Evolution and Non-Glacial Eustasy, Northern South America, SEPM Special Publication No 58, p. 283-318.
- Wright, J. 2004. Aruba and Curacao: Remnants of a collided Pacific oceanic plateau?, Initial results from the BOLIVAR Project. American Geophysical Union (AGU), Fall Meeting 2004, abstract # T33B-1367.
- Wright J. E., S. Wyld, and F. Urbani. 2008. Late Cretaceous subduction initiation Leeward Antilles / Aves Ridge: Implications for Caribbean Geodynamic models. *2008 Geological Society of America Joint Annual Meeting*, Abstracts with Programs, p. 103.
- Yoris F. and Albertos de Yoris M. A. 1989: Medidas de Paleocorrientes en la secuencia de la Formación Guárico y sus equivalentes en las secciones: Altagracia de Orituco, Guatopo y Gamelotal – San Francisco de Macaira, estados Guárico y Miranda (Paleocurrents in Guárico Formation and Equivalents, Altagracia de Orituco-Guatopo and Gamelotal-San Francisco de Macaira sections, Guárico and Miranda States). Caracas, *Geos*, 29:152-159.
- Yoris F. and M. Ostos. 1997. Petroleum Geology of Venezuela, *in*: Singer J. M. (ed.) 1997. *Well Evaluation Conference*. Caracas, Schlumberger, p. 1-44.
- Zapata, Eglee. 1976. Estudio de la Formación Guárico en el área de la Laguna de Unare, estado Anzoátegui (Study of the Guárico Formation in the area of Laguna de Unare, Anzoátegui state). Universidad Central de Venezuela, Thesis.

## **CHAPTER 4**

### **CONCLUSIONS**

Maastrichtian-Miocene turbidite deposits occur in northern Venezuela (Matatere Formation, Martínez & Valleta, 2008; Guárico Formation, Zapata, 1976, Albertos, 1989; Pampatar Formation, Muñoz 1973; Los Arroyos Formation, Alvarez et al., 1985; Caratas Formation, Galea, 1986), Curacao (Lagoen and Midden Curacao Formations; Beets, 1972), Trinidad (Chaudière and Point-a-Pierre Formations) and Barbados (Scotland Formation, Pudsey & Reading, 1982). These units overlie Cretaceous sediments and record the first interactions between the Caribbean and the South American plates since Late Cretaceous time (Kasper & Larue, 1986; James, 1997; Meschede & Frisch, 2002; Pindell et al., 1998). Provenance studies in Venezuela using petrographic and paleocurrent data have indicated at least two different sources of sediments, a northern volcanic arc source and a southern continental margin source (Matatere Formation, Kasper & Larue, 1986; Martinez & Valleta, 2008; Guárico Formation, Albertos, 1989; Yoris & Albertos, 1989; Pampatar Formation, Moreno & Casas, 1986). Sources located to the west (Colombian Andes) have also been suggested (Van Andel, 1958; Kasper & Larue, 1986).

This study integrates LA-ICP-MS U-Pb detrital zircon geochronology and petrography to determine the provenance of Early Cretaceous and Late Cretaceous – Miocene units in northern Venezuela and Curacao. The Early Cretaceous units (Barranquín, Aguardiente, Bobare and Agua Blanca Formations) represent a continental passive margin, derived from sediments of the Precambrian Guayana Shield; whereas the Late Cretaceous – Miocene units (Lagoen, Midden



Curacao, Guárico, Matatere, Pampatar, Caratas, and Los Arroyos Formations) are associated with the first interactions between the Caribbean and the South American plates.

### **EARLY CRETACEOUS PASSIVE MARGIN UNITS**

Ages of zircons in the Early Cretaceous passive margin units range between Late Archean ( $2731.8 \pm 26.7$  Ma, Barranquín Formation) and Early Devonian ( $415 \pm 4.1$  Ma, Aguardiente Formation). No grains of Triassic or Jurassic age were identified in these rocks.

The detrital zircon data show signatures that indicate the presence of at least three different sources:

- Precambrian (2.7 – 1.5 Ga) source: Grains of these age correlate with rocks from the Guayana Shield: Imataca (2736 Ma), Cuchivero (1995 Ma) and Roraima (1806 Ma) provinces. Detrital zircons with ages of about 1518 Ma seem to be diagnostic of the Parguazan Granite of the same shield.
- “Grenville” (1.3 – 1.0 Ga) source: Not reported in outcrops nor in the basement of Venezuela, but identified in fluvial grains in the Orinoco basin (Goldstein et al., 1997). Meta-igneous rocks from the Eastern Cordillera of Colombia (Santa Marta and Santander Massifs) are the potential sources of the 960 and 1200 Ma detrital component.
- Paleozoic (415 – 490 Ma) source: Age distribution peaks of 488 Ma and 422 Ma can be related to Cambrian-Ordovician rocks of the El Baúl Massif (El Baúl Granitic Suite) and probably to Silurian-Devonian plutonic bodies in the Mérida Andes (Cerro Azul Granite).

Deposition during Early Cretaceous times was controlled by extensional structures, which received siliciclastics drained from the exposed Guayana Shield, El Baúl Massif, the Colombian Andes (Santa Marta and Santander) and probably the Merida Arch. Location of these sources

indicate general sediment transport directions as south to north (Guayana Shield), west to East and southwest to northeast. A proposed proto-Orinoco river could have flowed along the structural depressions of a SW-NE oriented structure (Espino Graben) and delivered prograded siliciclastic sediments from Colombia to north-eastern Venezuela. The deltaic deposits of Barranquín Formation may represent the outlet of this “Proto-Orinoco” river.

## **MAASTRICHTIAN – MIOCENE TURBIDITE DEPOSITS**

LA-ICP-MS U-Pb detrital zircon ages of Late Cretaceous-Miocene turbidite units in northern Venezuela (Matatere, Guárico, Pampatar, Caratas, and Los Arroyos Formations) and Curacao (Lagoen and Midden Curacao Formations) yielded ages that vary between 2800 Ma (Late Archean) and 40 Ma (Middle Eocene).

The mineral composition of the arenites and graywackes, although variable from west to east, is consistent with the detrital zircon data and show volcanic lithics, plagioclases and in some cases detrital hornblende, which suggest the proximity of a volcanic source. The petrographic data in general reflect mixed provenances of continental passive margin and volcanic island arc.

The sediments that compose these turbidite deposits were shed from three main areas:

- A southern, cratonic source represented by the Guayana Shield and exposed areas of the Early Cretaceous passive margin.
- A northern source identified as the Caribbean volcanic arc and associated accretionary prism which fed the foredeep basin with Early Cretaceous – Eocene volcanic sediments.

- A western source found in the uplifted areas of the Western, Central and Eastern Cordillera of Colombia, Perijá and probably Guajira Peninsula, which provided Precambrian (Grenvillian-age), Paleozoic and Jurassic-Triassic meta-igneous sediments.

Origin of the turbidite units is linked to the right-lateral oblique collision between the southern Caribbean and the northern South American plates. By Maastrichtian-Paleocene time, arrival of the southern margin of the Caribbean plate to western Venezuela was marked by the emplacement of a southeast-migrating peripheral bulge and formation of a SSW-NNE-oriented foredeep. A fluvial system (probably a paleo-Magdalena river) drained in a south to north direction along this foredeep, eroding exposed areas of the forebulge, Guayana Shield, Western, Central and Eastern Cordillera of Colombia, and Perijá, and transporting continental and orogenic sediments into the distal parts of a delta complex in which mixing with components from the Caribbean volcanic arc occurred. This delta was located on an unstable platform, and provided favorable conditions for turbidity currents and gravitational slides (Matatere and Guárico Formations and associated olistoliths and olistostromes). Sediments of the Pampatar Formation probably accumulated in distal areas of the accretionary prism, whereas turbidites of Curacao were deposited in the proximities of the volcanic arc.

Starting the Middle Eocene, continuous eastward advance of the Caribbean plate thrust the Paleogene sequences into their current positions, along with diachronous emplacement of allochthonous terranes in northern Venezuela.

The detrital zircon data also recorded important magmatic and deformation events linked to the evolution of the Caribbean and its interactions with the South American plate:

- ca. 90 Ma: initiation of subduction magmatism, responsible of the generation of the Leeward Antilles arc on the basement of the Caribbean Large Igneous Province (CLIP).

- ca. 65 Ma: Cessation of arc magmatism caused by the collision of the arc with western Colombia and Ecuador.
- ca. 55 - 50 Ma: Renewed magmatic activation following collision of the arc with Colombia.

## REFERENCES

- Aguasuelos Ingeniería. 1991. Geología de la Serranía del Interior (Geology of the Serranía del Interior). Internal Corpoven Report. 237 p.
- Albertos, María. 1989. Estudio Geológico de las Secciones: Altagracia de Orituco – Agua Blanca y Gamelotal – San Francisco de Caira (estados Guárico y Miranda). Análisis Petrográfico y estadístico de la Formación Guárico (Geologic Study of the sections Altagracia de Orituco and Gamelotal – San Francisco de Caira, Guárico and Miranda states. Petrographic and statistical analysis of the Guárico Formation). Universidad Central de Venezuela, Thesis.
- Alvarez, Eduardo; Oliver Macsotay; Duggar Rivas and Victor Vivas. 1985. Formación Los Arroyos: Turbiditas de edad Mioceno Medio en la Región de El Pilar, edo. Sucre (Los Arroyos Formation: Turbidites of Middle Miocene age in the El Pilar Region, Sucre state). VI Congreso Geológico Venezolano, p. 1-32.
- Bartok, P. E., O. Renz, and G.E.G Westermann. 1985. The Siquisique opiolites, Northern Lara state, Venezuela: a discussion on their Middle Jurassic ammonites and tectonic implications. GSA Bulletin, 76:1050-1055.
- Bearsley, Amanga G; Virginia G, Sisson and H. G, Lallemand. 2008. Exhumation history of the Leeward Antilles coeval with regional deformation and island arc accretion. 2008 Annual GSA Joint Annual Meeting, Abstracts with Programs, p. 171.
- Beck C., Y. Ogacua and J. Dolan. 1990: Eocene Palaeogeography of the Southeastern Caribbean: Relations between sedimentation of the Atlantic Abyssal Plain at Site 672 and Evolution of

- the South America Margin. In: Moore J.C., A. Mascle et al. 1990. *Proceedings of the Ocean Drilling Program, Scientific Results*, 110:7-15.
- Beets, D. J. 1972. Lithology and Stratigraphy of the Cretaceous and Danian Succession of Curacao, Uitgaven “Natuurwetenschappelijke Studiekring voor Suriname en de Nederlandse Antillen, Utrecht, No. 70, 153 pag.
- Bellizia, A., 1986. Sistema montañoso del Caribe: Una Cordillera alóctona en la parte norte de América del Sur (Caribbean Mountain system: an Allochthonous cordillera in northern South America). *VI Congreso Geológico Venezolano*, 10: 6657-6836.
- Bellizia G., Alirio and Domingo Rodríguez G. 1966. Excursión a la Región de Duaca – Barquisimeto – Bobare (Field trip to Duaca – Barquisimeto - Bobare region). In: LEV, 2008, <http://www.pdvsa.com/lexico/excursio/exc-66.htm>
- Bizzi A. L. 2005. The Venezuelan Guayana Shield Basement dating Project. Progress Report. *Geos*, UCV, 38:112-194, in CD.
- Camposano Luis, Franco Urbani and Omar Contreras. 2005. Petrografía y Análisis Químico de Rocas Igneas halladas en Isla de Aves, Venezuela (Petrography and Chemical Analysis of the Igneous Rocks found in Aves Island, Venezuela) . *I Jornadas de Geología de Rocas Igneas y Metamórficas*, Programa General y Libro de Resúmenes, p. 22-23.
- Cardona Molina Agustin, Umberto G. Cordani and William D. MacDonald. 2006. Tectonic correlations of Pre-Mesozoic crust from the Northern termination of the Colombian Andes, Caribbean region. *Journal of South American Earth Sciences* 21:337-354.
- Cardona, A.; V., Valencia; P., Reiners; J., Duque; C., Montes; S., Nicolescu; G., Ojeda and J., Ruiz. 2008. Cenozoic exhumation of the Sierra Nevada de Santa Marta, Colombia;

- implications on the interactions between the Caribbean and South American plate. 2008 GSA Joint Annual Meeting, Abstracts with Programs, pag 104.
- Chew, David M.; Urs Schaltegger; Jan Kosler; Martin J. Whitehouse; Marcus Gutjahr, Richard A. Spikings and Aleksandar Miskovic. 2007. U-Pb Geochronologic evidence for the evolution of the Gondwanan margin of the north-central Andes, *GSA Bulletin*, 119(5): 697-711.
- Cordani U.G, A. Cardona, D.M. Jimenez, D. Liu and A.P Nutman. 2005. Geochronology of Proterozoic Basement Inliers in the Colombian Andes: Tectonic History of remnants of a fragmented Grenville Belt. *In*: Vaughan A.P.M., Leat P.T. and R.J. Pankhurst (eds.), *Terrane Processes at the margins of Gondwana*, Geological Society of London, Special Publications, 246:329-346.
- Dasch L. E. 1982. U-Pb Geochronology of the Sierra de Perijá, Venezuela. Case Western Reserve University, M.S. Thesis. 164 p.
- Diaz de Gamero, Maria L. 1995. The changing course of the Orinoco River during the Neogene: a review, *Palaeogeography, Palaeoclimatology, Palaeoecology*, 123:385-402.
- Dickinson, William R., L. Sue Beard, G. Robert Brakenridge, James L. Erjavec, Robert C. Ferguson, Kerry F. Inman, Rex A. Knepp, F. Alan Lindberg and Paul T. Ryberg. 1983. Provenance of North American Phanerozoic sandstones in relation to tectonic setting. *Geological Society of America Bulletin*, 94:222-235.
- Dickinson William R. 1985. Interpreting provenance relations from detrital modes of sandstones. *In*: G. G. Zuffa (ed.), *Provenance of Arenites*, p.333-361.

- Donnelly, Thomas W. 1989. Geologic History of the Caribbean and Central America. *In*: Bally A. W. and A. R. Palmer (eds.), *The Geology of North America – An overview: Geological Society of America, The Geology of North America*, A: 299-321.
- Driscoll Neal W. and John B. Diebold. 1998. Deformation of the Caribbean Region: One plate or two?, *Geology*, 26(11):1043-1046.
- Duncan, R. A. and R. B. Hargraves. 1984. Plate tectonic evolution of the Caribbean region in the mantle reference frame. *In*: Bonini, William E., Robert Hargraves and Reginald Shagam, *The Caribbean-South American Plate Boundary and Regional Tectonics*, Geological Society of America, Memoir 162, p. 81-93.
- Erickson J. P. and J. Pindell. 1998a. Cretaceous through Eocene sedimentation and Paleogeography of a Passive Margin in northeastern Venezuela. *In*: *Paleogeographic Evolution and Non-Glacial Eustasy, Northern South America*, SEPM Special Publication No 58, p. 218-259.
- Erickson J. P. and J. Pindell. 1998b. Sequence stratigraphy and relative sea-level history of the Cretaceous to Eocene passive margin of North-East Venezuela and the possible tectonic and eustatic causes of stratigraphic development. *In*: *Paleogeographic Evolution and Non-Glacial Eustasy, Northern South America*, SEPM Special Publication No 58, p. 261-281.
- Escalona, A. 2004. Tectonic reconstruction of sedimentary basins associated with the proto-Maracaibo and proto-Orinoco rivers: New constraints from BOLIVAR and GULFREX seismic data, *Eos Transactions AGU*, 85(47), Fall Meeting Suppl., Abstract T33B-1374.
- Feo-Codecido Gustavo, Foster D. Smith Jr., Nelson Aboud and Estela Di Giacomo. 1984. Basement and Paleozoic rocks of the Venezuelan Llanos Basin. *In*: Bonini, William E.,



- Robert Hargraves and Reginald Shagam, The Caribbean-South American Plate Boundary and Regional Tectonics, Geological Society of America, Memoir 162, p.175-187.
- Fox Paul J., Edward Schreiber and Bruce C. Heezen. 1971. The Geology of the Caribbean Crust: Tertiary sediments, granitic and basic rocks from the Aves Ridge. *Tectonophysics*, 12:89-109.
- French, Christofer D. and Christopher J., Schenk. 2004. Map Showing Geology, Oil and gas Fields, and Geologic Provinces of the Caribbean Region. USGS Open-File Report 97-470-K.
- Galea F. 1986. Bioestratigrafía y ambiente sedimentario del Grupo Santa Anita del Cretaceo Superior – Eoceno, Venezuela nor-oriental (Biostratigraphy and sedimentary environment of the Upper Cretaceous – Eocene Santa Anita Group, Northeastern Venezuela). *Memoria VI Congreso Geológico Venezolano*, 1:703-721.
- Goldstein S. L., N. T. Arndt and R. F. Stallard. 1997. The history of a continent from U-Pb ages of zircons from Orinoco basin river sediments. *Chemical Geology*, 139:271-286.
- Gonzalez de Juana C., J.M. Iturralde de Arozena, X. Piccard Cadillay. 1980. Geología de Venezuela y de sus Cuencas Petrolíferas, Caracas, Foninves, 1031 p.
- Gorney David, Alejandro Escalona, Paul Mann, M. Beatrice Magnani and BOLIVAR Study Group. 2007. Chronology of Cenozoic tectonic events in western Venezuela and the Leeward Antilles based on integration of offshore seismic reflection data and on-land geology. *AAPG Bulletin* 91(5):653-684.
- Ghosh, S.K. and E. Zambrano. 1996. The Eocene turbidites of the Trujillo Formation, Venezuelan Andes, AAPG Bulletin, 80(8):1294.

- González de Juana C., J.M. Iturralde de Arozena, and X. Piccard Cadillay. 1980. *Geología de Venezuela y de sus Cuencas Petrolíferas*, Caracas, Foninves, 1031 p.
- Grande, Sebastian. 2005. Rocas ígneas de la Península de Paraguaná (Igneous Rocks of the Paraguaná Peninsula, Venezuela. I Jornadas de Geología de Rocas Ígneas y Metamórficas, Programa General y Libro de Resúmenes. P. 28-30.
- Grande Sebastian, Franco Urbani and David Mendi. 2007. Presencia de un basamento Grenvilliano de alto grado en Venezuela noroccidental (Presence of a high-grade basement in northwest Venezuela of possible Grenville affinity). *Geos* 39:90.
- Guynn, Jerome. 2006. Comparison of Detrital Zircon Age Distributions using the K-S Test. Arizona LaserChron Center. <http://www.geo.arizona.edu/alc/Analysis%20Tools.htm>
- Hackley Paul C., Franco Urbani and Alexander W. Karlsen. 2005. Geologic Shaded Relief Map of Venezuela. U.S. Geological Survey Open File Report 2005-1038. <http://pubs.usgs.gov/of/2005/1038/>.
- Holcombe Troy L., John W. Ladd, Graham Westbrook, N, Terence Edgar and Christopher L. Bowland. 1990. Caribbean marine Geology; Ridges and basins of the plate interior. *In*: Dengo G. and J. E. Case, The Caribbean region: Geological Society of America, The Geology of North America, H: 231-260.
- Hoorn, Carina; Javier Guerrero; Gustavo A. Sarmiento and Maria A. Lorente. 1995. Andean tectonics as a cause for changing drainage patterns in Miocene northern South America, *Geology*, 23(3):237-240.
- Iturralde-Vinent Manuel A., and Lisa Gahagan. 2002. Latest Eocene to Middle Miocene Tectonic Evolution of the Caribbean: some principles and their implications for plate

- tectonic modeling. In: Jackson, Trevor A. (2002): Caribbean Geology into the Third Millennium, *Transactions of the 15<sup>th</sup> Caribbean Geological Conference*, p.p. 279.
- Jácome Maria I., Kenny Rondón, Michael Schmitz, Carlos Izarra and Ernesto Vieira. 2008. Integrated seismic, flexural and gravimetric modelling of the Coastal Cordillera Thrust Belt and The Guarico Basin, North-Central Region, Venezuela. *Tectonophysics*, 459:27-37.
- James K. H. 1997. Distribution and Tectonic significance of Cretaceous–Eocene Flysch–Wildflysch deposits of Venezuela and Trinidad. *Memoirs from VIII Congreso Geológico Venezolano*, Margarita Island, Venezuela, p. 415-421.
- James K. H. 2006. Arguments for and against the Pacific origin of the Caribbean plate: discussion, finding for an inter-American origin. *Geologica Acta* 4(1-2): 279-302.
- James K. H. 2007. The Caribbean Ocean Plateau – an overview, and a different understanding. <http://www.mantleplumes.org/WebDocuments/CaribbeanPlateau.pdf>.
- Kasper D. C. and D. K. Larue. 1986. Paleogeographic and tectonic implications of quartzose sandstones of Barbados, *Tectonics*, 5(6):837-854.
- Keppie J. Duncan and F. Ortega-Gutierrez. 1999. Middle American Precambrian basement: A missing piece of the reconstructed 1-Ga orogen. In: Ramos Victor and J. Duncan Keppie (eds.), *Laurentia-Gondwana connections before Pangaea*. Geological Society of America, Special Paper 336:199-210.
- Kerr, Paul F. 1959. *Optical Mineralogy*, Third edition, McGraw-Hill Book Company, 441 p.
- Kerr, A., R. V. White, P. M. E. Thompson, J. Tarney, and A. D. Saunders. 2003. No oceanic plateau – No Caribbean plate? The seminal role of an oceanic plateau in Caribbean plate evolution, *in*: Bartolini C., R.T. Buffler, and J. Blickwede (eds.), *The Circum-Gulf of*

- Mexico and the Caribbean: Hydrocarbon habitats, basin formation, and plate tectonics, AAPG Memoir 79, p. 126-168.
- Kroner, Alfred and Umberto Cordani. 2003. African, southern Indian and South American cratons were not part of the Rodinia supercontinent: evidence from field relationships and geochronology. *Tectonophysics*, 375: 325-352.
- Lallemant H. G. and Sisson V. B. 2005. Caribbean – South American Plate Interactions, Venezuela, The Geological Society of America, Special Paper 394, 346 p.
- Léxico Estratigráfico Venezolano (LEV). <http://www.pdvsa.com/lexico/>. (November 2008).
- Levander A. and the BOLIVAR working Group. 2005. BOLIVAR: Continental Growth and Deformation along South American – Caribbean Plate Boundary. *17<sup>th</sup> Caribbean Geological Conference, San Juan Puerto Rico*, pag. 46-47.
- Levander A., M. Schmitz, H. G. Ave Lallemant, C. A. Zelt, D. S. Sawyer, M. B. Magnani, P. Mann, G. Christeson, J. Wright, G. Pavlis and J. Pindell. 2006. Evolution of the Southern Caribbean Plate Boundary. *EOS Transactions*, American Geophysical Union, 87(9): 97,100.
- Lopez, Rafael. 1976. Estudio de la Formación Matatere en el area de Carora, estado Lara (Study of the Matatere Formation in the area of Carora, Lara state). Universidad Central de Venezuela, Thesis.
- Macsoy O., 1972. Observaciones acerca de la edad y paleoecología de algunas formaciones de la región de Barquisimeto, Estado Lara, Venezuela (Observations about age and paleoecology in some formations of the Barquisimeto region, Lara state). *Memorias IV Congreso Geológico Venezolano.*, Ministerio de Minas e Hidrocarburos, Caracas, 3: 1673-1701.

- Macsotay, Oliver; Victor Vivas; Nelly Pimentel de Bellizia and Alirio Bellizzia G. 1986. Excursion: Estratigrafía y Tectónica del Cretáceo – Paleógeno de las islas al norte de Puerto La Cruz – Santa Fe y regiones adyacentes (Field Trip: Stratigraphy and Tectonics of the Cretaceous – Paleogene of the islands north of Puerto La Cruz – Santa Fe and adjacent regions). *Memoria VI Congreso Geológico Venezolano*, 10:7125-7174.
- Macsotay O.; J. F., Stephan, and E. Alvarez, 1987. Grupo Lara: Sedimentitas oceánicas y peninsulares en el Cretáceo alóctono de Venezuela occidental (Lara Group: Oceanic and peninsula sedimentites in the Cretaceous allochthonous of western Venezuela). *Bol. Geol.*, (28): 3-78.
- Magnani, M.B; C.A., Zelt; A., Levander and the BOLIVAR Working Group. 2005. BOLIVAR: A snapshot of the Caribbean – South american plate boundary at 67.5 W. 17th Caribbean Geological Conference 2005, San Juan, Puerto Rico.
- Mamberti, Marc; Henriette, Lapierre; Delphine, Bosch; Etienne, Jaillard; Raynald, Ethien; Jean, Hernandez, and Mireille Polve. 2003. Accreted fragments of the Late Cretaceous Caribbean-Colombian Plateau in Ecuador. *Lithos*, 66:173-199.
- Martínez Gladys and Graziana Valleta. 2008. Petrografía de las facies gruesas de la Formación Matatere y otras unidades del Centro-Occidente de Venezuela (Petrography of the coarse grained facies of Matatere Formation and other units from Central-Western Venezuela), Universidad Central de Venezuela, Thesis, 280 p. Unedited.
- Maury R. C., G. K. Westbrook, P. E. Baker, Ph. Bouysse and D. Westercamp. 1990. Geology of the Lesser Antilles. *In*: Dengo G. and J. E. Case, The Caribbean region: Geological Society of America, The Geology of North America, H:141-166.

- Maze, W.B., 1984. Jurassic La Quinta formation in the Sierra de Perijá, northwestern Venezuela: geology and tectonic environment of red beds and volcanic rocks. *In*: Bonini, William E., Robert Hargraves and Reginald Shagam, The Caribbean-South American Plate Boundary and Regional Tectonics, Geological Society of America, Memoir 162, p. 263-282.
- Mendoza V. 2005. Geología de Venezuela. *Geos* 38. CD.
- Meschede Martin and Wolfgang Frisch. 2002. The Evolution of the Caribbean Plate and its Relation to Global Plate Motion Vectors: Geometric Constrains for an Inter-American Origin. *In*: Jackson, Trevor A. 2002. Caribbean Geology into the Third Millennium, *Transactions of the 15<sup>th</sup> Caribbean Geological Conference*, p.1-14.
- Molina Agustin Cardona, Unberto G. Cordani and William D. MacDonald. 2006. Tectonic correlations of Pre-Mesozoic crust from the Northern termination of the Colombian Andes, Caribbean region. *Journal of South American Earth Sciences* 21:337-354.
- Moreno Joselys and Johnny Casas. 1986. Estudio Petrográfico y estadístico de la secuencia flysch Eocena de la Isla de Margarita (Petrographic and statistic study of the Eocene flysch sequence from Margarita Island), Universidad Central de Venezuela, Thesis.
- Muñoz J., Nicolas Gerardo. 1973. Geología Sedimentaria del Flysch Eoceno de la Isla de Margarita, Venezuela (Sedimentary Geology of the Eocene Flysch of Margarita Island, Venezuela). *Geos*, 20:5-64.
- Ostos M., F. Yoris, and H. A. Lallemand. 2005. Overview of the Southeast Caribbean – South American Plate Boundary Zone. *In*: Lallemand H. and V. Sisson, Caribbean-South American Plate Interactions, Venezuela. The Geological Society of America, Special paper 394, p. 53-89.

- Peirson III, A. L.; A. Salvador and R.M. Stainforth, 1966. The Guárico Formation of north-central Venezuela. (La Formación Guárico, Venezuela nor-central). *Boletin Informativo, Asociacion Venezolana de Geología, Minas y Petroleo*, 9(7): 183-224.
- Persad, K.M. 1990. The Espino Graben – An Aulacogen?. *Transactions of the Geological Conference of the Geological Society of Trinidad & Tobago*, 2:25.
- Pettijohn F.J., P.E. Potter and R. Siever. 1987. *Sand and Sandstone*, 2<sup>nd</sup> edition, Berlin, Springer-Verlag, 553 p.
- Pindell, James L. and Stephen F. Barrett. 1990. Geological evolution of the Caribbean region; A plate-tectonic perspective. In: Dengo, G. and Case, J. E. (eds.), *The Caribbean region*, Geological Society of America, *The Geology of North America*, H:405-431.
- Pindell J. L., R. Higgs, and J. F. Dewey. 1998. Cenozoic palinspatic reconstruction, paleogeographic evolution and hydrocarbon setting of the northern margin of South America. In: *Paleogeographic Evolution and Non-Glacial Eustasy, Northern South America*, SEPM Special Publication No 58, p.45-85.
- Pindell James and Lorcan Keenan. 2001. Kinematic Evolution of Mexico and the Caribbean. *GCSSEPM Foundation 21st Annual Research Conference, Petroleum Systems of Deep Water Basins*, p. 193-220.
- Pindell, James; Lorcan, Keenan; Walter V., Maresch; Klaus-Peter, Stanek, Grenville, Draper and Roger, Higgs. 2005. Plate-Kinematics and crustal dynamics of circum-Caribbean arc-continent interactions: Tectonic controls on basin development in Proto-Caribbean margins. In: Lallemand H. and V. Sisson, *Caribbean-South American Plate Interactions*, Venezuela. The Geological Society of America, Special paper 394, p. 7-52.

- Pindell James, L. Kennan, K.-P. Stanek, W. V. Maresch and G. Draper. 2006. Foundations of Gulf of Mexico and Caribbean Evolution: Eight Controversies Resolved. *Geologica Acta*, 4(1-2):303-341.
- Priem, H.N.A; D.J. Beets and E.A.Th. Verdurmen. 1986. Precambrian rocks in an Early Tertiary conglomerate on Bonaire, Netherlands Antilles (southern Caribbean borderland): evidence for a 300 km eastward displacement relative to the South American mainland?, *Geologie en Mijnbouw* 65:35-40.
- Pudsey, C. J. and H. G. Reading. 1982. Sedimentology and Structure of the Scotland Group, Barbados. In: Legget, J. K. (ed.): Trench Forearc Geology, Geological Society of London, Special Publication, 10:291-308.
- Rekowski F., and L. Rivas, 2005. Integración Geológica de la Isla de Margarita, estado Nueva Esparta (Geologic integration of Margarita Island, Nueva Esparta state). Universidad Central de Venezuela, Thesis.
- Renz, O. y K. C. Short, 1960. Estratigrafía de la región comprendida entre el Pao y Acarigua, estados Cojedes y Portuguesa (Stratigraphy of the region between El Pao and Acarigua, Cojedes and Portuguesa states). *III Congreso Geológico Venezolano*, Caracas, 1: 277-315.
- Rodriguez Inirida and Josmat Rodriguez. 2003. Gravity and Magnetic Modelling across the Guárico Sub-basin, Espino Graben, Venezuela. *Andean Geodynamics: Extended Abstracts*. Institut de Reserche pour le développement IRD – Université Paul Sabatier. p. 533-536.
- Rogers, J. W. and M. Santosh. 2004. *Continents and Supercontinents*. Oxford University Press, 289 p.
- Ruiz Joaquin, Richard M. Tosdal, Pedro A. Restrepo and Gustavo Murillo-Muneton. 1999. Pb Isotope evidence for Colombia-southern Mexico connections in the Proterozoic. In: Ramos



- Victor and J. Duncan Keppie (eds.), *Laurentia-Gondwana connections before Pangea*. Geological Society of America, Special Paper 336:183-197.
- Santamaria, Francisco and Carlos Schubert. 1974. Geochemistry and Geochronology of the Southern Caribbean – Northern Venezuela plate boundary. *Geological Society of America Bulletin*, 7:1085-1098.
- Schneider Santos J.O., P.E. Potter, N.J. Reis, L.A. Hartmaun, I.R. Fletcher and N.J. McNaughton. 2003. Age, source, and regional stratigraphy of the Roraima Supergroup and Roraima-like outliers in Northern South America based on U-Pb geochronology. *GSA Bulletin*, 115(3):331-348.
- Schubert, C.; R. S. Sifontes; V. E. Padrón; J. R. Vélez , J. R. and P. A. Loaiza, 1979. Formación La Quinta (Jurásico), andes merideños: geología de la sección tipo (Jurassic La Quinta Formation, Merida andes: Geology of the type section). *Acta Científica Venezolana*, 30: 42-55.
- Sinton, C.W.; R.A. Duncan, M. Storey, J. Lewis and J.J. Estrada. 1998. An Oceanic Flood Basalt Province within the Caribbean Plate. *Earth and Planetary Science Letters*, 155:221-235.
- Sisson V., M. Ostos, A. E. Blythe, L. W. Snee, P. Copeland, J. Wright, R. Donelick and L. R. Guth. 2005. Overview of radiometric ages in three allochthonous belts of northern Venezuela: Old ones, new ones, and their impact on regional geology. In Lallemant H. and V. Sisson, *Caribbean-South American Plate Interactions, Venezuela*. The Geological Society of America, Special paper 394, p: 91-117.
- University of Arizona Laserchron Laboratory. <http://www.geo.arizona.edu/alc/>.

- French Christopher D. and Christopher J. Schenk. 2004. Map Showing Geology, Oil and Gas Fields, and Geologic Provinces of the Caribbean Region. U.S. Geological Survey, Open File Report 97-470-K.
- Urbani Franco. 2005. Geological Field Trip Cordillera de la Costa, Venezuela. 2005 Annual Meeting of the Projects BOLIVAR and GEODINOS.
- Urbani, Franco. 2006. Geología de la region de Siquisique, estado Lara (Geologi of the Siquisique region, Lara state). *Geos* 39, 85 p.
- Urbani F., J. Wright, S. Grande and P. Viscarret. 2007. La Metadiorita de Todasana, estado Vargas: Geología y Geocronología (The Todasana Metadiorite in Vargas state: Geology and Geochronology). *IX Venezuelan Geological Congress*.
- Valdes D'Gregorio, Carmen. 1980. Geología de superficie, Sedimentología, Estratigrafía y Tectónica de un Área entre Carora – Barquisimeto, estado Lara (Las Peñitas – Pozo Guapo). (Surface Geology, Sedimentology, Stratigraphy and Tectonic o fan area between Carora – Barquisimeto, Lara state; Las Peñitas – Pozo Guapo). Universidad Central de Venezuela, Thesis.
- Vallejo Cristian, Richard A. Spikings, Leonard Luzieux, Wilfried Winkler, David Chew and Laurence Page. 2006. The early interaction between the Caribbean Plateau and the NW South American Plate. *Terra Nova*, 18:264-269.
- Van Andel, Tjeerd. 1958. Origin and Classification of Cretaceous, Paleocene and Eocene sandstones of Western Venezuela. *Bulletin of the American Association of Petroleum Geologists*, 42(4):734-763.
- Villamil Tomas and James Pindell. 1998. Mesozoic Paleogeographic Evolution of Northern South America: Foundations for sequence stratigraphic studies in passive margin strata

- deposited during non-glacial times. In: Paleogeographic Evolution and Non-Glacial Eustasy, Northern South America, SEPM Special Publication No 58, p. 283-318.
- Viscarret Patxi, James Wright and Franco Urbani (2007). Dataciones U/Pb SHRIMP en circon de rocas del Macizo El Baúl, estado Cojedes, Venezuela (U-Pb SHRIMP zircon geochronology of El Baúl massif, Cojedes state, Venezuela). *Geos*, 39:94-95.
- Von der Osten, E., 1954. Geología de la región de la bahía de Santa Fé, estado Sucre (Geology of the region of Santa Fe bay, Sucre state). Venezuela, *Boletín de Geología* 3(8): 123-211.
- Weber, John. 2007. Using GPS to help unravel Cenozoic – Recent Caribbean – South American and Adria – Eurasia Plate motions and plate boundary zone tectonics (abstract). 2007 *Geological Society of America Annual Meeting*, Abstracts with Programs, 39(6):47.
- Wright, J. 2004. Aruba and Curacao: Remnants of a collided Pacific oceanic plateau?, Initial results from the BOLIVAR Project. American Geophysical Union (AGU), Fall Meeting 2004, abstract # T33B-1367.
- Wright J. E., S. Wyld, and F. Urbani. 2008. Late Cretaceous subduction initiation Leeward Antilles / Aves Ridge: Implications for Caribbean Geodynamic models. 2008 *Geological Society of America Joint Annual Meeting*, Abstracts with Programs, p. 103.
- Yoris F., and Albertos de Yoris M. A. 1989: Medidas de Paleocorrientes en la secuencia de la Formación Guárico y sus equivalentes en las secciones: Altagracia de Orituco, Guatopo y Gamelotal – San Francisco de Macaira, estados Guárico y Miranda (Paleocurrents in Guárico Formation and Equivalents, Altagracia de Orituco-Guatopo and Gamelotal-San Francisco de Macaira sections, Guárico and Miranda States). Caracas, *Geos*, 29:152-159.
- Yoris F., and M. Ostos. 1997. Petroleum Geology of Venezuela, *in*: Singer J. M. (ed.) 1997. *Well Evaluation Conference*. Caracas, Schlumberger, p. 1-44.

Zapata, Eglee. 1976. Estudio de la Formación Guárico en el área de la Laguna de Unare, estado Anzoátegui (Study of the Guárico Formation in the area of Laguna de Unare, Anzoátegui state). Universidad Central de Venezuela, Thesis.

## **APPENDICES**

# **APPENDIX A** **SAMPLE INVENTORY**

Table A1. Location of the visited sites.

GPS SITE	SAMPLE	UNIT	Location	Geographic	
				Lat	Long
329	VMN-5	Matatere	La Mamita stream	10° 17' 14.8"	70° 23' 10.7"
331	VMN-6	Matatere	El Oro stream	10° 21' 44.6"	70° 17' 06.8"
332	VMN-7	Aguardiente	Carora	10° 08' 47.7"	70° 06' 32.4"
333	VMN-8B	Matatere	El Palito stream	10° 23' 22.5"	70° 04' 55.4"
334	VMN-8A	Matatere	El Palito stream	10° 23' 22.8"	70° 04' 55.8"
335	no sample	Matatere/Castillo	La Mesa	10° 22' 33.2"	70° 03' 19.0"
336	VMN-9	Matatere	Los Carrillos river	10° 24' 58.1"	69° 54' 51.6"
337	VMN-10	Matatere	Horno Negro stream	10° 23' 49.0"	69° 55' 31.6"
339	VMN-11	Matatere	Puz stream	10° 29' 23.7"	69° 49' 23.1"
340	VMN-12	Matatere	Las Petacas stream	10° 36' 53.9"	69° 48' 32.5"
341	no sample	Gabbro	Siquisique	10° 36' 53.7"	69° 49' 09.4"
342	no sample	Matatere/Castillo	Siquisique	10° 36' 40.4"	69° 49' 19.5"
343	VMN-13	Matatere	Siquisique	10° 37' 19.9"	69° 38' 12.4"
	VMN-14				
	VMN-15				
347	VMN-16	Bobare	south Carora	10° 26' 13.6"	69° 26' 41.2"
348	VMN-17	Bobare	south Carora	10° 24' 08.8"	69° 24' 29.8"
349	VMN-18	Agua Blanca	Acarigua	09° 40' 12.2"	69° 05' 49.3"
350	VMN-19	Guárico	San Carlos	09° 39' 51.0"	68° 35' 37.0"
352	VMN-20	Guárico	San Juan de los Morros	09° 46' 30.3"	67° 21' 18.1"
356	VMN-23	Guárico	Camatagua	09° 49' 05.7"	66° 56' 34.5"
364	VMN-28	Guárico	Boca de Uchire	10° 06' 44.9"	65° 23' 09.3"
368	VMN-32	Barranquín	Cerro La Laguna	10° 13' 58.2"	64° 32' 06.2"
369	VMN-33	Barranquín	Mochima	10° 16' 35.3"	64° 26' 13.7"
370	VMN-34	Barranquín	Mochima	10° 19' 35.0"	64° 20' 23.7"
371	VMN-35	Barranquín	Santa Fe	10° 17' 31.0"	64° 23' 21.5"
379	VMN-39	Pampatar	Pampatar	10° 59' 48.5"	63° 47' 16.3"
380	VMN-40	Pampatar	Pampatar	10° 59' 47.3"	63° 47' 01.0"
381	VMN-41	Pampatar	Playa Moreno	10° 59' 02.0"	63° 48' 20.9"
382	VMN-42	Los Arroyos	El Pilar	10° 33' 34.5"	63° 09' 17.6"
383	VMN-43	Los Arroyos	El Pilar	10° 33' 20.9"	63° 09' 08.0"
N/A	CUR-14z	Midden Curacao	Curacao	12° 13' 15.0"	69° 02' 17.0"
N/A	CUR-21	Lagoen	Curacao	12° 21' 07.0"	69° 08' 14.0"
N/A	CUR-22	Lagoen	Curacao	12° 21' 07.0"	69° 08' 42.0"

Datum: WGS 84

Table A2. Sample Inventory and macroscopic description

LOCATION	UNIT	GEOLOGICAL CONTEXT	SITE	SAMPLE	DESCRIPTION	
Western Venezuela	Matatere Fm (Paleocene - Eocene)	Flysch	GPS 329 Qda La Mamita	VMN-5a	Compact and dense sandstone. Dark colored. Medium grain sized. Dark components, probably low content of Qz. Equivalent to sample LA 1501 (in Martinez & Valleta 2008)	
				VMN-5b	Qz-Sandstone. Coarse to conglomeratic. Light colored. Some dark grains and some red grains, probably of volcanic origin	
			GPS 331 Qda El Oro	VMN-6a	Qz-Sandstone. Medium to fine grains. Probably representing a channel fill. Similar to VMN-5b, although the red grains are not seen	
				VMN-6b	Dark, fine grained sandstone. Equivalent to VMN-5a and LA1504 (in Martinez & Valleta 2008). Very compact and dense. Dark gray to black in color. Low in Qz	
			GPS 333 Qda El Palito	VMN-8b	Medium grained Qz-Felsp sandstone. Dark colored. Felspars are gray	
			GPS 334 Qda El Palito	VMN-8a	Conglomeratic sandstone. Angular Qz grains. Rich in Qz. Equivalent to LA1510A. Iron-rich cement	
			GPS 336 Qda Los Carrillos	VMN-9	Sandstones with conglomeratic levels. Equivalent to LA1521. Some chert fragments into the conglomerate.Conglomerates are matrix supported. Qz-Felsp and chert (arkose)	
			GPS 337 Qda Horno Negro	VMN-10	Conglomeratic sandstone similar to VMN-9. Sandstones are very feldspatic (Plag). Bigger grains are rounded. Some Qz. Greywacke	
			GPS 339 Qda de Puz	VMN-11	Coarse sandstones and dark colored shales with olistoliths of limestones from Upper Cretaceous La Luna Fm. Equivalent to sample LA1524 in Martinez & Valleta (2008). Graywacke.	
			GPS 340 Qda Las Petacas	VMN-12	Fine grained sandstone.Porous (so far all the samples have been compact). Proportions: Feldspars>Dark grains>Qz.	
			GPS 343 Siquisique	VMN-13	granite pebbles from the conglomerate. Pebbles are about 2-5 cm in diameter. Equivalent to LA1530G and LA1530K (Martinez & Valleta, 2008). Fragments of volcanic rocks, granite, smoked Qz, ftanites.	
				VMN-14	Fine grained greywacke. Taken from outcrop of Matatere along the creek. Equivalent to LA1530A. Felspars, few Qz, drak grains	
				VMN-15	Granite pebble from other block of conglomerate from the same unit. This pebble is about 15 cm in diameter. Sample taken downstream, down the	
			Yumare	VMN-44	Fine grained greywacke.	
		Aguardiente Fm (K inf)		GPS 332 Carora	VMN-7	Fine grained sandstone. Qz, grey in color. Section is shaly at the base(? , NE side of outcrop). Sandy at the top(?). Reddish color when weathered
		Bobare Fm (low K)		GPS 347 South Carora	VMN-16	Mid to coarse grained sandstone. Qz-Feldsp, some dark grains (probably volcanic or chert)
			GPS 348 South Carora	VMN-17	Coarse grained sandstone. Qz-rich, Feldsp, Mica. The section is faulted	
		Agua Blanca (K)		GPS 349 Acarigua	VMN-18	Qz-mica-schist. Dark grains, probable smoked Qz. Schist with similar mineralogic composition as the first samples from Matatere Fm. Medium grain. Foliation hardly noticed
	Guarico Fm (late K - early T)	Flysch	GPS 350 San Carlos	VMN-19	Fine grained sandstone. Reddish in weathered surface. Muscovite and dark minerals, probably Qz. Almost a graywacke. Shaly outcrop. Just a few and thin sand beds	
Central Venezuela			GPS 352 San Juan de los Morros	VMN-20	Fine grained graywacke. Feldsp + dark components + Qz	
			GPS 356 Camatagua	VMN-23	Medium grained sandstone. Rich in Qz. Some chert grains. Also some Fe-rich grains	
Eastern Venezuela				GPS 364 Boca de Uchire	VMN-28	Grauwackic sandstone. Medium size grained

LOCATION	UNIT	GEOLOGICAL CONTEXT	SITE	SAMPLE	DESCRIPTION
Eastern Venezuela	Los Arroyos (Miocene)	Flysch	GPS 382 El Pilar	VMN- 42	Graywake. Medium grain sized, redish in color. Dark fragments plus angulose quartz. Outcrop very weathered and covered by vegetation
			GPS 383 El Pilar	VMN- 43	Medium to coarse grained sandstone. Graywake. Highly weathered
	Caratas Fm (Eocene)	Flysch	GPS 365 Ferry	VMN- 29	Fine grained sandstone. Dark grey in color. Sample was collected from the highest point of the outcrop. Minerals too small to identify. Some Qz
			GPS 366 Pto La Cruz	VMN- 30	Qz-Felsp sandstone. Medium grained. Light colored. Weathered
			GPS 367 Otra Banda	VMN- 31	Grauwakic sandstone. Medium to fine grained
	Barranquin Fm (early K)	Passive Margin	GPS 368 Cerro La Laguna	VMN- 32	Coarse grained, Qz-sandstone
			GPS 369	VMN- 33	Qz-Feldsp-sandstone. There is a big sand body, a channel fill. Medium grained
			GPS 370 Mochima	VMN- 34	Coarse grained Qz-Feldsp-sandstone. Faults everywhere on the outcrop
			GPS 371 Sta Fe	VMN- 35	Coarse grained Qz-sandstone. New section of Puerto La Cruz – Cumana highway
Margarita Island	Pampatar Fm (Eocene)	Flysch	GPS 379 Pampatar	VMN- 39	Dark colored sandstone. Graywacke
			GPS 380 Pampatar	VMN- 40	Conglomerate with volcanic fragments. Dark grey colored. No Qz seen
			GPS 381 Pampatar	VMN- 41	Medium-grained to conglomeratic sandstone. Dark colored (dark gray). No Qz. Dark minerals. Similar composition as conglomerate in sample VMN-40



**APPENDIX B**  
**FIELD WORK PHOTOGRAPHS**

**BARRANQUIN FORMATION**



Figure B.1. Outcrop of the Barranquín Formation (Taguarumo Member) at site GPS-368. The arrow indicates where sample VMN-32 was collected



Figure B.2. Outcrop of the Barranquín Formation at site GPS-369. Sample VMN-33 was collected where indicated by the arrow





Figure B.3. Outcrop of the Barranquín Formation at site GPS-370. Sample VMN-34 was collected where indicated by the arrow

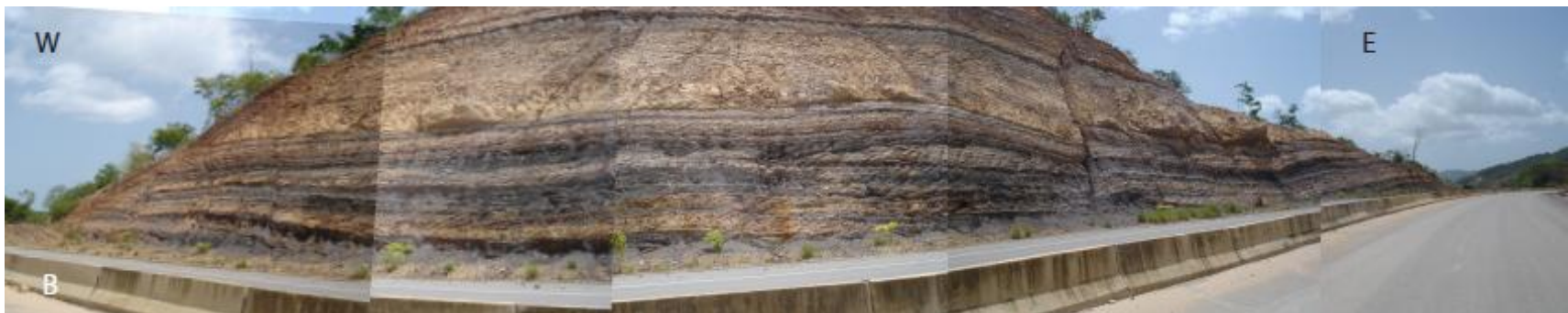


Figure B.4. Outcrop of the Barranquín Formation at site GPS-371, sample VMN-35. (A) Northern side of the road, where the sample was collected (pointed by arrow); (B) southern side of the road.



## BOBARE FORMATION



Figure B.5. Outcrop of the Bobare Formation, site GPS-348. The sample VMN-17 was collected where indicated by the arrow

## AGUARDIENTE FORMATION



Figure B.6. Outcrop of the Aguardiente Formation, south of Carora, site GPS-332, sample VMN-7



## BARQUISIMETO FORMATION



Figure B.7. The Barquisimeto Formation at site GPS-328; sample VMN-4. (A) Outcrop view and place where the sample was collected; (B) Outcrop view across the road; (C) phyllites of the Barquisimeto Formation

## GUARICO FORMATION



Figure B.8. Outcrop of the Guárico Formation, south of San Juan de Los Morros. Site GPS-352, sample VMN-20





Figure B.9. Reverse fault and associated drag fold in a turbidite sequence of the Guárico Formation, site GPS-352; sample VMN-20



Figure B.10. The Guárico Formation in the Boca de Uchire area; Site GPS-364; Sample VMN-28. Image taken from LEV (2008)



## MATATERE FORMATION



Figure B.11. Outcrops of the Matatere Formation at the La Mamita stream, site GPS-329; samples VMN-5A (picture B) and VMN-5B (picture A)



Figure B.12. (A) Outcrop of the Matatere Formation at the El Oro creek, Site 331.



Figure B.12(B) Outcrop of the Matatere Formation at the El Oro creek, Site 331; Sample VMN-6

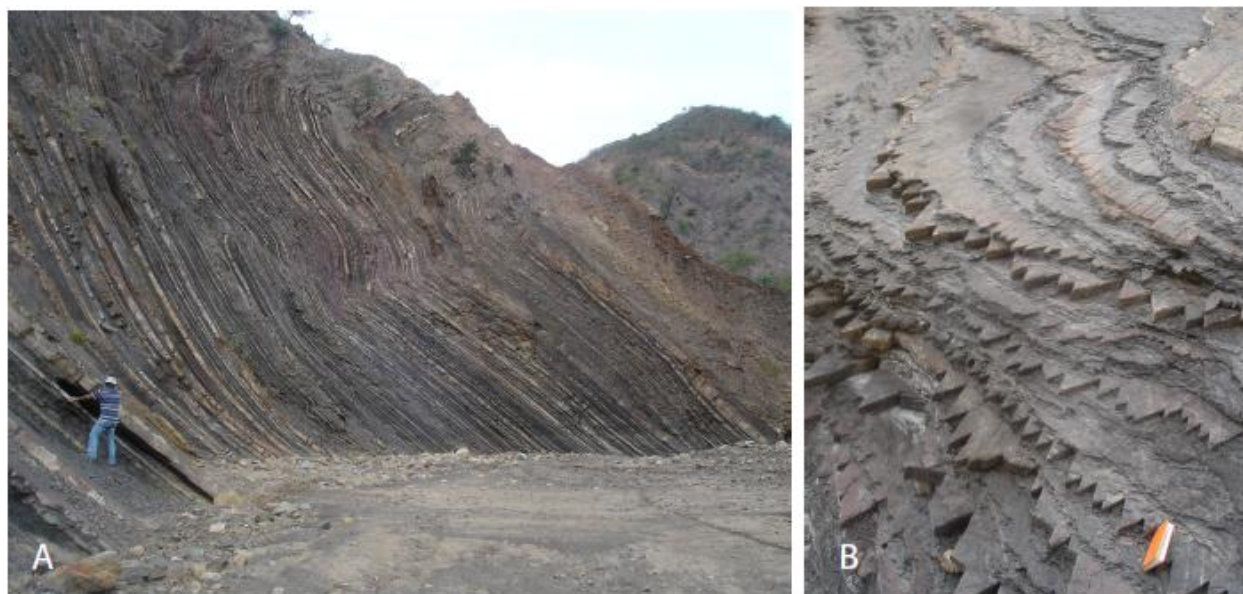


Figure B.13. Outcrop of the Matatere Formation at El Palito stream; Site GPS-333; sample VMN-8B. (A) General view of the outcrop; (B) fracture pattern of the sandstones



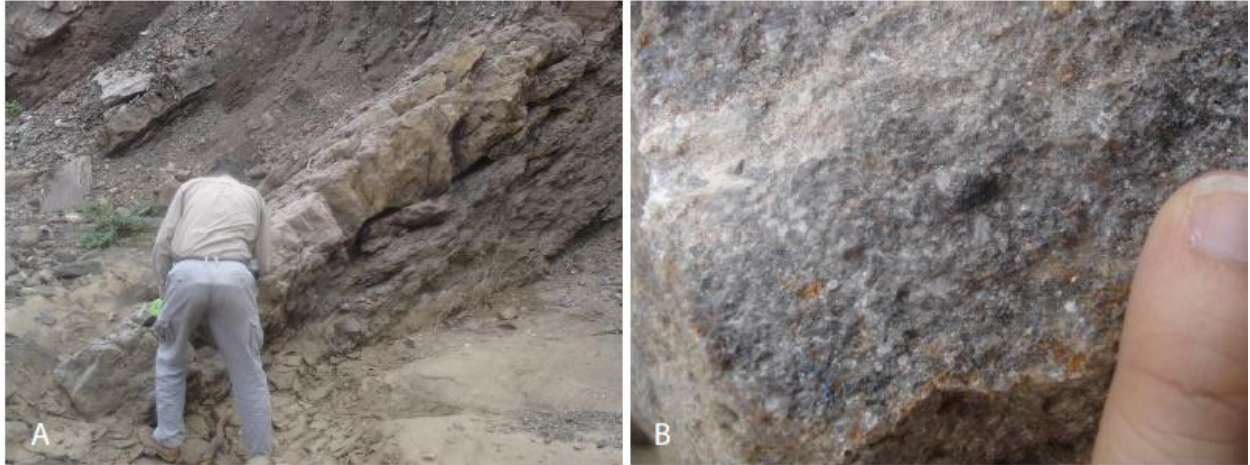


Figure B.14. (A) Outcrop of the Matatere Formation at El Palito stream; Site GPS-334; sample VMN-8A. (B) Quartz-rich graywacke



Figure B.15. (A) Conglomeratic level in the Matatere Formation; (B) Polymict composition of the conglomerate; Site GPS 336, sample VMN-9



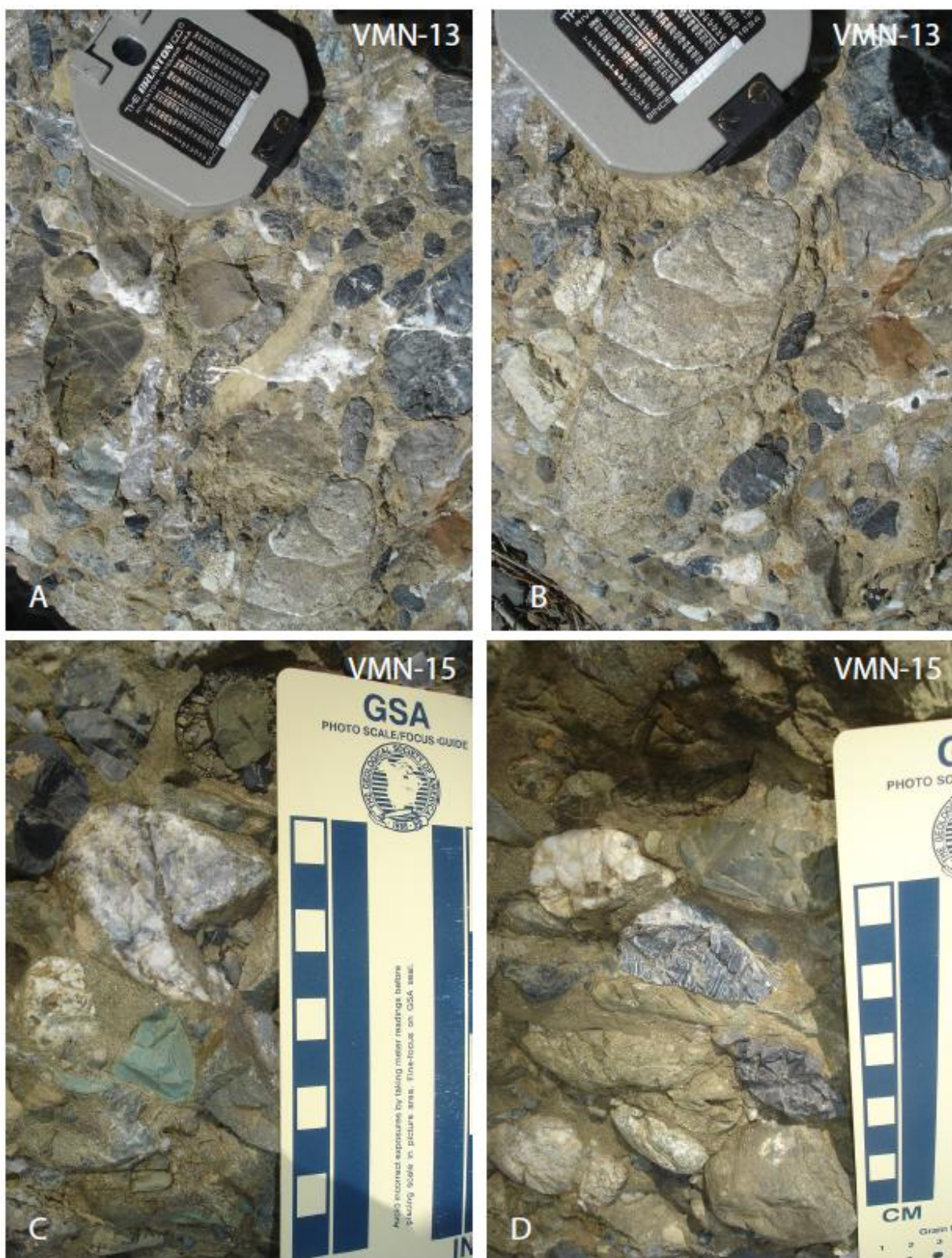


Figure B.16. Lithic conglomerates in the Siquisique area; Site GPS-343; samples VMN-13 and VMN-15.

## PAMPATAR FORMATION



Figure B.17. Outcrop of the Pampatar Formation in Margarita Island; Site GPS-380; sample VMN-40. The plastic bag at the right is about 40 cm tall



## CARATAS FORMATION



Figure B.18. The Caratas, Jabillos and Areo Formations at Site GPS-384

## LOS ARROYOS FORMATION



Figure B.19. Outcrops of the Los Arroyos Formation at the El Pilar area. (A) Site GPS-382; sample VMN-42; (B) Site GPS-383; sample VMN-43

## APPENDIX C

### PETROGRAPHIC DATA

Table C.1. Grain count data of passive margin samples

		SAMPLE	Quartz										Total Qz	Feldspar								Total F	Lithic Fragments														Total Lt				
			Monocrystalline					Polycrystalline						Plag					K-spar	X	Ls					Lm					Lv										
			undulose, non polyg	undulose, polyg	straight, non polyg	straight, polyg	in rock fragments	Total Qm	Qz	Chert	Chalcedony in rock fragments	Total Qp		undiff	Albite	Andesine	Labradorite	Bytownite in rock fragment			Total Ls		undiff	Phyllite	Qz-Mica- Schist	Quartzite	Metachert	Total Lm	Undiff	Andesite	rhyolite	malic- ultramafic	glass	pyroclastic	Total Lv						
Ag	Bo	VMN-7	288	19	7	0	0	314	5	0	0	0	5	319	0	0	0	0	0	0	0	0	0	0	0	0	0	0	0	0	1	0	1	0	0	0	0	0	0	0	1
AB	Bo	VMN-16	211	64	32	0	0	307	24	0	0	0	24	331	0	0	0	0	0	0	0	0	1	1	0	0	0	0	0	0	0	0	0	0	0	0	0	0	0	1	
		VMN-17	227	25	28	2	0	282	12	0	0	0	12	294	0	0	0	0	0	0	0	0	2	2	0	3	0	0	0	0	0	0	0	0	0	0	0	0	0	3	
		VMN-18	256	44	3	1	0	304	6	0	0	0	6	310	0	0	0	0	0	0	0	1	1	0	0	0	0	0	0	0	0	0	0	0	0	0	0	0	0	0	
Barraquin	AB	VMN-32	315	21	5	2	0	343	4	1	0	0	5	348	0	0	0	0	0	0	0	0	0	0	0	0	0	0	0	0	0	0	0	0	0	0	0	0	0	3	
		VMN-33	325	25	16	1	0	367	11	0	0	0	11	378	11	0	0	0	0	0	0	0	11	0	0	0	0	0	6	0	6	0	0	0	1	0	1	0	0	0	7
		VMN-34	258	36	14	1	0	309	19	0	0	0	19	328	4	0	0	0	0	0	0	0	1	5	0	0	0	0	5	0	5	0	0	0	0	0	0	0	0	5	
		VMN-35	291	52	9	2	0	354	16	3	0	0	19	373	0	0	0	0	0	0	0	0	0	0	0	0	0	0	1	0	1	0	0	0	0	0	0	0	1		
		AB	VMN-36	291	52	9	2	0	354	16	3	0	0	19	373	0	0	0	0	0	0	0	0	0	0	0	0	0	0	1	0	1	0	0	0	0	0	0	0	1	

Aq: Aqardiente Formation

AB: Agua Blanca Formation

Bo: Bobare Formation

		SAMPLE	Miscellaneous																				Total Misc		
			Micas			Hornblende	Prelimite	Glauconite	Heavy minerals							Oxides & other alteration products								Unknowns	Fossils
			Muscovite	Biotite	Chlorite				Zircon	Rutile	Tourmaline	Pyrite	Chalcopyrite	Apatite	Sphene	Opacues	Hematite	Leucocore	Magnetite	Sericite	Clays	Calcite			
Ag	VMN-7	5	2	0	0	0	0	2	0	2	0	0	0	1	0	5	1	0	5	0	0	0	0	23	
Bo	VMN-16	10	0	3	0	0	0	0	0	0	0	0	0	1	0	0	2	0	1	0	0	0	0	17	
	VMN-17	8	1	0	0	0	0	0	0	0	0	0	0	0	0	0	3	0	0	0	0	0	0	12	
AB	VMN-18	24	7	0	0	0	0	1	0	0	0	0	0	0	0	0	1	0	0	0	0	0	0	33	
Barranquin	VMN-32	1	0	0	0	0	0	0	0	0	0	0	0	0	0	0	2	0	0	0	0	0	0	3	
	VMN-33	0	0	0	0	0	0	0	0	0	0	0	0	0	0	0	0	0	0	0	0	0	0	0	
	VMN-34	3	0	0	0	0	0	1	0	1	0	0	0	0	0	0	3	0	0	2	0	0	0	10	
	VMN-35	1	0	0	0	0	0	1	0	0	0	0	0	0	0	0	0	0	0	1	0	0	0	3	



Table C.2. Grain count data of turbidite samples

	SAMPLE	Quartz										Total I Qz	Feldspar								Total I F	Lithic Fragments																				Total al Lt					
		Monocrystalline					Polycrystalline						Plag									Ls					Lm					Lv															
		undulose, non polyg	undulose, polyg	straight, non polyg	straight, polyg	in rock fragments	Total Qm	Qz	Chert	Chalcedony	in rock fragments		Total Qp	undiff	Albite	Oligoclase	Andesine	Labradorite	Bytownite in rock fragment	Kapap		undiff	Shale	siltstone	sandstone	Chert	Limestone	Total Ls	undiff	Phyllite	Qz-Mica- Schist	Qz-Mica- gneiss	Qz-Mica- unfoliated	Amphibolite	Quartzite	Metachert	Total Lm	undiff	Andesite	Dacite	rhyolite		midic- ultramafic	glass	pyroclastic	Total Lv	
Matatere Fm.	VMN-5A	260	23	66	0	0	349	3	9	0	12	361	0	0	0	0	0	0	0	0	0	0	3	0	3	0	2	3	0	0	0	3	0	8	1	0	0	0	0	0	0	0	0	1	12		
	VMN-5B	223	67	118	4	0	412	7	2	0	9	421	0	0	0	0	0	0	0	0	0	0	1	0	3	1	0	1	0	0	0	3	0	5	0	0	0	0	0	0	0	0	0	0	8		
	VMN-6A	203	52	44	2	0	301	2	3	0	5	306	0	0	0	0	0	0	0	0	0	0	0	0	0	0	1	1	0	0	0	1	0	3	1	0	0	0	0	0	0	0	0	1	4		
	VMN-6B	142	28	86	3	0	259	9	8	0	17	276	2	0	0	0	0	0	0	0	2	1	0	0	1	0	2	0	0	1	0	0	1	0	2	1	0	0	0	0	0	0	1	5			
	VMN-8A	104	242	21	0	2	369	35	1	0	0	36	405	0	0	0	0	0	0	0	0	0	0	0	12	12	0	0	0	0	0	1	0	1	0	0	0	0	0	0	0	0	0	13			
	VMN-8B	175	85	47	0	1	308	3	0	0	0	3	311	0	0	0	0	0	0	0	0	0	8	3	0	0	3	14	0	0	0	0	0	0	0	0	1	0	0	0	0	0	0	1	15		
	VMN-9	71	35	10	0	4	120	25	26	0	1	52	172	16	0	0	4	0	0	0	0	20	0	4	0	1	0	5	0	3	7	0	0	0	0	10	34	1	0	11	0	0	0	46	61		
	VMN-10	77	34	59	6	11	187	43	40	0	1	84	271	90	0	0	4	4	0	4	0	102	0	5	0	1	0	0	6	1	14	14	0	0	0	29	35	13	0	6	7	0	0	61	96		
	VMN-11	57	59	28	3	1	148	42	26	0	0	68	216	39	1	0	1	2	0	0	0	43	0	1	0	1	0	2	4	0	6	8	0	0	0	14	26	4	3	3	4	0	0	0	43	58	
	VMN-12	41	29	37	7	0	114	32	49	0	0	81	195	52	0	0	5	2	0	0	0	59	0	0	0	0	0	0	4	3	0	0	0	0	7	69	28	0	1	2	2	0	0	100	109		
VMN-14	52	33	36	1	0	122	27	34	6	0	67	189	40	1	0	6	1	1	0	0	49	0	0	1	0	0	0	1	0	3	3	0	0	0	6	39	8	0	9	0	3	1	60	67			
VMN-44	42	34	33	4	1	114	32	28	1	0	61	175	36	0	0	1	4	0	0	11	52	0	0	0	0	0	0	1	1	1	0	0	0	3	0	6	28	0	0	5	2	0	18	63	59		
Guarico Fm	VMN-19	173	11	40	0	0	224	8	33	19	0	60	284	14	0	0	1	0	0	0	15	0	9	0	0	0	0	9	0	1	3	0	0	0	4	21	5	0	1	9	0	0	3	66	52		
	VMN-20	174	27	18	1	0	220	17	19	5	0	41	261	18	0	0	1	1	0	0	20	0	21	0	0	0	0	21	0	9	6	0	0	0	1	16	25	1	0	24	0	0	0	0	69	87	
	VMN-23	246	86	19	0	0	351	19	9	0	0	28	379	6	0	0	0	0	0	0	6	0	0	1	0	13	0	14	0	2	4	0	0	0	4	10	0	0	0	3	0	0	0	3	27		
	VMN-28	251	26	16	0	0	293	8	11	0	0	19	312	38	0	0	2	2	0	0	0	42	0	39	0	0	10	0	49	0	6	0	0	0	0	6	2	1	0	0	0	0	0	0	3	58	
Curacá/Pampatar	VMN-39	120	13	22	0	0	155	6	12	4	0	22	177	75	2	0	2	0	0	0	10	89	0	5	0	0	3	4	12	0	4	4	0	0	2	0	10	34	6	4	30	16	3	1	34	116	
	VMN-40	28	5	9	0	0	42	12	23	5	0	40	82	21	2	0	0	1	0	2	4	30	0	0	0	0	4	0	4	0	0	0	3	0	0	4	7	44	21	8	20	18	0	46	107	168	
	VMN-41	31	4	4	0	0	39	19	8	8	0	35	74	12	0	0	1	1	0	3	3	20	0	1	0	0	2	0	3	0	0	0	0	5	0	0	1	6	10	12	5	8	8	0	50	63	102
	CUR-14z	124	10	13	1	0	148	10	27	0	0	37	185	67	2	2	1	1	0	0	5	78	0	2	0	0	0	1	3	0	2	2	0	2	0	0	6	8	2	1	16	1	0	0	26	37	
	CUR-21	27	4	7	0	1	39	6	4	4	0	14	53	##	4	0	0	1	0	5	1	125	0	0	0	0	0	1	1	0	3	5	0	2	1	0	0	11	14	18	0	12	37	0	4	65	97
	CUR-22	16	1	1	0	0	18	2	1	0	0	3	21	88	7	10	1	0	0	0	0	106	0	1	0	5	1	2	9	1	2	9	3	4	0	6	25	8	30	0	6	35	0	3	63	116	

Table C.2. (cont.)

SAMPLE		Miscellaneous																				Total Misc	Total grains					
		Micas			Hornblende	Pyroxene	Epidote	Prehnite	Feldspathoid	Glauconite	Heavy minerals							Oxides & other alteration products						Unknowns	Fossils			
		Muscovite	Biotite	Chlorite							Zircon	Rutile	Tourmaline	Pyrite	Chalcopyrite	Apatite	Sphene	Opques	Hematite	Leucoxene	Magnetite					Sericite	Clays	Calcite
Matatere Fm.	VMN-5A	0	0	1	0	0	0	0	0	0	4	1	3	0	0	0	1	0	1	0	0	4	0	0	0	0	15	388
	VMN-5B	1	0	4	0	0	0	0	0	0	8	0	3	0	0	1	0	0	10	0	1	0	3	0	0	0	31	460
	VMN-6A	0	0	0	0	0	0	0	0	0	3	1	1	0	0	0	1	0	2	1	0	0	3	0	0	0	12	322
	VMN-6B	0	0	3	3	0	0	0	0	0	2	0	1	7	0	1	0	0	1	2	0	0	0	14	0	0	34	317
	VMN-8A	0	0	0	0	0	0	0	0	0	0	0	0	0	0	0	0	0	5	0	0	0	0	0	1	0	6	424
	VMN-8B	0	1	0	0	0	0	0	0	0	0	0	0	1	0	0	0	1	0	0	0	0	0	0	1	17	21	347
	VMN-9	2	0	1	0	0	0	0	0	0	1	0	0	0	0	0	0	2	1	0	0	0	27	35	0	8	77	330
	VMN-10	9	7	19	2	0	0	0	0	0	0	0	0	0	1	0	0	0	4	3	2	0	10	8	0	1	66	535
	VMN-11	2	1	6	0	0	0	0	0	0	1	0	0	1	0	1	0	0	1	0	0	0	7	16	0	14	50	367
	VMN-12	2	2	12	1	0	0	0	0	0	0	0	0	1	0	0	0	0	0	3	0	0	8	4	0	0	33	396
Guarico Fm.	VMN-14	1	4	38	0	0	0	0	0	0	1	0	0	0	0	1	0	0	1	2	1	12	0	6	0	0	67	372
	VMN-44	4	5	31	1	0	0	0	0	0	2	0	0	0	0	0	0	0	0	3	0	2	0	0	0	0	48	334
	VMN-19	0	0	4	1	0	0	0	0	0	0	0	0	0	0	0	0	0	0	1	1	0	18	0	0	0	25	376
	VMN-20	0	19	9	1	0	0	0	0	1	0	0	1	1	0	0	0	5	0	3	0	0	5	0	0	0	45	413
	VMN-23	1	0	3	2	0	0	2	0	0	0	1	0	0	0	0	0	0	0	0	0	0	1	0	0	0	10	422
	VMN-28	9	2	1	0	0	0	0	0	0	0	0	1	0	0	0	0	0	0	2	0	0	0	0	0	0	15	427
	VMN-39	1	5	25	3	1	1	0	0	0	1	0	1	0	0	0	0	0	0	5	0	0	0	9	3	0	55	437
	VMN-40	0	0	9	0	0	3	0	0	0	0	0	0	1	0	0	0	0	0	0	0	0	0	23	1	48	85	365
	VMN-41	0	0	4	0	0	0	0	0	0	0	0	0	0	0	0	0	0	0	0	0	0	0	65	0	111	180	376
	Curacá	CUR-14z	5	0	18	1	1	0	0	3	0	0	0	0	0	0	0	0	0	0	3	1	3	1	14	6	1	57
CUR-21		1	0	10	28	3	9	0	2	0	0	0	2	8	0	1	0	0	0	0	11	0	0	0	0	2	77	352
CUR-22		0	3	17	24	17	0	0	0	0	0	0	0	12	0	0	0	0	0	3	0	0	5	0	0	3	0	84

## **APPENDIX D**

### **DETRITAL ZIRCON DATA**

Table D.1 Passive margin units

VMN-7		VMN-16		VMN-17		VMN-18		VMN-32		VMN-35	
Age	Error	Age	Error	Age	Error	Age	Error	Age	Error	Age	Error
415.1	4.1	451.4	4.4	613.9	28.2	491.1	6.7	427.0	4.1	464.8	4.7
423.0	4.3	594.9	6.1	618.5	7.9	502.4	4.8	489.7	4.7	485.0	8.3
428.6	6.4	635.9	6.1	868.4	22.7	965.1	61.1	568.4	5.4	532.8	5.5
441.3	8.7	650.0	10.1	885.9	27.7	1175.6	71.2	578.5	7.7	541.2	5.7
474.1	6.6	881.3	12.3	902.3	19.6	1373.8	30.6	605.9	5.8	588.0	6.0
494.0	7.3	894.0	8.3	904.1	21.0	1384.7	20.8	794.4	13.8	866.7	19.5
494.5	35.8	896.0	8.4	904.4	8.4	1388.9	29.8	909.1	14.3	928.1	12.5
500.4	15.2	897.6	8.4	907.1	8.5	1391.6	32.3	965.1	9.0	942.7	15.3
506.6	6.5	910.2	8.5	908.7	17.5	1394.2	46.3	970.4	50.0	970.3	67.1
517.6	5.0	913.0	8.5	914.7	27.4	1408.3	22.7	976.1	32.7	992.0	38.6
532.4	8.5	923.8	8.6	921.3	8.6	1412.9	19.9	985.6	27.9	1011.9	26.7
592.5	10.8	934.5	17.3	923.3	8.6	1413.5	45.4	986.5	31.4	1015.1	34.3
599.7	5.7	935.3	8.7	938.2	10.3	1417.1	52.6	987.2	34.8	1020.4	23.9
613.6	10.2	938.0	8.7	939.5	8.7	1424.8	31.5	994.6	44.3	1021.8	23.8
651.9	13.8	938.4	8.7	944.2	8.9	1426.7	19.1	1000.0	30.7	1031.2	47.3
655.5	6.2	952.8	9.3	947.7	9.2	1427.7	46.0	1008.0	36.0	1031.6	31.2
850.6	8.0	958.5	8.9	951.0	14.8	1431.8	27.3	1012.3	20.7	1034.5	41.5
936.9	8.7	961.5	9.3	953.4	8.9	1434.4	29.3	1015.9	36.5	1044.6	43.4
956.1	22.6	962.9	10.6	956.7	50.9	1444.4	23.1	1046.8	25.3	1068.7	43.9
988.5	42.7	964.2	9.0	957.1	26.9	1445.6	30.5	1058.4	36.0	1073.0	22.0
996.4	41.8	965.8	16.6	959.2	27.1	1450.3	50.0	1133.2	32.0	1096.3	40.3
1017.7	39.7	968.3	10.8	964.7	9.0	1455.6	38.5	1173.1	24.4	1122.7	38.5
1025.9	32.8	973.4	9.0	970.8	37.6	1456.6	36.0	1216.5	21.0	1166.6	53.3
1044.7	27.3	987.5	30.3	971.9	38.3	1460.4	39.4	1256.0	42.6	1169.3	25.6
1096.6	76.5	998.0	61.4	972.4	40.3	1462.5	90.9	1262.7	34.1	1172.6	50.3
1115.0	20.1	999.2	50.2	972.9	9.1	1465.4	46.9	1349.0	46.2	1198.6	22.2
1134.3	38.4	999.8	36.8	976.3	36.2	1468.6	20.0	1364.7	55.8	1215.2	19.7
1161.8	50.3	1000.4	38.0	978.0	30.8	1473.7	28.3	1375.7	28.7	1216.2	23.3
1165.9	31.7	1000.6	33.8	986.5	42.0	1481.2	37.2	1384.0	36.7	1224.4	37.6



Table D.1 (cont)

VMN-7		VMN-16		VMN-17		VMN-18		VMN-32		VMN-35	
Age	Error	Age	Error	Age	Error	Age	Error	Age	Error	Age	Error
1174.9	38.1	1008.2	32.6	988.8	28.2	1493.0	91.2	1388.7	21.8	1230.3	34.8
1200.0	30.0	1009.1	28.0	989.1	73.4	1493.3	25.6	1397.3	30.7	1258.7	24.6
1210.9	19.8	1023.5	20.3	993.0	44.4	1494.9	23.0	1405.5	24.1	1274.6	28.7
1216.3	31.1	1024.9	32.0	993.4	23.5	1502.7	59.0	1411.0	21.9	1327.7	28.5
1240.2	29.8	1026.5	50.5	994.1	24.5	1507.5	19.2	1412.9	19.2	1369.1	40.8
1243.1	40.3	1028.5	26.9	996.5	30.1	1513.2	29.5	1421.1	19.1	1380.3	87.5
1245.2	29.2	1030.5	27.6	998.3	58.9	1514.1	37.5	1431.2	26.9	1395.9	25.7
1254.3	22.5	1033.5	44.1	998.5	32.7	1517.0	65.1	1433.3	19.4	1396.8	34.1
1256.4	26.8	1038.3	32.0	1000.7	33.6	1518.5	29.4	1449.3	19.1	1403.3	40.7
1257.5	19.6	1042.6	35.2	1004.1	59.8	1528.4	46.6	1454.3	30.7	1411.8	43.1
1323.0	25.1	1043.1	30.9	1008.0	21.2	1528.6	30.7	1458.2	19.1	1412.1	46.7
1363.1	27.5	1051.3	51.3	1008.3	21.4	1529.0	56.2	1461.1	66.2	1430.3	29.6
1388.3	40.6	1082.0	89.3	1009.2	32.0	1573.4	22.9	1465.6	21.7	1453.1	50.1
1397.2	26.7	1109.3	41.2	1010.2	28.0	1775.7	18.3	1482.8	24.1	1455.0	27.7
1406.6	27.8	1114.4	35.7	1010.5	37.8	1779.0	38.9	1497.9	21.8	1466.9	23.9
1410.1	41.9	1115.7	34.9	1011.5	32.9	1779.0	21.9	1507.7	25.5	1481.2	28.0
1412.9	33.1	1131.2	27.3	1016.3	37.1	1779.6	18.3	1507.8	40.9	1481.8	29.3
1418.4	25.8	1139.2	25.9	1019.1	22.8	1795.0	18.3	1508.8	27.1	1489.1	27.1
1419.7	19.5	1159.5	25.0	1020.9	33.9	1795.1	23.2	1509.6	25.6	1493.9	22.1
1419.9	58.3	1168.8	44.0	1021.5	37.8	1797.1	27.4	1513.4	33.8	1495.4	24.6
1432.0	19.9	1179.3	35.2	1024.3	34.3	1797.1	25.2	1515.4	22.3	1499.9	55.5
1444.3	33.1	1201.1	25.3	1026.2	29.0	1800.8	29.2	1515.8	43.6	1517.2	23.6
1447.7	58.4	1214.3	25.5	1030.0	24.1	1801.6	50.0	1520.9	30.8	1527.6	40.2
1449.0	19.1	1239.8	29.7	1030.2	20.3	1802.8	33.1	1525.4	23.1	1544.8	35.0
1454.3	21.3	1241.9	28.4	1031.3	57.1	1803.3	26.4	1527.2	20.0	1550.1	30.4
1457.2	30.5	1323.9	26.1	1040.2	25.0	1806.9	25.5	1539.4	36.3	1550.9	18.8
1464.6	20.5	1378.1	77.2	1054.7	31.1	1807.6	31.3	1553.2	25.7	1556.5	27.4
1478.0	25.6	1388.9	43.3	1082.7	33.4	1811.4	18.2	1563.0	63.6	1559.4	21.0
1504.3	18.9	1429.2	30.4	1144.8	46.2	1813.8	35.4	1566.0	39.5	1566.3	29.6
1509.8	24.4	1483.1	81.0	1163.9	38.4	1814.9	37.8	1567.6	38.7	1590.8	24.7

Table D.1 (cont)

VMN-7		VMN-16		VMN-17		VMN-18		VMN-32		VMN-35	
Age	Error	Age	Error	Age	Error	Age	Error	Age	Error	Age	Error
1531.6	20.6	1486.3	19.0	1167.3	27.4	1815.0	34.0	1569.3	38.6	1605.3	23.3
1546.2	31.2	1491.8	50.0	1175.5	29.1	1815.7	24.0	1574.9	18.8	1635.1	18.6
1548.5	38.6	1516.0	42.3	1180.6	27.9	1816.9	28.2	1586.4	25.5	1685.9	24.1
1550.6	19.9	1516.3	36.2	1194.6	25.5	1817.4	22.5	1735.4	22.6	1755.8	18.3
1559.6	35.1	1533.3	19.8	1208.3	22.5	1823.6	39.3	1773.1	18.3	1761.1	22.3
1580.2	27.3	1535.9	19.6	1210.4	23.0	1825.4	37.7	1774.2	40.0	1777.2	22.4
1586.2	20.0	1536.3	25.8	1222.5	31.7	1828.8	26.3	1777.6	18.3	1787.8	30.1
1592.3	18.8	1563.7	25.5	1260.0	22.9	1834.9	42.6	1787.6	25.4	1790.1	18.2
1611.5	43.7	1577.2	18.7	1301.9	37.3	1835.9	42.6	1792.3	29.7	1792.3	23.0
1654.6	23.4	1609.8	18.6	1333.5	49.2	1836.0	37.7	1796.9	18.2	1796.9	25.3
1705.8	24.3	1622.2	32.4	1339.4	23.4	1844.5	50.1	1797.5	18.2	1798.1	25.3
1717.7	45.8	1671.7	18.5	1342.8	33.3	1845.3	18.1	1799.8	20.1	1804.2	20.2
1729.9	18.4	1766.1	53.0	1365.1	31.9	1847.6	31.7	1809.7	22.6	1812.0	50.7
1730.1	29.4	1772.4	25.6	1380.2	70.6	1850.5	42.5	1812.0	19.5	1818.2	18.2
1730.6	23.9	1796.4	37.3	1387.1	23.7	1851.4	39.3	1815.1	18.7	1821.6	18.2
1738.6	20.3	1810.4	24.7	1413.6	38.7	1884.7	36.0	1816.5	18.2	1824.1	23.3
1750.8	18.3	1812.4	18.2	1424.2	39.4	1914.9	36.4	1818.9	32.2	1834.8	31.9
1783.2	123.7	1813.3	20.5	1462.7	19.1	1922.4	30.5	1820.0	18.2	1835.6	38.6
1798.3	22.9	1816.9	23.8	1463.7	39.8	1926.6	18.7	1824.3	28.5	1838.8	29.5
1805.1	29.9	1888.6	23.8	1470.6	38.7	1926.7	17.9	1824.9	18.1	1839.8	28.3
1807.4	19.3	1901.8	18.1	1480.6	53.1	1968.8	43.2	1825.9	18.1	1845.2	20.5
1808.9	18.2	2004.9	17.8	1511.4	29.3	1978.1	17.8	1828.9	18.7	1851.1	25.3
1811.1	23.3			1522.2	23.1	1979.6	20.0	1843.0	33.1	1871.1	18.1
1813.1	31.8			1526.9	18.8	1982.4	17.8	1848.1	23.6	1878.4	22.0
1815.2	25.4			1542.4	20.9	1982.6	21.9	1852.2	23.2	1888.3	31.7
1815.3	22.5			1604.5	18.7	1986.0	27.1	1949.3	59.6	1892.0	19.6
1815.6	18.2			1638.4	37.3	1987.7	17.8	1970.3	19.3	1900.4	18.0
1819.9	21.4			1692.7	22.5	1988.5	17.8	1972.9	25.8	1939.9	39.4
1844.8	20.3			1737.1	74.9	1990.1	35.9	1990.5	28.1	1975.7	18.4
1872.7	18.0			1749.7	32.8	1993.8	32.7	1998.1	25.1	1995.0	18.0

Table D.1 (cont)

VMN-7		VMN-16		VMN-17		VMN-18		VMN-32		VMN-35	
Age	Error	Age	Error	Age	Error	Age	Error	Age	Error	Age	Error
1876.1	52.0			1791.8	18.2	1998.1	17.8	1998.4	28.1	2009.5	19.0
1888.8	18.4			1801.2	19.7	1999.8	23.1	2000.6	41.9	2059.1	17.7
1896.7	27.7			1813.8	25.8	2006.3	38.2	2015.9	30.9	2215.7	20.2
1937.0	22.9			1822.8	34.4	2015.0	34.6	2025.0	32.8	2243.0	24.2
2097.1	22.8			1832.8	23.6	2015.8	45.8	2033.1	28.5		
2126.5	17.9			2151.2	35.3	2021.1	30.5	2073.4	23.3		
2719.3	24.6					2024.8	42.3	2731.8	26.7		
						2036.9	34.4				
						2123.9	31.0				
						2134.2	18.0				

Table D.2. Turbidite units. Curacao island.

Curacao									
Age	Error	Age	Error	Age	Error	Age	Error	Age	Error
66.4	3.8	73.5	1.9	81.4	1.8	333.1	2.1	980.5	18.6
67.2	2.7	73.5	2.2	83.1	1.4	340.8	3.5	1000.6	15.3
69.4	3.5	73.7	2.3	86.1	1.5	414.1	7.9	1019.9	50.5
69.7	4.9	73.9	2.0	86.2	1.5	448.9	8.6	1021.7	49.7
70.3	2.7	73.9	1.7	88.8	5.6	453.2	3.8	1028.6	50.4
70.4	3.5	73.9	3.2	91.2	7.5	478.0	4.9	1049.0	24.2
70.7	2.7	74.0	1.9	104.7	1.4	486.6	15.5	1093.4	6.6
70.7	1.9	74.0	1.8	130.6	4.0	495.0	6.9	1093.7	12.5
70.8	1.6	74.1	1.4	171.3	9.5	495.0	6.8	1115.6	24.2
70.9	1.9	74.2	2.0	217.2	9.2	513.4	7.0	1120.7	56.4
71.2	2.8	74.3	4.9	235.2	2.4	560.3	6.1	1127.5	11.6
71.3	3.2	74.3	3.2	238.2	2.4	567.0	8.6	1137.9	66.2
71.3	2.3	74.4	2.4	238.8	2.5	581.1	16.5	1156.2	71.8
71.5	2.5	74.4	1.3	244.2	2.0	583.5	14.3	1178.8	7.8
71.5	1.7	74.8	1.2	244.7	8.5	597.4	9.8	1186.9	35.5
71.5	5.4	74.9	2.0	246.3	2.4	606.5	19.9	1197.8	7.6
71.8	3.6	74.9	2.0	246.9	4.7	612.1	9.9	1214.7	5.8
72.0	2.5	75.3	3.8	247.3	2.0	624.8	15.7	1228.3	25.3
72.1	1.3	75.9	2.3	247.9	2.6	631.2	3.5	1231.2	21.1
72.2	2.6	76.0	1.6	248.8	2.9	638.5	15.4	1296.6	11.8
72.2	2.7	76.1	2.5	249.6	3.1	642.9	12.3	1462.6	37.5
72.6	4.2	76.4	1.5	251.4	2.4	644.5	9.0	1463.5	34.6
72.6	1.6	77.1	1.8	253.4	3.0	663.0	16.9	1544.0	26.5
72.7	2.2	77.4	4.0	253.6	2.1	679.9	48.1	1544.5	24.2
72.8	1.4	77.6	1.2	262.1	1.3	786.8	16.8	1594.6	47.9
72.9	1.2	78.0	3.4	264.9	7.5	860.7	5.0	1726.7	25.0
73.0	6.7	78.1	2.5	304.1	4.5	935.5	5.6	1790.9	14.3
73.1	1.6	80.2	1.7	305.9	3.2	970.4	8.8	1810.7	18.1
73.2	3.7	80.2	2.2	314.3	2.0	970.5	17.5	2079.0	41.1
73.3	1.9	80.5	3.2	330.8	6.2	978.3	20.0	2525.5	20.8
								2684.9	16.8

Table D.2. Turbidite units. Matatere Formation

VMN-5A		VMN-5B		VMN-6A		VMN-6B		VMN-9		VMN-10		VMN-11		VMN-12		VMN-14	
Age	Error	Age	Error	Age	Error	Age	error	Age	Error	Age	Error	Age	Error	Age	Error	Age	Error
58.3	0.7	43.9	0.9	39.4	1.5	78.7	0.8	53.2	0.5	49.8	1.0	68.4	1.4	53.8	2.7	54.0	2.8
59.1	2.0	159.9	1.6	47.1	0.5	79.4	2.0	54.2	1.2	51.0	1.6	69.1	1.7	54.9	1.4	71.3	1.8
134.2	3.1	163.4	1.6	47.3	0.7	80.0	0.9	55.3	0.9	51.2	4.2	69.5	2.7	62.0	2.8	73.5	2.1
155.7	1.9	226.7	2.2	50.0	1.5	81.9	0.8	57.3	0.6	53.6	0.8	70.7	0.9	69.8	1.3	74.2	0.7
179.7	6.0	261.1	6.8	53.4	0.9	85.2	0.8	57.3	1.5	56.4	1.5	71.3	1.7	70.1	1.1	75.3	2.8
192.6	2.3	269.0	6.6	60.8	0.6	97.5	1.0	58.6	0.9	66.9	1.4	93.2	1.4	70.3	1.1	76.5	1.4
222.9	2.2	269.7	3.9	92.0	3.6	155.0	1.5	58.9	1.3	68.3	1.0	277.2	6.4	70.8	2.1	77.4	4.4
228.4	6.5	276.9	3.7	132.5	1.7	156.5	4.2	61.2	0.8	68.9	1.5	399.7	32.5	71.1	0.8	78.7	1.2
264.3	2.6	360.5	3.5	134.3	1.3	223.7	5.0	62.2	1.4	69.2	2.5	596.9	5.7	72.0	1.4	87.4	1.9
475.4	4.6	582.9	5.6	143.6	2.7	225.3	3.5	66.9	1.4	71.5	0.7	818.7	74.8	72.2	1.0	88.8	2.6
622.6	10.9	594.5	11.8	144.5	4.2	253.8	10.8	68.2	1.0	72.8	2.2	840.3	14.0	74.0	1.9	89.5	2.1
773.1	8.2	600.2	5.7	147.8	1.5	274.7	3.4	69.7	2.9	97.9	1.0	861.9	72.2	75.0	3.3	90.2	2.0
852.8	11.4	628.3	6.0	203.4	2.0	277.3	3.5	70.2	0.9	144.3	3.3	884.4	8.3	75.8	3.0	95.2	2.0
905.3	11.1	879.9	8.4	222.1	3.2	281.6	2.9	70.8	1.1	177.1	3.7	888.3	8.3	76.4	0.8	95.6	3.6
917.5	8.6	926.8	8.6	225.2	4.9	487.0	14.9	71.7	1.6	233.3	6.3	897.8	14.4	79.0	0.9	100.8	1.9
958.1	8.9	992.1	35.2	267.9	3.9	497.3	4.8	73.9	0.9	234.0	2.3	898.7	16.9	80.3	1.6	101.7	1.3
980.9	63.5	1009.2	34.3	278.3	4.3	502.7	4.8	76.3	1.0	252.0	2.5	905.2	18.1	82.9	1.0	103.2	1.2
982.0	36.4	1023.3	50.7	328.6	3.2	562.9	5.4	79.1	2.5	252.2	3.9	944.4	11.4	85.0	1.2	211.4	4.1
989.5	84.7	1029.9	59.0	336.9	3.3	564.5	5.4	241.2	4.9	252.4	4.5	946.9	8.8	85.7	1.4	223.0	2.2
999.2	39.6	1032.4	36.0	341.5	3.3	572.7	5.5	245.1	2.4	274.0	6.1	974.7	29.0	86.5	2.3	225.4	2.6
1004.7	24.4	1034.1	20.2	475.8	18.9	580.7	5.6	265.9	2.7	281.4	2.8	1009.7	36.8	90.7	1.3	231.4	4.3
1054.8	45.6	1049.7	24.6	518.0	5.9	583.9	7.1	268.6	4.8	287.9	3.4	1016.9	34.3	91.1	0.9	231.6	3.4
1086.2	20.2	1173.1	56.1	550.1	6.4	636.0	6.1	279.6	7.9	572.3	6.1	1061.6	22.4	96.0	2.1	232.4	5.6
1145.1	22.5	1187.0	46.4	552.1	5.6	685.9	6.5	814.8	12.1	606.3	16.0	1091.2	52.0	152.6	3.2	232.5	2.5
1163.3	38.5	1203.4	26.6	659.2	65.4	803.0	15.8	868.1	16.7	898.0	27.1	1121.5	44.3	223.0	2.2	236.5	3.4
1205.6	32.2	1209.4	22.6	679.1	6.4	964.0	9.1	869.0	15.3	909.1	10.9	1133.9	63.0	224.9	2.2	239.6	4.8
1209.1	21.5	1225.2	29.7	680.8	10.9	989.0	32.6	883.0	8.3	928.6	20.2	1152.4	100.4	235.1	2.3	240.3	3.0
1272.8	36.2	1273.0	48.2	697.1	13.5	1003.7	30.4	907.7	8.5	944.9	24.9	1158.4	54.7	238.0	2.3	240.4	2.7
1308.2	21.6	1285.7	33.5	748.1	24.2	1010.9	30.8	927.9	11.4	961.1	20.5	1161.0	30.9	238.4	2.3	242.7	2.6
1309.6	19.5	1304.7	112.8	931.6	8.7	1042.4	21.7	949.8	20.7	970.6	29.1	1162.8	25.0	238.6	3.6	244.0	2.4
1322.8	30.7	1313.8	27.4	934.2	8.7	1110.4	22.2	986.1	49.1	989.0	35.1	1177.7	26.5	238.7	3.4	245.4	3.7
1324.7	19.5	1319.9	19.6	994.0	25.2	1116.2	37.8	993.0	40.8	992.3	52.0	1180.7	31.4	242.4	6.5	250.2	2.5
1335.3	21.3	1323.7	25.4	1019.4	23.6	1149.4	52.0	999.6	61.8	994.9	23.9	1216.9	50.4	242.5	2.4	250.7	2.5
1347.2	19.3	1325.1	21.1	1032.0	31.4	1191.9	89.7	1009.1	59.8	995.0	61.7	1221.5	34.6	245.4	2.4	252.2	2.5
1379.3	19.3	1327.7	51.3	1049.3	75.4	1193.4	49.4	1011.5	31.3	1015.2	39.8	1271.0	37.7	247.3	3.0	254.0	3.3
1382.1	42.0	1333.9	43.0	1082.3	30.0	1229.5	35.1	1017.1	24.4	1049.6	32.2	1277.1	34.5	254.4	2.5	254.2	2.5
1392.0	28.7	1352.2	29.5	1090.8	31.1	1267.4	29.9	1021.8	38.9	1057.2	28.7	1280.1	32.6	264.1	2.6	254.7	8.6
1414.7	27.0	1357.5	69.4	1182.8	26.2	1268.6	33.6	1021.8	36.5	1069.8	32.8	1286.4	54.7	264.6	3.3	257.1	3.6
1418.3	29.3	1360.9	19.4	1196.9	24.9	1311.9	22.1	1043.8	33.7	1093.5	67.2	1314.1	41.5	271.2	2.7	258.0	2.5
1440.3	32.1	1372.6	22.3	1200.3	34.3	1341.3	97.9	1057.5	44.1	1118.5	48.0	1339.9	23.4	277.5	2.7	274.5	3.9
1440.4	51.6	1437.8	35.0	1211.7	20.4	1383.6	35.8	1087.7	47.1	1141.2	72.5	1340.5	36.0	305.0	3.0	287.6	2.8
1450.0	26.1	1438.9	83.4	1234.5	20.8	1438.4	19.1	1096.7	29.8	1142.6	29.1	1370.1	48.7	323.6	3.2	322.3	3.1
1466.9	49.7	1442.2	29.9	1263.0	40.3	1442.6	34.1	1107.3	56.4	1151.1	30.9	1384.2	80.7	330.5	4.3	367.9	4.7
1483.8	30.8	1454.8	31.6	1284.9	22.6	1456.9	21.2	1116.9	43.2	1168.7	30.8	1441.4	32.6	359.3	5.8	376.7	3.7

Table D.2. (cont.)

VMN-5A		VMN-5B		VMN-6A		VMN-6B		VMN-9		VMN-10		VMN-11		VMN-12		VMN-14	
Age	Error	Age	Error	Age	Error	Age	error	Age	Error	Age	Error	Age	Error	Age	Error	Age	Error
1488.7	21.4	1457.0	19.0	1307.1	19.5	1474.9	24.5	1120.3	27.3	1169.5	61.1	1441.7	34.6	362.6	5.8	464.1	4.5
1492.2	31.1	1478.0	37.9	1312.8	23.3	1477.4	29.1	1126.4	38.3	1169.6	37.8	1486.3	26.0	426.2	4.1	518.1	10.4
1500.1	29.8	1486.4	27.3	1324.8	32.2	1481.7	41.0	1127.8	53.3	1180.9	30.5	1532.6	20.8	435.8	13.4	563.0	11.1
1502.5	37.2	1494.5	28.7	1325.6	20.0	1482.3	25.1	1129.6	41.8	1188.7	108.1			483.1	14.4	590.6	6.8
1506.0	20.2	1496.9	43.0	1330.9	25.6	1491.1	28.9	1134.2	71.9	1194.1	50.9			494.9	5.1	597.8	6.5
1509.7	19.1	1499.2	39.0	1332.8	23.8	1503.4	27.2	1135.9	24.1	1194.7	68.9			501.1	4.8	657.5	6.3
1510.7	34.5	1499.6	20.1	1347.8	39.3	1514.0	46.9	1136.9	38.0	1196.4	19.7			548.2	10.6	666.0	20.7
1512.0	37.3	1501.0	41.9	1367.7	53.0	1517.5	25.2	1149.3	28.1	1209.2	34.1			594.9	5.7	746.5	8.1
1517.4	31.9	1501.5	28.2	1367.9	37.8	1519.9	50.1	1150.4	26.6	1214.9	23.7			608.6	5.8	1024.4	35.3
1531.6	35.5	1501.7	38.5	1417.3	24.9	1520.6	27.3	1155.4	31.4	1217.2	45.7			792.1	17.7	1042.4	20.2
1532.9	20.2	1510.4	45.1	1456.9	21.6	1535.9	26.2	1156.5	52.4	1226.7	34.2			801.9	11.1	1042.4	31.1
1541.7	37.8	1518.6	30.0	1470.5	38.8	1542.6	19.4	1157.5	37.4	1227.1	31.6			816.2	7.7	1098.9	26.0
1544.3	27.6	1527.8	25.1	1485.7	24.8	1543.5	22.8	1159.4	25.6	1252.6	34.4			821.1	7.7	1100.2	43.6
1546.5	19.0	1528.7	22.5	1506.7	50.9	1546.8	31.7	1167.5	26.0	1253.4	88.7			830.1	7.8	1151.0	43.9
1547.1	23.0	1540.5	56.3	1508.0	29.8	1549.1	20.5	1176.3	32.4	1276.5	65.8			921.1	8.6	1172.7	75.6
1551.1	22.0	1543.7	34.1	1510.7	127.4	1549.4	22.1	1178.2	27.1	1277.4	49.6			971.5	49.7	1177.8	36.9
1557.2	34.6	1549.0	34.9	1532.0	23.0	1554.1	35.0	1178.7	19.8	1300.8	64.1			984.5	32.2	1213.7	55.4
1558.2	27.9	1550.4	40.6	1540.3	18.8	1557.4	26.9	1179.3	50.3	1318.8	26.8			989.5	36.5	1273.6	40.8
1558.4	18.8	1565.6	21.6	1541.8	22.2	1558.3	38.0	1180.3	25.3	1324.5	37.8			993.7	96.0	1308.7	38.7
1578.9	30.9	1577.8	72.8	1572.4	25.0	1562.4	25.3	1185.8	48.6	1326.6	30.8			1025.6	37.6	1480.4	72.3
1580.3	19.3	1582.9	20.8	1575.0	28.7	1563.7	18.8	1192.7	31.4	1333.5	39.9			1059.5	32.5	1535.4	57.2
1586.7	23.2	1600.9	65.0	1578.8	18.7	1564.0	24.6	1197.9	30.2	1398.6	43.9			1087.4	63.2	1559.0	41.4
1700.9	33.0	1618.2	20.5	1579.8	18.7	1572.2	61.8	1198.7	25.0					1128.3	84.2	1591.4	24.3
1741.5	33.5	1713.8	26.7	1608.4	39.3	1574.5	28.0	1198.9	26.4					1138.5	40.7	1832.6	54.2
1793.9	18.2	1745.0	21.3	1628.8	19.7	1581.8	36.1	1199.5	31.2					1177.6	36.8	1859.6	20.8
1796.6	43.3	1758.0	18.3	1663.1	23.9	1672.4	36.2	1202.3	29.7					1183.0	25.0	1986.0	88.5
1798.5	18.3	1760.1	18.3	1676.5	43.1	1745.7	38.9	1206.7	43.7					1272.5	37.2	2101.4	46.0
1805.1	18.2	1767.9	40.0	1677.9	24.4	1767.0	22.7	1211.0	37.3					1300.7	21.0	2130.3	56.2
1808.5	29.3	1768.8	26.1	1709.6	18.4	1767.9	19.7	1218.8	30.1					1342.0	30.6	2168.2	27.5
1819.7	27.6	1788.2	19.7	1720.4	25.5	1824.5	48.1	1221.8	25.8					1377.2	26.8	2581.2	36.9
1830.5	20.0	1798.1	28.6	1763.5	31.1	1829.8	47.1	1224.0	30.3					1431.4	46.9		
1836.5	36.6	1830.9	24.1	1813.6	19.8	1831.4	20.1	1229.9	49.9					1601.0	18.8		
1861.0	22.4	1840.3	18.1	1822.8	20.1	1879.6	33.6	1232.2	33.6					1712.4	18.8		
1890.9	18.0	1859.8	27.6	1825.7	32.3	1905.4	18.0	1241.4	37.3					2841.1	16.3		
1903.0	18.0	1876.7	24.5	1847.8	34.5	1923.3	17.9	1244.0	61.0								
1934.3	40.3	2019.8	17.8	1896.5	18.0			1256.6	32.9								
		2059.5	34.9	1974.1	24.7			1257.1	46.5								
				2068.0	25.9			1257.9	47.3								
				2207.5	23.6			1264.1	79.8								
				2701.7	20.2			1270.8	34.0								

Table D.2. (cont.)

VMN-5A		VMN-5B		VMN-6A		VMN-6B		VMN-9		VMN-10		VMN-11		VMN-12		VMN-14	
Age	Error	Age	Error	Age	Error	Age	error	Age	Error	Age	Error	Age	Error	Age	Error	Age	Error
								1295.7	42.2								
								1299.6	45.3								
								1308.2	19.4								
								1312.1	84.2								
								1349.7	25.9								
								1370.8	22.1								
								1371.9	42.9								
								1393.0	28.8								
								1428.4	19.1								
								1501.9	29.3								



Table D.3. Turbidite units. Guárico and Pampatar Formations

GUARICO FORMATION								PAMPATAR FORMATION					
VMN-19		VMN-20		VMN-23		VMN-28		VMN-39		VMN-40		VMN-41	
Age	Error	Age	Error	Age	Error	Age	Error	Age	Error	Age	Error	Age	Error
71.7	1.9	63.1	4.6	67.3	1.7	74.7	1.1	49.6	0.8	49.1	0.9	51.3	1.5
263.0	3.5	66.9	1.3	77.9	2.5	83.3	2.3	49.6	1.0	49.4	1.3	51.6	0.7
450.3	4.3	67.2	0.9	81.3	0.8	85.8	2.0	49.8	0.5	50.2	1.3	52.4	0.7
512.7	12.9	71.6	1.8	82.0	1.2	94.6	2.4	50.1	1.3	50.6	0.5	53.0	0.5
974.6	43.7	72.7	4.0	83.2	3.0	155.6	3.6	52.8	1.0	50.7	0.8	53.5	0.8
989.8	46.5	80.3	1.5	86.5	0.9	160.9	1.6	69.6	1.6	52.0	0.7	54.8	0.6
995.3	93.6	97.7	1.0	96.5	1.7	166.6	1.6	72.2	0.7	52.6	0.6	55.4	0.6
1012.1	29.2	110.9	1.1	133.1	2.6	170.9	1.7	73.9	1.1	54.7	1.0	64.6	0.8
1028.0	31.6	164.2	2.2	153.0	13.2	182.2	8.4	75.7	2.0	67.2	2.4	74.1	0.7
1030.3	42.7	183.6	1.8	156.4	2.7	213.3	2.1	76.3	1.7	68.4	3.7	76.0	1.6
1177.5	26.7	220.0	2.2	156.6	2.6	232.6	2.3	77.5	0.8	69.1	0.9	76.4	0.8
1316.9	34.0	227.0	2.8	165.6	1.6	233.6	2.3	81.9	1.8	71.2	2.9	77.6	3.4
1330.1	26.9	228.6	3.4	167.0	4.3	239.4	2.4	83.2	1.3	71.2	1.5	80.6	2.1
1352.7	54.9	229.4	2.3	258.9	2.8	246.3	4.6	83.5	1.2	71.3	0.7	82.4	1.5
1373.0	24.3	230.6	3.3	278.3	10.2	250.9	2.5	85.9	0.9	72.6	0.7	89.6	1.2
1381.2	36.5	231.2	2.3	284.0	3.4	314.5	5.3	86.4	3.3	73.1	0.9	98.3	1.0
1391.0	25.9	231.9	3.8	287.7	3.5	335.2	5.2	213.7	6.8	73.5	1.2	105.3	2.7
1396.7	27.1	236.1	2.3	552.8	7.1	489.0	10.5	217.7	4.9	74.6	0.8	228.3	8.3
1401.6	29.5	246.1	2.4	557.5	6.1	490.6	9.0	220.3	10.4	74.6	1.0	232.9	2.3
1406.6	62.8	247.2	2.7	651.9	6.2	512.2	9.2	220.7	5.3	75.1	0.7	237.1	2.3
1423.9	22.8	247.8	7.5	801.4	7.5	547.8	11.8	222.7	2.2	75.7	0.8	241.4	2.4
1425.2	39.6	254.3	6.1	840.2	7.9	571.5	5.5	223.1	2.2	76.1	2.1	247.7	3.2
1425.3	32.3	263.0	3.1	902.3	9.9	579.6	7.6	224.5	2.2	76.5	0.8	249.0	2.4
1436.1	62.2	266.1	2.7	960.9	47.7	591.6	9.8	227.1	2.5	77.1	2.6	250.2	2.5
1445.1	23.7	279.7	2.9	963.0	12.4	628.8	20.5	228.0	2.2	77.8	0.8	273.9	2.7
1470.9	23.3	279.8	4.0	963.1	54.1	643.7	6.1	228.5	9.7	78.8	2.5	304.3	4.5
1478.1	49.3	306.2	3.0	1012.5	27.9	676.8	6.4	229.7	2.3	79.0	2.3	323.0	8.1
1486.4	50.5	315.7	6.8	1073.4	20.2	680.5	6.5	232.2	12.3	82.2	2.1	351.9	12.7
1508.3	23.4	392.1	3.8	1095.4	28.0	734.6	16.3	233.6	2.3	83.2	2.5	459.2	4.4

Table D.3. (cont)

GUARICO FORMATION								PAMPATAR FORMATION					
VMN-19		VMN-20		VMN-23		VMN-28		VMN-39		VMN-40		VMN-41	
Age	Error	Age	Error	Age	Error	Age	Error	Age	Error	Age	Error	Age	Error
1511.3	97.7	407.9	8.3	1229.5	39.3	736.3	25.2	233.7	2.3	86.7	0.9	500.2	9.8
1514.6	33.5	412.5	8.4	1236.0	77.9	791.0	19.6	234.0	6.1	92.8	0.9	535.7	5.1
1522.1	18.9	421.0	9.7	1287.6	48.4	853.2	8.2	235.2	2.8	93.2	0.9	541.4	5.2
1548.4	25.7	462.5	6.2	1353.6	49.1	899.0	11.8	236.7	2.3	237.4	2.3	558.3	9.9
1551.4	30.4	463.9	17.6	1356.8	23.6	933.0	8.7	237.0	6.1	238.3	5.3	568.2	13.4
1638.0	45.3	472.6	4.6	1378.5	19.3	1021.9	28.0	237.4	2.3	241.0	2.4	581.2	15.7
1779.2	45.3	473.7	5.7	1380.0	32.6	1048.9	29.1	237.5	2.3	241.7	2.4	584.0	5.9
1781.5	18.3	484.2	12.2	1384.8	41.0	1084.3	91.2	238.2	5.8	242.3	3.9	599.0	8.1
1806.4	18.2	489.9	14.6	1388.9	54.9	1087.5	20.0	238.2	5.9	243.2	2.4	611.8	12.0
1809.4	27.9	491.0	31.0	1443.1	25.0	1094.6	31.7	240.8	2.9	255.3	7.1	631.6	6.0
1810.9	28.2	508.8	10.6	1443.5	34.0	1103.9	20.0	241.4	2.4	257.3	2.6	722.1	12.5
1818.7	37.2	553.2	5.3	1492.1	19.8	1251.3	22.9	241.5	3.7	262.0	2.6	794.8	13.5
1863.1	147.4	563.6	23.3	1500.6	33.0	1252.7	23.5	242.7	2.4	275.5	2.7	912.2	8.5
1871.6	49.8	576.0	5.5	1504.8	41.6	1257.0	41.9	242.8	2.4	278.6	5.6	943.3	11.4
1908.5	27.1	581.9	5.6	1522.4	30.2	1277.3	52.1	243.6	3.0	302.7	3.0	999.0	45.6
1938.6	17.9	585.6	7.4	1527.8	30.9	1305.1	29.6	244.9	2.4	363.3	3.5	1022.3	34.9
1949.0	35.3	685.3	33.6	1537.2	18.8	1314.4	29.5	245.3	2.4	399.2	5.2	1035.1	27.6
1953.9	22.5	751.4	10.0	1543.3	37.8	1318.2	23.3	246.4	3.0	417.9	8.1	1040.5	40.0
1964.7	17.8	889.9	20.7	1552.7	32.0	1333.0	48.1	250.3	8.5	435.9	4.2	1055.6	42.3
1970.6	25.3	907.5	10.2	1557.7	33.4	1356.5	26.5	250.4	2.5	438.2	18.9	1069.0	31.8
1974.2	17.8	943.0	10.9	1561.6	51.9	1377.0	59.6	250.6	2.5	447.8	4.9	1085.7	71.0
1975.4	24.2	978.9	35.5	1562.9	22.3	1392.0	33.0	251.3	3.4	472.6	4.6	1116.1	27.1
1975.6	34.7	986.1	47.5	1581.4	21.9	1392.2	37.7	252.2	2.5	496.0	11.6	1147.1	35.4
1979.8	19.8	1006.1	65.9	1605.5	20.8	1465.9	28.9	253.0	2.9	532.7	13.0	1175.1	19.8
1984.4	32.6	1006.1	55.3	1608.6	20.9	1506.0	46.0	260.4	5.7	533.4	5.1	1184.0	65.6
1985.4	20.5	1011.9	42.5	1610.1	18.6	1522.2	20.4	266.4	2.8	546.1	23.4	1193.7	19.7
1987.5	23.0	1025.1	24.7	1622.6	36.0	1524.7	19.1	268.2	2.6	571.7	6.4	1200.6	45.8
1992.4	17.8	1039.6	48.8	1624.0	18.6	1564.9	37.1	269.8	3.9	584.3	5.6	1240.0	27.7
1996.2	17.8	1040.6	47.7	1632.1	31.8	1567.3	24.4	290.0	12.6	592.4	6.2	1275.6	31.6
1996.2	21.7	1044.2	23.0	1644.2	18.6	1616.9	86.6	308.4	13.0	594.0	5.7	1345.4	25.5
1997.6	26.5	1047.2	56.5	1653.3	29.3	1641.3	29.0	315.7	8.8	594.6	8.5	1765.5	28.0

Table D.3. (cont)

GUARICO FORMATION								PAMPATAR FORMATION					
VMN-19		VMN-20		VMN-23		VMN-28		VMN-39		VMN-40		VMN-41	
Age	Error	Age	Error	Age	Error	Age	Error	Age	Error	Age	Error	Age	Error
2000.7	39.3	1092.9	36.9	1665.5	53.9	1655.3	24.8	396.5	21.0	648.0	6.2	2207.5	36.3
2000.9	27.0	1120.5	41.8	1679.8	28.5	1758.8	34.0	414.9	24.7	682.9	10.7		
2010.5	27.3	1129.0	80.3	1755.6	21.4	1772.9	24.0	431.0	11.2	920.5	8.6		
2076.7	17.7	1143.1	61.1	1846.8	26.3	1797.6	18.6	454.8	5.0	942.1	8.8		
2113.7	24.9	1147.9	34.0	1908.9	35.7	1804.9	21.5	463.8	17.9	1022.7	31.7		
2138.2	32.0	1162.7	41.4	1966.9	17.9	1822.8	39.2	515.7	5.0	1042.1	25.7		
2208.6	29.0	1166.5	45.4	1983.5	174.7	1867.7	50.5	533.9	21.2	1044.2	20.4		
2534.4	30.0	1168.4	58.4	2195.0	21.4	1871.0	20.4	535.2	10.0	1050.0	21.9		
2697.1	22.3	1168.6	49.9			1932.2	31.7	541.7	25.0	1052.8	24.0		
		1173.8	24.4			1936.0	24.7	545.1	9.4	1056.8	24.2		
		1192.6	26.3			1944.0	20.4	575.5	8.2	1070.3	20.5		
		1196.1	57.8			1944.5	27.7	621.2	7.1	1079.1	40.0		
		1197.6	88.6			1994.6	19.4	637.7	6.1	1136.6	20.0		
		1200.4	66.5					865.3	9.3	1166.0	23.6		
		1203.8	49.1					991.3	46.0	1179.3	38.5		
		1208.0	43.7					1008.3	39.4	1211.3	20.3		
		1223.5	45.0					1011.7	20.3	1228.8	26.0		
		1267.7	44.6					1024.4	30.4	1332.9	19.4		
		1293.1	32.3					1035.2	88.8	1338.8	31.2		
		1780.0	49.8					1038.0	25.9	1389.7	23.4		
		1992.3	37.2					1083.3	77.5	1574.9	27.9		
		2962.1	26.1					1086.2	43.0	1903.5	18.7		
								1096.8	40.2	2000.5	17.8		
								1198.3	26.6	2059.2	21.2		
								1219.4	34.0	2075.2	17.6		
								1229.0	28.5	2626.8	16.6		
								1238.0	40.6				
								2051.3	57.4				
								2331.7	24.8				

Table D.4. Turbidite units. Caratas and Los Arroyos formations

CARATAS				LOS ARROYOS			
VMN-31				VMN-43			
Age	Error	Age	Error	Age	Error	Age	Error
2442.9	19.0	2132.0	19.4	1246.4	39.2	1514.6	18.9
2013.7	21.0	2001.2	40.2	499.1	9.4	1527.3	33.0
2011.8	33.0	1944.7	51.7	532.5	6.2	1531.4	18.9
1954.8	33.4	1992.2	22.4	617.1	8.7	1560.7	35.7
1464.5	46.4	1969.8	20.9	636.0	6.1	1563.8	37.7
2115.5	26.0	1425.0	23.7	758.4	8.6	1569.8	58.7
1957.8	40.7	1943.8	21.3	932.8	15.7	1578.1	33.0
1989.7	43.1	1972.2	24.2	968.5	49.5	1622.7	18.8
1869.5	18.1	2002.7	29.5	971.6	64.8	1651.1	18.6
1971.8	17.9	1989.4	21.7	987.8	28.5	1782.3	24.1
1969.2	26.4	1975.6	31.4	1035.4	53.4	1789.3	19.2
1972.6	27.1	2120.7	25.1	1037.9	24.1	1821.8	24.4
1996.2	24.4	2818.0	16.3	1043.3	46.2	1871.1	22.9
2434.3	23.6	2498.4	19.0	1077.8	31.9	1875.8	19.7
1984.9	29.2	2114.8	31.4	1183.3	22.0	1904.0	18.2
1970.7	18.6	2018.2	54.8	1212.8	30.7	1907.6	23.2
1998.6	21.2	1985.0	54.5	1223.2	47.7	1994.0	30.1
1873.3	22.0	2147.6	27.4	1239.8	20.4	1994.6	28.4
1980.9	21.4	2101.2	32.7	1243.9	26.3	2009.4	24.3
1995.2	30.8	1976.1	31.2	1260.4	53.2	2101.0	30.1
2127.8	24.9	2916.0	24.5	1399.5	28.5	2119.2	21.2
1995.0	23.5	2074.3	22.4	1458.4	114.4	2152.3	36.9
2147.7	23.8			1477.1	25.4	2292.8	34.2
1983.2	32.6			1487.0	45.0		

## **APPENDIX E**

### **SAMPLE PREPARATION**

#### **ZIRCON SEPARATION**

(more information available in <http://www.geo.arizona.edu/alc/Sample%20Processing.htm>)

The separation process for zircons can be separated in the following steps:

- 1) Crushing and grinding
- 2) Separation of the heavy fraction in the Gemini table
- 3) Hand Magnet separation
- 4) Methylene Iodide separation
- 5) Magnetic separation and/or hand picking

#### **STEP 1. Crushing and Grinding.**

The sample is first introduced in a jaw crusher (similar to the one on Figure E.1) to reduce the fragments to gravel size. Then, the sample is grinded to sand size in a mill; with the intention of separating the original framework grains of the rock without breaking them. In order to avoid contamination during the process, these machines must be cleaned before and after processing each sample.



Figure E.1. Carbide crushing plates in a jaw crusher. The upper plate moves in a semi-elliptical way against the fixed, lower plate, crushing the samples. Picture taken from <http://www.geo.arizona.edu/alc/Sample%20Processing.htm>

#### STEP 2. Gemini table (Figure E.2)

The pulverized sample is poured on a separation table (Gemini table) to separate the high density fraction (usually heavy minerals) from the low density fraction (quartz, feldspars, micas, clays). The table is tilted at a low angle (about 25 degrees) and shakes from side to side as long as water flows. The sediments are dragged by the current from the upper part of the table and distributed accordingly to their density along the several ridges on the table. The low density material will have the tendency to be washed away and flow to the outer ridges; heavier grains will run through the central ridges and be captured in containers located at the lower end of the table. Finally, to refine the process, the fraction captured on the containers is poured again on the table. Additionally, in order to keep the sample from contamination, this machine is cleaned before and after running each sample.



Figure E.2. Gemini table for gravitational separation. Note the dense material (in darker color) being separated from the lighter fraction (lighter color, at both left and right ends) towards the center of the table.

### STEP 3. Hand Magnet separation

Once the sample extracted from the Gemini table is dry (an acetone-wash and a lamp are usually used to speed this process, besides of preventing eventual rust of the iron-rich minerals) a hand magnet is passed over the powder. This will separate most of the iron-rich minerals (such as magnetite) that might be present in the sample. This step will ease the separation process performed on Step 4. At this point the remaining fraction should represent about 5% of the volume of the original sample (at time of collection).



#### STEP 4. Methylene Iodide (Diiodomethane) separation

Given the potential hazard of this substance, the separation is performed in a fume hood. The Methylene Iodide (MI) is poured in a glass balloon through a plastic funnel in which a paper filter has previously placed. Then, enough powder from the sample is poured into the balloon so it floats freely on the heavy liquid. The sample in the balloon is disturbed with a glass stirring rod and let to rest for about one hour. MI has a density of about 3.32 g/cc; zircon has a density of above 4.0 g/cc. Any material with a density higher than 3.32 g/cc (including zircons) will sink to the bottom of the balloon, the rest will keep floating. The fraction accumulated at the bottom is then flushed into another funnel with paper filter and therefore into a beaker. The sample is again disturbed, rested and flushed as many times as necessary until nothing sinks. The time of wait between each stir will depend on how quick the heavy minerals sink. To conclude, the new heavy fraction is carefully washed with acetone and put to dry.

#### STEP 5. Magnetic separation.

Depending on the composition of the sink fraction from Step 4, a magnetic separator is used. This equipment separates the minerals accordingly to their magnetic susceptibility. The sample is run through the machine gradually increasing the voltage. Intervals are 0.3, 0.5, 0.7 and 1.0, with a maximum of 2.2. Minerals will come off at different voltages; garnet at 0.3 and 0.5, monazite at 0.5 and sphene at 0.7-1.0. Most zircons will separate at the maximum setting and stay in the non-magnetic fraction. Some zircons with magnetically susceptible inclusions may separate together with the other minerals. If some minerals are trapped together with zircon after the magnetic separation, hand picking of the zircons can be performed.

## MOUNTING OF SAMPLES FOR LA-ICPMS ANALYSIS

All the mounting process was performed at the Laserchron Lab at the University of Arizona. For reference, the following steps were taken from <http://www.geo.arizona.edu/alc/Preparing%20mounts.htm>. Again, important care has to be paid in order to avoid contamination.

Materials needed:

- A 4" x 4" ceramic tile (smooth surface)
- Double-sided tape, 2" wide.
- Fine-point tweezers (#7 preferred)
- A small aluminum tube with divider
- Buehler ring forms
- Epoxy resin
- Wet or dry sandpaper of 2500 and 3000 grit

STEP 1: Mounting sample

- Firmly attach a 2" x 2" square of tape to the tile surface.
- Gently set aluminum tube on tape surface.
- Pour just enough sample into both sides of the tube to cover the exposed tape area (Figure E.3a).

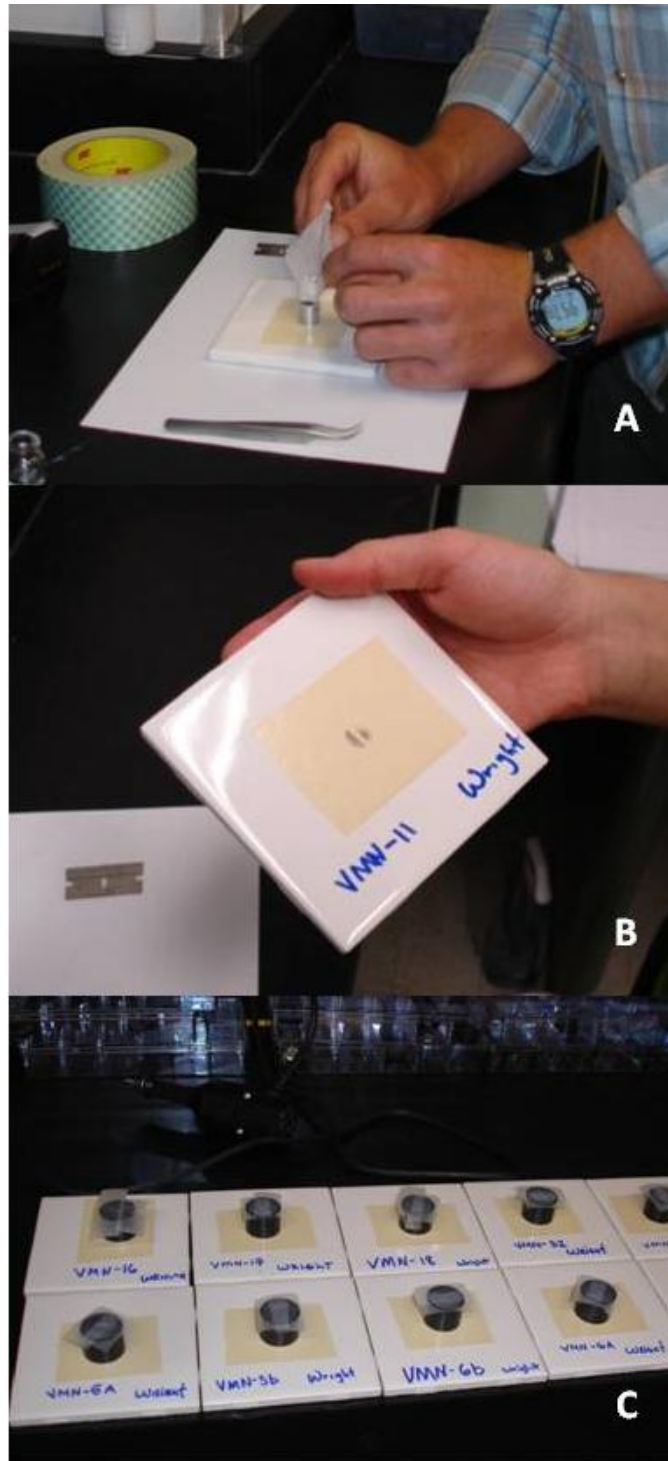


Figure E.3. Sample mounting. (A) Pouring zircons into the aluminum cylinder. (B) Zircons adhered on the tape; the “standard” grains are placed along the gap between the two halves. (C) Buehler rings moments before being filled with epoxy.

- Tilt and tap tile to spread grains evenly over exposed tape area. Pour off excess grains.
- Remove tube.
- Mount standards<sup>1</sup> in the gap between two semicircular halves (Figure E.3b).
- Place a Buehler ring in such a way that its walls are equidistant from the zircons (Figure E.3c).

#### STEP 2: Pouring epoxy

- Mix epoxy according to instructions.
- Pour epoxy into the ring, filling up to 3/8 inch.
- With a dissecting needle, loosen air bubbles from tape surface and under grains (but do not loosen grains from tape surface).
- Let harden for at least 24 hours.

#### STEP 3: Sanding

- Remove ring from tile and pull the tape from the mount surface.
- Using 2500 grit paper (and water), sand down so that you are part of the way into the smaller grains.

Switch to 3000 grit paper (with water) and continue sanding until you are about 1/3 to 1/2 of the way down into the smaller grains on the mount.

---

<sup>1</sup> *Standards* are fragments from a big zircon grain which age is previously known and calibrated

#### STEP 4: Imaging, trimming, and cleaning

- Take and print a picture of the mount surface with sufficient detail that individual crystals can be seen.
- Trim off the back of the mount (leave  $\sim 3/8$  thickness) and sand down back side for transparency.
- Wash mount thoroughly in soapy water and then spray hard with alcohol to clean surface.

## APPENDIX F

### ANALITICAL METHODS

#### LASER ABLATION ICP MASS SPECTROMETRY (LA-ICPMS)

Laser-Ablation ICP Mass Spectrometry (LA-ICPMS) allows a rapid determination of U-Th-Pb ages with micron-scale spatial resolution. The instrument used for this research is a Multicollector Inductively Coupled Plasma Mass Spectrometer (GVI Isoprobe, Figure F.1), located at the LaserChron Laboratory in the University of Arizona. This spectrometer is linked to a 193 nm wavelength Excimer laser ablation system. This device can also be applied in isotope geochemistry of Pb, Sr, Nd, Cu, Fe, U, Th, K, Ca and REE (Gehrels et al. 2006).

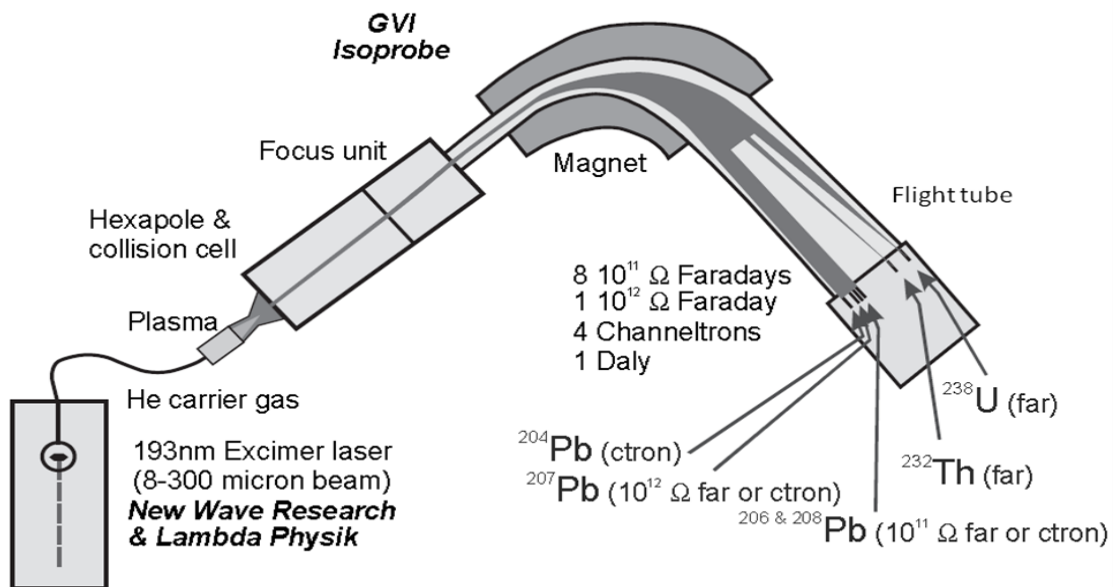


Figure F.1. Instrument used for U-TH-Pb geochronology at the Arizona LaserChron Center (Gehrels et al. 2006)

For geochronologic studies, the laser ablates the sample material, while the spectrometer analyzes U-Th-Pb isotopes. For detrital zircon analyses, a 35 or 25 micron beam diameter and a pit depth of ~15 microns is generally used. The ablated material is carried in helium gas into the plasma source of the multicollector inductively coupled plasma mass spectrometer. Simultaneously, U, Th and Pb isotopes are measured as long as they pass through the flight tube by Faraday collectors and channeltrons (ion counters, Figure F.1).

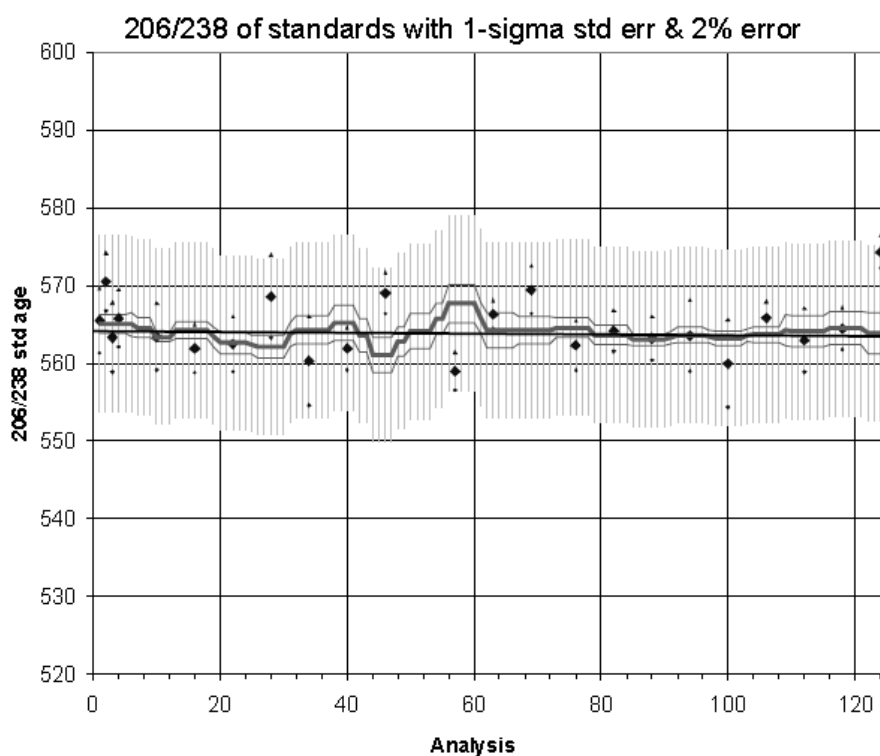


Figure F.2. Plot of standard samples analyzed (diamonds) to calibrate fractionation of  $^{206}\text{Pb}/^{238}\text{U}$ . The unknown samples are represented by the gray vertical bars; the tick, horizontal line (center) shows the average fractionization factor applied to the standards; the thin lines represent the standard error of this sliding window average (Gehrels et al. 2006).

Each analysis - performed on a single zircon grain - lasts about 90 seconds, during which a series of integrations of peaks is performed as the laser is firing and when it is off. In order to have a good statistical representation of the sample population, about 100 random zircon grains



are analyzed per rock sample. This gives an estimated time of 2.5 hours for a complete analysis of one rock sample.

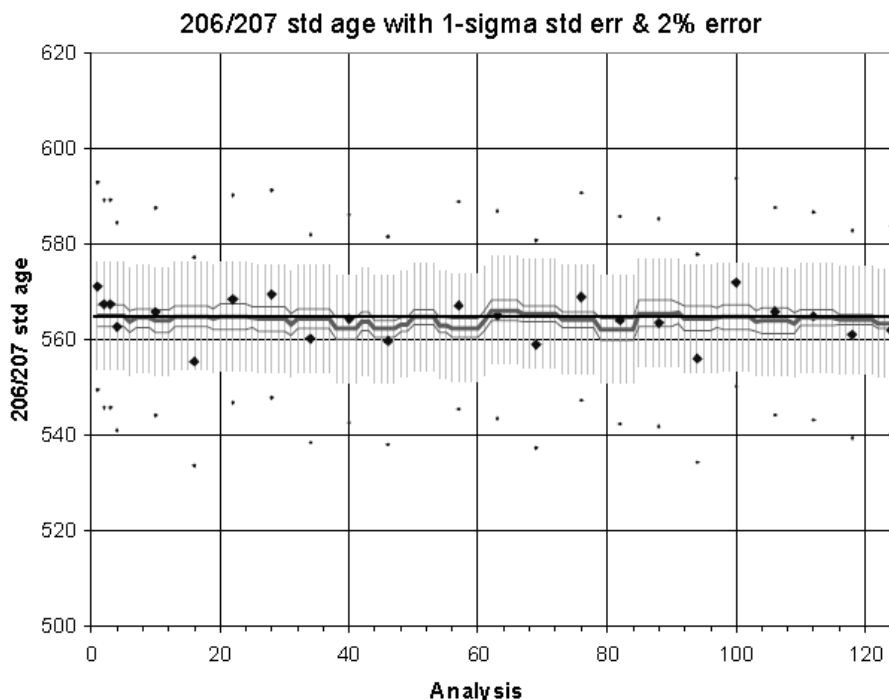


Figure F.3. Plot of standards analyzed to calibrate fractionation of  $^{206}\text{Pb}/^{207}\text{Pb}$  (GEHRELS *et al.* 2006).

Fractionization of Pb/U and Pb/Th occurs primarily in the laser pit, and this is highly sensitive to the rate of carrier gas flow across the sample surface. In order to correct this fractionization, fragments of a large zircon grain of highly-precisely known age (standards) are analyzed once every 5 unknown grains (Gehrels et al. 2006). The unknowns are then corrected against the closest 6 standards (Figure F.2). Additionally, fractionization of Pb isotopes, although minimal, is also removed by comparison with standards, by using the same procedure (Figure F.3).

For each zircon analysis, the errors in determination of  $^{206}\text{Pb}/^{207}\text{Pb}$  result in a measurement error of ~1-2% (at 2-sigma level) in the  $^{206}\text{Pb}/^{238}\text{U}$  age. Errors in measurement of  $^{206}\text{Pb}/^{207}\text{Pb}$  and  $^{206}\text{Pb}/^{204}\text{Pb}$  also result in ~1-2% (2-sigma) uncertainty in age for grains that are >1.0 Ga, but are substantially larger for younger grains due to low intensity of the  $^{207}\text{Pb}$  signal.

## DATA ANALYSIS

As previously mentioned, 100 randomly selected zircon grains per sample are analyzed for detrital zircon studies. This amount of grains would give a representative population from the sample for statistical analyses and will be used to identify the main age groups present in the rock. Once analyzed in the spectrometer, the data is filtered according to precision (10% cutoff usually used) and discordance (30% cutoff) and then plotted on Pb/U Concordia diagrams and relative age probability plots (Figure F.4). Other statistical treatments that can be applied are described below.

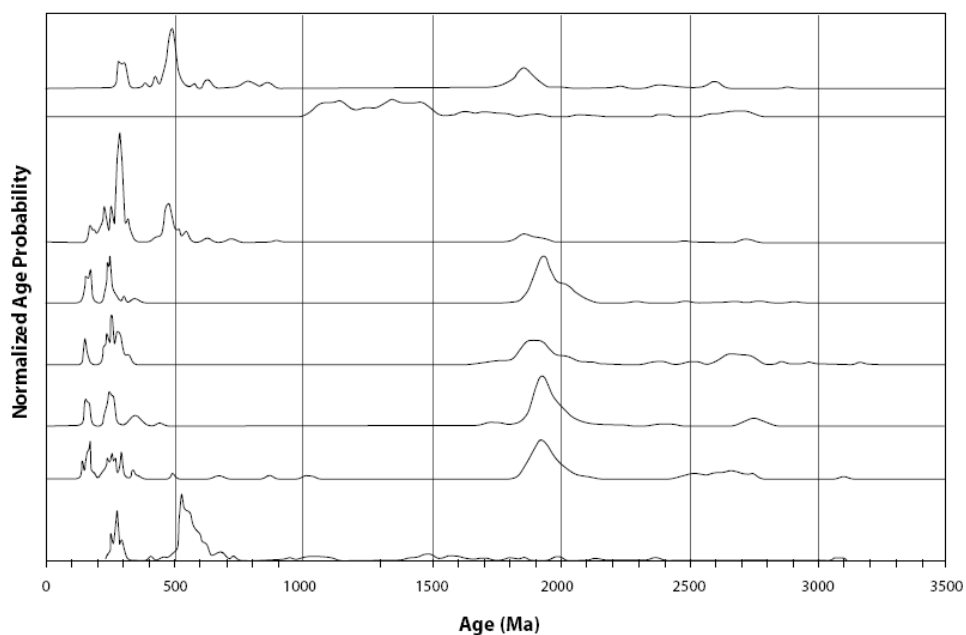


Figure F.4. Example of normalized relative age probability plots (Gehrels et al. 2006).

## Histograms

Histograms are one of the simplest ways to represent the distribution of the data. In a histogram, each bin will represent an age interval, and its height will be a reflection of the amount of grains that belong to a specific age interval.

## Probability Density Function (Figure F.5)

The Probability Density Functions (PDF) shows the probability of finding zircons of a particular age within the sample. The PDF is constructed by summing the normal distribution curve defined by each zircon's age and uncertainty (Guynn, 2006).

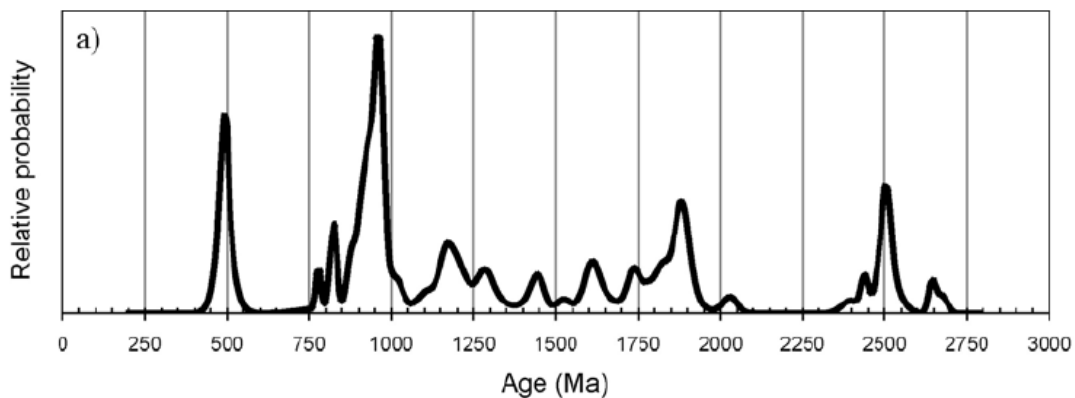


Figure F.5. Example of a Probability Density Function (Guynn, 2006).

## Cumulative Distribution Functions

The Cumulative Distribution Function (CDF, Figure F.6) is another application for showing detrital age spectra. They are similar to the probability density function with the exception that it sums the probabilities with increasing age. It shows the probability that a zircon will be younger than a certain age (Guynn, 2006).

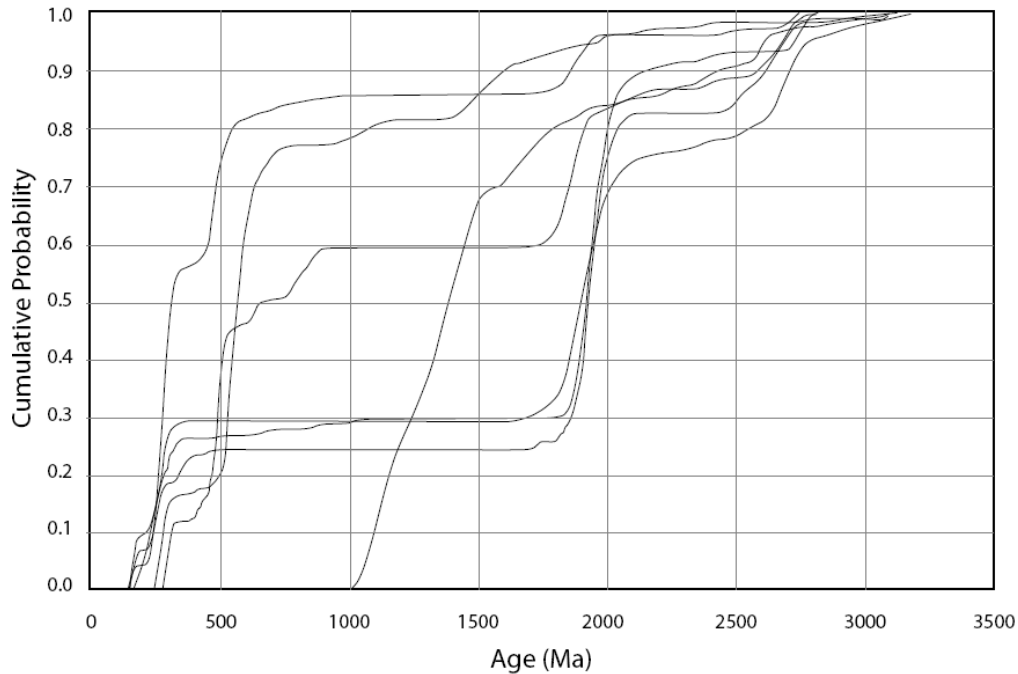


Figure F.6. Example of a cumulative probability plot (Gehrels et al. 2006).

### Kolmogorov - Smirnov (K-S) Test

The K-S test (Table F.1) compares two distributions to determine if they are statistically different at a certain level of confidence. It tests the null hypothesis that the two distributions (detrital zircon ages from two samples) are the same from the same parent population (Guynn, 2006).

The macro used in this work is provided by LaserChron. It returns a P-value that relates to the significance level of an observed D (The maximum probability difference between the two distributions). The P-value is the probability that the observed D could be due to random error. The smaller the P-value, the less likely that the observed D is due to random error, and more likely that the difference is because the distributions are not the same. The value (1-P) represents the probability that the two samples do not have the same distribution. So if P is high, the (1-P) is

low and it is unlikely that the two samples come from different populations. If P is low, the (1-P) is high and it is likely that the two samples come from different populations.

Table F.1. Kolmogorov – Smirnov test matrix.

	VMN-7	VMN-16	VMN-17	VMN-18	VMN-32	VMN-35
VMN-7		0.001	0	0	<b>0.24</b>	<b>0.533</b>
VMN-16	0.001		<b>0.848</b>	0	0	0
VMN-17	0	<b>0.848</b>		0	0	0
VMN-18	0	0	0		0.014	0
VMN-32	<b>0.24</b>	0	0	0.014		<b>0.847</b>
VMN-35	<b>0.533</b>	0	0	0	<b>0.847</b>	